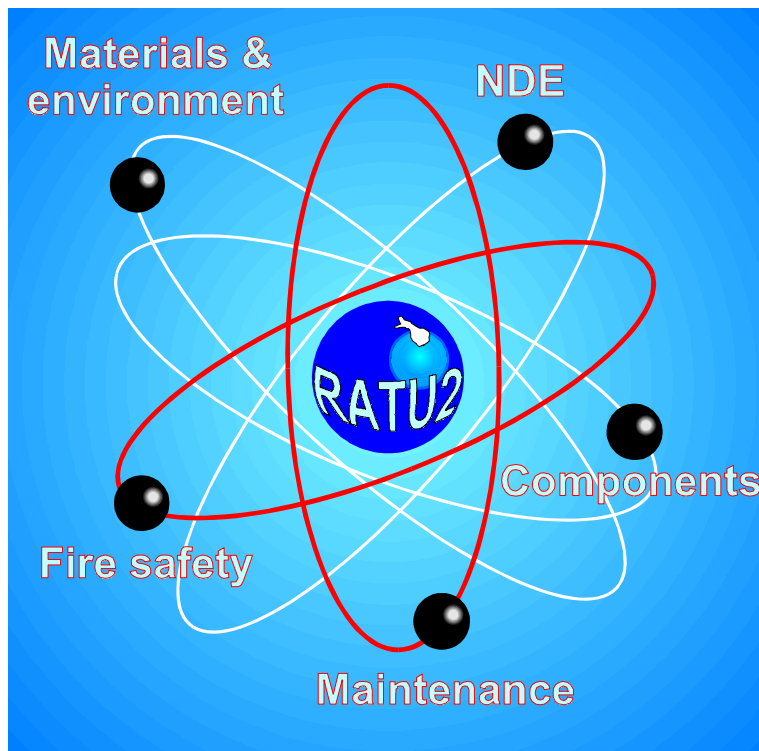


RATU2

The Finnish Research Programme on the Structural Integrity of Nuclear Power Plants

Synthesis of achievements 1995–1998



VTT SYMPOSIUM 190

Keywords: nuclear power plants, nuclear reactor safety, structural integrity, research programs

RATU2

**The Finnish Research Programme
on the Structural Integrity
of Nuclear Power Plants**

**Synthesis of achievements
1995–1998**

Espoo, 7 December, 1998

Edited by

Jussi Solin, Matti Sarkimo, Merja Asikainen & Åsa Åvall
VTT Manufacturing Technology

Organised by

VTT Manufacturing Technology



TECHNICAL RESEARCH CENTRE OF FINLAND
ESPOO 1998

ISBN 951-38-5263-6 (soft back ed.)

ISSN 0357-9387 (soft back ed.)

ISBN 951-38-5264-4 (URL: <http://www.inf.vtt.fi/pdf/>)

ISSN 1455-0873 (URL: <http://www.inf.vtt.fi/pdf/>)

Copyright © Valtion teknillinen tutkimuskeskus (VTT) 1998

JULKAISIJA – UTGIVARE – PUBLISHER

Valtion teknillinen tutkimuskeskus (VTT), Vuorimiehentie 5, PL 2000, 02044 VTT

puh. vaihde (09) 4561, faksi 456 4374

Statens tekniska forskningscentral (VTT), Bergsmansvägen 5, PB 2000, 02044 VTT

tel. växel (09) 4561, fax 456 4374

Technical Research Centre of Finland (VTT), Vuorimiehentie 5, P.O.Box 2000, FIN-02044 VTT, Finland

phone internat. + 358 9 4561, fax + 358 9 456 4374

VTT Valmistustekniikka, Voimalaitosten materiaalitekniikka, Kemistintie 3, PL 1704, 02044 VTT

puh. vaihde (09) 4561, faksi (09) 456 7002

VTT Tillverknings teknik, Material och strukturell integritet, Kemistvägen 3, PB 1704, 02044 VTT

tel. växel (09) 4561, fax (09) 456 7002

VTT Manufacturing Technology, Materials and Structural Integrity,

Kemistintie 3, P.O.Box 1704, FIN-02044 VTT, Finland

Phone international + 358 9 4561, Fax + 358 9 456 7002

Technical editing Maini Manninen

Oy Edita Ab, Espoo 1998

Preface

This Symposium summarises the scientific and technical achievements within the Finnish research programme on the structural integrity of nuclear power plants (RATU2). The programme began in 1995 and will be accomplished at the end of 1998. The main sources of the programme funding were public, i.e. the Ministry of Trade and Industry (KTM), VTT (Technical Research Centre of Finland) and the Radiation and Nuclear Safety Authority (STUK), but also the power companies Imatran Voima Oy (IVO) and Teollisuuden Voima Oy (TVO) has participated in the funding.

An outline of the programme is given in the first paper of this proceedings. The major scientific and technical results are described in the following technical papers. The main objectives and achievements within the programme are summarised in the last paper of this proceedings.

The presentations for this symposium have been selected by a team of the editors and project leaders Kim Wallin¹, Pertti Aaltonen¹, Pentti Kauppinen¹, Heli Talja¹, Kari Laakso², Olavi Keski-Rahkonen³. The members of the programme steering and project reference groups provided valuable efforts and experience for the planning and steering of the research. In addition, we are grateful to all colleagues participating in the research work and preparing of this symposium.

Espoo, November, 1998

Jussi Solin

Matti Sarkimo

Merja Asikainen

Åsa Åvall

¹ VTT Manufacturing Technology

² VTT Automation

³ VTT Building Technology

Contents

PREFACE	3
RATU2 research for safety and operability <i>Jussi Solin</i>	7
Fracture mechanical materials characterisation <i>Kim Wallin, Tapio Planman and Markku Nevalainen</i>	23
Fracture analysis of ductile elastic-plastic materials under mixed-mode I-II loading <i>Anssi Laukkanen</i>	45
Comparison of transition temperature criteria applied for KLST and ISO-V type Charpy specimens <i>Tapio Planman, Matti Valo and Kim Wallin</i>	77
Material deterioration due to neutron irradiation <i>Matti Valo and Kim Wallin</i>	91
Method development for studies of environmentally assisted cracking (EAC) <i>Päivi Karjalainen-Roikonen, Pekka Moilanen, Aki Toivonen and Pertti Aaltonen</i>	105
Modelling of environmentally assisted cracking <i>Pertti Aaltonen, Timo Saario, Hannu Hänninen, Jussi Piippo, Ulla Ehrnstén and Marjo Itäaho</i>	125
Oxide films in high temperature aqueous environments <i>Timo Laitinen, Kari Mäkelä, Timo Saario and Martin Bojinov</i>	145
Development of tools and models for computational fracture assessment <i>Heli Talja and Kari Santaoja</i>	177
Structural analysis of NPP components and structures <i>Arja Saarenheimo, Heikki Keinänen and Heli Talja</i>	195

Verification of analysis methods through participation in the NESC1 programme <i>Rauno Rintamaa, Tapio Planman, Heikki Keinänen, Heli Talja and Pentti Kauppinen</i>	221
Non-destructive inservice inspections <i>Pentti Kauppinen, Matti Sarkimo and Kari Lahdenperä</i>	237
Analysis of maintenance strategies <i>Kari Laakso and Kaisa Simola</i>	251
Models on reliability of non-destructive testing <i>Kaisa Simola and Urho Pulkkinen</i>	263
Human and organisational factors in the reliability of non-destructive testing (NDT) <i>Leena Norros</i>	271
Fire safety <i>Olavi Keski-Rahkonen, Jouni Björkman, Simo Hostikka, Johan Mangs, Risto Huhtanen, Helge Palmén, Arto Salminen and Antti Turtola</i>	281
RATU2 research objectives and achievements <i>Jussi Solin and Matti Sarkimo</i>	309
APPENDIX 1. List of publications	36 p.
APPENDIX 2. Contact information	6 p.

RATU2, research for safety and operability

Jussi Solin
VTT Manufacturing Technology
Espoo, Finland

1. Introduction

The Finnish research programme on the structural integrity of nuclear power plants, RATU2 was launched in 1995 for four years to coordinate the independent national research and development work aiming for structural safety in NPP's. The general planning and goal setting of the programme was based on the research need assessment and evaluation of the previous RATU programme. The research plans have been updated and refined annually on the basis of available funding.

The RATU2 programme is briefly introduced in this paper. The role of RATU2 in the national nuclear energy research field, the research areas, administrative data, main objectives and future plans are the topics of this presentation. See the following technical papers for the major scientific and technical results, and the last paper in this symposium for a summary of achievements within the RATU2 programme.

2. Nuclear energy research in Finland

In Finland about one third of the electrical energy is generated by nuclear power. Imatran Voima Oy runs two VVER type pressurized water reactors (PWR) in Loviisa and Teollisuuden Voima Oy runs two boiling water reactors (BWR) in Olkiluoto. Continued safe and economic operation of these plants is possible only when strict safety and reliability requirements are fulfilled.

Publicly funded nuclear energy research supplies impartial expertise for the regulation of nuclear energy. The public sector also has a major role in providing the necessary education system, personnel and equipment resources

for research and development, as well as in establishing the framework for international collaboration. This role is supported by focused public research programmes:

- Reactor Safety (RETU), 1995 - 1998,
- Structural Integrity of Nuclear Power Plants (RATU2), 1995 - 1998, and
- Publicly Administrated Nuclear Waste Management (JYT2001), 1997 - 2001.

Publicly funded research in the fields of programmable automation and environmental impacts is currently carried out in separate projects. Most of the public research is conducted by the Technical Research Centre of Finland (VTT). The universities participate to projects co-ordinated by VTT or have separate projects on specific topics. The power companies take care of the plant-specific issues and of the nuclear waste disposal.

In 1996 the RATU2 programme represented 6% of the nuclear energy R&D in Finland. An overview of the volumes of different research areas and the funding basis of the nuclear energy research in Finland in 1996 is shown in Fig. 1.

3. Main objectives of the RATU2 programme

The structural safety of nuclear power plants is largely dependent on materials and the design of the structures. Research in these areas aims to prevent accidents and unscheduled outages. Consequently, the concerns and risks arising from faults in equipment and structures can be kept to a minimum.

After a substantial operation time the ageing of the structures and components in the Finnish nuclear power plants is one of the main issues to be considered when safety and economic operation of the plants is evaluated. At the same time, ways are being sought to extend the lifetime of components.

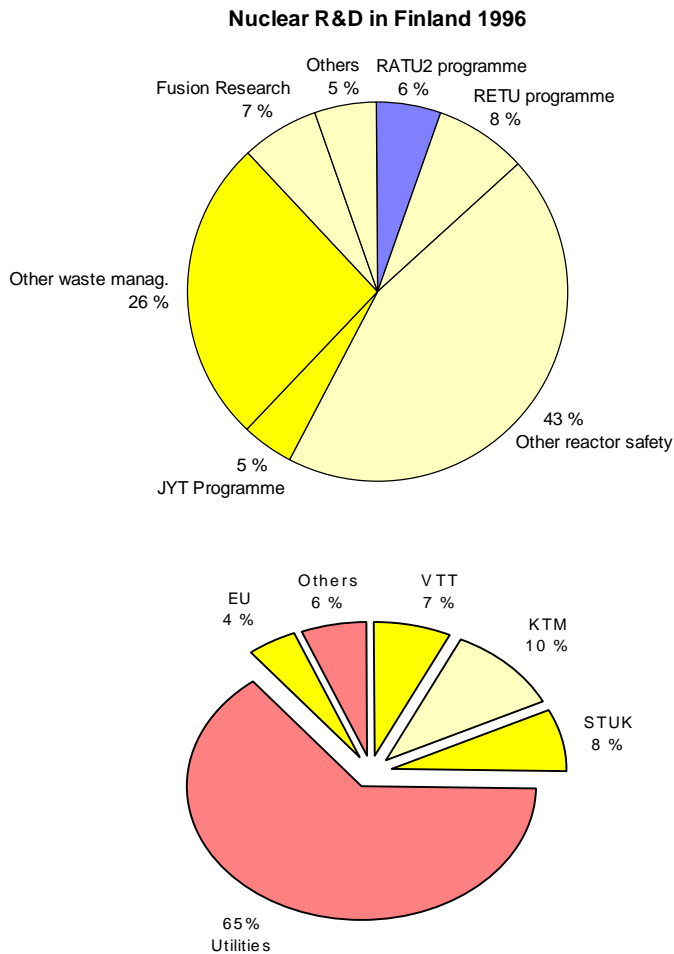


Figure 1. Funding of nuclear energy research in Finland in 1996.

The loading capacity of the critical main structures must always, during the operating time of the plant, exceed the loading stresses. One of the main objectives of the RATU2 research programme is to quantitatively evaluate the safety margins by developing and applying expertise in materials research, structural analyses, NDE, reliability and fire safety technology and also by applying various research, testing and analysis capabilities. Whenever feasible, the results of analyses and tests are compared and verified through participation in relevant international research programmes.

The RATU2 research programme also plays an important role in the education of new experts, technology transfer and international exchange of scientific results.

The aims and research plans for the RATU2 programme were compiled and published in the start-up phase (VTT, 1994).

4. Realisation of the RATU2 programme

4.1 Financial framework

The Finnish research programme on the structural integrity of nuclear power plants, RATU2 was launched in 1995 and it will be completed by the end of 1998. The annual budgets exceeded FIM 10 million, i.e., were round 2 million ECU per annum. This covered about 15 person-years of work for each year.

The project on material degradation in the reactor environment (RAVA) alone represents one half of the programme and the project on structural analyses for nuclear power plant components (RAKE) one fifth. The volume distribution between the projects is shown in Fig. 2.

4.2 Funding of the RATU2 programme

A summary of the funding of the RATU2 programme in 1995 - 1998 is shown in Figs. 3 and 4. The funding of the Ministry of Trade and Industry (KTM) has been allocated to the individual projects according to the original plans and suggestions of the steering group. VTT is funding the programme from its internal strategic research resources with the aim of developing most relevant expertise and facilities for this customer sector. The other parties have allocated their funding into specific tasks and thereby provided clear signals for steering of the projects. In addition to the here reported direct funding, the Radiation and Nuclear Safety Authority (STUK) and the Utilities (IVO and TVO) provide also significant work contributions to the RATU2 programme.

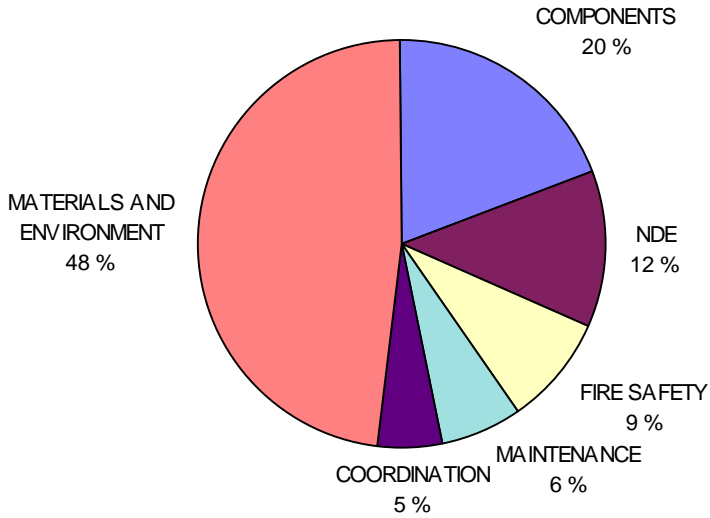


Figure 2. Distribution of expenses between the projects in RATU2 programme.

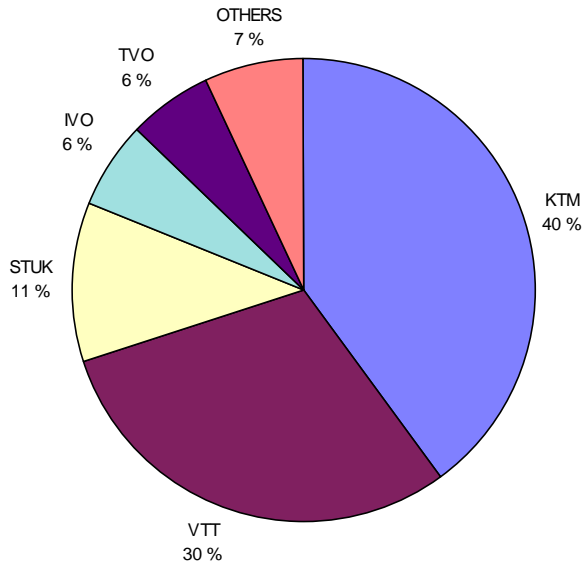


Figure 3. Funding organisations for the RATU2 programme in 1995 - 1998.

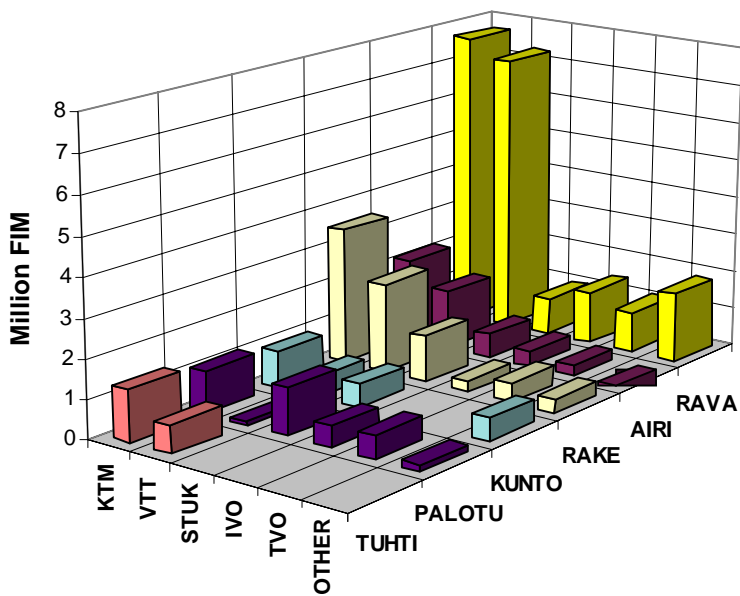


Figure 4. Distribution of funding for the projects within RATU2 in 1995 - 1998.

4.3 Organisation

For effective technical management, the RATU2 research programme is divided into five technical and one co-ordination projects as follows:

- Material degradation in the reactor environment (RAVA)
- Reliability of nondestructive inspections of nuclear power plants (AIRI)
- Structural analyses for nuclear power plant components (RAKE)
- Maintenance strategies and reliability (KUNTO)
- Fire safety (PALOTU)
- Co-ordination reporting and dissemination (TUHTI).

VTT Manufacturing Technology has the general responsibility of the programme, but for the project execution it closely co-operates with VTT Automation, VTT Building Technology, VTT Energy and Helsinki University of Technology. The co-ordination principles are documented in (Solin, 1997).

The programme is organised into five research projects, each having specific objectives, but transparent borders. In addition, a separate program is formed for general co-ordination. The programme organisation is illustrated in Fig. 5.

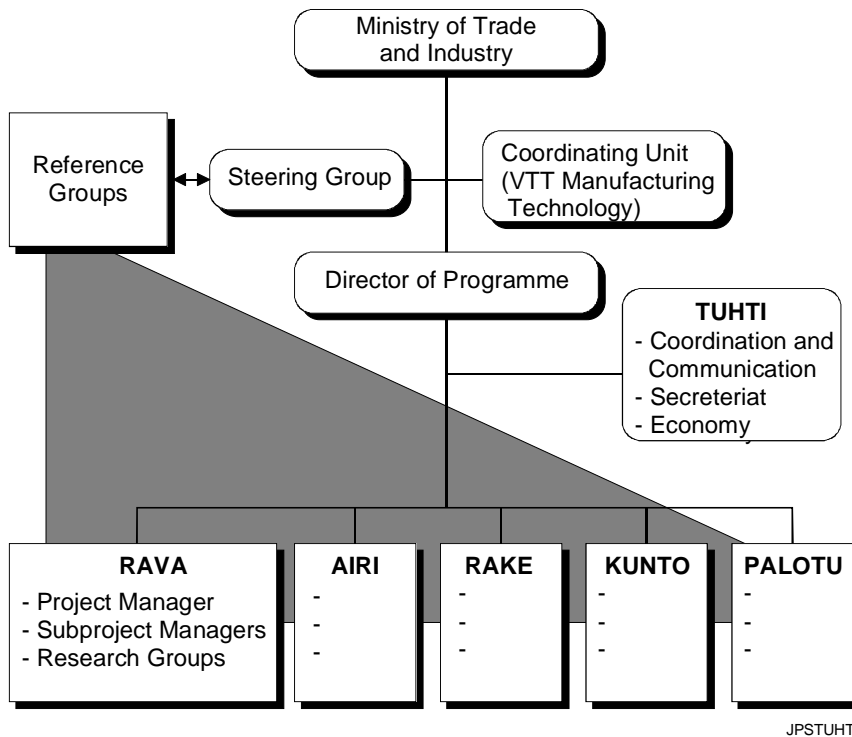


Figure 4. Organisation for steering the RATU2 programme (Solin, 1997).

Representatives of the Ministry of Trade and Industry (KTM), Radiation and Nuclear Safety Authority (STUK), utilities (IVO, TVO), VTT and Helsinki University of Technology form the steering group which is responsible of general steering of the programme. The project reference groups help in planning and technical follow-up of the projects.

4.4 Co-operation

Although each of the research projects has specific objectives and budget, the research work joins the project teams in flexible ways into the task groups. As the practical problems are multidisciplinary, some are dealt with in several projects within the RATU2 programme and/or linked to other international programmes. Perhaps the best example of this kind of cooperative work is the ongoing NESC1 activity:

The experimental verification of integrity assessments for nuclear power plant components requires expensive large scale tests, which could not be performed within the domestic research budgets without participation to the international network NESC. The participation to NESC1 is organised into two projects, AIRI and RAKE, where NDE and structural analysis are considered. However, the fracture mechanical assessment requires the experimental and analytical expertise for materials characterisation being developed in the RAVA project. Furthermore, the reliability modelling in the KUNTO project utilises the results of the nondestructive inspection round robins.

The networks, such as AMES, NESC and PISC, coordinated by the Joint Research Centre (JRC) of the European Union, as well as the Nordic NKS co-operation are considered very important for technology transfer and international exchange of results. The participation to the international CIR program coordinated by EPRI, to the OECD Halden reactor project, to the EURATOM Nuclear Fission Safety (NFS) projects and some other international projects is also organised through the RATU2 programme. This arrangement provides a forum for coordinated domestic funding and steering of these related activities. It also makes possible to use the existing technology transfer channels and reference groups together with the Finnish authorities and utilities.

5. Targetted research areas

5.1 Material degradation in the reactor environment

During the use of nuclear reactors the properties of the structural materials change. Variations in the operation environment, such as changes in water chemistry, may enhance the development and growth of flaws. Neutron radiation embrittles reactor pressure vessel materials. Radiation, together with water chemistry, increases the possibility of stress corrosion cracking in stainless steels and superalloys used in the reactor internal parts. Thermal ageing embrittles cast austenitic stainless steels. Research on structural materials endeavours to study the ageing mechanisms of materials, and the possibilities and methods of preventing or forecasting the damage caused to structures by ageing.

Research carried out on structural materials enables identifying various ageing phenomena and produces essential source data, which is used in estimating the safety of nuclear plants and their remaining operating life. The reliability of structural integrity analyses is directly dependent upon the relevancy and accuracy of material properties used as input for these analyses. Thus, it is imperative that the material properties determined experimentally are reliably transferable to describe the structural detail in question.

The RAVA project had originally four target areas:

- to improve the implementation, reliability and usability of fracture mechanical material characterization, and to develop new advanced models for the prediction of radiation damage,
- to study the mechanisms of radiation damage and recovery and to develop a new generation of radiation monitoring programmes, with special emphasis on the situation after thermal annealing,
- to evaluate the factors affecting the changes in material properties due to the environment and stresses and to assess their interrelationship, and

- to establish the applicability of the latest repair technologies and the reliability of the repairs, and to study the benefits of new materials and manufacturing technologies.

A fifth target area was introduced in 1997:

- to identify the correlation between the high temperature water chemistry, stress corrosion susceptibility and rise of radiation levels through contamination, and to prevent failures and activity rise by monitoring of the water chemistry.

5.2 Reliability of non-destructive inspections of nuclear power plants

During in-service inspections of nuclear power plants, flaws in the structures have to be detected reliably and also characterised. To be able to determine the criticality of flaws, the NDE methods must be able to assess not only the size but also the position, type and orientation of the flaw.

The cumulative plant operation data and experience gained from inspections are able to indicate the potential flaw areas. In these areas there is a need to apply versatile combination techniques and extensive post-analysis of inspection data. The elevation of radiation level and limited access of components cause inspection automation to become necessary.

The AIRI project has four target areas:

- to implement the validation practice of various NDT methods,
- to evaluate the reliability and accuracy of NDE results as a basis of the structural safety analysis,
- to implement automatic inspection systems, and
- to develop and implement new NDE techniques, particularly for problematic inspection tasks and continuous monitoring.

5.3 Structural analyses for nuclear power plant components

The ageing of the nuclear power plants raises continuing needs for structural analyses of structures, when the plant life time extension is planned or possibilities for power increase are evaluated. In such estimations, the effects of material properties degradation, the results of destructive full scale model tests as well as laboratory tests, numerical analyses, and operating experience are included. Additionally, realistic and reliable computational models are necessary. In particular, the real boundary conditions and loads acting on the structures in different operational situations are sometimes only known approximately. The use of improved models helps to assess the real safety margins of the power plants and to reduce unnecessarily large conservatism.

The main objective is to create, evaluate and apply effective and reliable structural analysis methods for the safety and availability assessment of nuclear power plant applications. In particular, they are applied on pressure vessels and piping.

The RAKE project has three target areas:

- to develop fracture assessment methods and tools,
- to assess structural behaviour under realistic loading cases, and
- to verify the assessment methods by results of large scale experiments.

5.4 Maintenance strategies and reliability

The ageing management of a nuclear power plant includes various decisions concerning e.g. the prioritization of different components for analyses and selection of their maintenance strategies. The maintenance tasks of a nuclear power plant include functional testing and calibration control, non-destructive testing, servicing, replacement of components, condition monitoring, repairs and modification work. The project is not directed to the reactor pressure vessel, steam generators being very expensive to replace, but on more easily

replaceable components and structures also important to plant safety and economy.

The aim is to develop and apply reliability and decision models, man-machine psychology for evaluation and development of maintenance strategies from the point of view of plant safety, availability and maintenance cost by using various plant information systems and data sources.

The KUNTO project has three target areas:

- to develop an analysis and decision support method for evaluation of the needs to change preventive maintenance programmes and replace components,
- to develop evaluation methods of structural integrity taking into account the results of probabilistic safety assessments and increasing knowledge on the degradation of materials, and
- to improve the reliability of the detection of flaws by developing and applying the knowledge of man-machine psychology in evaluating non-destructive testing.

5.5 Fire safety

According to experience and probabilistic risk assessments, fires present a significant hazard in a nuclear power plant. Fires may be initial events for accidents or affect safety systems planned to prevent accidents and to mitigate their consequences. The project consists of theoretical work, experiments and simulations aiming to increase the fire safety at nuclear power plants.

The PALOTU project has four target areas:

- to produce validated models for numerical simulation programmes,
- to produce new information on the behaviour of equipment in case of fire,
- to study applicability of new active fire protecting systems in nuclear power plants, and

- to obtain quantitative knowledge of ignitions induced by important electric devices in nuclear power plants.

5.6 Co-ordination, reporting and dissemination

In order to keep the research work focused and efficient, a separate co-ordination and communication project is included in the RATU2 research programme (Solin, 1997). This allows the experts to concentrate in the research work. Synergy and co-ordination is sought in multidiscipline technical areas as well as in the international co-operation.

6. Future research

6.1 Follow-on research programme on nuclear power plant safety 1999 - 2002

The Ministry of Trade and Industry (KTM) has decided to continue the national research efforts in a single research programme after completion of the parallel research programmes on Reactor Safety (RETU) and Structural Integrity of Nuclear Power Plants (RATU2).

The national advisory group was commissioned by the KTM to prepare a general plan and a recommendation on the organisation for the new programme. The recommendations of the international evaluation of the RATU2 and RETU programmes (Faidy and Hayns, 1998) and the opinions of national expert panels were taken into account in the resulting published proposal on the Finnish Research Programme on Nuclear Power Plant Safety (1999-2002) (Ydinenergianeuvottelukunta, 1998).

6.2 Priority topics in the follow-on research

When the RATU2 and RETU programmes were jointly evaluated in January 1998, the conclusions drawn by the external evaluators from France and U.K. and shared by the domestic support group included a clear recommendation on the future research priority:

“The evaluation team recognised a number of future trends which could have a strong influence on the direction of the programs. Above all, however, the team recognised that the Finnish plants are now at least twenty years old and, whilst they still have a long way to go before the end of their useful lives, they will require increasing attention to issues related to plant ageing. Along with many other countries, therefore, we anticipate a move towards research topics more directly related to underpinning the continued safe operation of the plant.” (Faigy and Hayns, 1998)

The Finnish Research Programme on Nuclear Power Plant Safety (1999-2002) is divided into three thematic research areas, which are Ageing, Accidents and Risks. The thematic research area of Ageing will have its main roots in the results of the RATU2 programme and is therefore of primary interest here. It will also reflect to the above cited recommendation of the RETU and RATU2 evaluation.

The research plans on ageing mechanisms include studies on phenomena limiting the applicability of mechanical and electrical components, fuel and constructions. The aim is to model effects of water environment and irradiation exposure to the ageing phenomena, and particularly effects of re-irradiation after annealing of pressure vessel material.

In the field of structural integrity the main objective is to create and verify experimental and computational methods for assessing the remaining lifetime of components and their ability to withstand possible accident situations. Systematic methods to improve and verify the reliability of non-destructive testing will be developed and techniques for continuous monitoring will be searched and evaluated.

In addition to the national research programme, other focused projects and actions will, hopefully, also utilise the results of the RATU2 programme. For example, there exist concrete plans on industry driven projects on plant life management.

7. Acknowledgements

The reported work was part of the Finnish Research Programme on the Structural Integrity of Nuclear Power Plants 1995 - 1998, project TUHTI on Co-ordination, reporting and dissemination.

Until September 1995, Dr. Rauno Rintamaa acted as the director the the RATU2 programme, and even thereafter, the reported co-ordination work has been carried out under his kind support and supervising.

The members of the steering group of the programme: Mr. Matti Ojanen, (Chairman), the Radiation and Nuclear Safety Authority, Mr. Ralf Ahlstrand, IVO Power Engineering Ltd., Mr. Juho Hakala, Teollisuuden Voima Oy, Prof. Hannu Hänninen, Helsinki University of Technology, Dr. Timo Haapalehto, Ministry of Trade and Industry, Dr. Lasse Mattila, VTT Energy, Dr. Rauno Rintamaa, VTT Manufacturing Technology, as well as the project leaders and members of the TUHTI co-ordination group: Ms. Merja Asikainen, Mr. Matti Sarkimo, Mr. Jari Niemi have given a significant contribution to steering of this research programme and are gratefully acknowledged of this co-operation.

References

Faidy, C. & Hayns, M. R. 1998. Evaluation of the RATU2 and RETU Research Programs. Helsinki: Ministry of Trade and Industry, Finland. 65 p. (Studies and Reports 8/1998).

Solin, J. 1997. RATU2 Suunnittelu, ohjaus ja raportointi; Tutkimusohjelman hallintomenettelyjen kuvaus. Espoo: VTT Manufacturing Technology. 15 p. + app. (Report VALB256). (In Finnish).

VTT 1994. Ydinvoimalaitosten rakenteellinen turvallisuus (RATU2) 1995 - 1998, Tutkimusohjelman suunnitelma. Espoo: VTT Manufacturing Technology. 50 p. (Report VALB41). (In Finnish).

Ydinenergianeuvottelukunta 1998. Kansallinen ydinvoimalaiosten turvallisuustutkimus 1999 - 2002; Ehdotus uuden tutkimusohjelman sisällöksi ja organisoinniksi. Helsinki: Ministry of Trade and Industry, Finland. 66 p. (Studies and Reports 15/1998). (In Finnish).

Fracture mechanical materials characterisation

Kim Wallin, Tapio Planman and Markku Nevalainen
VTT Manufacturing Technology
Espoo, Finland

1. Introduction

The experimental fracture mechanics development has been focused on the determination of reliable lower-bound fracture toughness estimates from small and miniature specimens, in particular considering the statistical aspects and loading rate effects of fracture mechanical material properties. Additionally, materials aspects in fracture assessment of surface cracks, with emphasis on the transferability of fracture toughness data to structures with surface flaws have been investigated. Further a modified crack-arrest fracture toughness test method, to increase the effectiveness of testing, has been developed.

2. Re-evaluation of the thermal shock experiment results based on the VTT master curve

One important step in fracture mechanical research has been the thermal shock experiments (TSE). The TSE's are exceptional because many of them had extremely long crack fronts. As a trend, the TSE initiation fracture toughness results form a lower bound to the small specimen data used for material characterization.

The present work has led to an ASTM testing standard for fracture toughness testing in the transition region (ASTM E 1921-97). The standard is based on the VTT approach for statistical treatment of fracture toughness data. Key components in the VTT approach are statistical expressions for describing the data scatter and for predicting a specimens size effect and an expression for the fracture toughness temperature dependence.

In order to examine the validity of the statistical size effect assumption, the TSE's were re-evaluated with the VTT approach. The statistical analysis was based on the VTT statistical brittle fracture model, which gives for the scatter of fracture toughness,

$$P[K_{IC} \leq K_I] = 1 - \exp\left(-\left[\frac{K_I - K_{\min}}{K_0 - K_{\min}}\right]^4\right) \quad (1)$$

where $P[K_{IC} \leq K_I]$ is the cumulative failure probability, K_I is the stress intensity factor, K_{\min} is the theoretical lower bound of fracture toughness and K_0 is a temperature and specimen size dependent normalization fracture toughness, that corresponds to a 63.2% cumulative failure probability being approximately $1.1 \cdot \bar{K}_{IC}$ (mean fracture toughness). The model predicts a statistical size effect of the form,

$$K_{B_2} = K_{\min} + [K_{B_1} - K_{\min}] \cdot \left(\frac{B_1}{B_2}\right)^{1/4} \quad (2)$$

where B_1 and B_2 correspond to respective specimen thickness (length of crack front).

Close to the lower shelf of fracture toughness ($K_{IC} \ll 50 \text{ MPa}\sqrt{\text{m}}$) the equations are expected to be inaccurate. The model is based upon the assumption that brittle fracture is primarily initiation controlled, even though it contains a conditional crack propagation criterion, which among others is the cause of the lower bound fracture toughness K_{\min} .

On the lower shelf, the initiation criterion is no longer dominant, but the fracture is completely propagation controlled. In this case there is no statistical size effect and also the toughness distribution differs (not very much) from Eq. 1. In the transition region, which is of main interest for the present work, however, Eqs. 1 and 2 should be valid as long as loss of constraint and/or ductile tearing do not play a significant role.

The VTT approach includes the "master curve" describing the temperature dependence of fracture toughness,

$$K_0 = 31 + 77 \cdot \exp(0.019 \cdot [T - T_0]) \quad (3)$$

where T_0 is the transition temperature where the mean fracture toughness, corresponding to a 25 mm thick specimen, is 100 MPa√m and K_0 is 108 MPa√m.

Eq. 3 gives an approximate temperature dependence of the fracture toughness for ferritic structural steels and it is comparatively well verified. Keeping the temperature dependence fixed, decreases the effect of possible invalid fracture toughness values upon the transition temperature T_0 .

For a randomly censored data set with the maximum likelihood concept (MML) the estimate of T_0 becomes

$$\sum_{i=1}^n \frac{\delta_i \cdot \exp\{c \cdot [T_i - T_0]\}}{a - K_{\min} + b \cdot \exp\{c \cdot [T_i - T_0]\}} - \sum_{i=1}^n \frac{(K_{IC_i} - K_{\min})^4 \cdot \exp\{c \cdot [T_i - T_0]\}}{(a - K_{\min} + b \cdot \exp\{c \cdot [T_i - T_0]\})^5} = 0 \quad (4)$$

from where T_0 can be solved iteratively. The Kronecker's delta (δ_i) is one (1) when K_{IC} corresponds to failure by brittle fracture and $\delta_i = 0$ when K_{IC} corresponds to non-failure (end of test value).

When the test temperatures are in the range $T_0 - 50^\circ\text{C} \dots T_0 + 50^\circ\text{C}$, the theoretical standard deviation of the estimate is approximately $\sigma_{T_0} \approx 17/\sqrt{r}$ ($^\circ\text{C}$).

As an example, the analysis of TSE 5A is presented in Figs. 1 and 2 where the raw and re-evaluated data are shown. Based on the re-evaluation the following main conclusions can be drawn:

- Application of the statistical size correction to the small specimen material characterization data succeeded in all cases to bring the material characterization data in line with the TSE results.
- Thermal shock loading does not decrease the fracture toughness below standard specimen deep crack (size corrected) fracture toughness. The "shallow flaw" effect is, however, not visible in the TSE data.

- Statistically defined size corrected lower bound estimates based on the master curve provide a conservative, but realistic, estimate of the TSE behaviour.
- Subsequent initiations in the TSE correspond always to a higher fracture toughness than previous ones. The behaviour can be explained by the WPS effect connected to the crack arrest event.

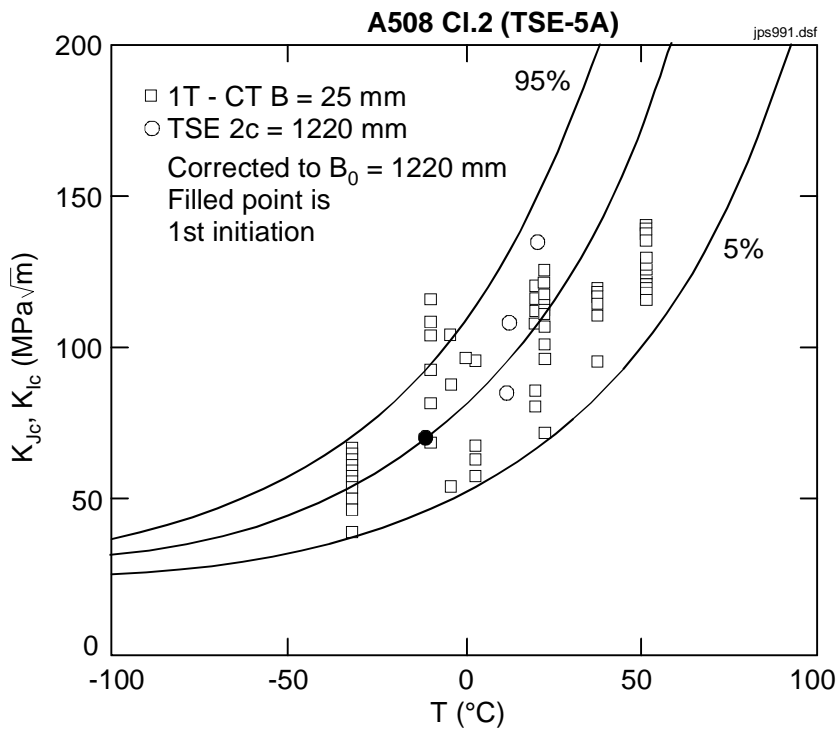


Figure 1. Original TSE-5A data. Filled point corresponds to first initiation event.

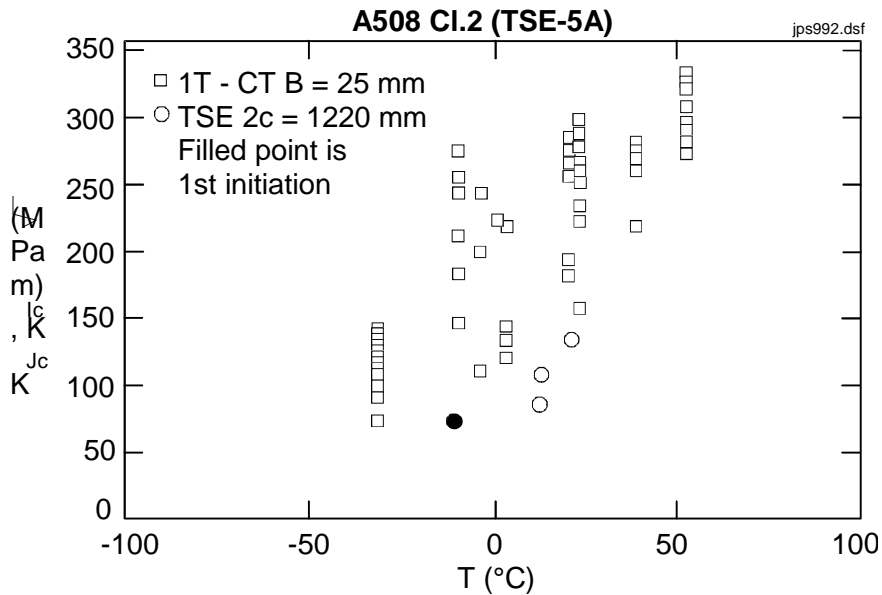


Figure 2. Size corrected TSE-5A data together with master curve.

3. Effect of loading rate on fracture toughness

The master curve concept describes a materials fracture toughness in the transition region, with the help of the reference temperature T_0 . It forms the basis for the new ASTM testing standard for fracture toughness testing in the transition region and it is also a candidate for structural integrity assessment codification. Normally, T_0 is determined for (quasi) static strain rates, while

often dynamic values are required. The master curve concept can of course be applied also to dynamic tests, but this would require more testing. Therefore, if the effect of loading rate on T_0 can be quantified with a sufficient accuracy, the applicability of the master curve concept for structural integrity assessment codification would be strongly enhanced. For this purpose, fracture toughness data, corresponding to different loading rates, found in the literature was analysed by the master curve concept.

Strain rate effects on the yield strength have classically been described with the Zener-Hollomon strain rate parameter, which combines the effect of temperature and strain rate into one, activation energy based, expression. In this study, the Zener-Hollomon strain rate parameter was applied to T_0 in order to develop a simple semiempirical expression for the strain rate dependence of T_0 .

A typical example of the master curve analysis result is presented in Fig. 3 for a western pressure vessel steel. All data sets were not suitable for the master curve analysis. In many cases, the individual fracture toughness results were missing or were too scarce. Based on earlier experience, only data sets including a minimum of three proper fracture toughness results were included in the master curve analysis.

MASTER CURVE ANALYSIS OF SA533B Cl.1 (HSST02) EPRI DATA BASE

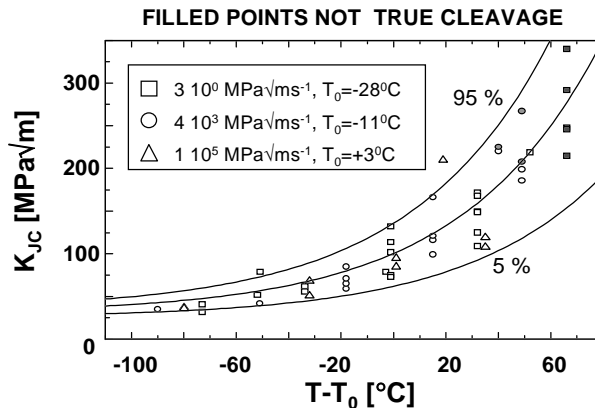


Figure 3. Master curve analysis of SA 533B Cl.1 (HSST 02) EPRI data base. Filled points are not true cleavage fractures.

The Zener-Hollomon strain rate parameter is usually expressed in the form

$$\sigma_y = f \left(T \cdot \log \left\{ \frac{A}{\dot{\varepsilon}} \right\} \right) \quad (5)$$

where T is the temperature in Kelvin and A is the strain rate parameter being a function of the activation energy of the yield process.

A major difference between a tensile test and a fracture toughness test is the definition of strain rate. For a crack, the stress and strain distribution is not uniform, but varies strongly in front of the crack tip. There have been attempts to prescribe a cracked specimen an effective strain rate value, but this is a very crude approximation of the real situation. Clearly better is to express the fracture mechanical loading rate in terms of the stress intensity factor and not the strain. This leads to the use of the loading rate parameter, \dot{K}_I , in stead of the strain rate parameter, $\dot{\varepsilon}$.

The results show that the shape of the master curve is essentially unaffected by the loading rate. Thus it is not sensible to apply the Zener-Hollomon strain rate parameter directly to the fracture toughness, but to the transition temperature T_0 . In this case, the strain rate parameter can be expressed as

$$T_0 \cdot \ln \left(\frac{A'}{\dot{K}_I} \right) = \text{constant} \quad (6)$$

with T_0 in Kelvin degrees.

The “constant” in Eq. 6 can be expressed in terms of a reference loading rate transition temperature. A simple reference is constituted by T_{01} which refers to the quasistatic loading rate $\dot{K}_I = 1 \text{ MPa}\sqrt{\text{m}}\cdot\text{s}^{-1}$. Renaming $(\ln A')$ as (Γ) simplifies the resulting equation to

$$T_0 = \frac{T_{01} \cdot \Gamma}{\Gamma - \ln(\dot{K}_I)} \quad (7)$$

The master curve T_0 estimates were fitted with Eq. 7 in order to determine T_{01} and Γ for each data set. A typical result is presented in Fig. 4 for the material presented earlier.

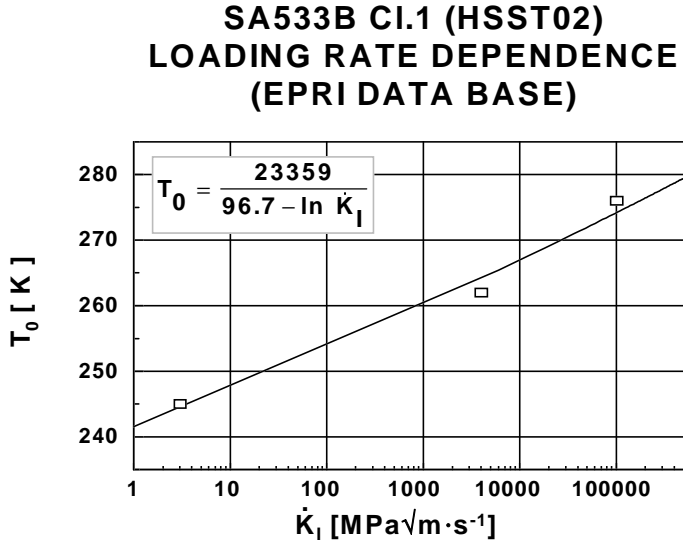


Figure 4. Loading rate dependence for material from Fig. 3.

The cases where the temperature shift was less than 15°C were not included in the subsequent analysis, because the uncertainty in T_0 causes the Γ estimate to be highly unreliable. Based on a simple pattern recognizing procedure, it was found that Γ can be successfully described by the yield strength and the static transition temperature and that their effect is essentially independent from each other. The best result was obtained with the equation presented in Fig. 5 and Eq. 8.

$$\Gamma_{\text{calc}} = 9.9 \cdot \exp \left\{ \left(\frac{T_{01}}{190} \right)^{1.66} + \left(\frac{R_{eL}}{722} \right)^{1.09} \right\} \quad (8)$$

The standard deviation of the equation is only 19.4%. The true standard deviation of the loading rate dependence expression is actually likely to be even less than 19.4%, because, it not only includes the inaccuracy of the correlation itself, but also the inaccuracy in the T_0 determination. Especially for large Γ

values and small loading rate differences (small temperature shifts), the quality of the data will affect the scatter considerably. The static transition temperatures used in the fitting of Eq. 8, all correspond to subzero temperatures, but limited results on irradiated materials indicate that an extrapolation to temperatures close to +100°C is appropriate.

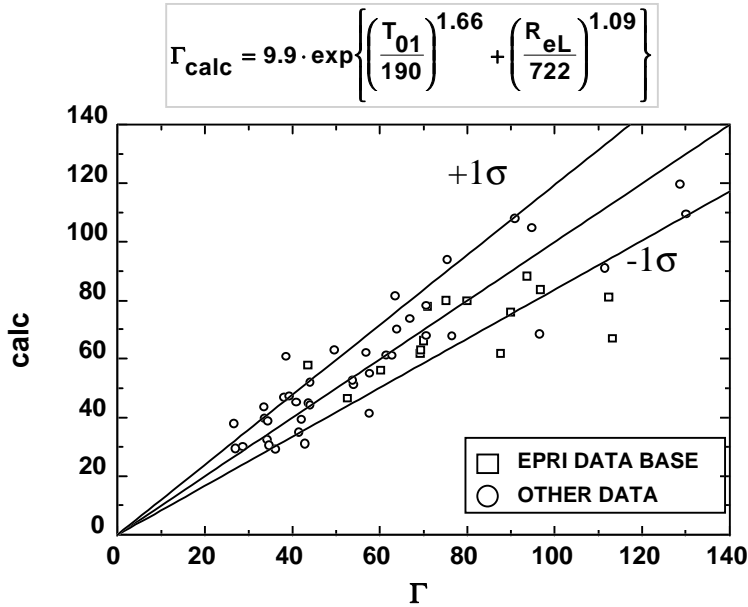


Figure 5. Material property dependence of strain rate parameter Γ . Boxes refer to EPRI pressure vessel material data base.

In terms of temperature shift, the accuracy is estimated to be of the order of $\pm 20\%$. The combination of Eqs. 7 and 8 is shown graphically in Fig. 6 for a dynamic loading rate of $1 \cdot 10^6 \text{ MPa}\sqrt{\text{m}}\cdot\text{s}^{-1}$. As expected, the shift increases when the yield strength or the quasistatic transition temperature decreases.

DYNAMIC LOADING RATE SHIFT OF MASTER CURVE TRANSITION TEMPERATURE

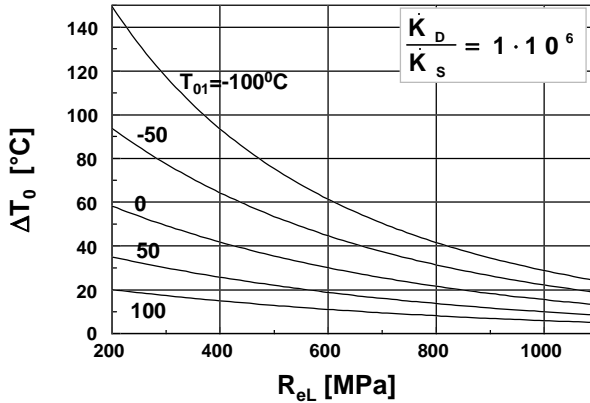


Figure 6. Transition temperature (T_0) shift due to severe dynamic loading rate as a function of yield strength and quasistatic transition temperature (T_{01}).

Based on the study it can be concluded that:

- the master curve concept is applicable also for dynamic loading rate fracture toughness data,
- based on the room temperature yield strength and the “static” fracture toughness transition temperature it is possible to describe the effect of loading rate with a $\pm 20\%$ accuracy,
- the loading rate dependence expression was developed for loading rates between $1 \cdot 10^{-1} - 1 \cdot 10^6 \text{ MPa}\sqrt{\text{m}\cdot\text{s}^{-1}}$, strength levels between 200 - 1000 MPa and static transition temperatures between -180 - 0°C, but extrapolation to higher transition temperatures appears appropriate.

4. Miniature fracture toughness testing

One fundamental issue in fracture mechanics testing has been the definition of a specimen size, which is required for a so-called valid measurement. Theoretically, the loss of constraint at the crack tip of a small specimen can be

calculated, but so far no universal way is available for transforming the measured fracture toughness to a standard parameter like K_{IC} . On the other hand, the application of constraint-based specimen size criteria leads to unrealistically large specimens, e.g., for use in reactor pressure vessel (RPV) surveillance.

According to the concept proposed by VTT, the critical value of the J-integral (J) at the onset of cleavage fracture is measured and transformed to the fracture toughness (K) which is then used in analysing the results statistically. The statistical cleavage fracture model used has been well verified for a large number of various structural steels and specimen geometries down to the 10*10*55 mm specimen size. For most structural steels the temperature dependence of fracture toughness can be described with only one material-specific parameter, i.e. the reference temperature T_0 (100 MPa \sqrt{m}).

The testing capabilities have now been developed further to smaller (ultra-small) specimens, i.e. three-point-bend specimens of size 3*4*27 mm, 5*5*27 mm, 5*10*55 mm and 10*10*55 mm. This development programme was completed in 1997 and it was followed by a test programme in order to demonstrate the restrictions and applicability of these specimens in fracture mechanics testing (Valo et al. 1997). The objectives of the programme for these ultra-small specimens were as follows:

- To assess the validity of fracture toughness data measured.
- To find approximate estimates for the measuring capacity of specimens.
- To clarify the need to have some kind of constraint correction.
- To verify the applicability of the cleavage fracture model.

As concerns testing and analysing data, there are no special restrictions or requirements in using ultra-small specimens. The test temperature should, however, be low enough to initiate cleavage fracture in the test. Due to the limited "measuring capacity", such small specimens are best suitable for characterising cleavage initiation. In the ductile area, the small ligament size does not allow sufficient crack growth in the specimen and practically only the blunting line can be measured experimentally.

Two pressure vessel steels were used in the study. The first was the ASTM Round Robin exercise material, i.e. plate HSST-3 of grade A533B. The second material was VVER 440 RPV steel 15Kh2MFA (VVER), a quenched and tempered Cr-Mo-V type forging. In addition, some fracture mechanics tests with ultra-small specimens had been conducted previously with a Cr-W-V fusion reactor structural steel.

The tests were performed following ASTM E 1152-87 whenever applicable. Load, load line displacement and crack opening displacement were measured when testing 5*10 mm, 10*10 mm and larger specimens. The crack length of a specimen was measured during the test with unloading compliance technique and a crack growth correction was applied. The tests were continued until cleavage fracture occurred or until a practical limit of the specimen displacement was reached. A simple crack growth correction (9) was made for the small specimens based on the initial and final crack lengths measured from the fracture surfaces. The amount of this correction was in general small.

$$J_{\text{corrected}} = J_0 \times \left(1 - \frac{0.5 \times \Delta a}{W - a_0}\right) \quad (9)$$

The specimens were prepared by an electric discharge machine. They were precracked with a PC controlled device under continuous monitoring of the load and crack length. In prefatiguing K_{max} of 10 - 12 MPa $\sqrt{\text{m}}$ and load ratio of $0 < R < 0.1$ were used. All specimens were side grooved to 2*10% after the prefatigue.

Most of the tests were performed in the transition range and ended at cleavage fracture, but some tests were also conducted in the temperature range of ductile fracture behaviour. The statistical size correction was made for the test results to convert them to the 25 mm specimen thickness. The combined (size-corrected) fracture toughness (K_{Jc}) data and corresponding fracture probability curves measured on the two materials are shown in Figs. 7 and 8.

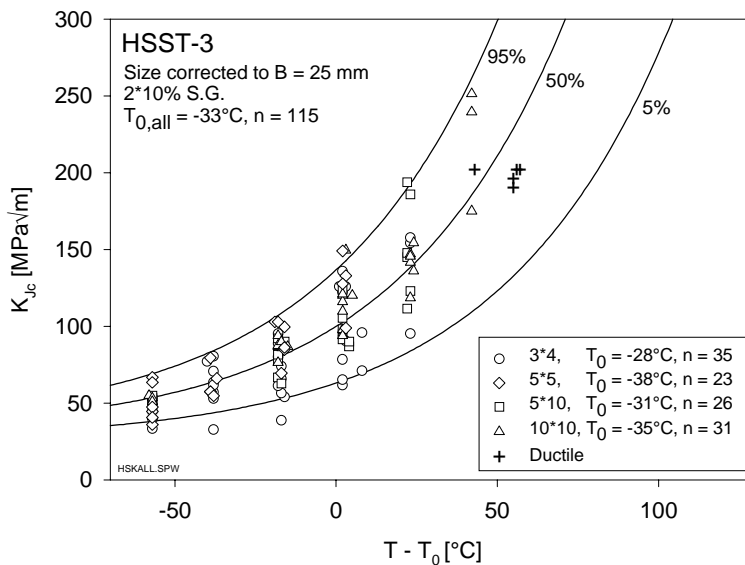


Figure 7. Fracture toughness K_{Jc} vs. temperature measured with HSST-3 specimens (size-corrected) and the fracture probability curves. T_0 ($100 \text{ MPa}\sqrt{\text{m}}$) = -33°C .

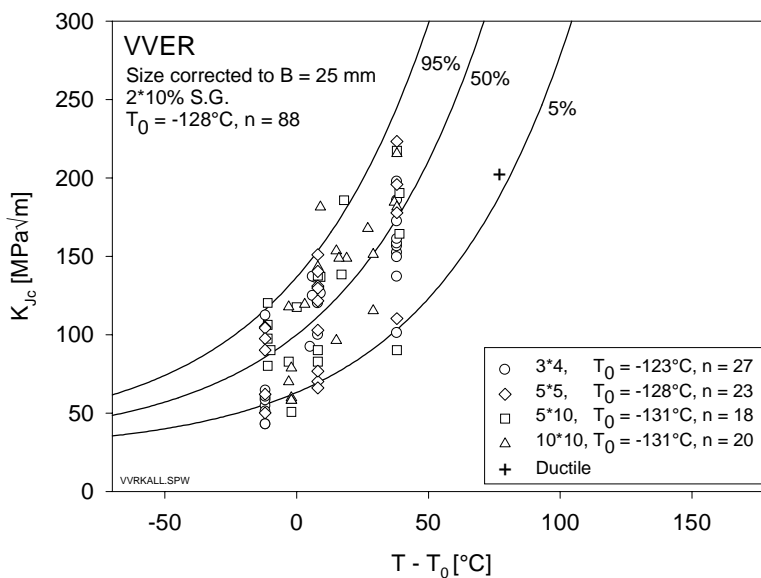


Figure 8. Fracture toughness K_{Jc} vs. temperature measured with VVER specimens (size-corrected) and the fracture probability curves. T_0 ($100 \text{ MPa}\sqrt{\text{m}}$) = -128°C .

In general, the results of the test programme were very promising, showing that the values of the $100 \text{ MPa}\sqrt{\text{m}}$ level reference temperature (T_0) determined even with 3×4 mm specimens are in good agreement with those of larger specimens. In addition, the statistical specimen size correction of the cleavage fracture model proved to be sufficient for all specimen types used, suggesting that no constraint correction is needed even with the 3×4 mm specimen.

Moreover, measurements made on the ductile area indicated that nearly similar fracture resistance curves can be obtained with 5×10 mm and larger specimens up to the J-level of 500 kN/m . Beyond this toughness level, curves measured with small specimens started to deviate from the curve of the larger specimen (Figs. 9 and 10). The proportional crack growth, i.e. the ratio $\Delta a/\text{ligament}$, was a parameter limiting the measuring capacity of a specimen in the area of ductile tearing.

The study indicated that:

- Small three-point-bend specimens (3×4 and 5×5 and 5×10 mm) are applicable in characterizing the fracture toughness in the transition region by applying the statistical cleavage fracture model of VTT, employing only the statistical specimen size correction included in the model.
- Microstructural factors do not cause excessive scatter in fracture toughness data measured even with the smallest applied specimen (3×4 mm).
- The 5×10 mm three-point-bend specimens give fracture resistance curves consistent with those of larger specimens (10×10 mm) up to J values of 400 kN/m on the steels used.

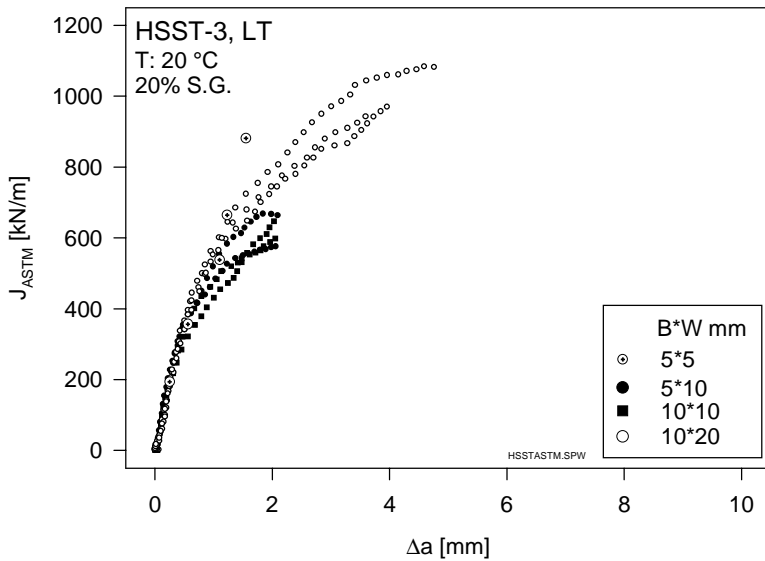


Figure 9. Fracture toughness vs. crack growth measured with HSST-3 specimens.

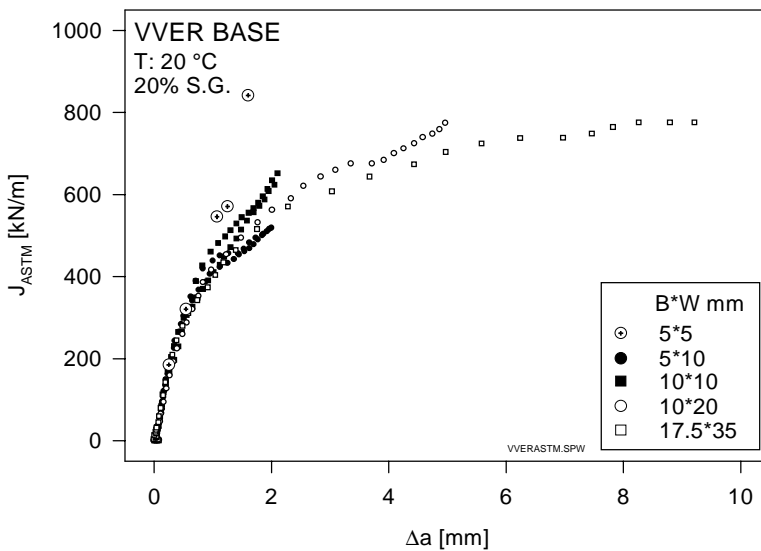


Figure 10. Fracture toughness vs. crack growth measured with VVER specimens.

5. Modified crack-arrest fracture toughness determination

A novel feature has been developed for the procedure of crack-arrest fracture toughness determination according to the standard ASTM E 1221-88, to overcome difficulties encountered in weld preparation for cleavage crack initiation in the higher transition temperature range of a bainitic pressure vessel steel.

The crack initiation process zone was produced by thermal treatment to a controlled brittle state. An electron-beam welding machine was used to accurate and reproducible quenching of the notch root. No welding was applied. Some specimens were additionally given a reversed bending treatment to homogenise the residual stresses. As a result, the control of the initiation stress intensity levels was greatly facilitated. An additional deflection restraining compression to the specimen sides was optionally employed to limit crack opening and thus to arrest the cleavage crack within acceptable limits.

With this 'restraint' method valid test results were obtained at temperatures corresponding to the upper transition temperature region of cleavage cracking. Linear finite-element analyses were conducted to determine the effect of the specimen side compression on stress intensity factor at cleavage crack initiation and arrest (K_Q , K_a).

Also, a set of instrumented Charpy tests were conducted to determine the crack arrest load as a function of test temperature for comparison to other similar materials.

The restrain method together with the developed notch root treatment provides good conditions for the crack-arrest fracture toughness determination. Results were obtained at higher temperatures than is possible, strictly following the standard procedure. This finding has been made both with a russian 15KH2MFA pressure vessel steel and previously with a tool steel. The results have been verified by comparing determined transition temperature with other, similar type of steels, and the validity has been found to be good.

Table 1. Test results in testing order. Test either a standard test or with side-compression (restraint). Heating time refers to time under EB-heating. K_Q is the stress intensity factor at crack initiation and K_a is the stress intensity factor at crack arrest.

Test number	Test temperature (°C)	Standard test / Compression load (kN)	Heating time (min)	K_Q (MPa√m)	K_a (MPa√m)
1	+22	300	20	235	110⁴⁾
2	+40	300	25	225	160
3	+40	100	25	210	- ²⁾
4	+60	0	35	- ¹⁾	- ²⁾
5	+40	Standard test	25	235	101⁴⁾
6	+60	Standard test	30	226	- ²⁾
7	+50	Standard test	25	250	197
8	+50	Standard test ³⁾	25	207	- ²⁾
9	+22	Standard test	30	192	92⁴⁾
10	+40	Standard test	30	176	- ²⁾
11	+50	Standard test	25	237	126⁴⁾
12	+60	Standard test	25	240	211
13	+80	Standard test ³⁾	25	367	- ²⁾
14	+70	Standard test ³⁾	30	- ¹⁾	-
15	+50	Standard test ³⁾	30	191	- ²⁾

1) No one clear incidence of crack initiation. Several acoustic indications of small stepwise crack growth.

2) Crack propagation principally in quenched region, not in virgin material. K_a -value meaningless.

3) No pre-compression of the specimen.

4) A valid result according to the ASTM standard, (K_{Ia}).

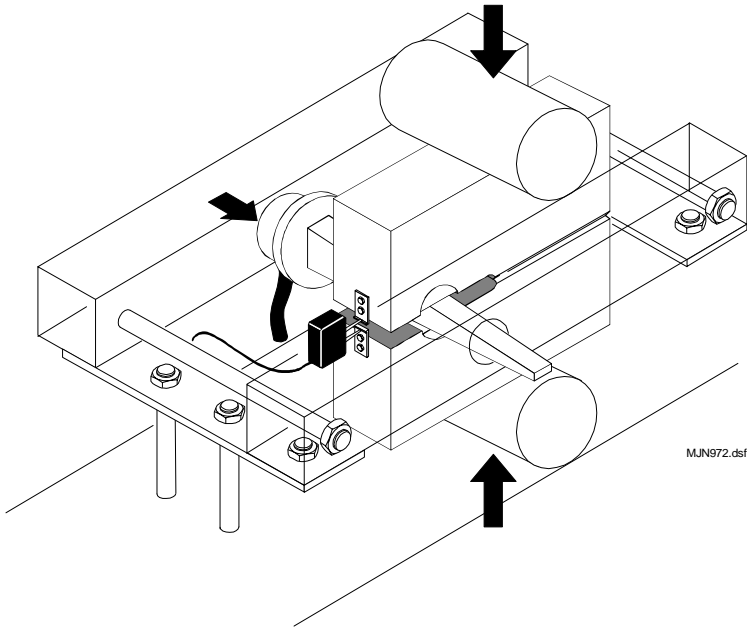


Figure 11. The schematic test arrangement.

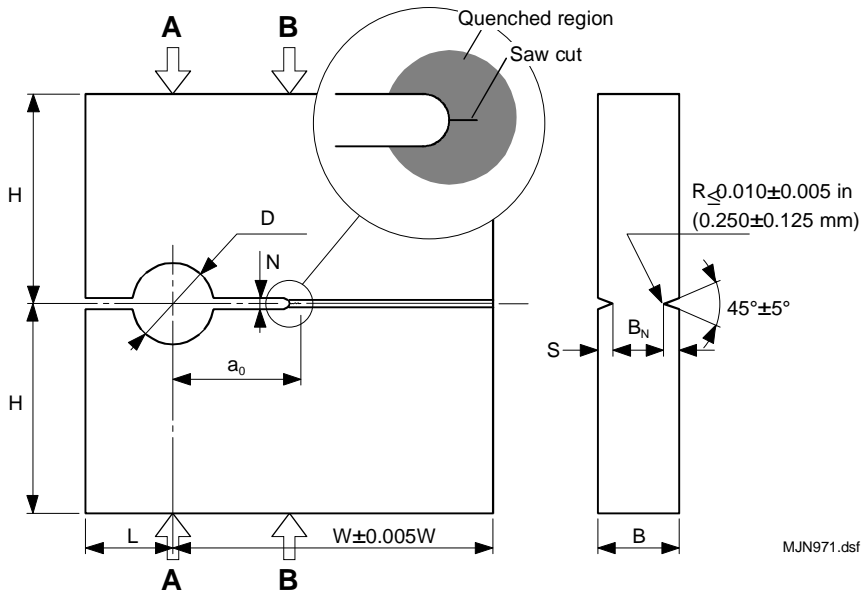


Figure 12. The specimen configuration.

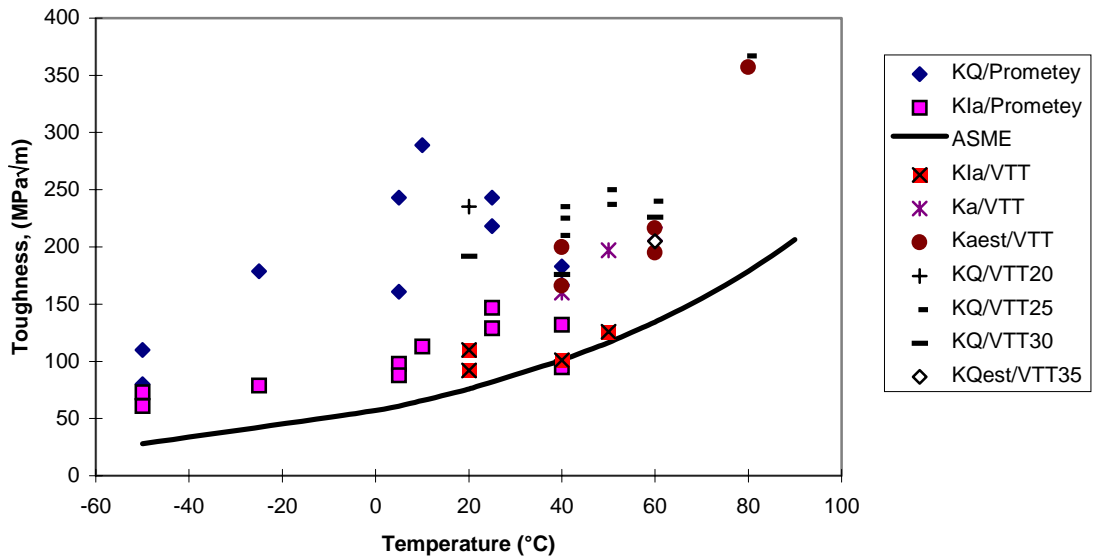


Figure 13. The results of VTT and ‘Crim’ Prometey. K_Q refers to crack initiation fracture toughness, while K_a and K_{Ja} refer to non-valid and valid crack-arrest fracture toughness. Numbers 20-35 refer to minutes under EB-heating. ASME lower bound curve is presented for reference.

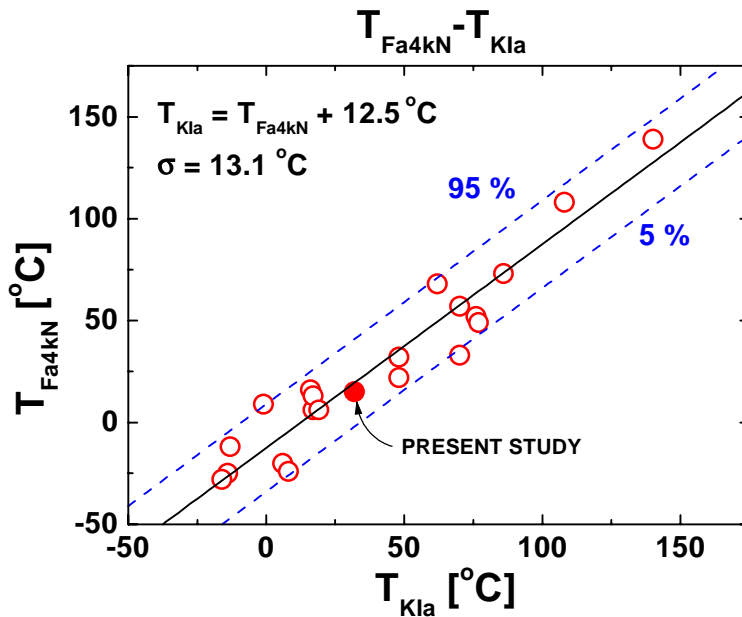


Figure 14. K_{Jd} vs. K_{Ja} correlation for previously investigated materials and present 15KH2MFA steel.

6. Conclusions

From above, it can be concluded that the research has been highly successful. However, due to the empirical nature of some of the parameters, more work is still needed before all the present findings are suitable for codification.

7. Acknowledgements

The reported work was part of the Finnish Research Programme on the Structural Integrity of Nuclear Power Plants 1995 - 1998, subproject RAVA1 on Material Degradation in Reactor Environment. The work for Chapter 2 was completed in 1995, Chapters 3-4 in 1996 and Chapters 5-6 in 1998.

Co-operation with Rainer Rantala and Matti Ojanen from the Radiation and Nuclear Safety Authority, STUK, Ralf Ahlstrand and Jyrki Kohopää from IVO Ltd. together with Matti Valo, Klaus Rahka and many other colleagues is gratefully acknowledged.

References

- ASTM E 1921-1997. Test method for the determination of reference temperature, T_0 , for ferritic steels in the transition range. ASTM Books of Standards.
- Rintamaa, R. & Sarkimo, M. (Eds.). 1995. RATU - Nuclear power plant structural safety research programme 1990 - 1994, Final report. Helsinki: Ministry of Trade and Industry, 166 p. (Ministry of Trade and Industry Studies and Reports 135/1995). ISSN 1236-2352; ISBN 951-739-116-1
- Rintamaa, R., von Estorff, U., Mc Garry, D., Hurst, R. C. & Wintle, J. B. 1997. Pre-test material characterization of the NESC spinning cylinder (ICONE5-2279). Proc. of ICON 5: 5th Int. Conference on Nuclear Engineering, Nice, France, May 26 - 30.

Wallin, K. & Rintamaa, R. 1995. Re-evaluation of the thermal shock experiment results based on the VTT approach for statistical treatment of fracture toughness data. 21. MPA-Seminar, Approaches to Lifetime Extension of Nuclear Power Plants, Vol. 1. Pp. 2.1 - 2.18.

Wallin, K. 1997. Effect of strain rate on the fracture toughness reference temperature T_0 for ferritic steels. In: Recent Advances in Fracture, R. K. Mahidhara, A. B. Geltmacher, P. Matic and K. Sadananda (Eds.). The Minerals, Metals & Materials Society. Pp. 171 - 182.

Valo, M., Planman, T. & Wallin, K. 1997. The applicability of small and ultra-small fracture toughness specimens for material characterization. In: Small Specimen Test Techniques, ASTM STP 1329, W.R. Corwin, S.T. Rosinski, and E. van Walle, (Eds.). Philadelphia: American Society for Testing and Materials. (To be published).

(See Appendix 1 for a comprehensive listing of publications)

Fracture analysis of ductile elastic-plastic materials under mixed-mode I-II loading

Anssi Laukkanen
VTT Manufacturing Technology
Espoo, Finland

Abstract

In order to evaluate the mixed-mode fracture behavior of elastic-plastic metallic materials, experimental tests and numerical calculations were carried out. Since the transition of fracture toughness between opening and in-plane shear modes with ductile materials is a question of controversy, single-edge notched bend (SENB) specimens were subjected to asymmetric four-point bending (ASFPB) to provide various mode portions using four materials: A533B pressure vessel steel, F82H ferritic stainless steel, sensitized AISI 304 austenitic stainless steel and CuAl25 copper alloy. Fracture resistance curves were determined and fractographical studies performed. Numerical studies focused on determining the J-integral and stress intensity factor (SIF) solutions for the experimental programme and the Gurson-Tvergaard constitutive model was used to simulate continuum features of the fracture process. The results demonstrate that mode II fracture toughness of ductile metallic materials can be significantly lower than mode I fracture toughness. Studies of the micromechanical aspects of fracture demonstrate the factors and variables responsible for the behavior noted in this investigation.

1. Introduction

Mixed-mode fracture research has traditionally dealt with brittle materials behaving in a linear-elastic manner. The results in case of brittle fracture (see e.g. [1-3]) have demonstrated that the mode II fracture toughness is usually close to or larger than the mode I fracture toughness, indicating that the mode I fracture toughness is a conservative estimate of the fracture resistance of the material. When considering ductile materials and their mixed-mode fracture

toughness, the results are not as unequivocal. Different researchers with different materials as well as experimental setups have obtained opposite and controversial results. Some researchers, e.g. [4-5], have found that in mode II fracture toughness is higher than in mode I, but other researchers have obtained inverse results suggesting that in mode II fracture toughness is lower than in mode I, e.g. [6-7]. The area of elastic-plastic mixed-mode fracture toughness suffers also from lack of studies, meaning that relatively few studies have been published. One reason for this is the difficulty associated with controlling nonlinear elastic-plastic two-dimensional situations, both in numerical simulations and in experimental work.

The basic idea and background for the question why mixed-mode fracture and fracture toughness can not be taken as conservative with respect to mode I stems from the basic thinking in mode I, which typically neglects differences in fracture micromechanisms. Since it appears that the mode II brittle fracture toughness is higher than the mode I toughness, we can think that mode II ductile fracture toughness would be higher than mode I, with the same simple analogy. This reasoning and others like it, on the other hand, lacks the information regarding the differences in fracture micromechanisms and, thus, is not correct. The right approach for brittle mixed-mode and mode II fracture is obtained when starting from the simplified result that brittle fracture is controlled by stresses, usually the hydrostatic stress or the first principal stress ahead the crack. When introducing a shear component to the crack loading, this decreases the value of hydrostatic tension and as a consequence causes an increase in macroscopic fracture toughness. But when considering ductile fracture, we are faced with a situation where the fracture micromechanisms are mainly controlled by strains. When introducing a shear-component to the crack loading we at the same time increase the values of strain when considering J_2 -plasticity. Because of this general and simple result, the macroscopic fracture toughness should be lower in ductile fracture and the situation has a principal difference compared to brittle material behavior.

Experimental work in the field of mixed-mode fracture has generally been quite extensive for the past few decades. Yet, several issues still remain open, and when considering ductile materials behaving in an elastic-plastic manner the results currently available are pretty scarce. Generally, several studies with ductile materials suffer from weaknesses associated with analysis of results,

meaning that very few studies have focused on characterizing the mixed-mode fracture toughness in terms of J-integral or other associated parameters. Concentrating on studies related to ductile behavior of metallic materials, Maccagno and Knott [4] used the asymmetric four-point bend (ASFPB) setup in determining the fracture toughness transition of HY130 pressure vessel steel. The study recorded the modes of fracture as well as the ductile fracture transition. The transition in micromechanical terms refers to a shear-type of crack nucleation in comparison to more typical, mode I fibrous crack extension. In a revised study Bhattacharjee and Knott [8] focused on micromechanical changes associated with different degrees of shear loading. Both studies suffered from inadequate analysis of results, i.e. the results were mostly presented in terms of load-displacement curves. Shi et al. [5] and Shi and Zhou [9] examined the fracture toughness of HT100, HT80 and A36 steels in modes I and II. They found differences in micromechanical features, as well as that in their test series the fracture toughness in mode II was higher than in mode I. Several studies suffer from uncertainties related to experimental setups (instrumentation, friction, measurement of crack length) in addition to the other weakness, analysis of results.

Numerical analysis of mixed-mode I-II crack behavior has mainly dealt with using the Gurson-Tvergaard constitutive model in simulating the effects of shear-stresses on crack nucleation behavior, if we neglect the numerous driving force solutions for different specimen geometries. Tohgo et al. [7] used the original Gurson's model and were able to demonstrate the competition between two different nucleation processes depending on the degree of shear-loading, i.e. crack nucleation from the blunted side of the notch and from the sharpened tip. Aoki et al. [10] continued along the same lines and focused on the crack tip deformation behavior with different mode proportions. Ghosal and Narasimhan [11, 12] focused on determining the fields of equivalent plastic strain, hydrostatic tension and void volume fraction with the Gurson-Tvergaard model including nucleation and accelerated void growth after certain critical void volume fraction. They found the same results as before but most of all, they were able to present their results with better correspondence to micromechanics of fracture, priming their consideration on typical mode I type of fracture process consisting of nucleation, growth and coalescence of voids. Ghosal and Narasimhan [11, 12] used different initial void populations, mainly simulating a situation where a large void existed ahead of the crack and the ligament failed

according to porous failure criterion of the Gurson-Tvergaard model. They were able to determine the simulated fracture nucleation toughness envelope between modes I and II, and found that when the nucleation is taken to be strain controlled, the fracture toughness had a decreasing value when moving towards mode II, but near mode II it had again a rising trend due to transition to pure shear fracture. Mode II fracture toughness as given by their simulations was lower than mode I fracture toughness.

This work focuses on determining the micromechanical aspects of mixed-mode fracture, the transition of fracture toughness between modes I and II and using numerical simulations in interpreting different aspects of the fracture process. Elastic-plastic ductile materials were studied, because earlier work has provided some controversial results and in addition the background in form of micromechanical features remains quite unknown.

2. Numerical simulations

2.1 SIF and J-integral solutions

Linear-elastic two-dimensional plane strain finite element (FE) modeling was utilized in order to determine the SIF-solutions for the ASFPB-configuration. When comparing SIF-solutions available in the literature, large differences were noted (e.g. [2] contra [13]) and since the range of applicability of the results was somewhat unclear, it was found that specific analyses for the current work were required. The ASFPB-setup was chosen because of the simplicity of a bend-type specimen and is presented with its characteristic dimensions in Fig. 1.

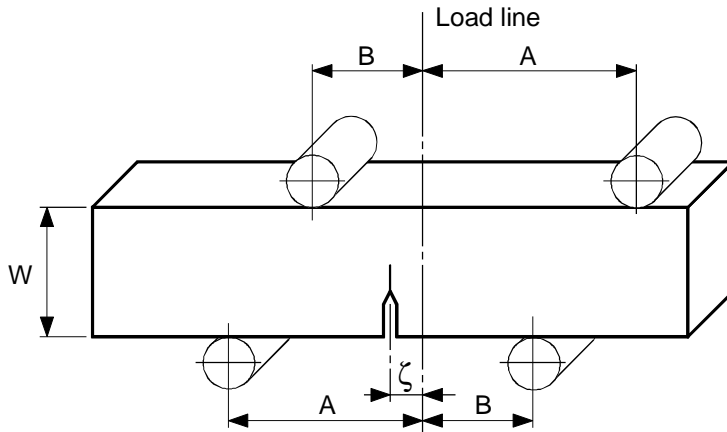
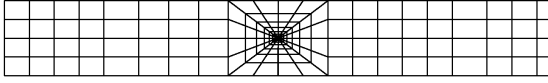
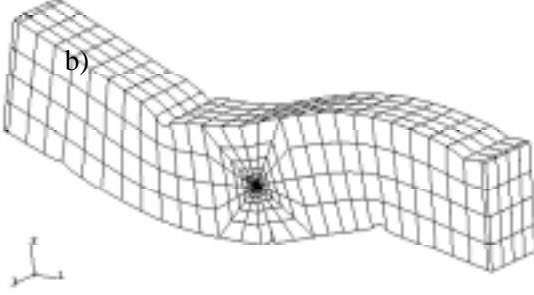


Figure 1. Asymmetric four-point bend arrangement for single edge notched bend specimens with characteristic dimensions.

The variable ζ controls mode mixity, i.e. $\zeta = 0$ refers to mode II loading and $\zeta = \infty$ to mode I. Because measures A and B presented in Fig. 1 do not have any influence on the mode mixity, they were chosen based on suitability for experimental purposes. J-integral was calculated following the domain integral routine presented by Li et al. [14]. Because the mode mixity under different loading conditions is of interest, the J-integral must be partitioned to mode I and II contributions. This was achieved by using the filtering method presented by Mattheck and Moldenhauer [15]. The idea of the filtering technique consists of applying suitable constraint equations to reduce the situation back to either mode I or mode II loading. This is achieved with restraining the displacements either symmetrically or antymmetrically, depending on whether mode I or mode II contribution is to be filtered from the total J-integral. A typical FE-mesh used in the calculations is presented in Fig. 2a. Three-dimensional calculations were performed to determine the variations of equivalent and hydrostatic stresses in the thickness direction with different values of ζ , and a deformed mesh from these calculations is presented in Fig. 2b.



a)



b)

Figure 2. Finite element meshes; (a) two-dimensional mesh and (b) deformed three-dimensional mesh.

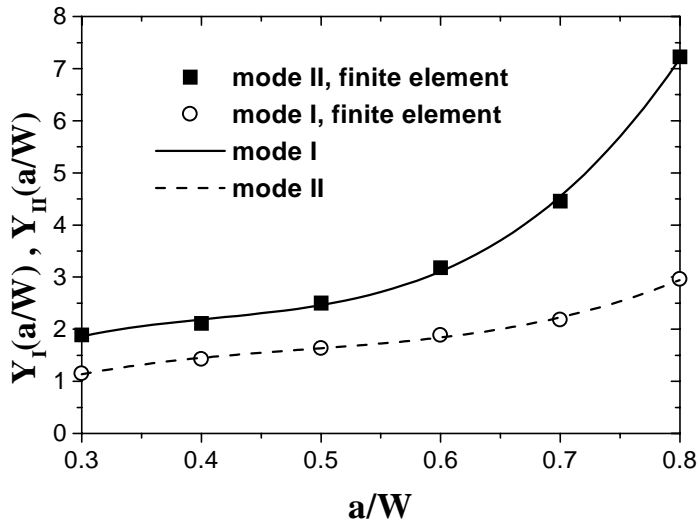
In order to produce the results as a function of a single parameter depending on proportions of mode I and mode II loading, an equivalent mode angle is presented:

$$\beta_{eq} = \tan^{-1}\left(\frac{K_{II}}{K_I}\right), \quad (1)$$

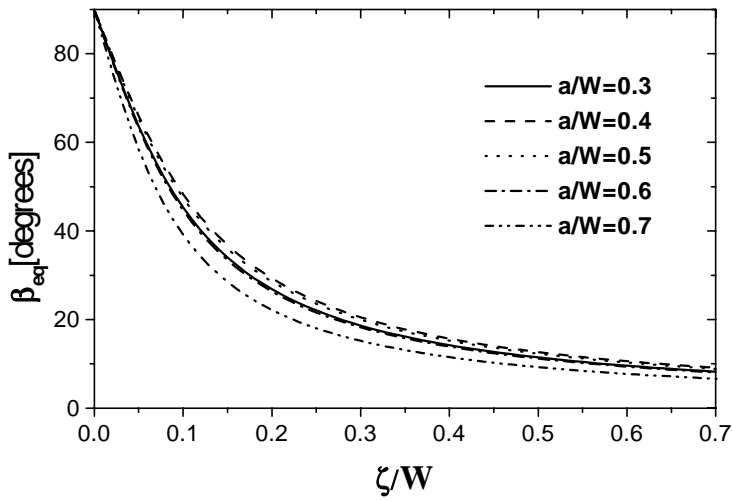
where K_i denote the corresponding SIFs. The results of the linear-elastic calculations were fitted to polynomial form and are presented in Fig. 3a. The equivalent mode angle of eq. (1) can be given for the ASFPB configuration as

$$\beta_{eq} = \tan^{-1}\left(\frac{WY_{II}\left(\frac{a}{W}\right)}{6\zeta Y_I\left(\frac{a}{W}\right)}\right), \quad (2)$$

which is a necessity in controlling the experimental tests and is presented with different values of a/W and ζ in Fig. 3b.



a)



b)

Figure 3. Non-dimensional stress intensity factor results; (a) correction functions and (b) equivalent mode angle.

The J-integral solutions were determined according to the formalism presented by Rice et al. [16]. The η_i -factors for modes I and II were determined based on an ideal-plastic material model and are presented in Fig. 4.

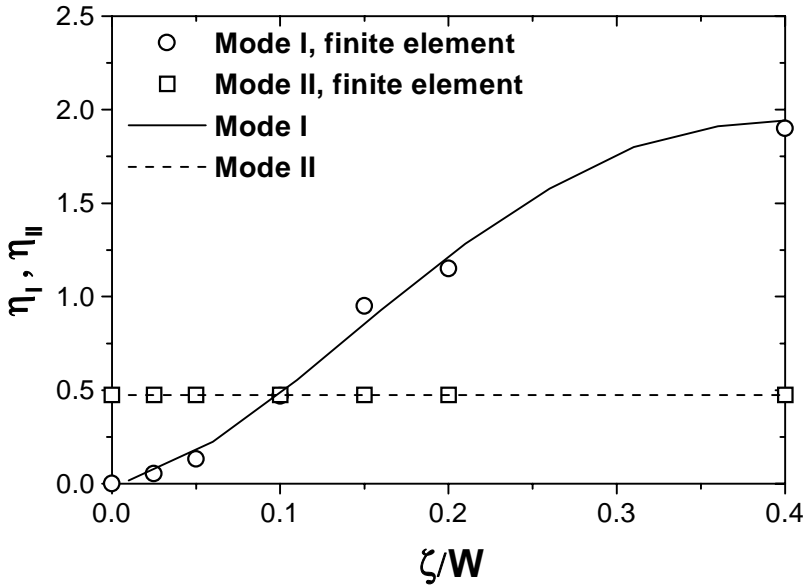


Figure 4. η_i -solutions for J-integral determination.

The calculations required great concern and exact interpretation of results, because of the two-dimensionality of the deformation field. Since the behavior under mixed-mode loading is neither symmetric nor antisymmetric, effects such as friction must be considered when the solution is compared to realistic behavior. These additional boundary conditions need to be examined during calculations to form physically sound solutions. The assumptions made regarding the ideal-plastic material behavior were verified using incremental plasticity analysis and the assumptions were found valid within the range of observation. Three-dimensional results presented the uniform decay in the state of hydrostatic tension ahead the crack front while the deviatoric stress state remained in proportion nearly constant at a fixed observation point ahead the crack tip.

2.2 Simulations with the Gurson-Tvergaard constitutive model

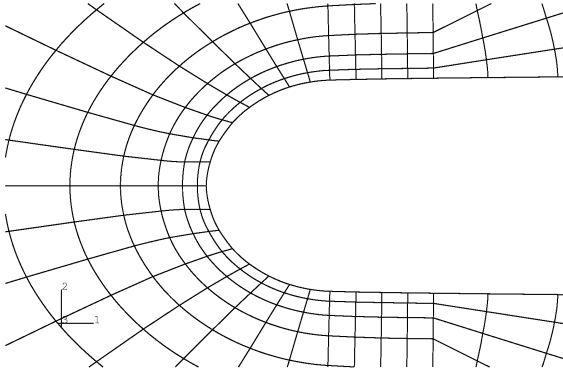
The Gurson-Tvergaard model was used to simulate the ductile fracture process in order to provide numerical background for describing the micromechanical features of the fracture process. The results presented here are a part of a wider modeling effort related to numerical modeling of the ductile fracture process, but only some of the results important for this study will be presented here. It is to be remembered that the Gurson-Tvergaard model does have severe limitations with respect to practical use even in mode I, and in mixed-mode and mode II these features surface even more vividly. The theoretical background is quite lengthy and because several good presentations already exist, reference to publications [17, 18], where the features of the model are under closer examination, is provided. The results presented here pertain to pure mode I and mode II. Because the changes associated with the continuum fields under observation are continuous and monotonic, we can assess the general trends without requiring to present a huge number of contour plots.

The simulations were performed with a two-dimensional boundary-layer model. The matrix material followed J_2 -theory of plasticity and finite strains. The Gurson-Tvergaard model correction constants were given values $q_1 = 1.5$, $q_2 = 1$ and $q_3 = q_1^2$. In these calculations we will consider a situation where no initial void distribution nor density is given. Nucleation is taken to be strain controlled according to the presentation of Chu and Needleman [19]:

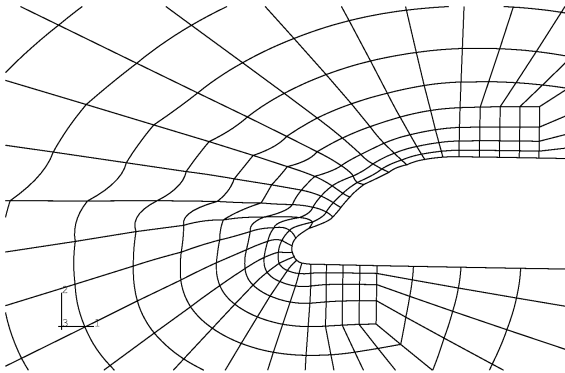
$$\dot{f}_{\text{nucl}} = A \dot{\epsilon}_m^{\text{pl}} = \frac{f_N}{s_N \sqrt{2\pi}} e^{\left[-\frac{1}{2} \left(\frac{\epsilon_m^{\text{pl}} - \epsilon_N}{s_N} \right)^2 \right]} \dot{\epsilon}_m^{\text{pl}}, \quad (3)$$

where $\dot{\epsilon}_m^{\text{pl}}$ is the equivalent plastic strain rate. The parameters are chosen followingly: $f_N = 0.1$, $s_N = 0.1$ and $\epsilon_N = 0.3$. The selection of parameters was performed according to traditional values used in literature, because within the contents of this presentation the features we are looking for are not dependent on the numerical values of the parameters as long as they are within reasonable limits. The results of crack tip deformation, distributions of

hydrostatic stress, equivalent plastic strain and void volume fraction are presented in Figs. 5 and 6. Fig. 5 demonstrates that in mode I the crack tip experiences a typical opening deformation pattern, while in mode II the crack tip sharpens due to extensive shearing. At the same time from Fig. 6 we note that the maximum value of hydrostatic tension decreases and rotates clockwise, while the values of equivalent plastic strain increase tremendously and localize on the sharpened tip. A formation of a slip-band of intense shearing is visible from mode II calculations. When observing the damage formation with the void volume fraction, a transition in fracture mechanisms can be found. In near mode I situations and thereof the crack tip deforms in a way that the other side is blunted while the other tip sharpens. At near mode I the damage formation is strongest at the blunted side, due to nucleation of voids as a consequence of plasticity and growth of existing voids because of hydrostatic tension, indicating crack nucleation from the blunted side. When approaching mode II and in mode II, the damage formation is more rapid in the sharpening tip due to an increase in plastic straining and a decrease in hydrostatic tension on the blunted side, causing the crack to nucleate from the sharpened tip. These features will be considered in more detail in the discussion section.

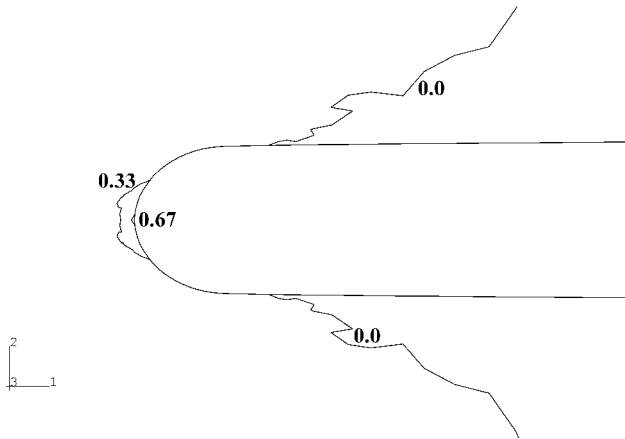


a)

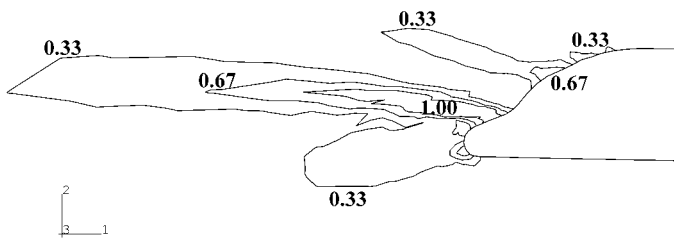


b)

Figure 5. Results of numerical simulations with the Gurson-Tvergaard model. Crack tip deformation under (a) mode I and (b) mode II.

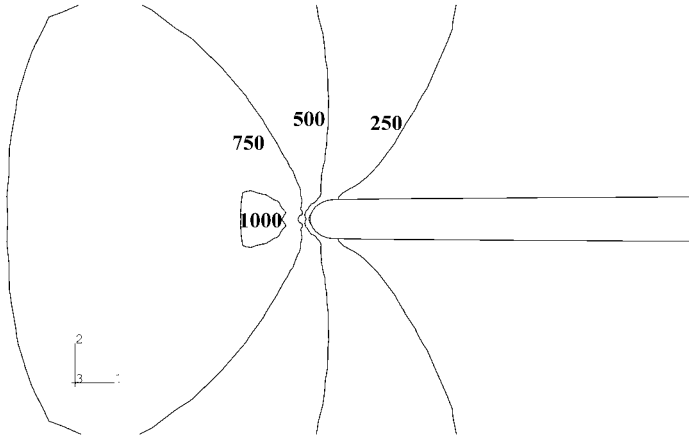


a)

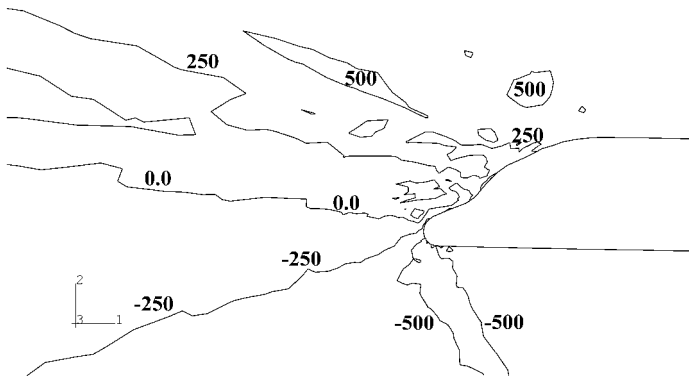


b)

Figure 6. Contours of equivalent plastic strain under (a) mode I and (b) mode II; Contours of hydrostatic tension (MPa) under (c) mode I and (d) mode II; Contours of void volume fraction under (e) mode I and (f) mode II; All results with equivalent loading.

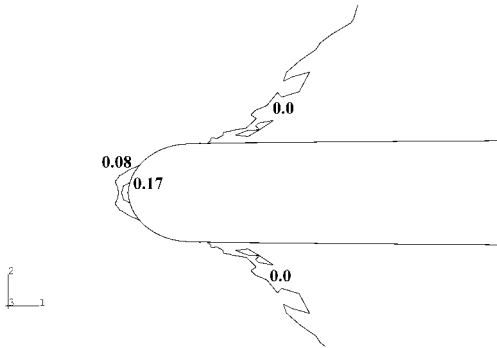


c)

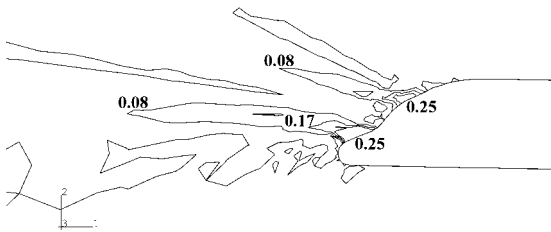


d)

Figure 6. Continues.



e)



f)

Figure 6. Continues.

3. Experimental work

3.1 Materials and specimens

The configuration chosen for the experimental tests was the ASFPB-setup first presented by Gao [3], where the equivalent mode angle can be adjusted continuously starting from mode II. The SENB-specimens were either Charpy-size, or following the current mode I fracture toughness testing standards, sizes with cross-sections of $10 \times 20 \text{ mm}^2$ (thickness \times width) or $15 \times 30 \text{ mm}^2$. Orientation was for A533B, F82H and AISI 304 specimens T-L and for CuAl25 specimens L-T. The basic mechanical properties of the materials tested are presented in Table 1.

Table 1. Properties of experimental materials.

Material	Yield strength MPa	Tensile strength MPa	Fracture toughness (I), kN/m
F82H	530	640	310
A533B	505	670	540
AISI 304	250	600	350
CuAl25	315	428	105

Experiments were performed under displacement control measuring the global force-displacement curve, which decomposes to the strain energy of the loading rolls depending on the choice of A and B. Instrumentation was found more accurate and less prone to rotational errors in this method of measurement when compared to measuring the local displacement variables. PD-method was utilized following current procedures provided by several mode I fracture resistance testing standards.

Several different experimental configurations for mixed-mode testing have been presented and a general consensus regarding the most suitable choice has not been achieved. The deficiencies of different setups can be divided in three categories: instrumentation, measurement of crack growth and friction.

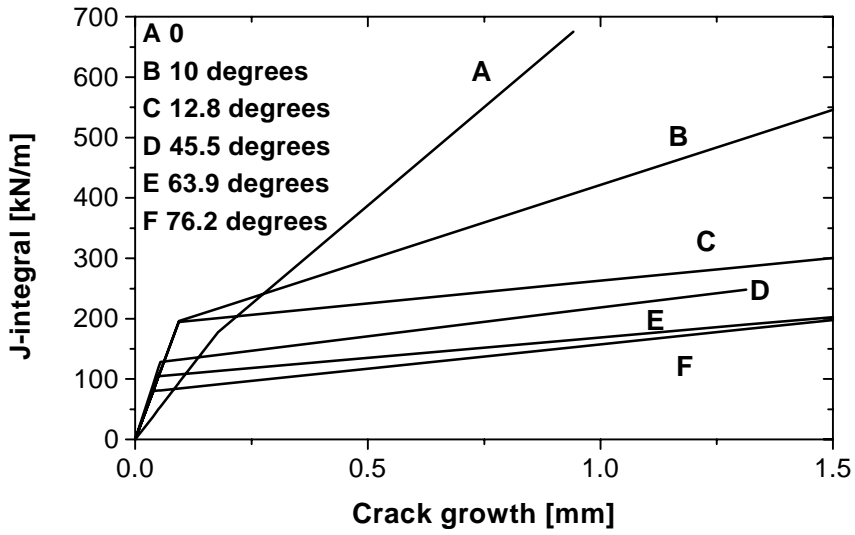
Instrumentation deficiencies are related to the fact that mechanical gages etc. are very prone to errors when the deformation field is two-dimensional, meaning that different types of corrections are needed, and on the other hand, the correct measurement of the displacement variables under mixed-mode loading is under question. Additional difficulty in instrumentation is a consequence of large displacements, which are often encountered in mixed-mode testing. Measurement of crack growth is another problem. Compliance solutions do not exist and even so, the stiffness of the specimen will be dependent on the mode angle and makes the arrangement susceptible to additional errors. Potential drop (PD) measurements can be affected by the shearing of the crack front during loading, resulting in more significant geometry changes than in mode I testing, and cause the voltage signal to have a drop of unknown quantity related to current deformation state. Multiple specimen methods are naturally available, but demand many specimens. In this work the PD-method was used with partial success. The third problem is friction, because, when mode II is approached it is most likely that the crack faces will experience additional contact, making the results depend on the current crack length with an additional frictional component doing the work as well. An easy way around the problems associated with friction is to avoid testing in mode II and to perform the tests near mode II where the crack faces separate due to a small opening component.

3.2 Fracture resistance curves

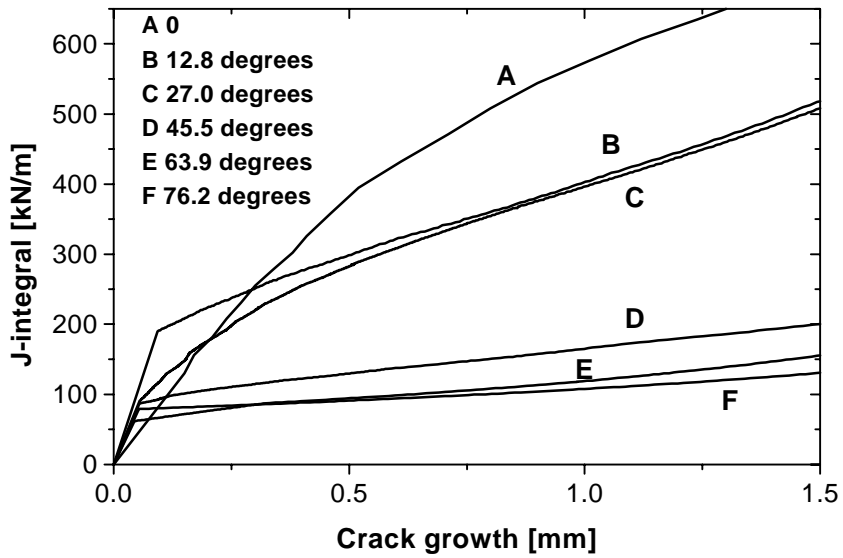
Fracture resistance curves were determined for all materials as a function of the equivalent mode angle and are presented in Fig. 7. In Fig. 7a the resistance curves for F82H are shown, which demonstrate a trend of decreasing fracture resistance. In near mode II (near 90°) the curves are very flat, i.e. the tearing modulus is very small. Similar results are presented for A533B in Fig. 7b, while in Fig. 7c the results of AISI 304 present even a more dramatic decrease of fracture toughness, which will be referred to microstructural features in the discussion part of the work. The fracture resistance curves of CuAl25 alloy indicate a drop in fracture resistance at a certain discrete mode portion rather than a continuous drop, as presented in Fig. 7d. This effect is most likely related to microstructural orientation effects and anisotropy and is a subject of further studies.

3.3 Fractographical results

The fracture surfaces were investigated with a scanning electron microscope (SEM) and energy dispersive x-ray (EDS) analyses were used to study the crack formation micromechanics. The results were basically similar in all materials studied with some different details related to microstructural factors, which will be referred to later. In Fig. 8 the fracture surfaces of F82H steel in mode I and with a modal angle of 76.2° are presented. The fracture surface of Fig. 8a is a typical surface of mode I dimple fracture. Fig. 8b presents the morphology of a fracture surface near mode II. The differences between the fracture surfaces are clear: the near mode II surface is usually characterized as being macroscopically flat, which is not the case in microscopical terms. The morphology of the fracture surface formed at mode angle of 76.2° contains areas of extremely small dimples formed around second phase particles and the areas are connected to each other through deviations in the macroscopic fracture plane, which can be characterized as asperities. The dimple size decreases and becomes more sheared consistently when moving from mode I towards mode II. The dimple size experiences a large drop at the beginning stages of the mode locus.

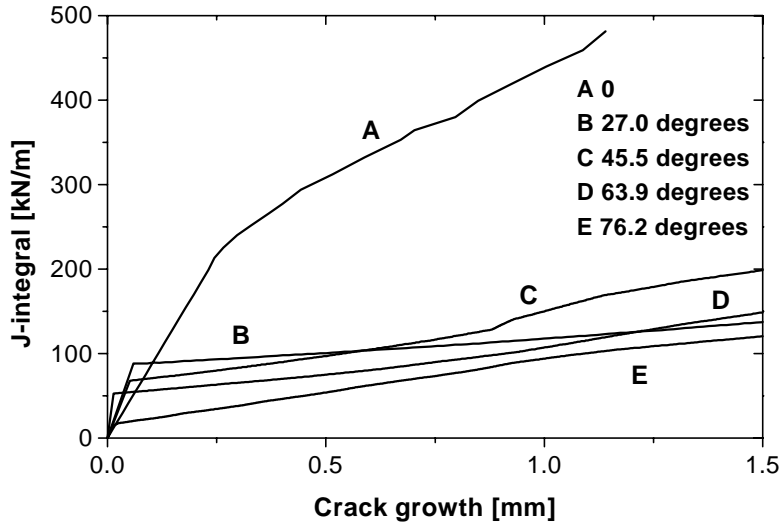


a)

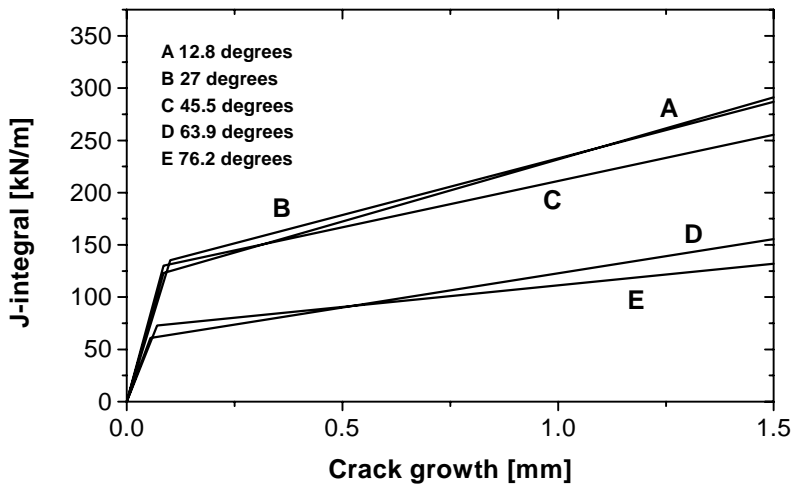


b)

Figure 7. Fracture resistance curves as a function of the equivalent mode angle. (a) F82H, (b) A533B, (c) AISI 304 and (d) CuAl25.

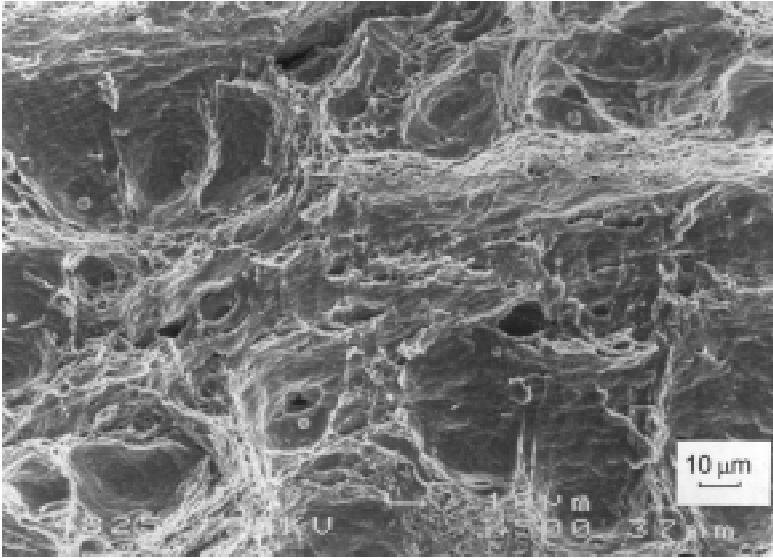


c)

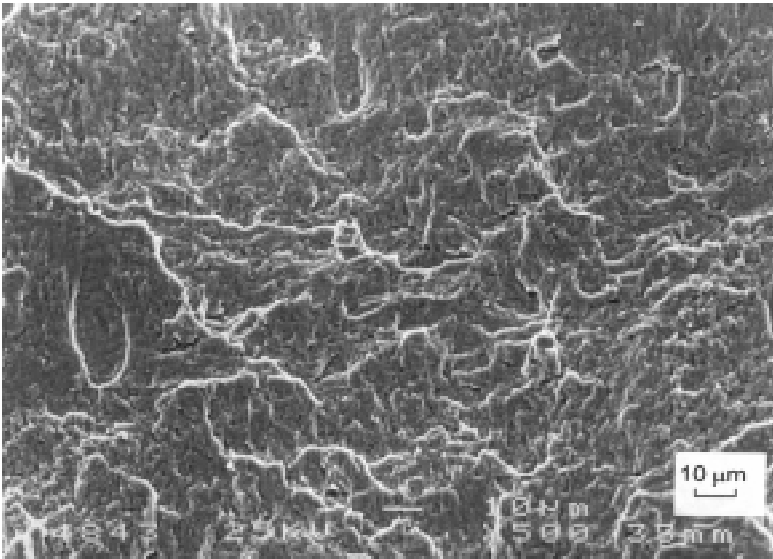


d)

Figure 7. Continues.



a)



b)

Figure 8. Fracture surface morphology of F82H steel under (a) mode I and (b) equivalent mode angle of 76.2° .

3.4 Fracture nucleation angles and modes

Crack nucleation angles followed similar trends with all materials with respect to the equivalent mode angle. In Fig. 9 the nucleation angles are presented as a function of β_{eq} for F82H steel. The difference compared to typical linear elastic results is drastic. Based on linear-elastic treatments it has generally been accepted that the crack nucleation angle in mode II is approximately 70° , while based on these results nucleation even in mode II occurs nearly self-similarly and between the modes a nearly quadratic variation is observed.

Crack nucleation process in elastic-plastic ductile mixed-mode propagation pertains the competition between mode I and mode II type of crack nucleation and growth. Crack nucleation with these materials was found to change from mode I to mode II type of crack growth with an equivalent mode angle of approximately $40\text{-}60^\circ$. This observation was made based on transitions in the nucleation angles and nucleation values of fracture toughness. The macroscopic crack growth, on the other hand, was found to alter its appearance closer to the mode II end, when the zigzags of a mode I crack diminished and the crack propagated macroscopically like a shear crack. This fact is most likely related to local conditions since nucleation and propagation are influenced by the near crack tip material properties, the mode of crack growth near the transition of first nucleation may not be stable with respect to propagation and different modes can exist at different stages. Macroscopically mode II crack growth was observed in tests where the mode angle was 76.2° .

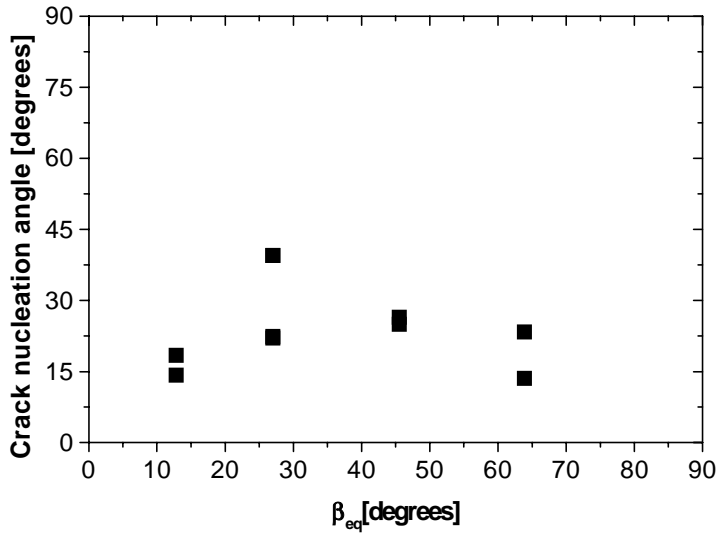


Figure 9. Fracture nucleation angles of F82H steel with different mode angles.

4. Discussion

4.1 Micromechanics of mixed-mode I-II fracture

The numerical calculations demonstrated the decrease of hydrostatic tension as the loading was altered from mode I towards mode II. At the initial stages of mode II loading the rate of decrease of hydrostatic tension is high. Naturally, if we consider an infinitesimal situation, under mode II the crack front would not experience a hydrostatic stress state at all. With finite strains, it is noticed that the maximum of the hydrostatic tension rotates clockwise and decreases in value. Also, at mode II the sharpened tip of the crack experiences hydrostatic compression, while the weak peak of hydrostatic tension is far from the area of crack propagation.

The deviatoric stress state and thus the plasticity experienced by the near crack tip region is enhanced by the introduction of the shear loading component. The maximum values at mode II are found from the sharpened crack tip and as known even from the basic linear-elastic crack stress field solutions, the extent

of the plastic region is several times larger in comparison to mode I loading. This feature can also be understood as an expansion of the process zone of fracture.

Numerical simulations also reveal the modes of crack nucleation, which have been verified experimentally by several researchers (referred above to e.g. [7,10-12]). The calculations demonstrate that near mode I the rate of damage formation is highest at the blunted side of the initial notch, indicating crack nucleation from the blunted side, while on the sharpened tip at these mode angles the void formation is less severe. When enhancing the mode II loading component, it is found that as the hydrostatic tension stress state decreases and the plasticity localizes in a more volatile manner to the sharpened tip, the damage accumulation of the sharpened tip overcomes that of the blunted side. In mode II, the lack of hydrostatic tension in the blunted side impedes void growth and because the plastic strain concentrations are extremely strong at the sharpened tip, for crack propagation from the blunted side is unfavorable. The damage formation at the sharpened tip is extremely strong causing the crack to nucleate as a thin shear crack through an intensive plastic localization, the process being usually referred to as mode II type of crack nucleation.

The differences caused by the previous factors to micromechanisms of fracture under mode II loading are presented in Fig. 10. Fig. 10a presents a typical mode I dimple fracture, which is divided into stages of nucleation, growth and coalescence for reference. The first abnormality when comparing to the mode II fracture of Fig. 10b is related to the nucleation process. Typically in mode I the situation is such that the nucleation of voids from large particles is

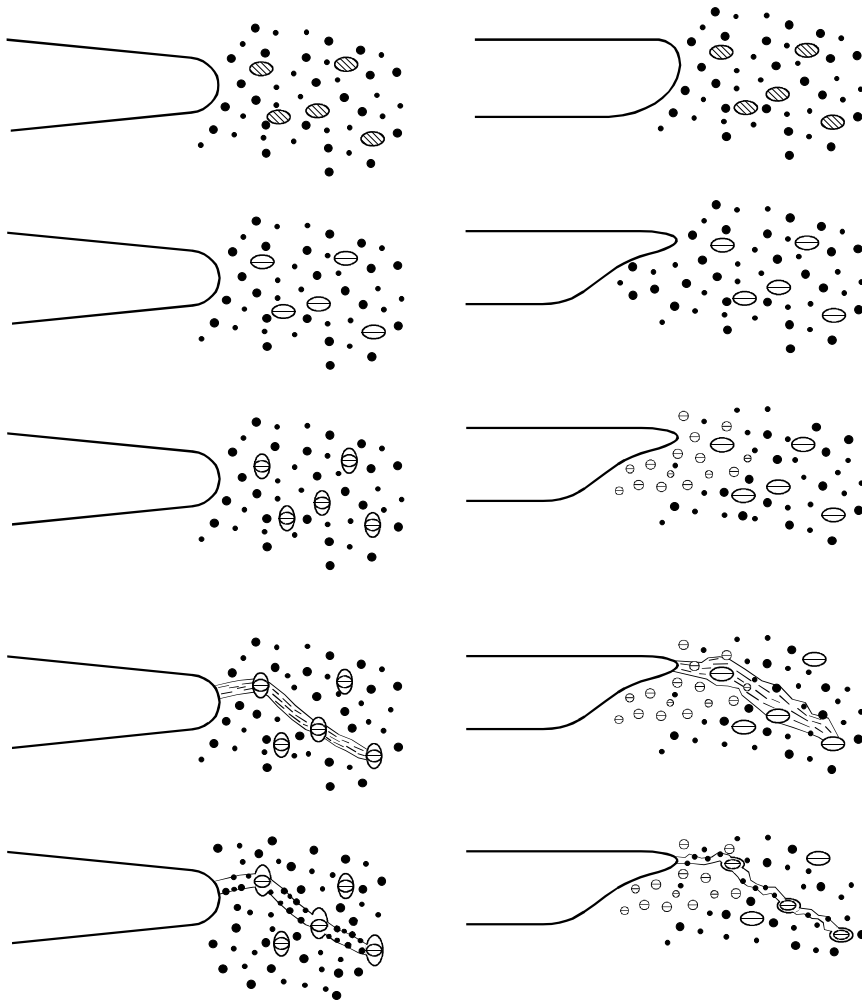


Figure 10. Micromechanical stages of fracture under (a) mode I and (b) prominent mode II.

stress controlled, while smaller particles of secondary populations nucleate with a strain controlled mechanism (stress controlled [20], strain controlled [21]). The plastic strains experienced by the near crack tip areas in mode II are large enough to cause nucleation in smaller particles as well fairly early in the rupture process, because otherwise the dimple sheets as seen in SEM-studies could not have been formed. The nucleation process takes place throughout the crack front at near tip regions, which is referred to the large plastic zone and strain controlled nucleation of different particle populations, because the interface

stress controlled nucleation can be considered a milder criterion compared to nucleation through plasticity. In mode I type of fracture the strain controlled nucleation of smaller particles is related to the coalescence stage, where the localization caused by the grown large voids initiates a formation of void sheets through smaller particles contributing to the coalescence and final fracture. At the next stage in mode II type of fracture, due to the lack of hydrostatic tension, the voids which have formed as a result of the nucleation process do not have any prospects of growing, but will remain near their initial forms which are in relation to the original inclusion sizes. In contrast, the strong influence of void growth on mode I fracture and the typically exponential relation between void growth rate and stress triaxiality has been demonstrated in several studies (e.g. [22]). At this stage we have a crack tip with a large plastic zone, which, when considering nucleation, can be considered as the process zone of fracture, and a fine distribution of voids. The next stage of fracture is the coalescence of voids, which occurs as a local rupture between the small voids. It can be argued that this stage can occur with much smaller energy consumption than in fibrous crack extension even if considering microscopically rectilinear crack growth, because we are considering a sheet of very fine voids connected with small ligaments and the loading with reference to localized plasticity is strong. The asperities connecting the void sheets are related to the process zone through microstructural inhomogeneities and the fracture process. Comparing to a traditional mode I crack propagation, the mode II crack possesses more degrees of freedom, to say. The micromechanical level at which the fracture process occurs is smaller due to the lack of void growth, and it causes a situation where the microstructural inhomogeneities, such as particle distribution and matrix properties and their anisotropy, have an effect to the end result. The larger process zone provides the crack with degrees of freedom to propagate in the intense slip-zone with respect to non-continuum properties, causing the asperite surface to form during crack growth. The fracture resistance curves presented previously support the concepts of micromechanical observations and numerical simulations. The drastic decrease of the tearing modulus with all materials is a direct result of the increase in plastic zone with mode II loading leading to a larger process zone, which can be interpreted as easing the fracture process and decreasing the energy associated with plastic dissipation. Thus, the crack has several possible paths to advance, from which it selects the one of lowest resistance, which on the other hand is formed as a result of grain orientation and other effects causing anisotropy.

The mixed-mode fracture surfaces are formed with mechanisms that are between both far ends. The decrease of hydrostatic tension is quite rapid at small values of the mode angle, which is reflected as a decrease of void growth rate and the formation of smaller dimples even at small values of the equivalent mode angle. Otherwise the asperity formation etc. follow intermediate values when encompassing between modes I and II.

4.2 Material characteristics of the fracture micromechanisms

The materials considered in this study possessed naturally some characteristic properties with responses to mixed-mode loading. The F82H steel is relatively clean in microstructural terms, and the sparsity of second phase particles is in mode I reflected as large dimples surrounded by void sheets of smaller particles. This is reflected to a mixed-mode situation in a sense that in near mode I the differences in dimple size are larger between different populations, and larger dimples exist among sheets of smaller dimples. The A533B steel studied has a very fine particle distribution, which is reflected as sheets filled with small dimples even at near mode I situations. AISI 304 was found to contain additional impurities which had formed copper-sulfide and the initial void volume fraction was very high. This reflected as a drastic decrease in fracture toughness, even at the early stages of the loading spectrum near mode I. The CuAl25 alloy had a strong texture due to complex manufacturing process (internally oxidized, rolling and hot-isostatic pressing), which was found to cause a discontinuity type of decrease in fracture toughness. This effect was considered to be a consequence of anisotropic material behavior associated with different crack nucleation mechanisms, but the studies were not perceived further.

4.3 Modeling considerations with respect to ductile mixed-mode I-II fracture

The general idea of simulating mixed-mode ductile rupture with the Gurson-Tvergaard model is related to finding the deficiencies of the model, which can then be better understood for mode I and general loading. It can not be pursued

that using the model for mixed-mode or mode II fracture analysis is entirely a valid effort, because several features of the model have been committed to more or less strictly mode I type of loading and as such we are definitely not discussing about a general fracture model.

Because the model basically defines a von Mises material enhanced with dilatation effects, in principle there are no basic features limiting its use. The limitations and questions are more related to the latter variants, the damage evolution equation and the dilatational part. At first, the q_i factors were chosen by Tvergaard [23] in order to present interaction and coalescence effects for a mode I type of ductile failure and are unlikely to be material parameters in terms of different loading modes. Additionally, the basic model is formed for a spherical void in a characteristic unit cube, which may not reflect the size scale consistently. Since in the case of mode II or mixed-mode fracture, the interaction between voids is likely to be more severe and certainly the concept of unit cube containing a void of cylindrical geometry forming typically under high stress triaxiality is under question. Also, local anisotropy due to changes in length-scale is to be considered. Similar arguments can be given for the general two-dimensional modeling of crack nucleation and propagation, but unfortunately three-dimensional numerical modeling is still an obstacle in many cases. Similar comments can be given for the choice of nucleation functions and the acceleration of void growth due to coalescence. Taking into account the previous factors more general models for simulating ductile fracture should be considered and some of the shortcuts taken in present modeling identified.

4.4 Parameters and criteria

Based on results for the nucleation angle and associated behavior, the work done within linear-elastic mixed-mode criteria for predicting crack nucleation direction and fracture toughness locus lacks in background. Criteria related to plastic strain, shear stress and deviatoric stresses should be used instead and some first steps have been taken. Naturally, criteria based on energy release rate could be considered as the most feasible ones. Another issue are the changes in crack nucleation and growth modes, which cause an entirely another fact to characterize. Also, because the transition between brittle and ductile mixed-mode fracture behavior is dependent on for example microstructural features,

the modeling efforts are more complicated. Behavior of two materials very close to each other in terms of composition and properties can differ with respect to mixed-mode brittle and ductile as an example, and as such great care must be taken.

A similar question arises when considering parameters for assessing ductile mixed-mode fracture. This study used J-integral to characterize the behavior, but it is to be questioned whether some other parameter should be used. In a mixed-mode situation, for example both components of the J-vector have nonzero values and neglecting the second component does not have any grounds. Several conservation integrals have been presented, but their suitability has not been assessed with detailed accuracy containing numerical and experimental work. Finding the correct parameter would solve several, even most, of the problems facing the understanding of mixed-mode fracture.

5. Conclusions

Mixed-mode fracture resistance curves were determined for four metallic elastic-plastic materials experiencing a ductile fracture mechanism. Results involving transitions of fracture toughness, and concerning crack nucleation angle and fracture morphology together with numerical modeling were used to describe the micromechanics of the fracture process and some comments for modeling were provided with respect to mixed-mode loading.

The conclusions from this work are:

- Fracture toughness in ductile materials can be lower under mixed-mode or mode II loading than in mode I. The effect appears most pronounced with materials of great practical importance, such as structural and stainless steels.
- The different micromechanical features of ductile failure under mixed-mode I-II loading have been demonstrated to be due to differences in the continuum fields characterizing the fracture process. The stages of fracture are different because of a lack of hydrostatic tension and an increase in quantitative values of plastic strain when the shear loading component is introduced.

- In terms of mixed-mode behavior, linear-elastic and elastic-plastic materials differ in many fundamental ways and theories and criteria for brittle materials are unable to assess the behavior of ductile materials.

6. Acknowledgements

The reported work was part of the Finnish Research Programme on the Structural Integrity of Nuclear Power Plants 1995 - 1998, subproject RAVA1 on Material Degradation in Reactor Environment. The work was performed in 1997 - 1998.

Co-operation with Rainer Rantala and Rauli Keskinen from the Radiation and Nuclear Safety Authority, STUK, Ralf Ahlstrand and Alpo Neuvonen from IVO Ltd. and Paulus Smeekes from TVO Ltd. together with Kim Wallin, Päivi Karjalainen-Roikonen, Seppo Tähtinen and many other colleagues is gratefully acknowledged. The work presented was partly funded by the Finnish Fusion Energy Research programme, FFUSION.

References

- [1] Maccagno, T. M. and Knott, J. F. The Fracture Behavior of PMMA in Mixed Mode I and II. *Engineering Fracture Mechanics*, Vol. 34, 1989, pp. 65–86.
- [2] Suresh, S., Shih, C. F., Morrone, A. and O’Dowd, N. P. Mixed-Mode Fracture Toughness of Ceramic Materials. *Journal of the American Ceramic Society*, Vol. 73, 1990, pp. 1257–1267.
- [3] Gao, H., Zwang, Z., Tang, C. and Zhou, A. An Investigation on the Brittle Fracture of K_I - K_{II} Composite Mode Cracks. *ACTA Metallurgica Sinica*, Vol. 15, 1979, pp. 380–391.
- [4] Maccagno, T.M. and Knott, J.F. The Mixed Mode I/II Fracture Behavior of Lightly Tempered HY130 Steel at Room Temperature. *Engineering Fracture Mechanics*, Vol. 41, 1992, pp. 805–820.

- [5] Shi, Y.W., Zhou, N.N. and Zhang, J.X. Comparison of Mode I and Mode II Elastic-Plastic Fracture Toughness for Two Low Alloyed High Strength Steels. *International Journal of Fracture*, Vol. 68, 1994, pp. 89–97.
- [6] Aoki, S., Kishimoto, K., Yoshida, T., Sakata, M. and Richard, H.A. Elastic-Plastic Fracture Behavior of an Aluminum Alloy Under Mixed Mode Loading. *Journal of the Mechanics and Physics of Solids*, Vol. 38, pp. 195–213.
- [7] Tohgo, K., Otsuka, A. and Gao, H.W. The Behavior of Ductile Crack Initiation from a Notch under Mixed Mode Loading. *Proceedings of Far East Fracture Group Workshop*, M. Sakata, Ed., Tokyo Institute of Technology, 1988, pp. 101–108.
- [8] Bhattacharjee, D. and Knott, J.F. Ductile Fracture in HY100 Steel under Mixed Mode I/II Loading. *Acta Metallurgica et Materialia*, Vol. 42, 1994, pp. 1747–1754.
- [9] Shi, Y. W. and Zhou, N. N. Comparison of Microshear Toughness and Mode II Fracture Toughness for Structural Steels. *Engineering Fracture Mechanics*, Vol. 51, 1995, pp. 669–676.
- [10] Aoki, S., Kishimoto, K., Yoshida, T. and Sakata, M. A Finite Element Study of the Near Crack Tip Deformation of a Ductile Material under Mixed Mode Loading. *Journal of the Mechanics and Physics of Solids*, Vol. 35, 1987, pp. 431–455.
- [11] Ghosal, A. K. and Narasimhan, R. Mixed-Mode Fracture Initiation in a Ductile Material with a Dual Population of Second-Phase Particles. *Materials Science and Engineering A*, Vol. 211, 1996, pp. 117–127.
- [12] Ghosal, A. K. and Narasimhan, R. Numerical Simulations of Hole Growth and Ductile Fracture Initiation under Mixed-Mode Loading. *International Journal of Fracture*, Vol. 77, 1996, pp. 281–304.
- [13] Wang, K. J., Hsu, C. L. and Gao, H. Calculation of Stress Intensity Factors for Combined Mode Specimens. *Advances in Fracture Research*, ICF 4, 1977, pp. 123–133.

- [14] Li, F. Z., Shih, C. F. and Needleman A. A Comparison of Methods for Calculating Energy Release Rates. *Engineering Fracture Mechanics*, Vol. 21, 1985, pp. 405–421.
- [15] Mattheck C. and Moldenhauer, H. Mode-Extraction from Mixed Mode Analysis of Cracks by Special Filter-Technique. *International Journal of Fracture*, Vol. 34, 1987, pp. 209–218.
- [16] Rice, J. R., Paris, P. C. and Merkle, J. G. Some Further Results of J-integral Analysis and Estimates. *Progress in Flaw Growth and Fracture Toughness Testing*, STP 536, D.T. Read and R.P. Reed, Ed., American Society for Testing and Materials, 1973, pp. 118–133.
- [17] Gurson, A.L. Continuum Theory of Ductile Rupture by Void Nucleation and Growth: Part I – Yield Criteria and Flow Rules for Porous Ductile Materials. *Journal of Engineering Materials and Technology*, Vol. 99, 1977, pp. 2–15.
- [18] Tvergaard, V. Material Failure by Void Growth to Coalescence. *Advances in Applied Mechanics*, Vol. 27, 1990, pp. 83–151.
- [19] Chu, C.C. and Needleman, A. Void Nucleation in Biaxially Stretched Sheets. *Journal of Engineering Materials and Technology*, Vol. 102, 1980, pp. 249–256.
- [20] Argon, A. S., Im, J. and Safoglu, R. Cavity Formation from Inclusions in Ductile Fracture. *Metallurgical Transactions A*, Vol. 6A, 1975, pp. 825–837.
- [21] Cox, T. B. and Low, J. R. An Investigation of the Plastic Fracture of AISI 4340 and 18 Nickel-200 Grade Maraging Steels. *Metallurgical Transactions A*, Vol. 5A, 1974, pp. 1457–1470.
- [22] Rice, J.R. and Tracey, D. M. On the Ductile Enlargement of Voids in Triaxial Stress Fields. *Journal of the Mechanics and Physics of Solids*, Vol. 17, 1969, pp. 101–127.
- [23] Tvergaard, V. Influence of Voids on Shear Band Instabilities under Plane Strain Conditions. *International Journal of Fracture*, Vol. 17, 1981, pp. 389–407.

Comparison of transition temperature criteria applied for KLST and ISO-V type Charpy specimens

Tapio Planman, Matti Valo and Kim Wallin
VTT Manufacturing Technology
Espoo, Finland

1. Introduction

A great deal of test data have been obtained on reactor pressure vessel steels using the standard Charpy-V test. Although more advanced test methods, based on elastic-plastic fracture mechanics, are both recommendable and already in use in the surveillance programmes of some nuclear power plants (NPPs), Charpy tests are still required, e.g., by regulatory guides.

Besides the normal-size (ISO-V) Charpy specimen ($10*10*55 \text{ mm}^3$), various types of sub-size specimens have been introduced. One standardised sub-size specimen being in use is the so-called KLST specimen, the size of which is $3*4*27 \text{ mm}^3$ with 1 mm central notch (DIN 50 115). So far the test data published for the KLST specimen, as well as sub-size specimens in general, is still limited.

The results from small specimen testing are typically used for evaluating the fracture behaviour of the ISO-V Charpy specimen and if there are no test results available for the correlation, as there usually is not, a general correlation has to be applied to evaluate the fracture behaviour of the ISO-V specimen. The availability of a sub-size specimen depends therefore significantly on how reliably this relationship has been established.

Impact test data measured with different specimens have been correlated using some appropriate criterion (or criteria) and since a total transition curve is normally measured, there are several ones available. The criterion can be a fixed energy or lateral expansion level describing the transition temperature or the

level can be derived from the upper-shelf energy (USE). In general, the proposed criterion can be divided into two groups: those *derived from the dimensions* of the specimens and those *derived empirically* from experimental data.

Test data measured with ISO-V and KLST -type Charpy specimens are discussed and the validity of two proposed, basically different transition temperature criteria and the resulting differences in the temperatures, that are inevitable because of the different size ligaments, studied. Specimens' capability to describe consistently the transition temperature shift characteristic of ferritic steels due to irradiation and recovery annealing is discussed as well. The data consists of the test results published previously [1] and more recent test data measured at VTT with KLST-type specimens for non-irradiated and irradiated FFA, JFL and JRQ pressure vessel steels in an IAEA Co-ordinated research programme.

2. On proposed correlations

One of the best established correlations for the KLST specimen, including over 30 transition curves, has been determined for absorbed energy and lateral expansion 1.9 J, 3.1 J and 0.3 mm (KLST specimen) and 41 J and 68 J and lateral expansion 0.9 mm (ISO-V specimen), respectively. The criteria have been derived using the mean ratio of USEs as a normalising factor. The resulting mean difference in the transition temperatures was found to be as follows [2]:

$$T_{\text{KLST}} = T_{\text{ISO-V}} - 65^{\circ}\text{C} \quad \begin{array}{l} \text{(KLST: 1.9 J, 3.1 J and 0.3 mm lateral exp.)} \\ \text{(ISO - V: 41 J, 68 J and 0.9 mm lateral exp.)} \end{array} \quad (1)$$

The three proposed criteria are to be used together [2].

There has been presented also another way of correlating the transition temperatures [3]. The appropriate energy level for the KLST specimen (or the ratio of energies) was derived from the definition of the J-integral, according to which the J-integral, describing the elastic-plastic fracture toughness of a material, is inversely proportional to the ligament area of the specimen. When energy criterion 28 J is normalised in relation to the ligament area, the

corresponding criterion for the KLST specimen is about 3.1 J (3.15 J), that is 35 J/cm^2 .

The 35 J/cm^2 transition temperature has in a previous study been determined for various types of steels as a function of specimen thickness (B) by dynamic tests [4]. In relation to the normal-size Charpy-V specimen, the transition temperature difference (ΔT) was found to depend on specimen thickness (B) as follows:

$$\Delta T = 51.4 \cdot \ln[2 \cdot (B / 10)^{0.25} - 1] \quad (^\circ\text{C}) \quad (2)$$

The standard deviation of the function was less than 5°C for specimens with $B \geq 3 \text{ mm}$. The formula (2) is expected to be valid for various low-alloy steels having the yield strength within range 200 - 1000 MPa [4]. The measured data and the function fit are shown in Fig. 1.

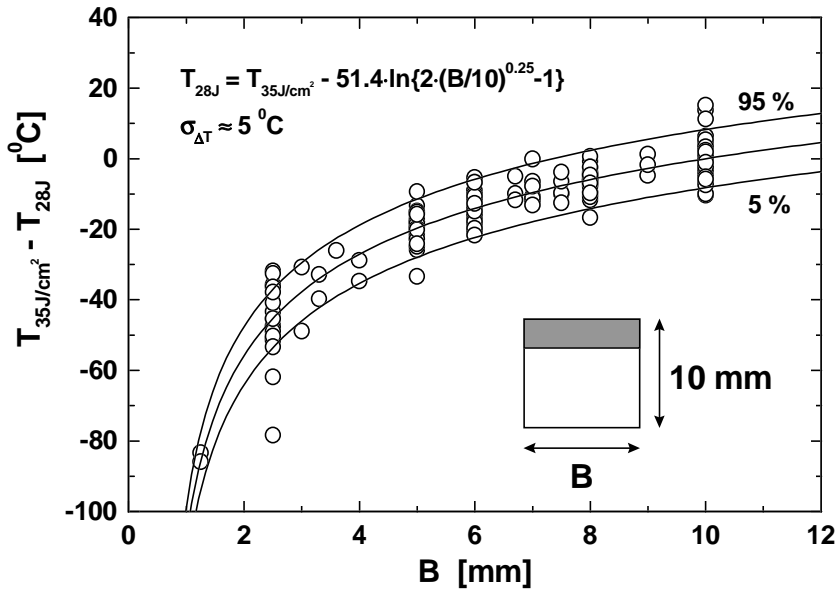


Figure 1. Effect of specimen thickness on the 35 J/cm^2 transition temperature [4].

When the formula (2) is applied to the KLST specimen, ignoring the fact that the formula takes into account only the effect of specimen thickness, the correlation becomes as follows:

$$T_{\text{KLST}} = T_{\text{ISO-V}} - 38^{\circ}\text{C} \quad \begin{array}{l} \text{(KLST: 3.15 J and 0.3 mm lateral exp., e.g.)} \\ \text{(ISO - V: 28 J and 0.3 mm lateral exp., e.g.)} \end{array} \quad (3)$$

On the basis of fracture mechanics the lateral expansion criterion should be equal for both specimens, independently of specimen size, for example 0.3 mm [3].

The transition temperature(s) is typically the primary parameter to be determined by Charpy tests. The second one is the notch toughness at higher temperatures, i.e. the mean upper-shelf energy (USE) which can also be estimated from the sub-size specimen data. Such a procedure for evaluating the USE of the ISO-V specimen can be derived from fracture mechanics [3]. By combining the defining formula of the J-integral and power-law fit $J = (\Delta a)^m$ describing stable crack growth, the following relationship was derived between the USEs:

$$E_{\text{ISO-V}} = E_{B \cdot b} \cdot \frac{10}{B} \cdot \left(\frac{8}{b}\right)^{1+m} \quad (4)$$

where B is specimen thickness, b is ligament width and m is a material and geometry factor.

The value of m depends on specimen size, dimensions of the notch and material. Factor m can be determined empirically from the USEs measured with different specimens. The value of m has been shown to depend primarily on the USE of the material [3].

3. Materials

The materials tested in this study were low-alloy quenched and tempered pressure vessel steels. Most data have been measured on 15X2MFA-type Cr-Mo-V steels with different irradiation conditions. The six examined material

states consisted of two heats in either non-irradiated, irradiated or both irradiated and annealed condition. In addition, six states of the corresponding weld materials, with roughly the same contents of alloying elements but different main impurity contents, were tested. The IAEA CRP 3 steels, FFA, JFL and JRQ, were tested both in non-irradiated and irradiated conditions. The materials have been characterised in detail in an IAEA co-ordinated research programme (IAEA CRP 3). The Charpy ISO-V test data measured in this programme were in part used for this study. The irradiated sub-size specimens were fabricated from the halves of the corresponding tested ISO-V specimens. The other materials included in the study (three steels with different compositions) were non-irradiated and tested elsewhere.

4. Test and analyses methods

The impact energy used for testing the KLST specimens was 15 J and the impact velocity 3.8 m/s. For the ISO-V specimens the corresponding values were 300 J and 5 m/s. A pneumatic mechanism was used to transfer the specimen from thermal bath to the proper striking position accurately and with minimum delay time. The transition temperatures were determined from a tanh-function fit obtained by minimising the squared sum of temperature deviations.

5. Results

The transition temperatures based on the mean USE ratio of the ISO-V and KLST specimens [2] are compared in Fig. 2 which shows also the mean and 95% prediction bounds calculated for the measured data with slope 1:1. The difference between the transition temperatures given by the KLST specimens (at 1.9 J and 3.1 J) and the ISO-V specimens (at 41 J and 68 J) was approximately 63°C. The standard deviation of the correlation was 18°C. The result also shows (Fig. 2) that the temperatures hold the linear 1:1 relationship moderately up to about 70°C 68 J level but remain below the mean dependence at higher temperatures. The temperature difference (and the scatter with remarks) obtained here coincide with the result reported elsewhere (compare eq. 1) [2].

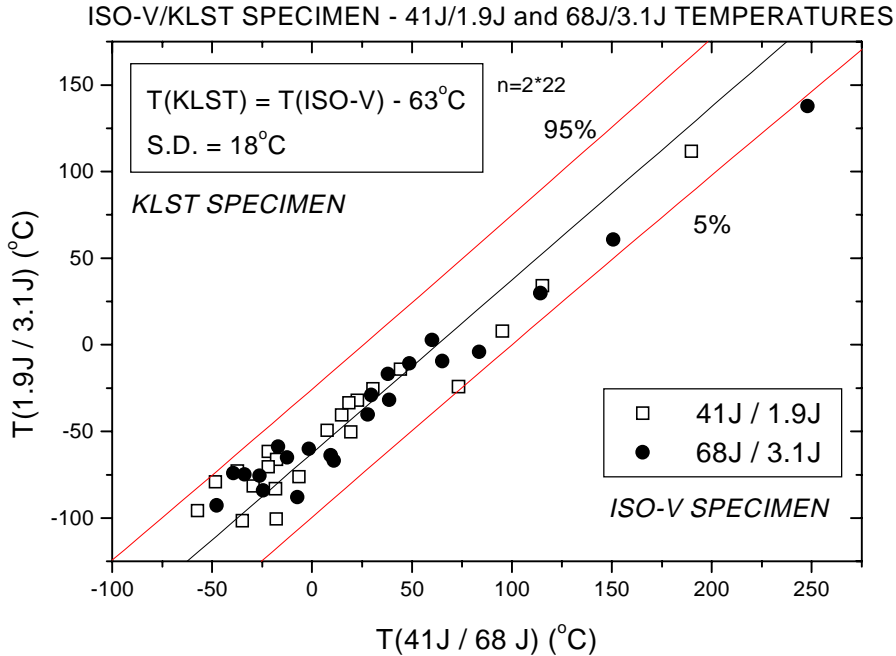


Figure 2. Comparison of transition temperatures 41 J / 68 J and 1.9 J / 3.1 J measured with ISO-V and KLST-type impact specimens. The values of lateral expansion are excluded.

For comparison, the transition temperatures were determined also at the energy levels proportioned to the real (measured) USE value of each material instead of the average value. Neither the transition temperatures nor the mean dependence of them showed, however, any marked difference as compared with the results based on the mean USE ratio. Moreover, the standard deviations were very close to each other, suggesting that no improvement can be achieved by employing the USE ratio measured for each material rather than the mean value.

The transition temperatures based on the ratio of the ligament areas, i.e. the 3.15 J and 28 J criteria, are compared in Fig. 3. The difference between the transition temperatures given by the KLST specimens (at 3.15 J) and the ISO-V specimens (at 28 J) was in this case approximately $37^{\circ}C$. The standard deviation of the correlation was $14^{\circ}C$, i.e. somewhat lower than that given by the USE-based energy criteria ($18^{\circ}C$). The result confirms that the thickness correction formula (2) [4] can be used for the KLST specimen (compare eq. 3) and also supports the validity of the formula (2) in general, i.e. the applicability of it for

(notched) impact specimens with various dimensions. The dependence of the transition temperatures (Fig. 3) is also distinctly linear and follows the 1:1 slope.

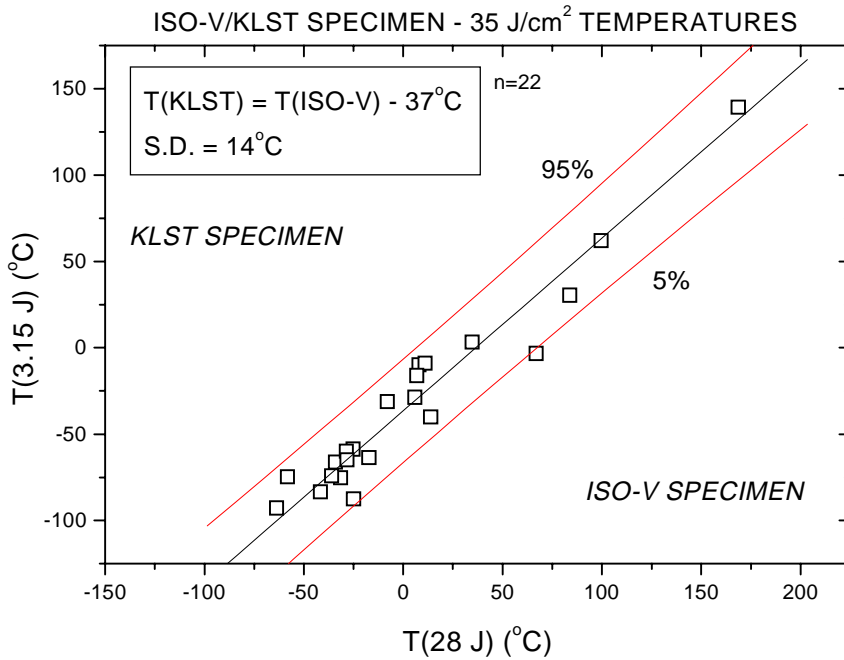


Figure 3. Comparison of transition temperatures 28 J and 3.15 J measured with ISO-V and KLST-type impact specimens.

The values of USE measured with the ISO-V and KLST specimens for the materials studied are shown together with the measurements published elsewhere for various steels [5] and for one 2 1/4Cr1Mo pressure vessel steel [6] in Fig. 4. These data were used for deriving the correlation between the USEs of the ISO-V and KLST specimens. An appropriate function [3] was fitted to the measured USE data so as to solve the unknown factor (m) in eq. (2) as follows:

$$m = \left(\frac{E_{\text{ISO-V}}}{A} \right)^n \quad (5)$$

where $E_{\text{ISO-V}}$ is the USE of the ISO-V specimen, and A and n are fit parameters. The values estimated for these parameters were 188 J and 0.32, respectively.

Using these values, the formulas (2) and (5) are now available for calculating, e.g. iteratively, the USE of the ISO-V specimen from the value measured with the KLST specimen.

The straight line in Fig. 4 shows the mean (constant) USE ratio, according to which energy criteria 1.9 J/3.1 J/0.3 mm vs. 41 J/68 J/0.9 mm have been determined [2]. The relationship used describes thus also the materials discussed in this study satisfactorily though it is not clear if the correlation actually is linear as it has been assumed.

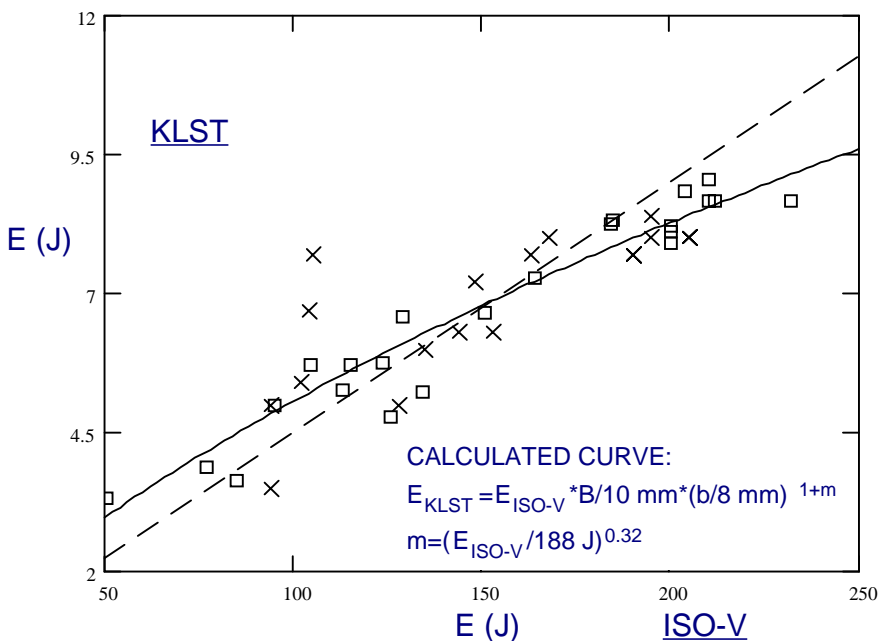


Figure 4. Correlation of upper-shelf energies. The curve shows an estimate of given type and the straight line the relationship used for determining the proposed [2] transition criteria. Data from this work (o) and from ref. [5] (x) are included.

The USEs of the ISO-V specimens were also estimated from the USEs measured with the KLST specimens by using the derived relationship. It proved that the USE of the ISO-V specimen is predictable by this means with the accuracy of about $\pm 20\%$. Three measurements [5] diverged clearly outside this prediction.

The irradiated KLST and ISO-V specimens (15X2MFA-type steels) had been prepared so that the neutron fluences were equal, which made it possible to compare the transition temperature shifts of the base and weld materials exhibited by different specimens. The results indicate that the irradiation shift shown by the KLST specimen tends to be lower than the shift shown by the ISO-V specimen, with the same material condition. The largest difference was measured to be as big as 51°C, and in one case was the difference to the opposite direction, the shift shown by the KLST specimen being 5°C higher than the shift shown by the ISO-V specimen.

The neutron fluences of the KLST and ISO-V specimens fabricated from the irradiated FFA, JFL and JRQ steels were close to each other as well and thus the irradiation shifts of the transition temperatures measured with different specimens comparable. The shifts measured at different energy levels are compared in Fig. 5.

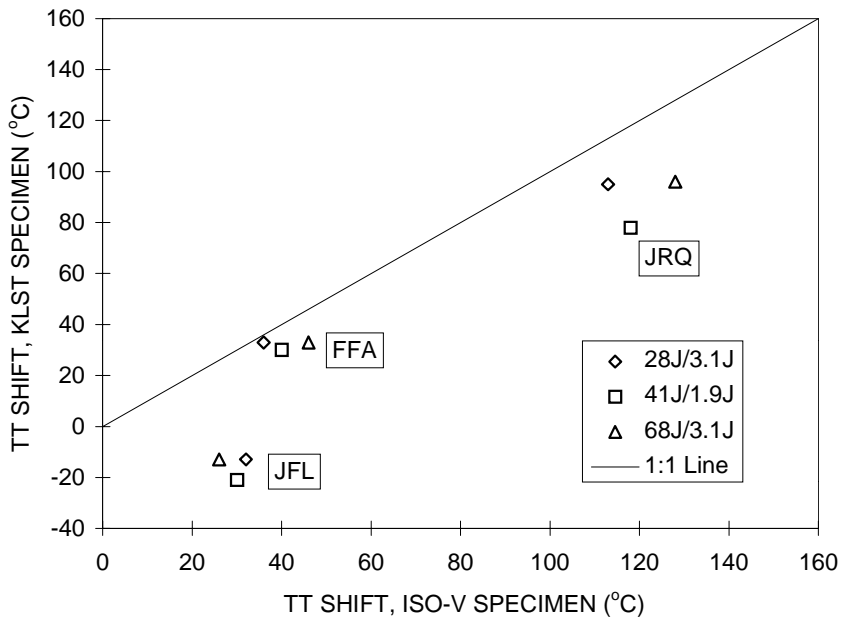


Figure 5. Comparison of the irradiation shifts of transition temperatures measured with ISO-V and KLST-type impact specimens at different energy levels for the IAEA CRP 3 steels.

The degree of recovery was predicted quite accurately by the KLST specimen for those steels where the transition temperature shift in annealing was large, but failed to predict the shift for the ones where it was small. The best correlation was obtained at the 28 J/3.15 J energy levels and, which is important, the degree of recovery measured with the KLST specimen was in each case lower than or equal to that measured with the ISO-V specimen. In general, the degrees of recovery at 68 J and 3.1 J showed a large variation between the values measured with different specimens.

6. Discussion

The relationship measured in this work between the transition temperatures of the ISO-V and the KLST type Charpy specimens at 41 J / 1.9 J and 68 J / 3.1 J is nearly equal to that reported elsewhere [2], supporting thus the validity of the 65°C temperature difference measured [2] for a large number of steels. On the other hand, the current result confirms that the formula (2) is valid also for the KLST specimen, according to which the transition temperature with this specimen is 38°C higher as compared to that of the ISO-V specimen at the 35 J/cm² energy level, i.e. when the absorbed energy is normalised in relation to the ligament area. The energy criteria would thus be, for example, 28 J and 3.15 J as it has been assumed in this work.

It has been shown (for a 15X2MFA steel) that lateral expansion criteria 0.9 mm / 0.3 mm are also consistent with the proposed energy criteria, i.e. the transition temperature difference is expected to be 65°C. However, the absorbed energy normalised in relation to the ligament area corresponds to a same lateral expansion for both specimens, which has been shown (for this steel) as well [3].

The discussed USE-based energy criteria (without lateral expansion) resulted in a standard deviation (18°C) that is equal or somewhat larger than that published elsewhere [2], i.e. around 15°C. According to the rather high standard deviation obtained in this work and the deviation from the linear 1:1 relationship observed with the USE-based criteria suggest that an improved (general) correspondence could be achieved, most likely with steels having a high transition temperature ($T_{68J} > 70^{\circ}\text{C}$), by applying the criteria based on the ligament area, for example the value 35 J/cm² used in this work. However, it is not feasible to definitely

address which one of the criteria discussed gives a better (general) correlation without including more different types of (structural) steels in the correlation. The relationship of the KLST and ISO-V transition temperatures has a slope close to 1:1 in both cases, but especially the 28 J/3.15 J correlation cannot be improved by estimating also the slope (Figs. 2 and 3).

Although the correlation of the transition temperatures between the different specimens could be described satisfactorily by employing the criteria based on the mean (and constant) ratio of USEs, the linear relationship of the USEs is not evident, but the dependence is following more likely the applied power law (5) than a linear relationship. The verification of this dependence is on the basis of only these measurements difficult because there was a quite large scatter in the USE values. One obvious reason for this scatter is that the USEs have been determined as an average of only a few test results. It follows also that the estimated parameters should be considered as first approximations rather than final values. By perceiving this fact the correspondence of the calculated and measured USEs can be regarded as moderate.

The deviations of the measured irradiation shifts in the transition temperatures is of major importance since the range of variation was large and the KLST specimens showed mostly lower shifts than the ISO-V specimens. For the 15X2MFA steels the shifts measured at the 68 J/3.1 J energy levels differed more than those measured at the other two levels, which can be explained by the low USEs of the irradiated weld materials. The ratios USE/68 J (ISO-V) and USE/3.1 J (KLST) were in both irradiated welds in the range 0.8–0.9. As the reason for the rest of the deviation in the irradiation shifts shown by the ISO-V and KLST specimens remain obscure, it should be recommended to add at least 30°C to any transition temperature shift measured with the KLST specimen, independently of the criteria, to ensure a conservative estimate for the ISO-V specimen. This "safety margin" also equals the 2*standard deviation measured for both correlations and hence, it can be regarded as a minimum margin for a transition temperature shift evaluation. Further, to avoid any excessive uncertainties, transition temperatures should not be measured at energy/lateral expansion levels exceeding approximately 75% USE. In general, the difference between the transition temperature shifts measured with ISO-V and KLST specimens for the 15X2MFA and IAEA CRP 3 steels are consistent, i.e. the

KLST specimen tends to give shifts of up to 30–40°C lower than those measured with the ISO-V specimen.

7. Conclusions

In total 22 structural steels or steel conditions were included in the study. Steels with four basic compositions were studied in the irradiated condition. The discussion is limited to various energy criteria proposed for determining Charpy transition temperatures from sub-size specimen data, excluding the lateral expansions. With these remarks the following general conclusions can be made from the results of this work.

1. The 3.1 J / 1.9 J / 0.3 mm transition temperatures of the KLST specimen are approximately 65°C lower than the 68 J / 41 J / 0.9 mm transition temperatures of the normal-size (ISO-V) Charpy specimen.
2. The 3.15 J transition temperature of the KLST specimen is approximately 38°C lower than the 28 J transition temperature of the ISO-V specimen, i.e. the difference is on the average equal to that measured with other types of impact specimens at the absorbed energy level normalised according to the ligament area, that is 35 J/cm².
3. The USE of the ISO-V specimen can be estimated from the USE measured with the KLST specimen by solving the formulas (4) and (5), where A and m have the values 188 J and 0.32, respectively. An iteration procedure can be used for solving $E_{\text{ISO-V}}$.
4. Transition temperatures should not be measured at energy/lateral expansion levels exceeding about 75% USE. The mean transition temperature shift (due to irradiation) measured with the KLST specimen should be raised by at least 30–40°C in evaluating the shift for the ISO-V specimen.

8. Acknowledgements

The reported work was part of the Finnish Research Programme on the Structural Integrity of Nuclear Power Plants 1995–1998, sub-project RAVA1 on Material Degradation in Reactor Environment. The work was performed in 1996–1997.

Co-operation with Rainer Rantala and Matti Ojanen from the Radiation and Nuclear Safety Authority (STUK), Ralf Ahlstrand and Jyrki Kohopää from IVO Ltd. together with many other colleagues is gratefully acknowledged.

References

1. Planman, T., Wallin, K., Valo, M., Ahlstrand, R. & Kohopää, J. Comparison of some impact test results on ISO-V and KLST type Charpy specimens. Espoo: VTT Manufacturing Technology, 1995. 13 p. (Report VTT VALB93).
2. Klausnitzer, E. N. Micro-specimens for mechanical testing. *Materialprüfung*, 1991, Vol. 33, No. 5, p. 132 - 134.
3. Wallin, K. Mini- ja normaalikokoisten Charpy-V-koesauvojen tulosten välinen korrelaatio. Espoo: Technical Research Centre of Finland, Metals Laboratory, 1992. 29 p. (Report VTT-MET B-207). (In Finnish).
4. Wallin, K. Murtumissitkeyskorrelaatiot. Espoo: Technical Research Centre of Finland, 1986. 31 p. + app. (VTT Research Reports 428). (In Finnish).
5. Amayev, A. D., Badanin, V. I., Kryukov, A. M., Nikolayev, V. A., Rogov, M. F. & Sokolov, M. A. Use of subsize specimens for determination of radiation embrittlement of operating reactor pressure vessels. In: Small specimen techniques applied to nuclear reactor vessel thermal annealing and plant life extension, ASTM STP 1204,

Eds. Corwin, Haggag and Server. Philadelphia: ASTM, 1993. Pp. 424 - 439.

6. Bryan, R. H. et al. Pressurized-thermal-shock test of 6-in.-thick pressure vessels. PTSE-2: Investigation of Low Tearing Resistance and Warm Prestressing. NUREG/CR-4888, ORNL-6377, Dec. 1987. P. 46.

Material deterioration due to neutron irradiation

Matti Valo and Kim Wallin
VTT Manufacturing Technology
Espoo, Finland

1. Introduction

IAEA CRP 3 was a major effort to develop and validate surveillance methodologies for irradiation embrittlement characterisation and it is hardly any more possible to carry out similar co-operative programmes due to resource limitations. The programme included material characterisation by tensile, Charpy-V and fracture toughness tests. The programme promoted considerably the acceptance of direct fracture toughness characterisation of the irradiated material condition.

Specimen preparation by reconstitution technique is becoming a common expertise in many laboratories. The VTT practice has been widely validated in the current programme. However, no international or co-operative validation programmes have not yet been performed with irradiated material, where the technique has its unique value but where possibility of incorrect application is also evident.

2. IAEA/CRP 3 fracture mechanical results

The key focus of the third phase of the IAEA co-ordinated research programme on neutron irradiation effects on advanced pressure vessel steels is upon advancing quantitative fracture mechanics methodology and assuring the extrapolation of qualitative fracture methods which have predominated in reactor vessel surveillance until recent years. One scope of the programme was fracture toughness testing. The participants performed a variety of different fracture toughness tests on many of the materials. The tests included static and

dynamic testing. For the final evaluation of the programme, it was decided that VTT Manufacturing Technology would make a centralised re-evaluation of the test results, with latest state of the art analysis methods.

The data included in the analysis were generally taken from the IAEA CRP 3 data base. The data was in all cases checked against the original national reports and complemented as necessary. VTT Manufacturing Technology performed also few additional tests to strengthen some of the conclusions drawn by the analysis. Nine countries performed static fracture toughness testing out of which three performed also dynamic testing. In one case (dynamic), the irradiation was performed in Switzerland and the testing in Finland.

Before re-evaluation, the data was screened. Only data deemed as descriptive of the true fracture toughness was included in the analysis. The prerequisite was that the fracture toughness is based on the elastic-plastic J-integral, or valid linear elastic (LEFM) fracture toughness K_{IC} . This meant that the Indian dynamic test results had to be excluded from the re-evaluation, because they were based on invalid LEFM results and equivalent energy maximum load results, which were not comparable with the other results.

The definition of ductile crack growth initiation toughness varied from laboratory to laboratory (lab-to-lab). Thus, the ductile fracture results showed such a large lab-to-lab variability that a comparative analysis of the results was impossible. Also, the quality of the data supplied to the data base was such that a systematic recalculation of the ductile initiation toughness was not possible. By necessity, the re-evaluation had to be restricted to brittle fracture initiation described by the elastic-plastic fracture toughness K_{IC} .

The statistical analysis was performed in accordance with the VTT method for assessment of fracture resistance. The majority of the fracture toughness testing was performed on the reference material JRQ. To study the effect of specimen size, type and orientation, the T_0 data was plotted as a function of specimen distance to the plate surface. The T_0 data included also the theoretical $\pm 1 \cdot \sigma$ confidence limits for the estimate. The scatter in the results was relatively large. It appears that estimates based on less than three specimens are too unreliable. Therefore, a second plot of the data including only estimates based on three or more specimens, was made in Figs. 1 and 2.

The result shows a much reduced scatter in T_0 (especially for the L-T orientation). No systematic differences between different specimen types are visible. Neither can be seen any size effects in addition to the statistical size effect included in the analysis. The L-T orientation seems to show a toughness gradient in the plate thickness direction, but not the T-L orientation. The data from the different countries is quite consistent, with one exception. The [JA] data differ from rest of the data. The reason for the difference is not known, but it was decided not to include the [JA] data in the subsequent analysis of JRQ. As a whole, the statistical analysis applying the VTT method seems to work well for JRQ in the reference state.

A comparison between the static fracture toughness transition temperature shift ΔT_0 and the most common Charpy-V transition temperature ΔT_{41J} was made. The result is presented in Fig. 2.

The result of the comparison is not very encouraging with respect to the reliability of the Charpy-V test. Only in one case (GWA), is the Charpy-V shift greater than the static fracture toughness shift. For the GWA material the Charpy-V shift corresponds to the T-L orientation whereas the fracture toughness shift corresponds to the L-T orientation. The Charpy-V shift underestimates the fracture toughness shift at maximum by approximately 70°C (GFB). Based on the comparison, it can be concluded that the Charpy-V shift is not appropriate for the estimation of the static fracture toughness shift.

In an attempt to improve the usability of the Charpy-V test, a direct correlation between the transition temperatures (not the shifts) was attempted. In this case many more results were available for the comparison. The result of the comparison is presented in Fig. 4.

A clear difference in the correlation is seen between irradiated and non-irradiated materials. Considering the scatter, a 95% "lower bound" correlation for the irradiated materials becomes, $T_0 \approx T_{41J} + 15^\circ\text{C}$. This relation, used together with the master curve, appears more applicable than the use of the Charpy-V shift combined with the ASME reference curve. Most favourable is, however, based on the analysis, the direct determination of the static fracture toughness.

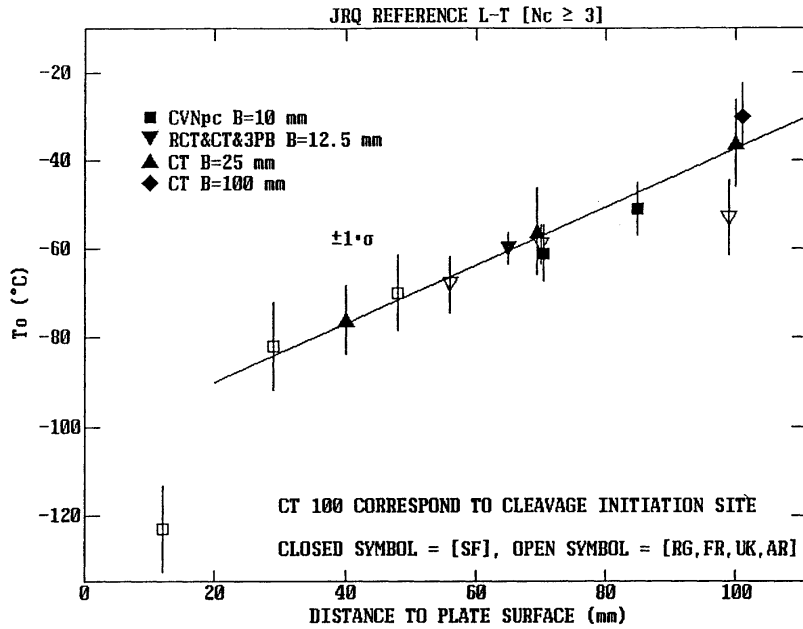


Figure 1. JRQ, L-T orientation, data with three or more specimens.

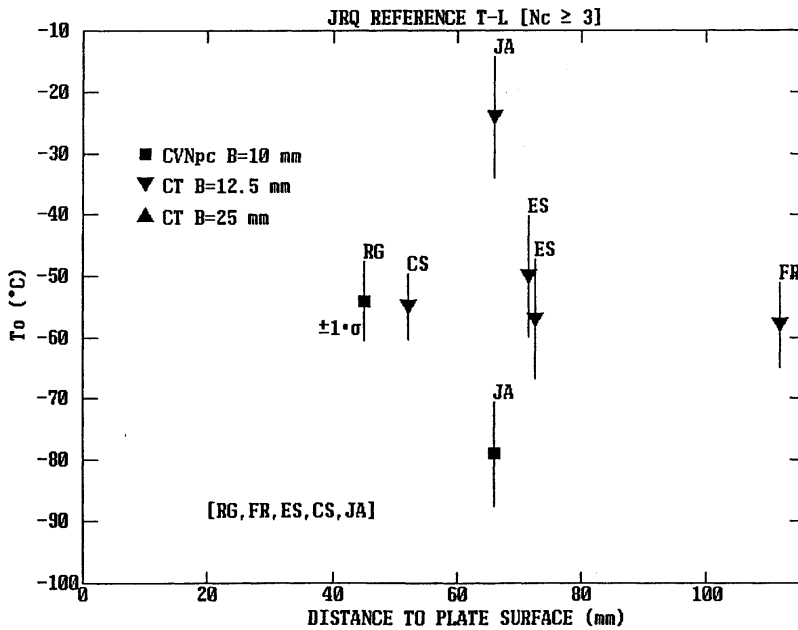


Figure 2. JRQ, T-L orientation, data with three or more specimens.

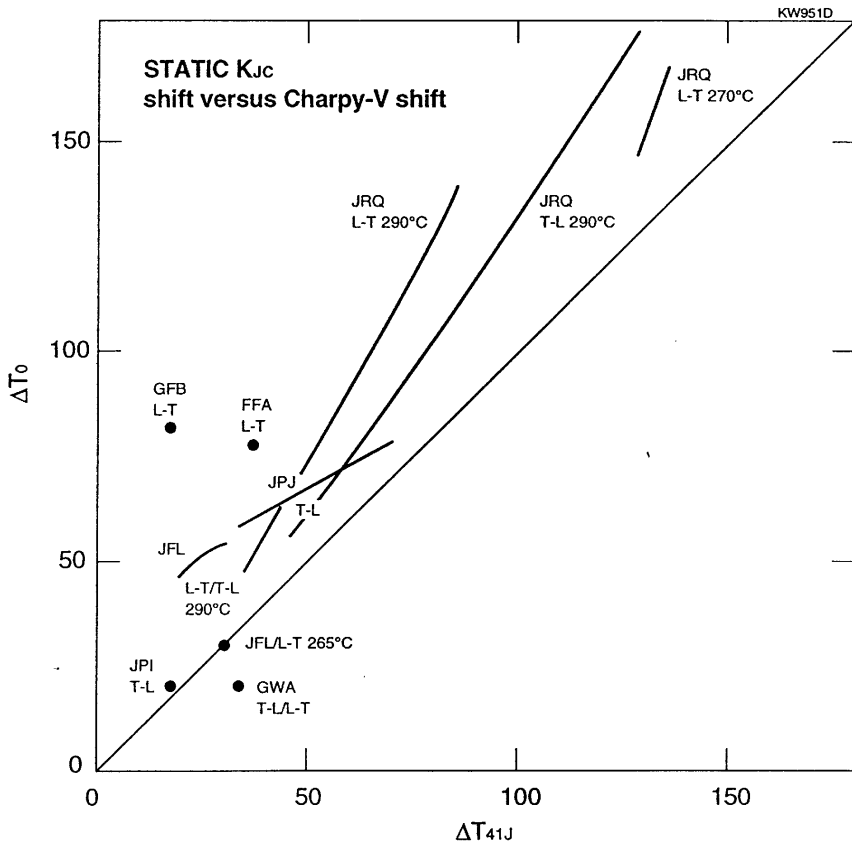


Figure 3. Comparison between the static fracture toughness shift ΔT_0 and Charpy-V shift ΔT_{41J} .

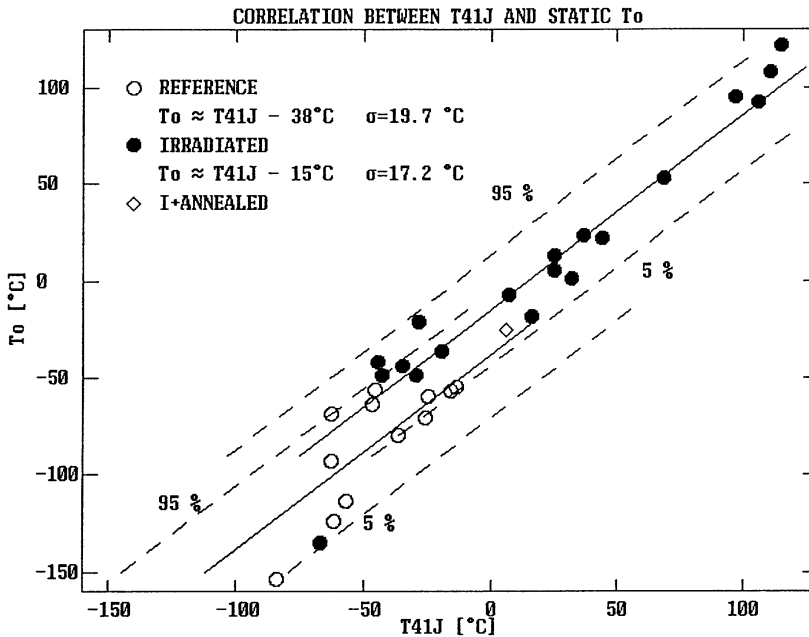


Figure 4. Correlation between T_{41J} and T_0 .

3. Irradiated specimen reconstitution techniques

Specimen reconstitution is a powerful technical means to utilise the available material effectively for material properties characterisation. If the pressure vessel of a NPP has been annealed, the original PV surveillance programme can be adapted to the new situation only with the help of reconstitution technique.

The stud arc welding technique utilised by VTT is described schematically in Fig. 5 and its nominal welding parameters are given in Table 1. Oversized end studs are used and the specimens are finished with a discharge machine. Square end studs of 12×12 mm for the 10×10 mm inserts and 6×6 mm for the 3×4 mm inserts are used. The end stud material is a fine grained, thermomechanical Mn-steel (RAEX 490 FORM, Rautaruukki Ltd). Its guaranteed test values are:

yield strength 554 MPa and tensile strength 679 MPa at 20°C and $E_{CH-V} = 139$ J at -20°C. An irradiated VVER-forging was used in the verification tests.

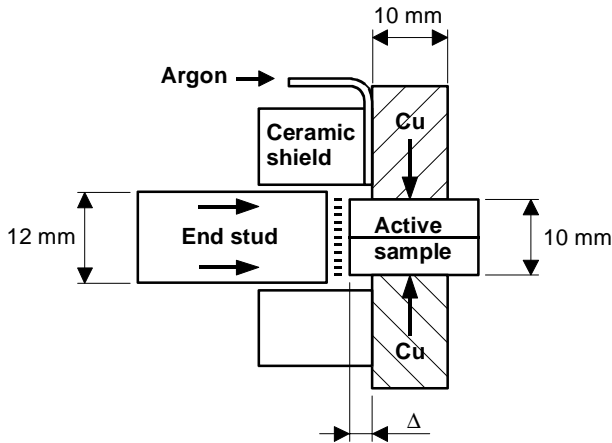


Figure 5. The welding rig for 10 × 10 mm specimens. $\Delta = 2$ mm is used for 10 × 10 mm and 3 × 4 mm cross-sectional specimens. The active sample is called also centre insert.

Table 1. The nominal welding parameters.

Specimen size (cross-section)	Current A	Time s	Voltage V	Energy kJ	Δ^* mm
3 mm × 4 mm	350	0.06	20-25	0.5	2.0
10 mm × 10 mm	800	0.10	c. 20	1.7	2.0

* see Figure 5

At best the amount of authentic material required for preparing one reconstituted specimen equals the volume, which is deformed in the test. Material can not be used more effectively for mechanical properties characterisation by qualified tests because in a mechanical test material responses to loading by deformation. The limitations of the technique are evident. Reconstitution is performed by welding, which leads to local melting and overheating of the material and consequently to local annealing of irradiation defects with a potential of creation of non-conservative data. The rapid post weld cooling of the weld on the other hand leads to hard weld seams,

which confine material deformation to the centre insert of the specimen in the test. This so called reconstitution constraint will tend to reduce the energy absorbed by the specimen in the test. Because primary pressure vessel material data is often created with reconstituted specimens, the technique needs proper validation.

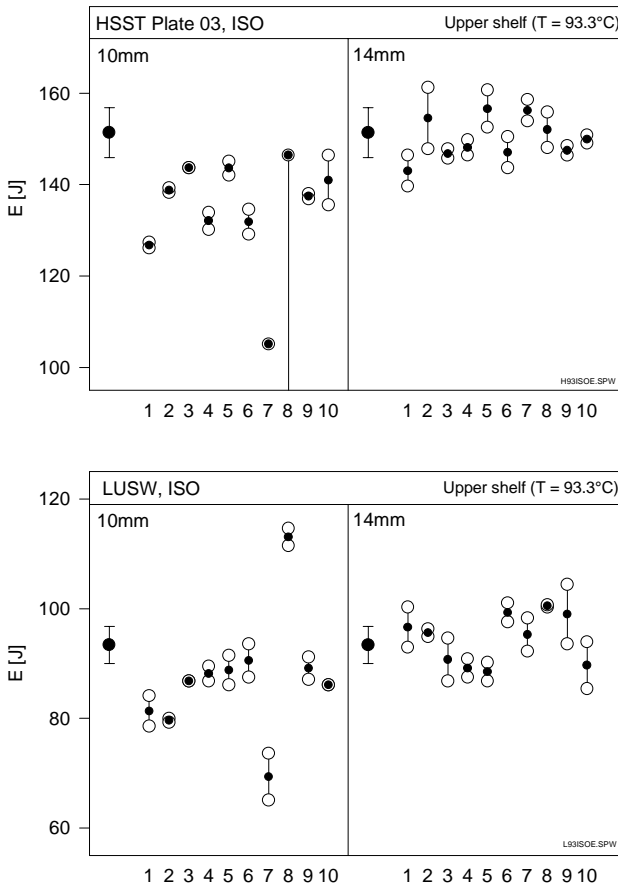


Figure 6. The measured upper shelf CH-V impact energies of reconstituted specimens in the ASTM reconstitution round robin exercise. Centre insert lengths of 10 mm and 14 mm and two materials HSST 03 and Linde 80 weld were used. Baseline upper shelf energies shown by the bars on the left side are 151 J for HSST-3 and 93.3 J for Linde 80 weld. The figure indicates that specimens of 10 mm insert measure reduced upper shelf energies but 14 mm inserts give the baseline values. VTT is participant number 3.

The first guide for irradiated material reconstitution was ASTM E 1253-88 (re-approved 93). In order to revise the guide ASTM organised recently a round robin exercise with ten international participants including VTT (see Onizava et al. 1998). Figure 6 shows the effect of the hard reconstitution weld seam on the upper shelf energy. The exercise was performed with unirradiated materials and hence it is not sensitive to material overheating. The last heat treatment of pressure vessels is performed at app. 600°C but irradiation defects anneal out already at app. 450°C.

Heat input in reconstitution welding is often minimised by using short weld pulses. It was shown by detailed measurements that the welding event of 0.1 s duration applied by VTT can well be modelled as a plane impulse heat source. The temperature profiles in the specimen after the reconstitution welding, Figure 7, can be estimated with reasonable accuracy based on the measured heat input.

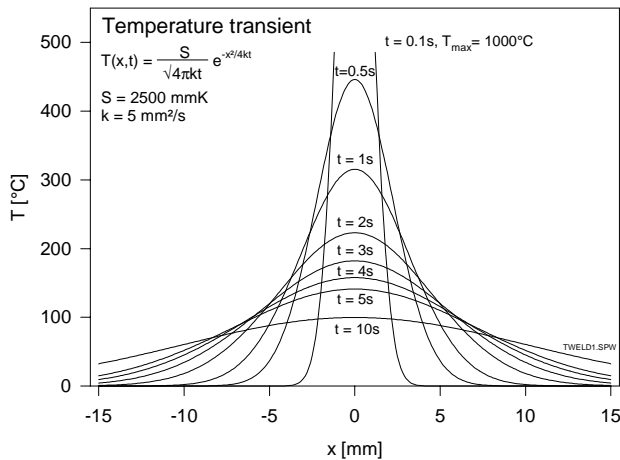


Figure 7. Calculated heat diffusion profiles in the specimen after the application of a plane heat impulse.

The new validation tests were performed with sub-size specimens of VVER base metal material, which was irradiated into a fluence of $16 \times 10^{19} \text{ n/cm}^2$, $E > 1 \text{ MeV}$. The $3 \times 4 \times 27 \text{ mm}$ specimen size was used for Charpy-V and

precracked specimen tests. Precracked specimens were side grooved by $2 \times 10\%$, had $a/W \sim 0.5$ and were precracked before side-grooving using $K_{\max} \sim 12 \text{ MPa}\sqrt{\text{m}}$ and load-ratio $0 < R < 0.1$. The specimens were tested in the cleavage fracture temperature range. Crack growth was not measured during the test. Crack growth (Eq. 1) and specimen size corrections (Eq. 2) were applied to the measured K_{IC} values. The measured Charpy-transition curves are shown in Figs. 8 and 9 and the fracture toughness test results in Fig. 10.

$$J_{\text{corrected}} = J_0 \times \left(1 - \frac{0.5 \times \Delta a}{W - a_0}\right) \quad (1)$$

$$K_{25\text{mm}} = 20 + (K_{\text{measured}} - 20) \times \left(\frac{3\text{mm}}{25\text{mm}}\right)^{0.25} \quad (2)$$

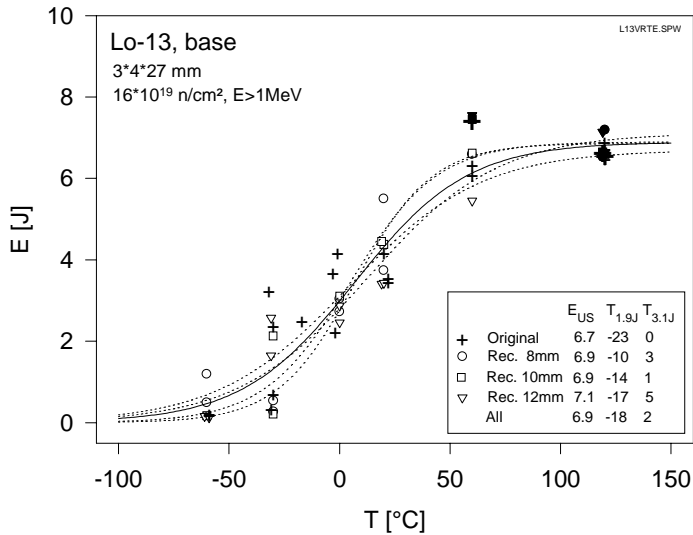


Figure 8. The measured transition curves for original and reconstituted subsized ($3 \times 4 \times 27 \text{ mm}$) Charpy-V specimens, impact energy, VVER base metal, neutron fluence $16 \times 10^{19} \text{ n/cm}^2$, $E > 1 \text{ MeV}$.

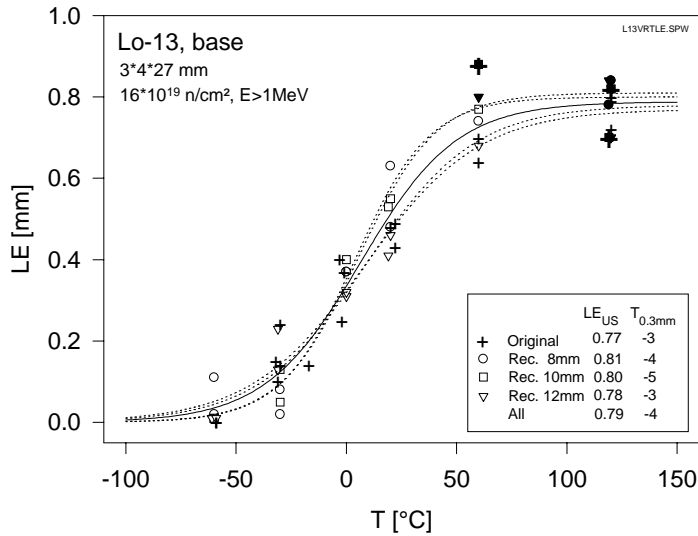


Figure 9. The measured transition curves for original and reconstituted subsized ($3 \times 4 \times 27$ mm) Charpy-V specimens, lateral expansion, VVER base metal, neutron fluence 16×10^{19} n/cm², $E > 1$ MeV.

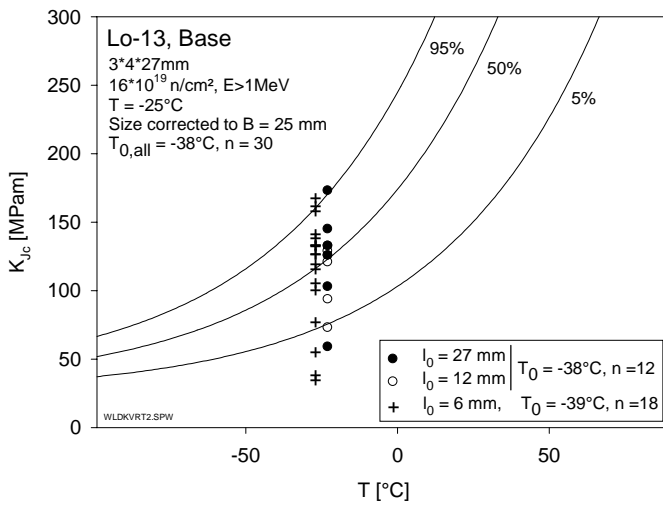


Figure 10. The cleavage fracture initiation K_{JC} for original and reconstituted $3 \times 4 \times 27$ mm three point bend specimens, 20% side grooves, $a/W \sim 0.5$, VVER base metal, neutron fluence 16×10^{19} n/cm², $E > 1$ MeV. The values are size corrected to $B = 25$ mm specimen size. Transition temperature defined by the $l_0 = 6$ mm specimens is compared to the transition temperature defined by the $l_0 = 12$ mm and original specimens.

Considerable scatter in Charpy-V and cleavage fracture properties is typical for the base metal used for the validation tests. Hence some uncertainty is included in the equality statement of data sets measured with reconstituted specimens of varying centre insert lengths. Reconstituted Charpy-V specimens give practically the same transition temperature values for $T_{3.1J}$ and $T_{0.3mm}$ as original specimens but values for $T_{1.9J}$ differ at most by 13°C as shown in Figs. 7 and 8. Irradiation embrittlement of the material measured with original $3 \times 4 \times 27$ mm specimens for the current fluence was app. 80°C . Consistency of the original and reconstituted specimen test values is considered to be good, when characteristic scatter in material properties and the number of test specimens used for measuring the transition curves is taken into account.

Fracture toughness data is shown in Fig. 10. Because the number of original specimens is rather small, the original and the $l_0 = 12$ mm reconstituted specimens are used as a reference group for the $l_0 = 6$ mm reconstituted specimens. The real length of the short inserts varied from 5.53 mm to 5.85 mm. The same transition temperature value is attained for both groups. The data is clearly biased towards the lower tail of the distribution as compared to the master curve description but this feature is a material property. The measured cleavage initiation values went up to $280 \text{ MPa}\sqrt{\text{m}}$, which is a high value for $B = 3$ mm specimens. However, the objective was to demonstrate only the equality of two data sets irrespective of size dependent validity criteria. Irradiation embrittlement of the material has not been measured with $3 \times 4 \times 27$ mm fracture toughness specimens but the Charpy-V irradiation shift of 80°C is a first estimate for the shift. The data shows that sub-size specimens reconstituted from 6 mm inserts work well.

4. Conclusions

The IAEA CRP 3 indicated clearly that quantitative assessment of irradiation embrittlement depends on the parameter, which is used in describing the response of material properties to irradiation, and on the detailed technical criteria applied. In addition laboratory to laboratory variation in the data was relatively large and partly due to technical incompetence. Master curve formalism appears as a clear and unifying approach in embrittlement characterisation. In addition better, physically based correlations between the

embrittlement sensitive parameters need to be developed. Sound critical attitude is also required, when assessing published data.

Specimen reconstitution is a reliably and powerful technique, which can be used in irradiated material testing, when applied with caution. The ASTM round robin exercise identified the limits of applicability of the technique, beyond which the measured data will be biased or misleading. The ASTM round robin also indicated rather large laboratory to laboratory variations. The inherent danger of annealing irradiation defects during specimen preparation can be critically assessed and revealed only in round robin exercises performed with irradiated material, which are non-existing now. In the current situation each laboratory, which aims to apply reconstitution technique to irradiated material, has first to verify his practice with irradiated material.

5. Acknowledgements

The reported work was part of the Finnish Research Programme on the Structural Integrity of Nuclear Power Plants 1995 - 1998, subproject RAVA2 on Material Degradation in Reactor Environment. The work for Chapter 2 was completed in 1996.

Co-operation with Rainer Rantala and Matti Ojanen from the Radiation and Nuclear Safety Authority, STUK, Ralf Ahlstrand and Jyrki Kohopää from IVO Ltd. together with many other colleagues is gratefully acknowledged. The work was co-ordinated to the IAEA/CRP3 programme. The ASTM Reconstitution Round robin was organised by Wayne Pavinich from Framatom Technologies Inc. and the co-ordinated specimen testing was performed by Mikhail Sokolov / ORNL.

References

Wallin, K. 1995. Summary of the IAEA/CRP 3 fracture mechanical results. Irradiation Embrittlement and Mitigation, IWG-LMNPP-95/5, Vol. 2. Vienna: IAEA. 27 p.

Valo, M. 1998. Reconstitution of sub Charpy-size V-notched and precracked specimens. Small Specimen Test Techniques, ASTM STP 1329. W. R. Corwin, S.T. Rosinski, and E. van Walle (Eds.). Philadelphia, USA: American Society for Testing and Materials.

Onizava K., van Walle E., Nanstadt R., Sokolov M. and Pavinich W. 1998. Critical Analyses of Results from the ASTM Round-Robin on Reconstitution. Small Specimen Test Techniques, ASTM STP 1329. W. R. Corwin, S. T. Rosinski, and E. van Walle (Eds.). Philadelphia, USA: American Society for Testing and Materials. (Summary of the ASTM Reconstitution Round Robin Exercise).

(See Appendix 1 for a comprehensive listing of publications)

Method development for studies of environmentally assisted cracking (EAC)

Päivi Karjalainen-Roikonen, Pekka Moilanen,
Aki Toivonen and Pertti Aaltonen
VTT Manufacturing Technology
Espoo, Finland

1. Introduction

During the use of nuclear reactors the properties of the structural materials change. Variations in the operation environment, such as changes in water chemistry, may enhance the development and growth of flaws. Neutron radiation causes embrittlement for in-core vessel materials. Radiation, together with water chemistry, increases the possibility of stress corrosion cracking in stainless steels and superalloys used in the reactor internal parts. Research on structural materials endeavours to study the ageing mechanisms of materials, and the possibilities and methods of preventing or forecasting the damage caused to structures by ageing.

The objective within the subproject “Material degradation due to corrosive environment” of the RATU2 project was to evaluate the factors affecting the changes in material properties due to the environment and stresses, and to assess their interrelationship. The subproject included among others the following tasks:

- Development of routine EAC crack growth testing method for small test specimens.
- Application of rising displacement testing to study irradiation assisted stress corrosion cracking (IASCC).

New simplified techniques for determination of fracture resistance curves in simulated reactor environments. Multi-specimen bellows loading system to

provide more experimental EAC data than can be obtained with previous servo hydraulic or mechanical loading systems.

2. The use of small fracture mechanical specimens in research of environmentally assisted cracking in simulated light water reactor environments

In recent years the use of fracture mechanics based approach has gained popularity in the research of environmentally assisted cracking, EAC. The basic test types utilising precracked specimens are constant load tests, constant displacement tests and determination of fracture resistance curves (J-R curves) with low displacement rate in an environment of interest. The information looked for is the susceptibility of a material to environmentally assisted cracking, EAC, crack growth rate, $(da/dt)_{EAC}$, as a function of stress intensity factor K or J-integral, and the stress intensity factor threshold value for EAC, K_{IEAC} , below which no environmentally assisted crack growth is assumed to occur, or the crack growth rate is very low.

The applicability of fracture resistance tests, i.e., J-R curve tests using small precracked three point bend specimens is evaluated as a method to reveal the EAC susceptibility of a material. Further, environmentally assisted crack growth rates $(da/dt)_{EAC}$ are determined from the J-R results using superposition based analysis method developed at VTT (Karjalainen-Roikonen & Wallin 1992). The possibility of initiation values, J_i or J_{Ic} (or corresponding stress intensity factor values, K_{ji}) for cracking, to represent stress intensity factor threshold value for EAC, K_{IEAC} , is discussed.

2.1 Experimental procedure - small specimens

Fracture resistance curves (J-R curves) in simulated BWR conditions with different constant displacement rates were determined for furnace sensitised austenitic stainless steel AISI 304 and for the HAZ of the welded AISI 321 Ti-stabilised austenitic stainless steel.

AISI 304 was furnace sensitised at 600°C for 2 hours. Three point bend specimens with the dimensions of 10×10×55 mm (AISI 304) or 10×5.5×55 mm (Ti-stabilised) were machined and prefatigued for the tests. The tests were performed with a servohydraulic testing machine in an autoclave attached with a water circulation loop. Load, deflection and crack length were monitored during the tests. The crack length during the tests was measured with a DC Potential Drop system.

The tests for sensitised AISI 304 were performed in simulated BWR primary water loop environment, oxygen content 200 ppb, conductivity < 0.3 μScm^{-1} , pH 7 and controlled potential +400 mV_{SHE} (AISI 304) or +200 mV_{SHE} (Ti-stabilised). The tests for the HAZ of the welded AISI 321 Ti-stabilised austenitic steel were performed under displacement control with constant displacement rates of 8×10^{-4} mms⁻¹, 1.2×10^{-5} mms⁻¹, 2.4×10^{-6} mms⁻¹ (AISI 304); 3×10^{-6} mms⁻¹ and 3×10^{-7} mms⁻¹ (Ti-stabilised).

After the tests the fracture surfaces were examined with a scanning electron microscope and the initial and final crack lengths were measured. The potential drop measurement data was fitted to the initial and final cracks and fracture resistance curves (J-R curves) were determined. The environmentally assisted crack growth rates $(da/dt)_{\text{EAC}}$ were calculated using superposition based analysis (Karjalainen-Roikonen & Wallin 1992).

2.2 Results - small specimens

The fracture resistance of both materials decreased with decreasing loading rate due to increasing proportion of environmentally assisted crack growth as can be easily observed in Figs. 1 and 2. The environmentally assisted crack growth rates were about 2 - 3×10^{-6} mms⁻¹ for AISI 304 and about 3 - 8×10^{-7} mms⁻¹ for the HAZ of the welded AISI 321 Ti-stabilised steel. The results are summarised in Table 1.

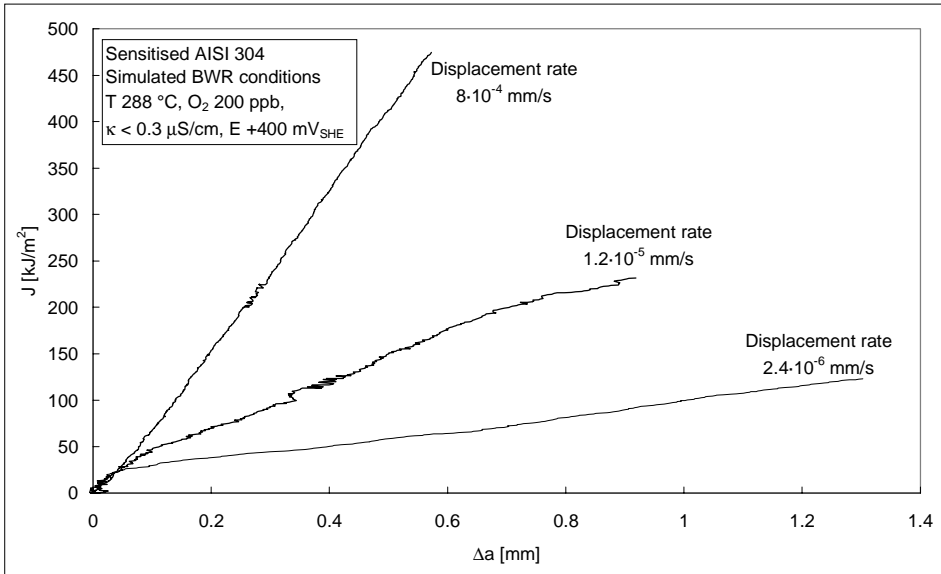


Figure 1. Fracture resistance curves for sensitised AISI 304 determined in simulated BWR environment (T 288°C, O_2 200 ppb, $\kappa < 0.3 \mu\text{S/cm}$, $E +400 mV_{SHE}$).

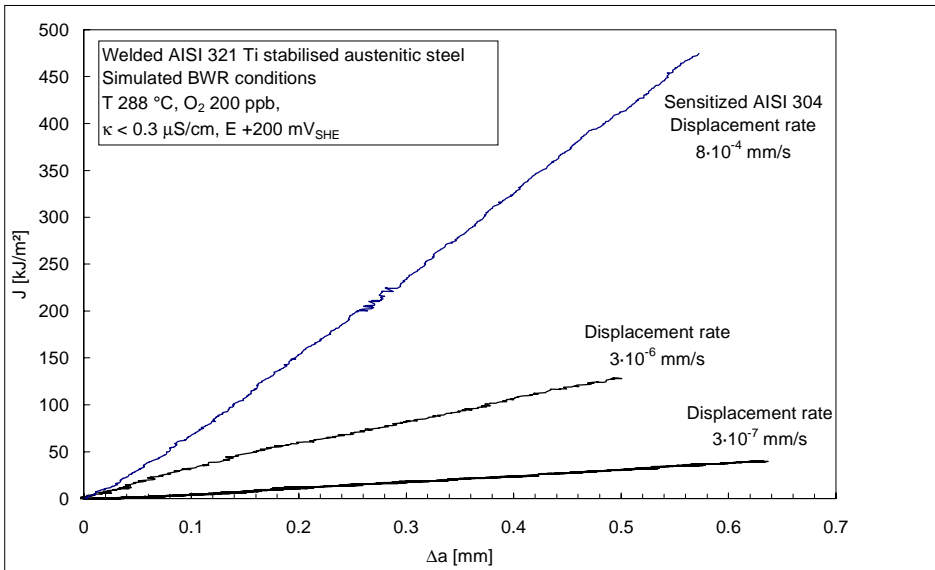


Figure 2. Fracture resistance curves for welded AISI 321 Ti stabilised austenitic stainless steel determined in simulated BWR environment (T 288°C, O_2 200 ppb, $\kappa < 0.3 \mu\text{S/cm}$, $E +200 mV_{SHE}$) as well as the reference curve (AISI 304).

Table 1. Test results obtained in simulated BWR-conditions, T 288°C, O_2 200 ppb, pH 7, κ 0.3 $\mu S cm^{-1}$, E +400 mV_{SHE} (AISI 304) or +200 mV_{SHE} (welded AISI 321).

Material	Displacement rate [mms^{-1}]	$(da/dt)_{EAC}$ [mms^{-1}]	Fracture surface appearance
304	8×10^{-4}	---	ductile 100%
304	1.2×10^{-5}	3×10^{-6}	IGSCC > 50%, TGSCC < 50%, ductile < 10%
304	2.4×10^{-6}	2×10^{-6}	IGSCC > 80%, TGSCC < 20%, ductile < 5%
Welded AISI 321	3×10^{-6}	8×10^{-7}	TGSCC > 70%, ductile < 30%
Welded AISI 321	3×10^{-7}	3×10^{-7}	IGSCC > 30%, TGSCC < 70%, ductile < 10%

* TGSCC, Transgranular Stress Corrosion Cracking; IGSCC, Intergranular Stress Corrosion Cracking

The amount of intergranular cracking on the fracture surface increases with decreasing loading rate.

2.3 Discussion and conclusions - small specimens

Fracture resistance curve of a material describes capability of a material to resist stable crack growth. In inert case when a fracture resistance curve is determined with standard loading / displacement rate and no environmental effect is present, the driving force for the fracture is mechanical loading only. Unless creep occurs, ductile fracture in an inert environment does not depend on time. When fracture resistance curve for a material is determined in an environment, an other driving force for cracking, i.e. environmental effect is introduced. Thus, two different components affect the crack growth rate during the test as well. When the loading / displacement rate is decreased the proportional environmental effect on the crack growth rate increases compared to the effect of mechanical loading. This effect is also visible on the fracture surfaces of the

specimens. Decreasing the loading / displacement rate increases the amount of IGSCC / TGSCC of the fracture surface and decreases the amount of ductile tearing.

Because both mechanical loading and the environment have an effect on the crack growth rate during the fracture resistance (J-R) test, the measured total crack growth rate does not represent environmentally assisted crack growth rate, $(da/dt)_{EAC}$ but includes also the crack growth rate due to mechanical loading. For the same reason, the initiation value for cracking, i.e. $J_{0.2}$ or J_{Ic} (or corresponding K-values) of the fracture resistance curves determined in an environment should not be used as a stress intensity factor threshold value, K_{IEAC} for environmentally assisted cracking. To get the environmentally assisted crack growth rate, $(da/dt)_{EAC}$, from the fracture resistance curves determined with low loading / displacement rate an analytical approach as used here should be applied.

The environmentally assisted crack growth rates, $(da/dt)_{EAC}$, seem to be dependent on the fracture mechanism, i.e., as the proportion of IGSCC increases the $(da/dt)_{EAC}$ decreases slightly. The calculated crack growth rates for sensitised AISI 304 seem to be in good accordance with those found in literature (MacDonald et al. 1985, Horn 1986, Hishida et al. 1986).

3. Irradiation effects on the fracture resistance of welded stainless steels in BWR environments

A study on the IASCC susceptibility of materials used in Finnish reactors has been conducted. The work of VTT performed within the RATU2 research programme is a part of the international Cooperative IASCC Research (CIR) Program which is coordinated by EPRI. The Finnish activity and results so far within CIR program are shortly introduced in following (Toivonen & Aaltonen 1997).

Stress corrosion susceptibility of irradiated and reference state austenitic stainless steel (SIS 2333) base metal and heat affected zone (HAZ) was studied by slow J-R tests in simulated BWR water. Test materials consisted of two base metal plates with a weld seam.

The specimens were prefatigued sub size 3PB specimens prepared by electric discharge machining (cross section 3 mm × 4 mm, length 27 mm). Due to small available test material pieces, the specimens were prepared by reconstitution welding.

The tests were performed in an autoclave which was connected to a water recirculation loop and equipped with a servohydraulic testing machine. Test temperature was 288°C, conductivity (feed water) 0.2 - 0.3 μS/cm, O₂ content 200 ppb, pH about 7 (at test temperature) and electrochemical corrosion potential varied between -500 mV_{SHE} and +200 mV_{SHE}.

Load, load line displacement and crack length were measured during the tests. Crack length measurement was performed with Direct Current Potential Drop, DC-PD. The J-R tests were performed according to ASTM E 1152 -87 with the exception of lower displacement rates. In this study, all J-R curves were measured with the same constant displacement rate, 2×10⁻⁶ mm/s.

Superposition based analysis method was used for the determination of environmentally assisted crack growth rates, (da/dt)_{EAC}. The method is based on the hypothesis that environmentally assisted cracking and cracking due to mechanical loading can be separated:

$$(da/dt)_{EAC} = (da/dt)_{TOT} - (da/dt)_{MECH} \quad (1)$$

The terms have the following meanings:

(da/dt)_{TOT} = total crack growth rate at a certain J integral value. Calculated from a slow J-R curve determined in the test environment.

(da/dt)_{MECH} = crack growth rate due to mechanical loading only. Calculated from a reference J-R curve with no environmentally assisted cracking.

The J-R curves and (da/dt)_{EAC} values indicate clear increase in stress corrosion susceptibility in irradiated material when compared with reference state material, especially in the case of HAZ. At the moment, it is not clear to what degree the effect is a result of irradiation and to what degree it is due to low

temperature sensitization (LTS, due to operating temperature, 288°C, and exposure time, about 80 000 hours). Most probably the increase in SCC susceptibility is a combination of both irradiation and thermal ageing.

In post-test fractographic examinations it was observed that the environmentally assisted cracking mechanisms were different in the irradiated and in the reference state materials at some - but not at all - electrochemical corrosion potentials.

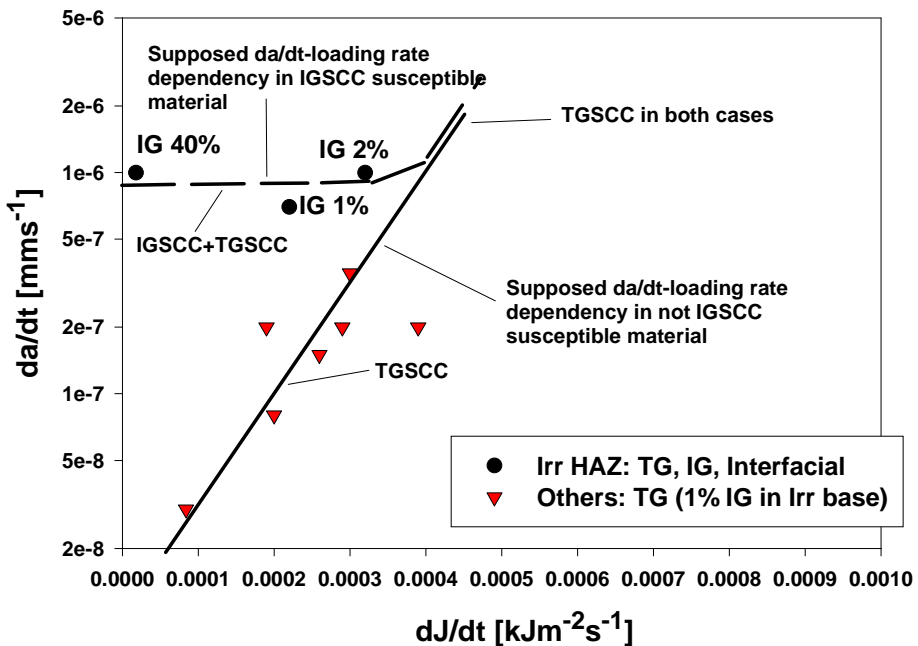


Figure 3. Supposed EAC morphology / EAC crack growth rate / loading rate dependency in IGSCC susceptible and IGSCC resistant austenitic stainless steels (solid and dashed lines). Materials were base metal (not IGSCC susceptible material) and heat affected zone of austenitic stainless steel AISI 304 (IGSCC susceptible material). Tests were performed under simulated BWR conditions: T 288°C, κ_{in} 0.3 $\mu\text{S}/\text{cm}$, O_{2in} 200 ppb, ECP +200mV_{SHE}.

Also, clear dependency between crack growth rate, loading rate and fracture morphology dependency was found, Fig. 3. For intergranular stress corrosion cracking (IGSCC) susceptible materials the amount of IGSCC increased with decreasing loading rate but the crack growth rate was about 9×10^{-7} mm/s

independently from the amount of IGSCC. For base metal AISI 304, that represented not IGSCC susceptible material, the environmentally assisted cracking mode was transgranular stress corrosion cracking (TGSCC) and crack growth rate was found to be linearly dependent on the loading rate.

In addition to J-R tests, DL-EPR tests were utilized to determine the degree of thermal sensitization of the test materials. The measured reactivation ratios do not support the assumption of thermal sensitization.

4. New simplified technique for determination of fracture resistance curves in simulated reactor environment

Fracture mechanics based tests to determine EAC crack growth rate under simulated light water reactor (LWR) conditions are usually performed in an autoclave using a loading system either with hydraulic or electric step motors. Pulling rod lead-in through the autoclave lid causes friction which may result in inaccuracy of load measurements. Typically, big 1T or 2T precracked C(T) specimens are used, and test facilities are designed for testing of only one specimen at a time. However, small specimens are needed when testing irradiated materials or when testing many specimens simultaneously.

In order to be able to test small specimens with accurate enough load measuring, a pneumatic servo-controlled fracture resistance measuring (PSFM-device) device was developed, (Moilanen 1995). In addition to increased sensitivity i.e. to avoid friction fall at pressure boundary, the pneumatic system has also several other advantages. Possible system leakage do not pollute the test environment and the system is easy to move and to calibrate into different test environments. With the system, constant load, constant displacement, corrosion fatigue and constant or various displacement rate tests in different test environments can be performed. Also, PSFM test facilities enabling testing of six specimens simultaneously under light water reactor conditions was developed.

The accuracy of the newly developed measuring device was determined through measuring the fracture resistance curves of sensitized AISI 304 stainless steel,

AISI 316 stainless steel and Inconel weld materials. The tests were performed in air at room temperature, in air at 288°C and under simulated BWR (Boiling Water Reactor) conditions.

4.1 Operating principle of PSFM-device

The main parts of the pneumatic servo-controlled fracture resistance measuring device are shown in Figure 4.

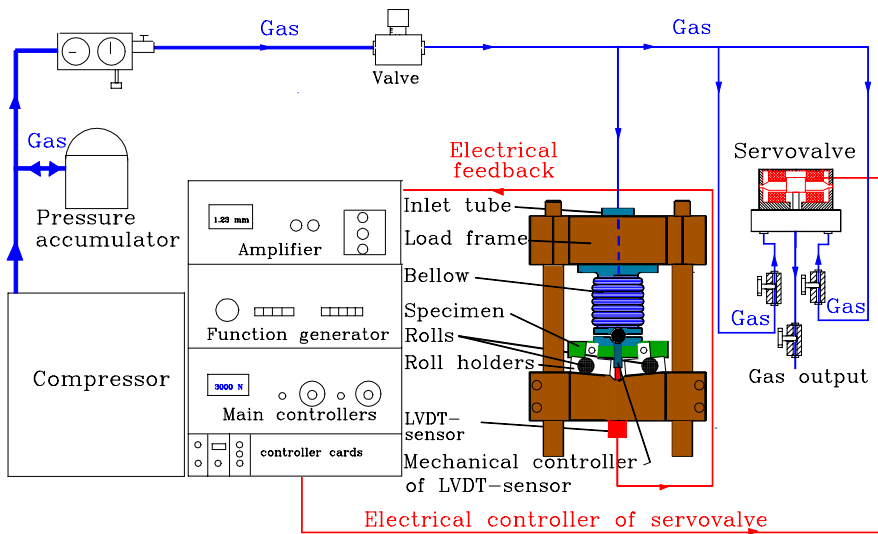


Figure 4. Pneumatic servo-controlled fracture resistance measuring device.

Specimen loading is provided by a bellows filled with a gas. The load is directly proportional to the pressure in the bellows. The pressure of the bellow i.e. load is adjusted by a servo controller and a servo valve with a feedback of either load or displacement. Load point displacement is measured with an LVDT-sensor (Linear Variable Differential Transformer), and the tests can be performed either load or displacement controlled. The servo valve needs 0.5...2 bar pressure level when the test is started. The pressure level at the beginning of the test depends on the size of the test specimen. Typically pre load directed to the test specimen is 50...300 N. A function generator is used to produce a constant displacement rate for the bellows. Technical specifications of the PSFM-device are presented in Table 2.

Table 2. Technical specifications for PSFM-device.

Maximum load	5000 N
Maximum displacement of the bellows	2.0 mm
Minimum displacement rate of the bellows	$0.6 \cdot 10^{-5}$ mm/min
Maximum operational pressure (pressure inside the bellows)	200 bar
The gas consumption of the servo valve under 120 bar pressure level	about 6-8 l/min
Maximum current for servo valves	30 mA
Gas types for servo valves	air, nitrogen and helium
Maximum number of test specimens to be tested simultaneously	6
Minimum specimen size	$3 \times 4 \times 27$ mm ³
Maximum specimen size	$10 \times 10 \times 55$ mm ³

4.2 Operational principles for multi-specimens PSFM-device

A multi-specimen PSFM-device was built for simultaneous testing of several specimens in order to increase testing capacity. Operational principle for the device i.e. the servo-controlled gas adjusting system is similar to the one specimen testing system presented above. A new kind of load frame including moveable specimen carrier was designed and manufactured for the system, Fig. 5. It made handling and preparing fixings for positioning of the specimens and DC PD wires easier. The test lay-out for multi-specimen PSFM-device consisting of simultaneous testing of five specimens in LWR environment and one in a high temperature furnace is presented in Fig. 6.

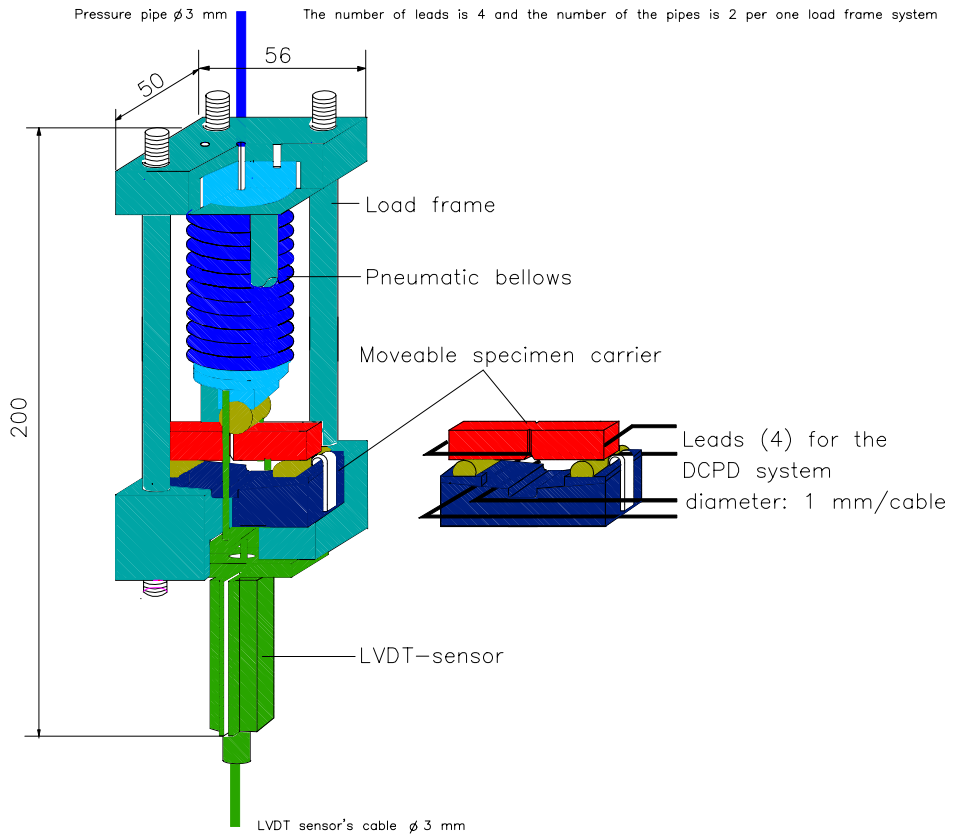


Figure 5. Load frame system for multi-specimen PSFM-device.

bellows, momentary crack length, as well as pressure, temperature and water chemistry parameters (pH, oxygen content and conductivity) were measured. The momentary crack length during both the tests in air as well as in simulated BWR conditions was measured using DC PD (Direct Current Potential Drop) technique. All fracture resistance tests were made displacement controlled.

4.4 Results - PSFM-device

Typical load and displacement curves as a function of time for AISI 304 stainless steel measured in air at a temperature of 288 °C with the PSFM-device are presented in Fig. 7.

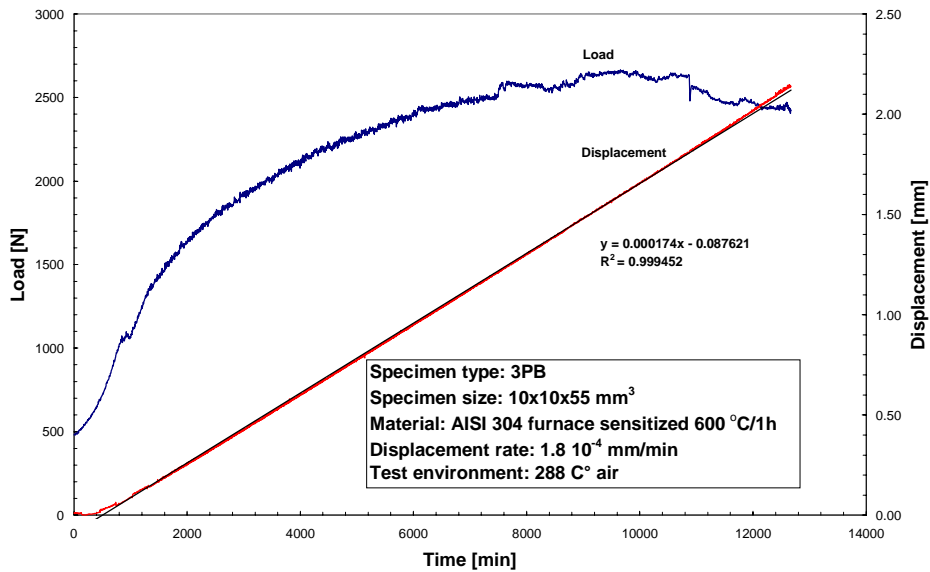


Figure 7. Typical load and displacement curves as a function of time in a fracture resistance test for AISI 304 determined with PSFM-device in air at a temperature of 288°C.

The displacement as a function of time shows linear behaviour except for the very beginning of the loading (time < 500 min). This non linearity is caused by compression of the gas in the bellow and compliance of the load frame. In order to be able to correct the non-linearity caused by load frame flexibility, the

compliance of the load frame system was measured with a calibration sample Fig. 8. Based on the data shown Fig. 8, the displacement non-linearity in the beginning of the test can be accounted for.

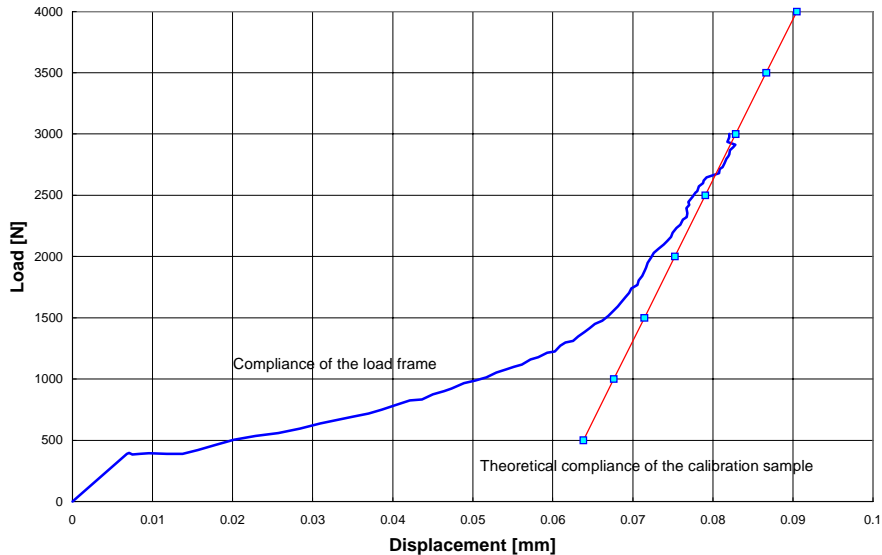


Figure 8. The compliance of the load frame and the calibration sample.

The target displacement rate in the test was $1.8 \cdot 10^{-4}$ mm/min. According to the measured data, the actual displacement rate was $1.74 \cdot 10^{-4}$ mm/min during the test, Fig. 7. The difference between the measured and the target displacement rates is small, i.e. 3.3%, and can be considered acceptable for all practical purposes.

In fracture resistance test performed for Inconel weld material under simulated BWR conditions using multi-specimen PSFM-device measured displacement and load as a function of time are presented in Fig. 9.

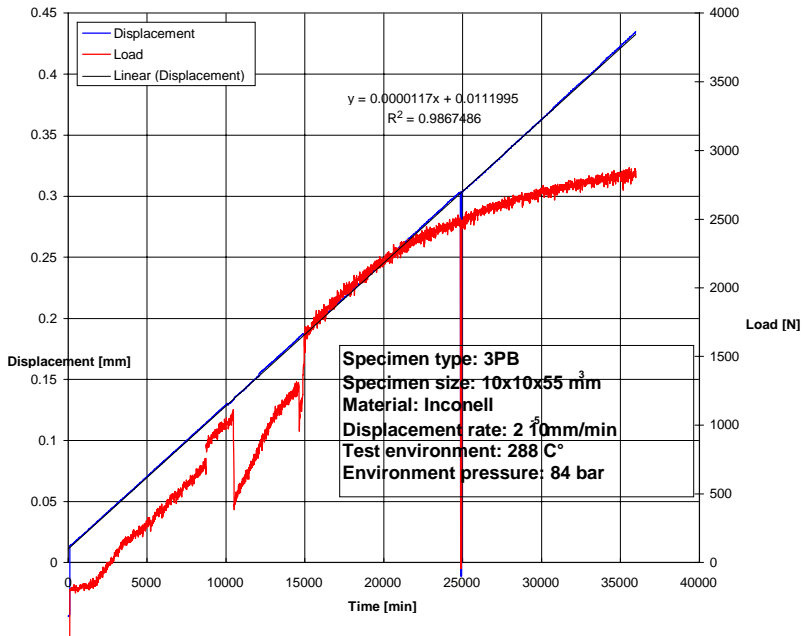


Figure 9. Displacement and load as a function of time in a slow fracture resistance curve determination for Inconel weld material performed with multi-specimen PSFM-device under simulated BWR conditions.

Also, under high temperature, high pressure BWR conditions the displacement rate produced by PSFM-device is constant and linear, Fig. 9. The maximum variation in the displacement values was $< 1 \mu\text{m}$. The target displacement rate was $1.2 \cdot 10^{-5} \text{ mm/min}$ and the actual displacement rate was $1.17 \cdot 10^{-5} \text{ mm/min}$ during the test, Fig. 9. The difference between the measured and target displacement rates is again small, i.e. 3.0%.

The possible pressure variations in the autoclave circulation loop was found not to have effect on the displacement rate. This is due to the accurate displacement feedback of the system.

4.5 Conclusions - PSFM-device

The newly developed pneumatic servo-controlled fracture resistance measuring device, PSFM-device, is suitable for performing constant load, constant displacement and constant displacement rate tests (fracture resistance curves) for small three point bend specimens in simulated light water environments. Even very low displacement rate, $0.2 \cdot 10^{-5}$ mm/min, can be achieved and accurately maintained constant in the fracture resistance test. The biggest advantages of PSFM-device are sensitivity in load and displacement control and measurements as well as its ability to compensate the pressure variations which test environment can cause. In addition, with multi-specimen PSFM-device simultaneous testing of six specimens is possible. This increases efficiency and lowers the costs for EAC data production remarkably.

5. Conclusions

- Small fracture mechanical three point bend specimens in constant displacement tests were found to reveal materials susceptibility for intergranular and transgranular stress corrosion cracking under simulated BWR conditions.
- Fracture mechanism (IGSCC / TGSCC) was found to be dependent on the loading rate.
- IGSCC crack growth rate is less sensitive to loading rate than TGSCC crack growth rate for austenitic stainless steel AISI 304 under simulated BWR conditions.
- Superposition based analysis method seems to be promising method for calculation of environmentally assisted crack growth rate.
- The newly developed pneumatic servo-controlled fracture resistance measuring device, PSFM-device, is suitable for performing constant load, constant displacement and constant displacement rate tests (fracture resistance curves) with great accuracy for small three point bend specimens in simulated light water environments. With multi-specimen PSFM-device

simultaneous testing of six specimens is possible. New testing facilities increase efficiency, lower the costs for EAC data production remarkably and enables testing of small irradiated specimens.

6. Acknowledgements

The reported work was part of the Finnish Research Programme on the Structural Integrity of Nuclear Power Plants 1995 - 1998, subproject RAVA3 on Material Degradation due to Corrosive Environment. The work presented in Chapter 2 was mainly made in 1996, in Chapter 3 in 1997 - 1998 and in Chapter 4 in 1995 - 1998.

Co-operation with Erkki Muttilainen from TVO Ltd, Rainer Rantala from the Radiation and Nuclear Safety Authority, STUK, Ossi Hietanen from IVO Ltd. as well as Prof Hannu Hänninen, Helsinki University of Technology together with many other colleagues is gratefully acknowledged. The work presented in Chapter 4 is a part of the international Cooperative IASCC Research (CIR) Program which is coordinated by EPRI. The work presented in Chapter was partly funded by the Finnish Fusion Energy Research programme, FFUSION.

References

Horn, R. M. 1986. Evaluation of crack growth in oxygenated high temperature water using full size pipe tests. Transactions of the ASME, 108, pp. 50 - 56.

Hishida, M., Saito, M., Hasegawa, K., Enomoto, K. and Matsuo, Y. 1986. Experimental study on crack growth behavior for austenitic stainless steel in high temperature pure water. Transactions of the ASME, 108, pp. 226 - 233.

Karjalainen-Roikonen, P. and Wallin K. 1992. Analysis of fracture mechanical tests for stress corrosion cracking. ECF 9, Reliability and Structural Integrity of Advanced Materials, Vol. II, S. Sedmak, A. Sedmak and D. Ruzic (Eds.).

MacDonald, D. D., Cragolino, G., Chung, P. C. and Yoshitake, A. 1985. Crack growth rates in type-304 stainless steel in simulated BWR water. California: EPRI.

Toivonen, A. and Aaltonen, P. 1997. Irradiation assisted stress corrosion cracking, IASCC. Progress report 1997. Espoo: VTT Manufacturing Technology (Report VALB228).

Moilanen, P. 1995. Pneumatic servo-controlled fracture resistance measuring device. Helsinki University of Technology, Faculty of Mechanical Engineering. M.Sc. Thesis. 87 p. (In Finnish).

(See Appendix 1 for a comprehensive listing of publications)

Modelling of environmentally assisted cracking

Pertti Aaltonen, Timo Saario, Hannu Hänninen*, Jussi Piippo**,
Ulla Ehrnstén, Marjo Itäaho*
VTT Manufacturing Technology
Helsinki University of Technology*
Cormet Ltd.**
Espoo, Finland

1. Introduction

During the use of nuclear reactors the properties of the structural materials change. Variations in the operation environment, such as changes in water chemistry, may enhance the development and growth of flaws. Neutron radiation causes embrittlement for in-core vessel materials. Radiation, together with water chemistry, increases the possibility of stress corrosion cracking in stainless steels and superalloys used in the reactor internal parts. Research on structural materials endeavours to study the ageing mechanisms of materials, and the possibilities and methods of preventing or forecasting the damage caused to structures by ageing.

2. Development of a Selective Dissolution - Vacancy Creep (SDVC) Model for environmentally assisted cracking of materials in high temperature water

Several mechanisms and models have been proposed to describe environmentally assisted cracking (EAC) principally in order to develop efficient remedial measures for this problem. Recent reviews describe most of the proposed EAC mechanisms and models in detail (Turnbull 1993, Newman

& Saito 1993, Hänninen 1986). The Selective Dissolution-Vacancy - Creep (SDVC) model (Aaltonen et al. 1996, Saario et al. 1995) has been proposed within the RATU2 programme. It is based on the idea of selective dissolution or oxidation, production of vacancies as well as deformation localisation to a shear band at the crack tip.

In this Selective Dissolution - Vacancy - Creep (SDVC) model for stress corrosion cracking (SCC) the rate determining step is the generation of cation vacancies by selective dissolution of metal cations through the existing passive film at the crack tip. The vacancies migrate towards the location of the maximum stress concentration enhancing and localising creep. Crack advance occurs by formation of a shear band at the crack tip, further influence of vacancies in the volume of the shear band and final breakdown of bonds between atoms as the vacancy concentration exceeds a critical value. Passivation of the freshly formed bare surfaces enhances generation of new cation vacancies, which then migrate towards the new location of the maximum stress concentration. After generation of a critical vacancy amount in the shear band ahead of the new crack tip, cracking can proceed. The environmental impact on SCC follows thus the changes in the film properties which has been characterised in water chemistry related sub-task within RATU 2.

The mathematical foundation, which is needed for development of the detailed model into a quantitative predictive tool has been formulated in a preliminary form. The model can be verified experimentally, and it can be used as a for basis of development of efficient remedial tools for mitigation and prevention of EAC problems in high temperature water. Important applications are expected for both secondary and primary water loops of NPP's.

The SDVC model was first verified for Alloy 600 in high temperature water environments. The latest research work has been devoted to expand the SDVC model to other materials known to be prone to environmentally assisted cracking. Key point in the conducted tests has been to verify various mechanisms of vacancy generation in brass, in hydrogen charged Alloy 600 and oxidised pure copper. Application of internal friction technique (IF) has been used to confirm the generation of excessive amounts of vacancies due to environmental surface reactions.

3. Application of the SDVC model on intergranular stress corrosion cracking (IGSCC) of Alloy 600, comparison with the experimental data

The SDVC model is suggested to be equally applicable to secondary and primary water SCC of Alloy 600 and it can be immediately used as a basis of development of efficient remedial tools for mitigation and prevention of e.g., intergranular stress corrosion cracking (IGSCC) in nuclear power plants (NPP).

The validity of the SDVC model was studied based on experimental and literature data. It was shown that the pH and temperature dependencies of IGSCC crack growth rate and the effects of zinc injection, hydrogen overpressure and grain boundary carbide distribution on the IGSCC crack growth rate of Alloy 600 are qualitatively in accordance with the model. The model also qualitatively predicts the effect of electrochemical potential on IGSCC crack growth rate. Based on the model a valid explanation was given for the experimentally observed IGSCC cracking at cathodic potentials. Also, the model was used to give a plausible explanation for the fact that IGSCC does not occur in Alloy 600 at potentials higher than about 0.3 V above the corrosion potential, as experimentally found in caustic solutions. In the following the SDVC model is compared with the experimental data on IGSCC of Alloy 600.

3.1 Effect of temperature - activation energy

The measured (apparent) activation energies of IGSCC of Alloy 600 range from 80 to 220 kJ/mol. All these values fall into the range expected for solid state diffusion of cations. In PWR primary water the activation energy in crack growth tests has been found to be about 160 kJ/mol. In the SDVC model for SCC of Alloy 600, the rate determining step is transport of cations through the existing passive film at the crack tip. Transport of cations requires a simultaneous flux of cation vacancies in the opposite direction. The activation energy of diffusion of iron cation in the oxide growing on AISI 316 stainless steel was found to be 145 kJ/mol, which is consistent with the activation energy of cation vacancy migration in magnetite and ferrite spinels. The fact that the activation energies of SCC crack growth for Alloy 600 are similar to the values

found for cation vacancy migration in spinel type oxides renders further credibility to the SDVC model.

3.2 Effect of pH

If transport of iron cations through the oxide film is both dominating the corrosion of Alloy 600 and the rate determining step in SCC of Alloy 600 in high temperature water, one would expect to have similar dependencies on pH and temperature for both phenomena. In fact, this is what is found when comparing the IGSCC crack growth rate of Alloy 600 as a function of pH and the similar dependency on pH at 300°C of the corrosion rate of stainless steel and Alloy 600. The rate of intergranular attack (IGA) of Alloy 600 in high temperature water also has the same dependency on high temperature pH. These data are in accord with the prediction based on the SDVC model.

3.3 Effect of hydrogen overpressure

In a review on the effect of hydrogen on SCC of Alloy 600 it was concluded at operating temperatures (320 to 330°C) the effect of hydrogen overpressure is small and that experiments can show either increasing or decreasing susceptibility to SCC.

Increase of hydrogen over-pressure is expected to increase the rate of hydrogen entry to the metal or to slow down the cathodic reaction. Also, from thermodynamic considerations it has been shown with mixing entropy calculations that ingress of hydrogen into the metal will increase the concentration of cation vacancies. This would be expected to increase shear band localisation and thereby also rate of SCC.

The SDVC model predicts that an increase in iron dissolution rate will increase the susceptibility to SCC of Alloy 600, because of increased production rate of cation vacancies.

3.4 Effect of Zn injection

Injection of Zn to primary water reduces the corrosion product release rate, i.e. dissolution rate, by a factor of about 3. At the same time the susceptibility of Alloy 600 to PWSCC decreases by a factor of roughly 2.5. Injection of Zn reduces the SCC crack growth rate of Alloy 600 in BWR water by roughly a factor of 2. Based on these results it seems plausible that Zn injection mitigates SCC through its decreasing effect on the dissolution rate. These data are considered to strongly support the basic ideas of the SDVC model.

3.5 Effect of yield stress and stress level

The maximum stress achievable ahead of the crack tip is relative to the yield stress. The higher the yield stress, the higher the maximum stress and the higher the vacancy concentration. Based on the SDVC model one expects that SCC crack growth rate increases when yield stress increases or when the amount of cold work increases. In pure water the SCC crack growth rate of Alloy 600 increases by roughly two orders of magnitude if the yield stress increases with a factor of roughly two. Cold work increases SCC velocity of Alloy 600 in both pure and primary water. It is also well established that cracking in operating steam generators is most likely to occur at locations of heavy cold work as well as at crevice areas.

3.6 Effect of grain boundary carbide distribution

In contradiction to the behaviour of sensitized stainless steel in BWR water, for Alloy 600 in PWR water a rather uniform coverage of grain boundaries by carbides is typically combined with a good resistance to IGSCC. Based on the SDVC model there are at least two plausible reasons for this occurrence. First, as described above, the fracture event in the SDVC model is preceded by formation of a shear band. A carbide at the grain boundary will most probably make the formation of the shear band more difficult and thereby mitigate IGSCC. Secondly, as discussed above, IGSCC of Alloy 600 occurs in the potential range where Fe^{2+} cation can exist in the passive film. Because carbon

when in solid solution is known to hinder the formation of Fe^{3+} on surface, partial removal of carbon from the metal near the grain boundaries by carbide precipitation will probably make formation of Fe^{3+} cation easier, thereby mitigating IGSCC.

4. Application of the SDVC model to hydrogen charging of Alloy 600

Hydrogen has been observed to affect significantly the initiation and growth of intergranular stress-corrosion cracking (IGSCC) of Alloy 600 in high-temperature aqueous environments. The better understanding of environmentally assisted cracking (EAC) of Alloy 600 requires improved knowledge of hydrogen behaviour in this alloy (Aaltonen et al. 1997a, Aaltonen et al. 1998a, Aaltonen et al. 1998d). Especially, the discrepancy between the low and high temperature hydrogen effects in EAC of Ni-base alloys needs more experimental data (Andresen & Angeliu 1997).

4.1 Experimental - hydrogen charging of Alloy 600

Hydrogen charging was performed in 1N H_2SO_4 + 5 mg/l NaAsO_2 solution in a thermostatic cell using a platinum counter electrode. Current density was kept constant during hydrogen charging and values from 0.3 to 100 mA/cm^2 were applied. Additionally, samples of about the same size were charged using current densities from 0.1 to 100 mA/cm^2 in the equivalent environment for hydrogen content measurements with a LECO equipment. Internal friction measurements were carried out with an inverted torsion pendulum in the temperature range of 90–500 K with the heating rate between 1 and 3 K/min.

4.2 Results - hydrogen charging of Alloy 600

A typical temperature dependence of internal friction and shear modulus for a hydrogen charged Alloy 600 sample is given in Fig. 1. In the temperature range of 100–500 K a complex damping process is observed, which can be separated into low-temperature, 100–270 K, and high-temperature, 270–500 K, peaks.

The height of the low-temperature peak does not depend on the oscillation frequency or heating rate at a current density of 1 mA/cm^2 , i.e., hydrogen content of about it. This is an evidence of its relaxation nature. The low-temperature hydrogen IF peak for the studied frequency range is localised in the temperature range of 175–195 K. Independence of the low-temperature peak position on frequency is typical for anelastic relaxation processes. On the other hand, the high-temperature peak changes its height when the frequency or the heating rate are changed. Such a behaviour, typical for a non-relaxation IF peak, allows one to assume that the high-temperature peak is caused by transition processes. Diffusion-controlled outgassing of hydrogen or hydride decomposition may be such processes, Fig. 1.

Strong evidence for the introduction of very high concentrations of vacancies and hydrogen-vacancy interactions has been obtained at high temperatures and high hydrogen pressures in Ni (Jagodzinski et al. 1995). No contribution of vacancies to the measured low-temperature IF peaks was observed in this study. In the case of vacancies the enthalpy of migration transitions in nickel would be higher, i.e., 1.32 eV (Shewmon 1989). The mixed effect of hydrogen atoms and vacancies can not be excluded. However, the binding energy between hydrogen and other interstitials like nitrogen, carbon or oxygen is expected to be about 0.1 eV or even smaller (Daw et al. 1983).

High-temperature IF peak revealed the formation of a hydride phase when the charging current density exceeded 1 mA/cm^2 . Cracks, obviously due to decomposition of the hydrides, became visible on the sample surfaces. In the PWR-plants hydride formation and crack initiation through hydride decomposition in creviced areas of Alloy 600 require reduced temperature and additionally reduced pH corresponding to the shut-down procedure (Andresen & Young 1995). That is why these observations can not be directly related to EAC of Alloy 600 in reactor environments at high temperatures, because hydrides are not stable at such a high temperature and additionally in hydrogen charging experiments using acidic electrolytes no oxide films were expected to be present. The results obtained may explain the initiation of IGSCC cracks observed in nuclear components. Thus, low temperature hydrogen embrittlement can be caused by the presence of hydrides and by the binding of hydrogen with dislocations.

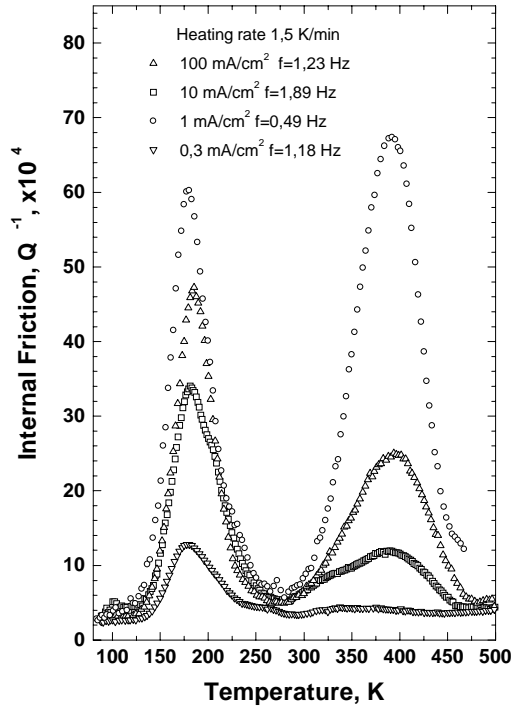


Figure 1. Internal friction peaks for Alloy 600 as a function of the charging current density.

The activation energy for Alloy 600 crack growth at high temperatures in reactor environments has been reported to be in the range of 80–220 kJ/mol (Cassagne et al. 1992). By assuming that Alloy 600 and nickel react in the same manner with hydrogen this value is higher than activation energy for hydrogen migration but approaches the value of migration activation energies for cations in oxides. The activation energy for the low-temperature hydrogen-induced cracking of steel is less than 20 kJ/mol (Andresen & Angeliu 1997), which corresponds well with the trapped interstitials in irradiated iron (Hasiguti 1973). It can, thus, be assumed that the crack growth rate of Alloy 600 in high temperature aqueous environments is mainly controlled by the changes taking place in the oxide film. The role of hydrogen in high temperature aqueous environments is believed to be related with the reduction or oxidation of nickel in the oxide (Totsuka & Szlarska-Smialowska 1987).

4.3 Conclusions - hydrogen charging of Alloy 600

In the hydrogenated Alloy 600 two internal friction peaks were detected in the temperature range of 100–270 K and 270–500 K, respectively. The low-temperature peak was shown to have a relaxation nature, while the high-temperature peak is caused by phase transformation processes.

The low-temperature peak is caused by a Snoek-like relaxation with an apparent enthalpy of activation of 38.5 kJ/mol, which corresponds to the data for hydrogen-induced Snoek-like peaks in Ni-base alloys.

A maximum in the peaks height dependency on the charging current density at 1.0 mA/cm² points out the formation of hydride phase in Alloy 600. Hydride phase decomposes during slow heating at temperatures lower than 500 K.

Crack initiation through hydride decomposition in creviced areas of Alloy 600 in PWR environments requires reduced temperature and pH corresponding to the shut-down procedure.

5. Application of the SDVC model to selective dissolution of brass

Selective dissolution of some of the alloying elements is an important consequence of interaction of alloys with passivating environments. In many models of environmentally assisted cracking (EAC) of alloys it is assumed that selective dissolution of passivated surfaces in alloys is accompanied with generation of significant amount of vacancies. The further dynamic reactions of these vacancies can lead to the initiation and growth of stress-corrosion / corrosion fatigue cracks.

Zinc alloys are known to suffer both selective dissolution as well as EAC. In this way they are useful alloys to validate partly the SVDC model and vacancy generation (Aaltonen et al. 1997b, Aaltonen et al 1998b).

5.1 Experimental - selective dissolution of brass

Creep tests of brasses carried out at constant load with electrochemical potential control in tap water at 80°C revealed a significant increase of the strain rate when the applied potential was increased to the level required for the formation of CuO as the outermost component of the oxide film on the brass surface (Itäaho 1995). Formation of CuO oxide on the top of the pre-existing ZnO and Cu₂O results in an increase of the electrical resistivity of the whole layer by more than two orders of magnitude and, respectively, in an increase of zinc dissolution provided by the cation current through the oxide layer, Fig. 2. According to the present ideas concerning anodic films (McDonald 1992), maintenance of the cation current requires vacancy generation at the metal/oxide/electrolyte film interface and their diffusion through the oxide film into the bulk metal.

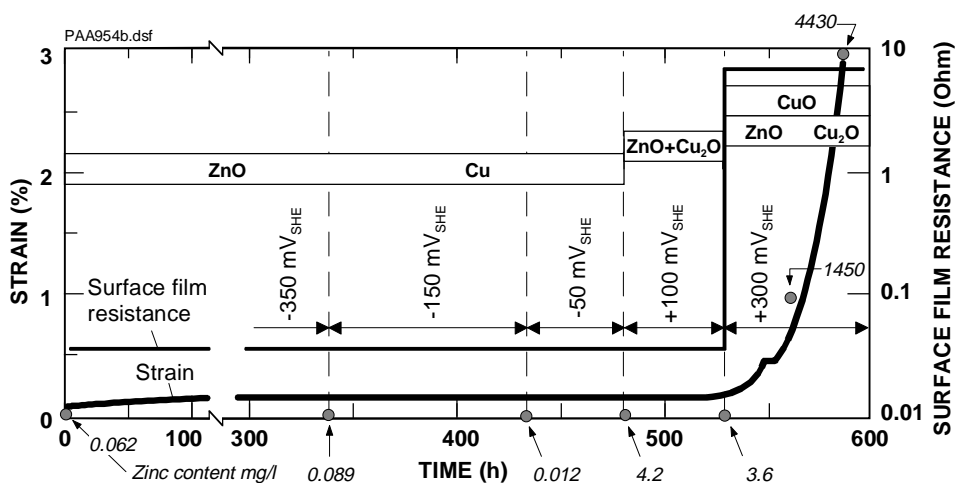


Figure 2. The measured strain in CuZnAlFe brass during constant load creep test in tap water at 80°C. The potential of the specimen was increased step-wise. The surface film resistivity and dissolved zinc content in test solution were measured at the end of each period at adjusted potential.

Oxidation of test materials for internal friction measurements were carried out in tap water at 80°C, i.e., the temperature at which industrial brasses with high Zn content exhibit rapid SCC in tap water (Itäaho 1995). Electrochemical

polarization was performed in two steps. First, Cu₂O component was introduced next to the pre-existing ZnO oxide film at the potential of +100 mV_{SHE} for 2 hours. In the immediately following second stage, at the potential of +350 mV_{SHE} CuO oxide film was formed on the top of the previous oxide layers for 10 hours. This resulted in a bilayer oxide film structure that consisted of ZnO/Cu₂O inner layer and CuO outer layer (Aaltonen et al. 1996).

IF measurements were carried out with an inverted torsion pendulum in the temperature range of 90–500 K with the heating rate of 1.5 K/min. Oscillation frequency was about 1 Hz and the amplitude was of the order of magnitude of 10⁻⁶. Samples with the dimensions of about 40 × 2 × 0.5 mm³ were cut by a diamond saw and polished with 800 grit emery paper.

5.2 Results - selective dissolution of brass

Temperature dependencies of IF in brass are given in Fig. 3. When electrochemical oxidation of brass leads to significant dissolution of Zn temperature dependencies of IF reveal well defined peaks in the temperature range of 200–350 K.

Complex two-component peak attributed to the interaction of excessive vacancies with dislocations is observed in the temperature range of 200–350 K in the temperature dependence of low-frequency internal friction of brasses after electrochemical oxidation and combined selective dissolution of Zn.

Comparison of the IF results with the positron annihilation data for dezincified brasses allows to conclude that peak P1 (at about 200 K) is related to unpinning and peak P2 (at about 300 K) to repinning of dislocations by excessive vacancies produced during oxidation.

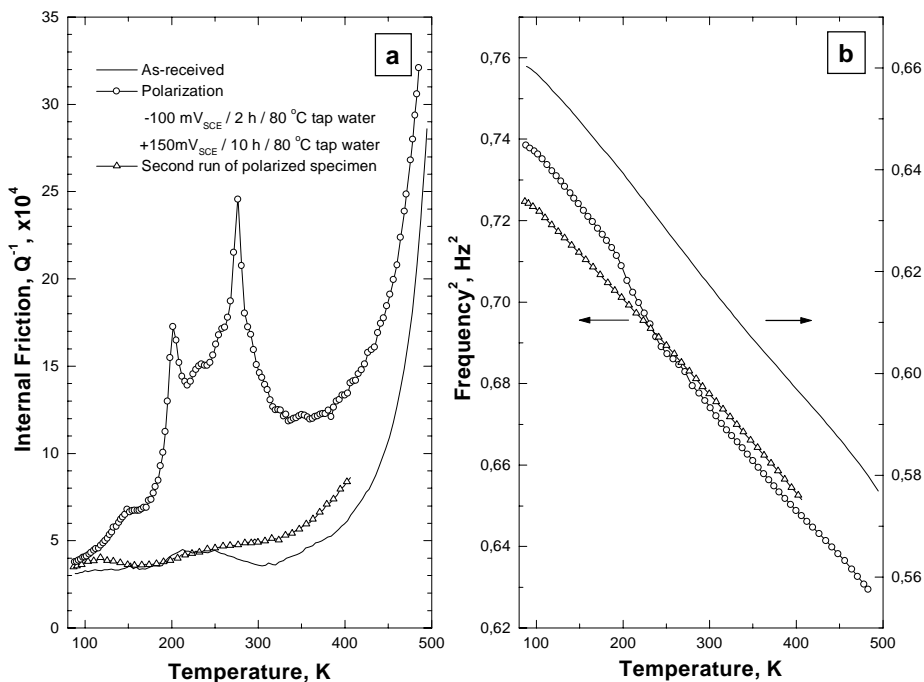


Figure 3. Temperature dependence of IF in brass oxidized in tap water at 80°C. During oxidation at +150 mV_{SHE} the selective dissolution of zinc has taken place.

5.3 Conclusions - selective dissolution of brass

Excessive amount of vacancies produced during oxidation in tap water at 80°C and the combined selective dissolution of Zn cause significant changes in the dislocation structure and, apparently, dynamic annihilation of vacancies play an important role in environmentally assisted creep and stress-corrosion cracking of these alloys.

6. Application of the SDVC model to oxidation of copper

Copper has two different types of oxides i.e., Cu_2O and CuO . The former grows through oxygen migration to the bulk metal but the latter grows through the copper cation migration through the Cu_2O film and oxidation at the electrolyte/oxide interface. As shown earlier for brass, polarisation to the range where CuO is the stable oxide results in excessive amounts of vacancies being rejected into bulk metal. It may be assumed that the same takes place for pure copper as well. In nitrite solutions at potentials where CuO is formed copper has been shown to suffer from SCC. The aim of this study is to reveal the changes in mechanical properties of bulk copper after oxidation in a passivating environment. The internal friction (IF) technique was also used in this study due to its high sensitivity to changes in the defect structure of metals (Aaltonen et al. 1998c).

6.1 Experimental - oxidation of copper

Temperature dependence of IF Q^{-1} and free oscillation frequency squared f^2 (in other words, shear modulus) were measured in the temperature range of 90–500 K with an inverted torsion pendulum. Torsion strain amplitude did not exceed $2.5 \cdot 10^{-6}$, frequency of free oscillation was about 1 Hz. Heating rate was maintained constant at the level of 1.5 K/min.

Oxidation was performed in 0.3 M NaNO_3 solution at 80°C for copper working electrodes. Oxidised conditions were selected based on the earlier EAC studies so that a thin layer of Cu_2O (dark brown film) was formed during 2 h at -150 mV_{SCE}, after which a layer of CuO (black film) was formed during 10 h at +100 mV_{SCE}. This oxidation sequence leads in a brass to a significant growth of the strain rate in the creep experiments and transgranular EAC in a tap water environment in brass (Itäaho 1995).

In addition to the annealed Cu samples subjected to oxidation and referred to as A-samples, cold deformed samples subjected to oxidation after deformation referred to D-samples were studied as well. D-samples were produced by

bending the annealed samples in two steps: first they were deformed up to 5% at room temperature, then after exposure for 10 min in air at room temperature they were bent back at liquid nitrogen temperature. The amount of cold deformation achieved exceeds significantly all non-controlled deformations possibly introduced during the sample installation into the IF machine.

6.2 Results - oxidation of copper

Temperature dependence of Q^{-1} and f^2 for A- and D-samples is given in Fig. 4. A set of peaks can be observed both for A- and D-samples. The temperature positions of the peaks suggest that they are the Hasiguti peaks (Okuda & Hasiguti 1963). The Q^{-1} dependence of both types of treatment is qualitatively similar, although in the whole temperature range the background and the heights of the peaks are higher for samples subjected to oxidation.

The results of the deconvolution of the IF peaks based on broadened Debye peaks are shown in Table 1. It was assumed that the observed peaks had a lognormal distribution of the relaxation time (Nowick & Berry 1972). Typical heights and temperature positions of the peaks (see Table 1) correspond to those of the Hasiguti peaks (Okuda & Hasiguti 1963, Koiwa & Hasiguti 1963). The temperature positions of the Hasiguti peaks P_1 , P_2 and P_3 were found to be 145, 166 and 230 K, respectively, for the frequency of 1 Hz (Nowick & Berry 1972).

Exposure of an A-sample at 310 K for half an hour after the first run diminishes significantly the P_3 peak. Low-temperature P_1 peak changes after this exposure only slightly, but it is completely suppressed after annealing at temperatures higher than 400 K (3-rd run in Fig. 4). The temperature positions of peaks P_1 , P_2 and P_3 observed in the present study (Table 1) are lower compared to the above mentioned values for the Hasiguti peaks at the frequency of 1 Hz, although the frequency of A-sample in this case was higher, about 1.5 Hz.

Table 1. Deconvolution of the IF peaks for A- and D-samples.

Sample Component	A-sample, 1-st run			A-sample, 2-nd run			D-sample		
	P ₁	P ₂	P ₃	P ₁	P ₂	P ₃	P ₁	P ₂	P ₃
Height of peak , ×10 ⁴	11.0	2.0	11.2	6.7	0.2	2.7	1.2	0.6	4.0
Temperature position of peak, K	144	161	226	145	162	226	134	153	218
Width of peak, β- parameter	4.3	1.1	4.2	0.7	3.5	4.2	0.01	2.3	1.9
Background, ×10 ⁴	23.0			19.0			10.3		

The A-samples revealed a significant decrease of the shear modulus after oxidation compared to the annealed state (see 1-st and 3-rd runs in Fig. 4b). This has also been observed in the case of pure copper irradiated with electrons (Marx et al. 1981). Modulus defect is as high as 3.3% at 250 K, which is about the same (3.8%) for the irradiated copper (Marx et al. 1981). After an exposure at 310 K for half an hour, partial recovery of the modulus defect takes place. The amount of the recovery is approximately 1%.

6.3 Conclusions - oxidation of copper

Oxidation of pure copper in 0.3 M NaNO₂ solution under certain electro-chemical conditions results in Hasinger peaks on the temperature dependence of low-frequency internal friction.

Formation of an oxide layer on the surface of copper in the studied passivating environment is accompanied with generation of excessive amounts of metal vacancies at the Cu/Cu₂O interface, which then diffuse into the bulk metal.

Flux of excessive vacancies results in dislocation multiplication and rearrangement of dislocation structures due to osmotic stress. Thus, oxidation of

the metal surface in a passivating environment inducing EAC is accompanied with long-range effects in the bulk metal.

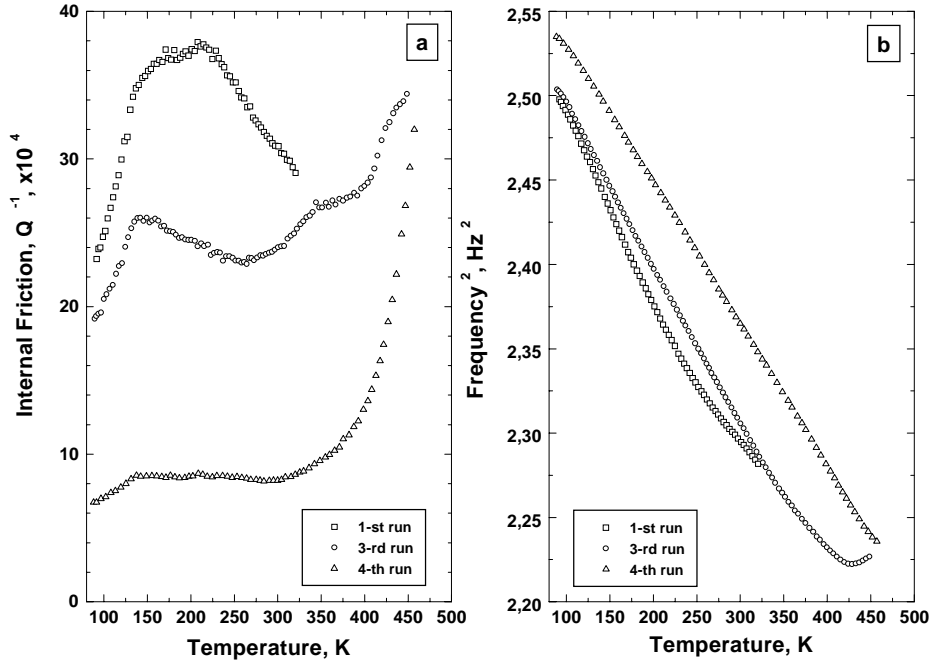


Figure 4. Temperature dependence of internal friction Q^{-1} (a) and oscillation frequency f^2 (b) for copper: A-samples were polarized in 0.3 M NaNO_2 solution for 2 h at $-150 \text{ mV}_{\text{SCE}}$ and for 10 h at $+100 \text{ mV}_{\text{SCE}}$ at 353 K (80°C). During first run and second run (not shown) heating was performed up to 320 K, and during third and fourth runs up to 450 K.

7. Conclusions

A new Selective Dissolution - Vacancy Creep (SDVC) model for environmentally assisted cracking (EAC) of materials in high temperature water is described. The model is based on the idea of selective dissolution or oxidation, production of vacancies as well as deformation localisation to a shear band at the crack tip. The experimental observations made for intergranular stress corrosion cracking (IGSCC) of Alloy 600, hydrogen charging of Alloy

600, selective dissolution of brass and oxidation of copper support SDVC-mechanism.

8. Acknowledgements

The reported work was part of the Finnish Research Programme on the Structural Integrity of Nuclear Power Plants 1995 - 1998, subproject RAVA3 on Material Degradation due to Corrosive Environment.

Co-operation with Erkki Mutttilainen from TVO Ltd. and Ossi Hietanen from IVO Ltd. together with many other colleagues is gratefully acknowledged.

References

Aaltonen, P., Saario, T., Karjalainen-Roikonen, P., Piippo, J., Tähtinen, S., Itäaho, M. & Hänninen, H. 1996. Vacancy-creep model for EAC of metallic materials in high temperature water. Corrosion '96, NACE, Denver, USA. Paper No. 81. 12 p.

Aaltonen, P., Jagodzinski, Y., Tarasenko, A., Smouk, S. & Hänninen, H. 1997a. Influence of hydrogen charging on mechanical behaviour of Inconel-600 alloy measured by internal friction. Proceedings of the 8th International Symposium on Environmental Degradation of Materials in Nuclear Power Systems - Water Reactors, Amelia Island, USA, 10 - 14 August 1997. Vol. 1. American Nuclear Society. Pp. 325 - 332.

Aaltonen, P., Saario, T., Ehrnstén, U., Itäaho, M. & Hänninen, H. 1997b. Selective dissolution-vacancy-creep model for EAC of brass. In: Magnin, Thierry (Ed.) Corrosion-Deformation Interactions CDI '96. Second International Conference on Corrosion-Deformation Interactions in conjunction with EUROCORR'96. Nice, France, 1996. The Institute of Materials. Pp. 35 - 44.

Aaltonen, P., Bojinov, M., Ehrnstén, U., Lagerström, J., Laitinen, T., Saario, T. & Sirkiä, P. 1998a. The effect of environment on the electric and electrochemical properties of surface films on alloy 600 and alloy 690 in pressurised

water reactor primary water (Poster). Proceedings of the International Symposium Fontevraud IV Contribution of Materials Investigation to the Resolution of Problems Encountered in Pressurized Water Reactors. Vol. II. Pp. 861 - 872.

Aaltonen, P., Jagodzinski, Y., Tarasenko, A., Smouk, S. & Hänninen, H. 1998b. Internal friction in brasses after oxidation in tap water by anodic polarisation. *Acta Materialia*, Vol. 46, No. 6, pp. 2039 - 2046.

Aaltonen, P., Jagodzinski, Y., Tarasenko, A., Smouk, S. & Hänninen, H. 1998c. Low-frequency internal friction of pure copper after anodic polarisation in sodium nitrite solution. *Corrosion Science*, Vol. 40, No. 6, pp. 903 - 908.

Aaltonen, P., Jagodzinski, Y., Tarasenko, A., Smouk, S. & Hänninen, H. 1998d. Study of Snoek-type relaxation in hydrogenated Inconel 600. *Philosophical Magazine*, Vol. A 78, No. 4, pp. 979 - 994.

Andresen, P. L. & Young, L. M. 1995. Characterization of the roles of electrochemistry, convection and crack chemistry in stress corrosion cracking. Proc. of Seventh Int. Symposium on Environmental Degradation of Materials in Nuclear Power Systems – Water Reactors. Breckenridge, Colorado, August 7 - 10, 1995. Houston, TX: NACE International. Pp. 579 - 591.

Andresen, P. & Angelu, T. 1997. Evaluation of the role of hydrogen in SCC in hot water. *Corrosion-97*, NACE, New Orleans, Paper No. 195. 12 p.

Cassagne, T., Combrade, P., Foucoud, M. & Gelpi, A. 1992. The influence of mechanical and environmental parameters on the crack growth behaviour of alloy 600 in PWR primary water. Proc. of 12th Scandinavian Corrosion Congress & Eurocorr '92, Espoo, Finland, 31 May - 4 June, 1992, Vol. 2. Helsinki: The Corrosion Society of Finland. Pp. 55 - 67.

Daw, M. S., Bisson, C. L. & Wilson, W. D. 1983. Calculation of the binding of hydrogen to fixed interstitial impurities in nickel. *Metallurgical Transactions A*, Vol. 14A, No. 7, pp. 1257 - 1260.

Hasiguti, R. R. 1973. Defect clusters in connection with the presence of impurity atoms in neutron irradiated BCC metals. Defect and Defect Clusters in B.C.C Metals and Their Alloys, Nuclear Metallurgy, Vol. 18, Ed. R. J. Arsenault. Gaithersburg, Maryland: National Bureau of Standards. Pp. 1 - 18.

Hänninen, H. 1986. Comparison of proposed stress corrosion cracking mechanisms. Proceedings of 10th Scandinavian Corrosion Congress, Stockholm, Sweden. Pp. 405 - 412.

Itäaho, M. 1995. The effect of environment on the creep and fracture behaviour of materials. Espoo: Helsinki University of Technology. MSc. Thesis. 96 p.

Jagodzinski, Y., Larikov, L. & Smouk A. 1995. Positron annihilation study of vacancy defects nucleation during deformation of hydrogen charged nickel. Physica Status Solidi, A, Vol. 149, No. 2.

Koiwa, M. & Hasiguti, R. R. 1963. Acta Metallurgica, Vol. 11, No. 1215.

Marx, F. P., Sokolowski, G. & Lücke, K. 1981. Influence of oxidizing and reducing pre-treatments on the internal friction of electron irradiated copper, Journal de Physique, Coll. C5, suppl. 10, 42, C5 241.

McDonald, D. D. 1992. The point defect model for the passive state. Journal of the Electrochemical Society, Vol. 139, No.12, p. 3434 - 3449.

Newman, R. C. & Sato, M. 1993. Anodic stress-corrosion cracking: slip-dissolution and film-induced cleavage. Proceedings of International Conference on Corrosion-Deformation Interactions, CDI'92, T. Magnin and J. M. Gras (Eds). Les Editions de Physique Les Ulis. Pp. 3 - 26.

Nowick, A. S. & Berry, B. S. 1972. Anelastic relaxation in crystalline solids. New York & London: Academic Press. 677 p.

Okuda, S. & Hasiguti, R. R. 1963. Acta Metallurgica, Vol. 11, No. 257.

Saario, T., Aaltonen, P., Karjalainen-Roikonen, P., Piippo, J., Mäkelä, K., Tähtinen, S. & Hänninen, H. 1995. Selective Dissolution - Vacancy - Creep

model for IGSCC of Alloy 600. Proceedings of the Seventh Int. Symposium on Environmental Degradation of Materials in Nuclear Power Systems - Water Reactors. Breckenridge, Colorado, USA, 7 - 10 August 1995. Houston, TX: NACE International. Pp. 841 - 854.

Shewmon, P. 1989. Diffusion in Solids. 2nd Ed. Warrendale, Pennsylvania: TMS. 241 p.

Totsuka, N. & Szlarska-Smialowska, Z. 1987. Effect of electrode potential on the hydrogen induced IGSCC of alloy 600 in high temperature aqueous environments. Corrosion, Vol. 43, pp. 734 - 738.

Turnbull, A. 1993. Modelling of environmental assisted cracking. Corrosion Science, Vol. 34, No. 6, pp. 921 - 960.

(See Appendix 1 for a comprehensive listing of publications)

Oxide films in high temperature aqueous environments

Timo Laitinen, Kari Mäkelä, Timo Saario and Martin Bojinov
VTT Manufacturing Technology
Espoo, Finland

1. Introduction

The evaluation of modified water chemistries as well as of the effects of increased power output in nuclear power plants is associated with a need to understand their effect on occupational dose rates and on environmentally assisted cracking as well as other types of corrosion of structural materials.

Occupational dose rates are due to activity build-up on the primary circuit components, which in turn depends on the dissolution, transport, deposition and incorporation of the activated corrosion products in the oxide films formed on material surfaces. Accordingly, activity build-up is influenced by the electrochemical and electric properties of the oxide films and by the water chemistry of the coolant. Concerning different types of corrosion, it can with good reason be assumed that both the oxidation reaction related to corrosion (e.g. crack growth) as well as the coupled cathodic reaction involve steps in which charged species are transported through the oxide films formed on material surfaces either within the crack or on surfaces exposed to the bulk coolant.

In spite of the significant work of Robertson [1] and others, it can be stated that a sufficient characterisation and a satisfactory model for the electrochemical behaviour and electric properties of the oxide films formed in nuclear power plants are not available. More experimental support is needed concerning especially the preferential paths and driving forces for ion transport as well as the nature of mobile species or defects. The lack of sufficient understanding has complicated the assessment of the applicability and possible side-effects of e.g.

noble metal water chemistry and the injection of zinc as a means to prevent the uptake of activated corrosion products into corrosion films.

The long-term aim of the work performed within the present research program is to minimise the risk of activity build-up, environmentally assisted cracking (EAC) and other types of corrosion, as well as to be prepared for the evaluation and introduction of modified water chemistries in Finnish power plants. To achieve this, the focus of this project is on understanding the mechanism of the incorporation of radioactive species into the different layers of the oxide film, as well as the transport phenomena contributing to stress corrosion cracking and other corrosion phenomena. This requires modelling the electrochemical behaviour and electrochemical and electric properties of oxide films formed on iron- and nickel-based alloys in relevant conditions.

The project is divided into four sub-projects as follows:

- Behaviour of oxide films in plant conditions
- Oxide films in simulated plant conditions
- Modelling the processes in oxide films on metal surfaces
- Development of electrochemical techniques for high-temperature measurements

2. Oxide films in real plant conditions

To correlate the extent of activity incorporation with the structural properties of oxide films in a VVER plant, stainless steel samples with different initial surface treatments were exposed to the primary coolant at Loviisa unit 2 and removed for analysis at regular intervals [2]. This was accompanied by high temperature water chemistry monitoring and analysis of grab samples of the coolant.

2.1 Results and discussion

The samples were made of OX18H10T stainless steel (similar to AISI 321 SS; a titanium stabilized stainless steel). Their surfaces were initially either pre-oxidised, polished or decontaminated. In the latter case the samples were prepared from pieces cut from the primary circuit drainage line at Loviisa unit 2.

Changes in the activity levels in oxide films as a result of exposure to the primary coolant at Loviisa unit 2 for various periods of time are shown in Fig. 1.

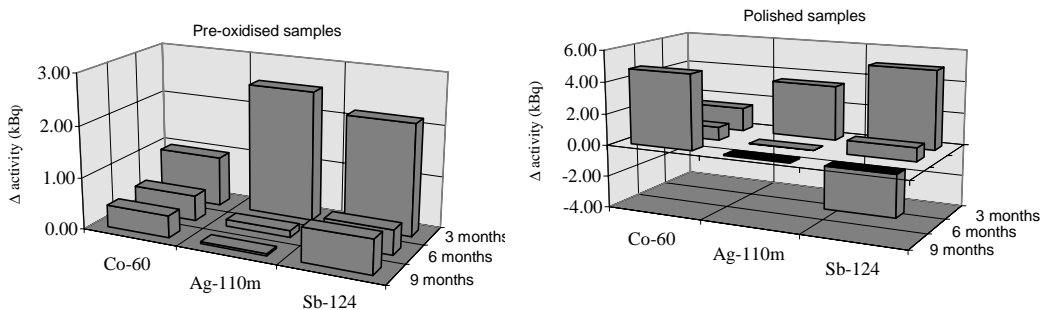


Figure 1. Changes in activity level (Δ) during successive exposure periods of 3 months.

The total activity in all of the studied oxide films increased during the first 9 months of the fuel cycle. However, contribution of different isotopes to total activity changed during the nine months exposure period. Furthermore some differences in activity incorporation into the oxide films were observed between samples with different initial surface treatments. In general, rather high rate of activity incorporation on all samples during the first exposure period of three months may be attributed to the high rate of oxide growth and to the changes in oxide structure. The highest increase in total activity levels was measured for the polished surface after the three months exposure period. The most significant contribution to the increase of activity levels came from Ag-110m and Sb-124 as shown in Figure 1. However, the contribution from these isotopes has become less important during the subsequent exposure periods for the polished samples and also for the decontaminated ones because of the decreasing contribution of Co-60. For the pre-oxidised surfaces the effect of

Sb-124 is still significant, due to the increasing contribution of Co-60 incorporation as shown in Figure 1.

The cross section Scanning Electron Microscope (SEM) micrographs taken from samples confirmed that the differences in activity pickup into the sample surfaces can be partly explained by the differences in oxide film thickness. The thicker the oxide, the more it can incorporate activated corrosion products. However, the elemental composition of the oxide film should affect the affinity of oxide to pick up activated corrosion products and therefore Secondary Ion Mass Spectrometry (SIMS) profiles of different alloying elements will be measured and analysed in detail in the near future.

2.2 Concluding remarks on oxide films in plant conditions

The activity levels increased in all of the studied oxide films, as expected, but some differences between samples was observed. At the moment it is unclear which have been the controlling parameters in reducing the Co-60 incorporation into the oxide film on pre-oxidised samples. Similarly more information is needed of the compositions of the oxide films on polished and decontaminated samples to evaluate the causes of an increase in Co-60 incorporation.

During the steady-state operation the levels of soluble and insoluble activated corrosion products in the coolant are known to be low resulting in a fairly low rate of activity in-corporation into the oxide whereas during the start-ups and shutdowns the situation is totally different. Therefore, in order to understand factors affecting activity incorporation into oxide films, this test program is being extended to cover the cool-down and heat-up stages as well. This will make it possible to search for correlations between different stages of the fuel cycle and the changes in oxide properties and oxide growth kinetics as well as factors mainly determining activity incorporation into the oxide films.

3. Oxide films in simulated plant conditions

3.1 Activity pickup in zinc doped PWR oxides

Several studies have been carried out to evaluate the effects of different blocking agents to reduce the incorporation of radioactive species into oxide films growing in typical PWR environments. The results have shown that dissolved zinc in the range of 10 to 40 ppb reduces the pickup of Co-60 by a factor of 8 to 10. The aim of the current work was to clarify the long-term beneficial effects of zinc addition as well as to find out the possible changes in activity pickup behaviour when the zinc addition is interrupted [3].

3.1.1 Results and discussion

The oxides formed on stainless steel samples exposed to simulated primary PWR coolant during three subsequent zinc injection periods were thin and dense, and the oxide thicknesses remained almost constant (see Fig. 2). After the zinc dosing periods, the oxide films were found to be enriched with Cr when compared with the base metal composition, and incorporation of Zn was clearly detected (see Fig. 3). Incorporation of Co-60 into the oxide films was found to be low during the zinc injection periods. The elemental depth profiles in the oxide films were found to remain unchanged during the subsequent injection of Zn.

The activity incorporation into the stainless steel oxides started to increase as soon as zinc dosing to the coolant was stopped (Fig. 2). However, the Co-60 concentration was lowest on the samples which were first oxidised in Zn containing primary coolant. This could indicate that zinc in the oxide continued to block the adsorption sites for Co-60 incorporation even though Zn concentration in the coolant was lower than 1 ppb. After the zinc injection period the thicknesses of all oxide films increased which partly explains also the increase in total activity incorporation.

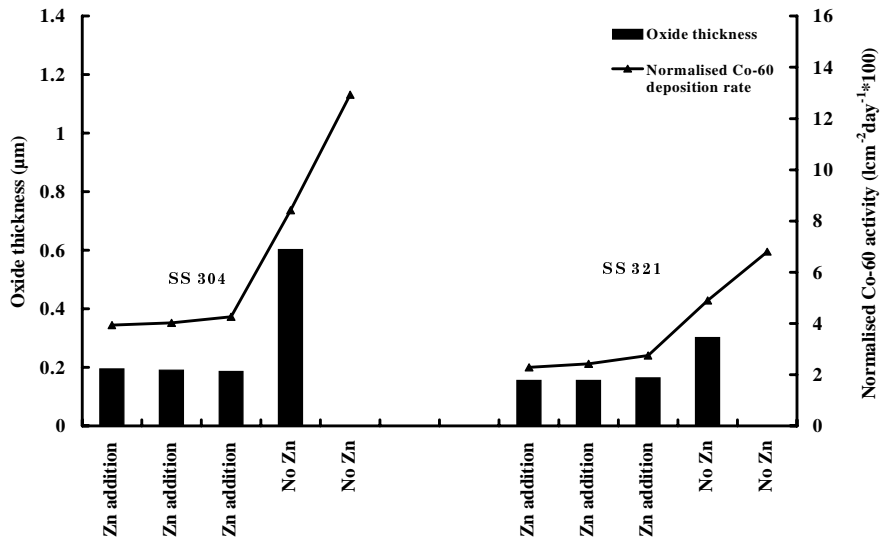


Figure 2. Oxide thicknesses and normalised Co-60 pickup rates onto the new SS samples during exposures to different test phases.

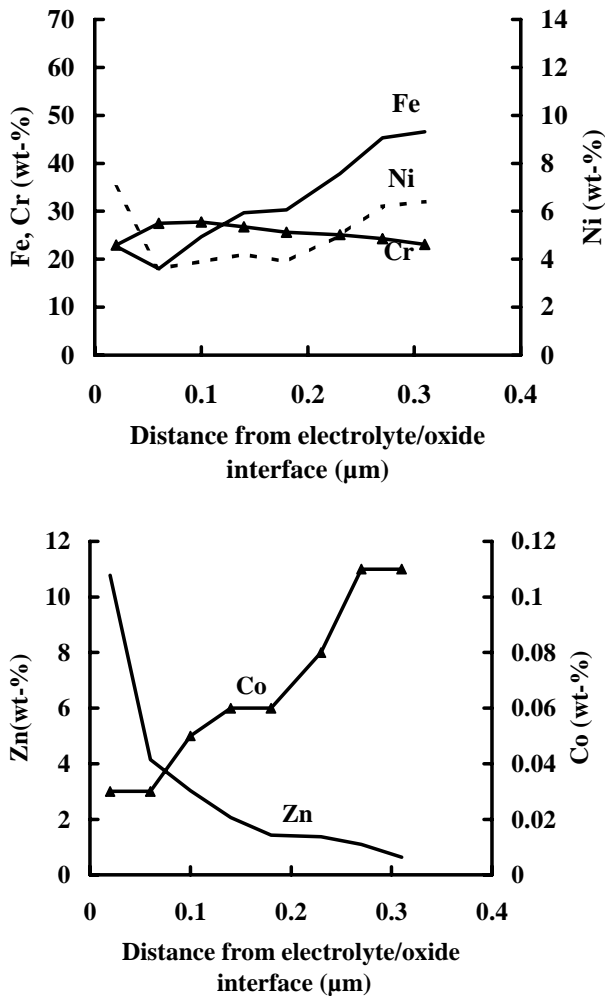


Figure 3. Profiles of alloying elements in the oxide on the new SS 304 sample after 3 zinc addition periods (over 300 days).

3.1.2 Concluding remarks on activity pickup

During the zinc injection periods the oxide films did not grow in thickness. This may indicate that zinc further inhibits ion transport through the chromium rich oxide film which typically behaves like a barrier layer for ion transport in the oxides. The lower ion transport through the oxide films should result in

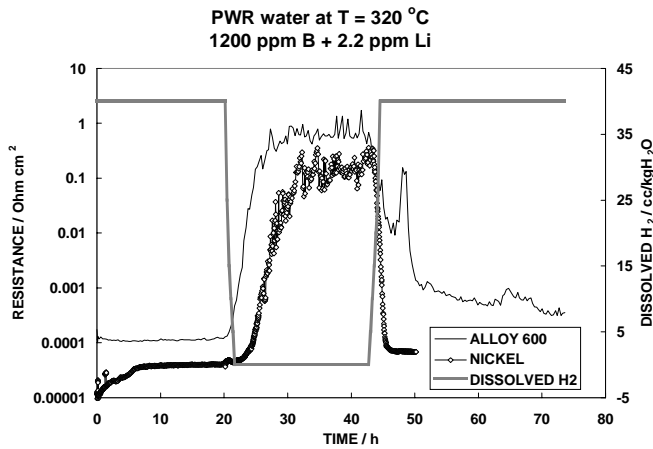
thinner oxides which was also observed in these measurements. As soon as the zinc injections were stopped, the activity incorporation into oxides increased and so did the measured oxide film thicknesses. Therefore, for zinc injection to be effective it should be carried out continuously. However, the actual mechanism by which Zn inhibits the activity incorporation into the oxides is still not clear. These studies suggested that zinc addition should be a cost effective method to reduce the rate of activity build-up on the primary circuit surfaces in PWRs as it has been shown to be in BWRs.

3.2 Comparison of surface films on Alloys 600 and 690 in PWR coolant

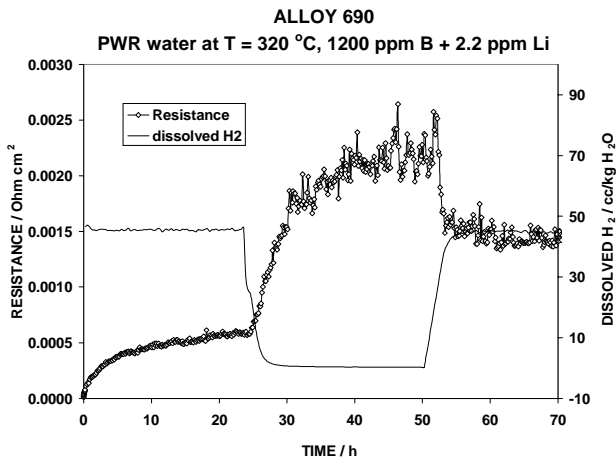
The objective of this study was to obtain *in situ* information on the electronic and electrochemical properties of surface films forming on Cr, Fe, Ni, Alloy 600 and Alloy 690 in PWR water at 320 °C both in the presence and absence of dissolved hydrogen [4]. This information is used as a basis to evaluate the validity of some assumptions used in existing models for high-temperature oxidation and environmentally assisted cracking of Alloy 600 and Alloy 690.

3.2.1 Results and discussion

The results shown in Fig. 4 demonstrate that the removal of hydrogen from the PWR coolant influences the electronic resistance on Alloy 600 and pure Ni (measured using the contact electric resistance (CER) technique) in almost equal ways: the value of the resistance increases significantly and reaches an almost constant level (see Fig. 4). In the case of pure Ni, the reason for the increase in the resistance may be the fact that metallic Ni is stable in the presence of sufficient amount of dissolved hydrogen, while NiO is formed when dissolved hydrogen is removed. The fact that Alloy 600 behaves in a similar way to pure Ni may indicate that the surface film on Alloy 600 resembles that of pure Ni. This interpretation is supported by the work of Fish et al. [5].



a)

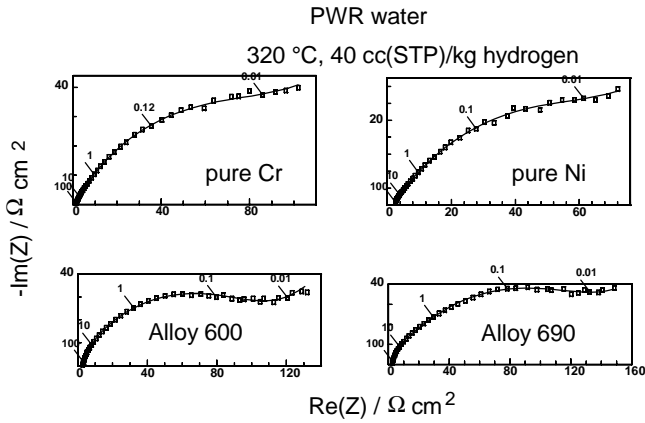


b)

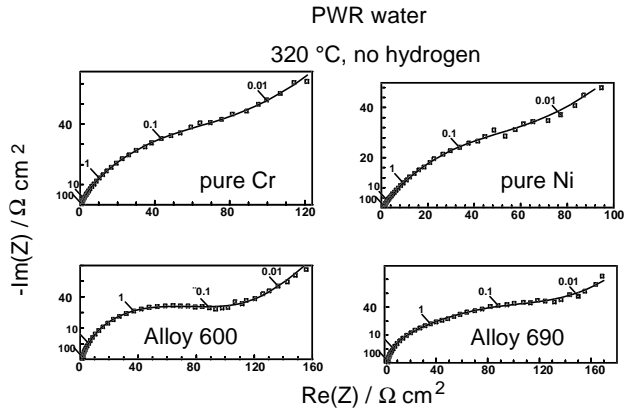
Figure 4. Effect of changes in the content of dissolved H₂ on the electronic resistance of Alloy 600 and nickel (a) and on that of Alloy 690 (b). Resistance measured using the CER technique.

In the case of Alloy 690, the removal of hydrogen resulted only in a small increase of the film resistance (see Fig. 4b). This suggests that the electronic properties of the oxide film on Alloy 690 are mainly controlled by the presence of Cr in the film.

The impedance spectra measured for pure Cr, pure Ni, Alloy 600 and Alloy 690 samples at 320°C in the presence and in the absence of 40 cc(STP)/kg hydrogen are shown as complex plane plots in Fig. 5. The spectra for all the materials point to two processes with different characteristic frequencies. The removal of hydrogen is clearly observed as an increase of the magnitude of the impedance values. Accordingly, the process related to at least one of the time constants must be influenced by the hydrogen content in the system.



a)



b)

Figure 5. Impedance spectra of pure Cr, pure Ni, Alloy 600 and Alloy 690 in PWR water at 320 °C. Hydrogen content 40 cc(STP)/kg water (a); hydrogen content < 0.1 cc/kg water (b). Parameter is frequency in Hz.

One of the characteristic frequencies can be ascribed to the anodic reaction occurring at the metal/film interface and subsequent cation transport, and the other to the cathodic reaction occurring at the film/solution interface. This interpretation is supported by the experimental observation that the oxide films formed under the studied conditions exhibit fair electronic conductivity, which should make the occurrence of the cathodic reaction, i.e. the evolution of hydrogen, at the outer interface highly probable.

Based on these concepts, the equivalent circuit shown in Fig. 6 was chosen in order to fit the experimental results. The contribution of the anodic reaction and processes connected with it is described by means of a capacitance (C_1) in parallel to a charge transfer resistance (R_1) in series with a Warburg impedance (Z_w), which is related to the transport of cations towards the film/solution interface. The processes related to the cathodic reaction are described by means of a capacitance (C_2) in parallel to a charge transfer resistance (R_2). The contributions of the anodic and cathodic processes are in series with each other and with the resistance of the electrolyte R_{el} . The best fit results according to the proposed model are shown in Fig. 5 as solid lines demonstrating the good correspondence between the calculated and the experimental data.

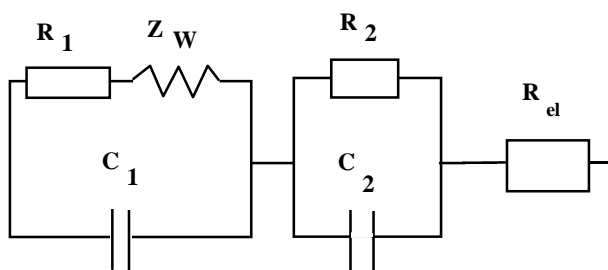


Figure 6. The equivalent circuit used to fit the experimental data measured for the different metal/oxide film/solution systems.

The results of the fitting showed that the cathodic process seems to be rate-determining for the overall corrosion reaction, as R_2 was almost a decade higher than R_1 in all the cases. The value of R_2 decreased with the removal of hydrogen, which is in good agreement with the fact that hydrogen evolution is facilitated in the absence of dissolved hydrogen. On the other hand, both the charge transfer resistance R_1 and the Warburg constant σ increased when

hydrogen was removed (except R_1 for Ni). This can be understood if R_1 and σ are associated with the anodic process of generation and transport of cation species at the metal/film interface and within the oxide film, respectively. The presence of hydrogen probably causes such changes in the film that the rate of cation transport in it is higher than in the absence of hydrogen. This might be connected with partial reduction of the film in the presence of hydrogen.

No significant difference was observed in the values of the charge transfer resistance R_1 for any of the materials studied. In addition, the removal of hydrogen did not result in such a big increase in R_1 as was observed for the electronic resistance measured for Ni and Alloy 600 when hydrogen was removed. Assuming that the electronic and ionic contributions to charge transfer in one and the same process should be interrelated, these facts suggest that the results obtained by CER measurements are most certainly connected with a phenomenon different from that described by the charge transfer resistance R_1 . This can be explained on the basis of the formation of electronically conductive channels consisting of metallic Ni, as discussed above, when the film is exposed to hydrogen-containing environment. These channels are not likely to act as short-circuit paths for cation species, but they increase the electronic conductivity of the film as a whole.

3.2.2 Concluding remarks on surface films on alloys 600 and 690

The results of this work can be used as a starting point to understand the earlier experimental observation, according to which the crack growth rate in Alloy 600 slightly increases when the resistance of the surface oxide film on the material increases [6]. If the increase in the electronic resistance of the oxide film is connected with the oxidation of well-conductive metallic Ni extending through the whole film e.g. to less conductive NiO, as discussed above, the existence of metallic Ni could be used as a criterion for conditions in which crack growth rate is minimised. The resistance of the studied alloys to general corrosion seems to be largely determined by the rate of the cathodic reaction (hydrogen evolution) proceeding presumably at the oxide film / electrolyte interface.

4. Modelling the processes in oxide films on metal surfaces

To understand the factors affecting the rate of transport of radioactive species into oxide films and the mechanisms leading to oxide film growth, the conduction mechanism in and the transpassive dissolution of the oxide films on Fe-Cr alloys [7, 8], on pure Cr [9, 10] and on commercial stainless steels was modelled on the basis of experimental results. The experiments were partly based on the electrochemical techniques developed in this project (see chapter 5). The modelling reported in this chapter was done in such environments (ambient temperature, sulphate solutions), in which relevant literature data was available. This was necessary in order to be able to compare the results with those from earlier investigations and to verify the techniques developed and used in this project. The modelling work is currently being extended to cover high-temperature conditions.

4.1 Experimental results

The electronic resistance (measured using the CER technique) of Fe-12%Cr, Fe-25%Cr and pure Cr shows a flat maximum in the potential region corresponding to the most passive behaviour (see Fig. 7), while the decrease of the resistance at both more positive and more negative values points to changes in the structure of the film.

The measurement of the impedance (Z) of Fe-Cr alloys (see Fig. 8 for the Fe-25%Cr alloy) at different potentials shows that the slope of the Z vs. frequency plot depends on potential. Accordingly, the charge carrier density of the film cannot be considered independent of potential. The phase angle curve points to capacitive behaviour over a wide potential range, but clear changes can be seen to take place when approaching the potential values at which the electronic resistance had been observed to exhibit low values (see Fig. 7).

The steady state polarisation curves measured after preoxidation in the passive range (see Fig. 9) demonstrate that the currents due to the transpassive oxidation are much higher and start to increase at lower potentials for the Fe-25%Cr alloy

than for the Fe-12%Cr alloy. In the case of the Fe-12%Cr alloy, a secondary passivation is observed.

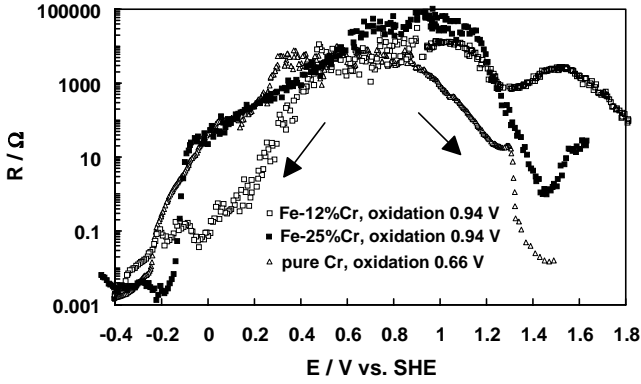


Figure 7. Resistance vs. potential dependences for Fe-12%Cr, Fe-25%Cr and pure Cr during potential sweeps (1 mVs^{-1}) in either positive or negative direction after oxidation in the passive region. Oxidation potentials shown in the legend of the figure.

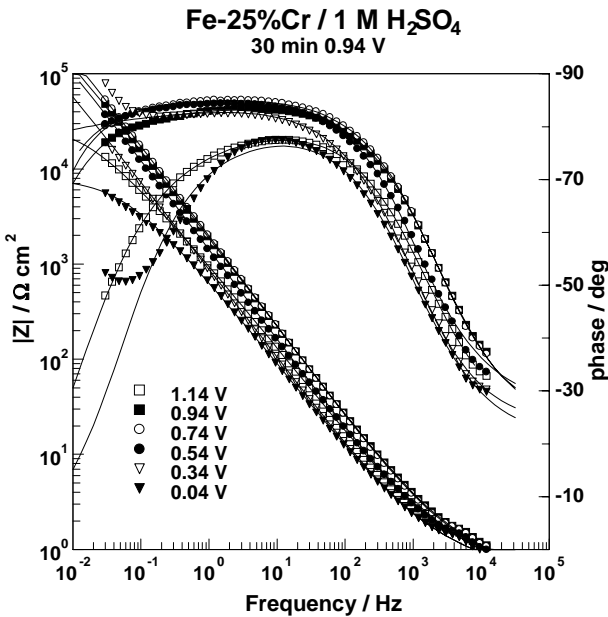
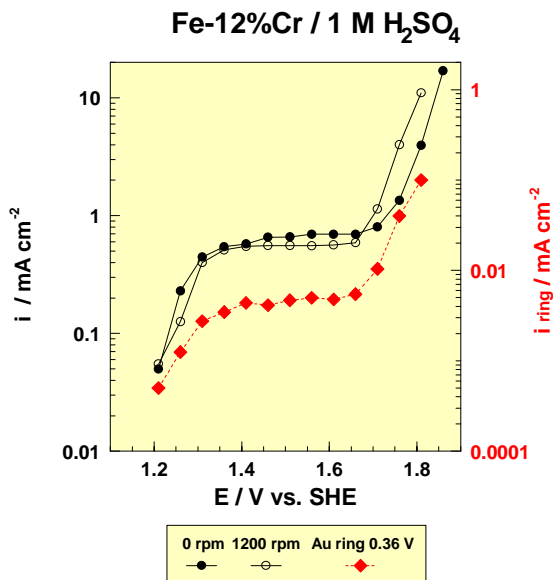
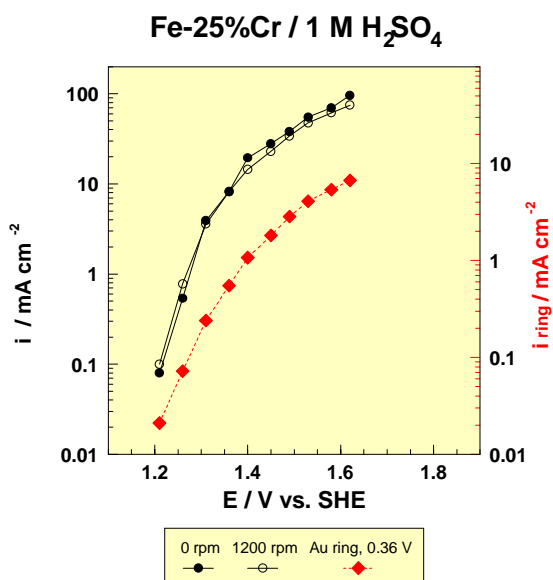


Figure 8. Impedance spectra of Fe-25%Cr alloy oxidised in the passive range with subsequent polarization at more positive and more negative potentials.



a)



b)

Figure 9. Steady state polarization curve for the transpassive dissolution of Fe-12%Cr alloy (a) and Fe-25%Cr alloy (b) in an acidic sulphate solution measured with a motionless (0 rpm) and a rotating (1200 rpm) disk electrode together with the steady state ring current due to detection of Fe(III) and/or Cr(VI) (ring potential 0.36 V vs. SHE).

Photoelectrochemical experiments showed that the magnitude of the mobility gap of the oxide film (i.e. intercept of the extrapolated square root of quantum yield vs. photon energy curve with the x axis) decreases with increasing potential on Fe-Cr alloys. Its value changes from about 2.7 eV to about 2.2 eV (Fig. 10). The latter value is typical for the film formed on pure Fe. This indicates that the film on the alloys at high potentials is transformed to a film resembling that on pure iron. This transformation can be ascribed to the transpassive dissolution of chromium from the film.

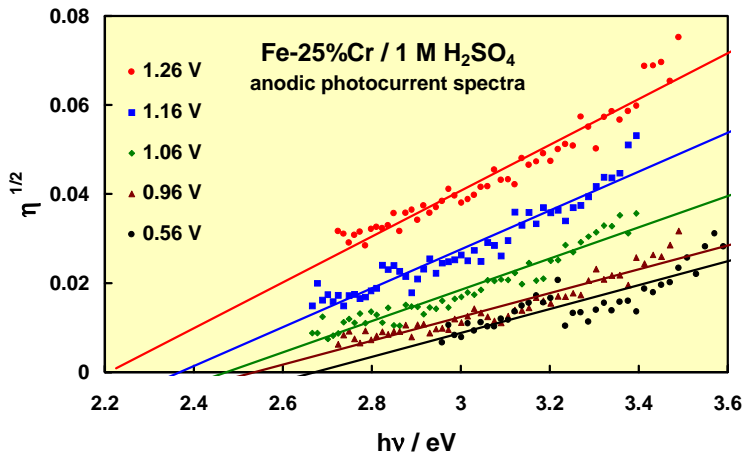


Figure 10. Plots of the square root of quantum yield vs. photon energy for pure Fe-25%Cr. The intercept with the x-axis gives the value of the band-gap of the semiconducting oxide film.

4.2 Discussion

The CER results show that the films on Fe-Cr alloys and Cr exhibit a high electronic resistance in the middle of the potential region corresponding to passive behaviour, while the resistance decreases at both negative and positive potentials. One way to describe this kind of behaviour is the so-called Young model [11, 12]. In this model it is assumed that as a result of defect formation at one interface the conductivity of the film is exponentially dependent of the distance from that interface as follows:

$$\sigma_d(x) = \rho_d^{-1} \exp(-x/x_0)$$

where the parameters are:

$\sigma_d(x)$ - defect induced conductivity

x - distance from the interface

ρ_d - specific resistivity at the interface at which the defects are generated

x_0 - a constant.

Müller [13] has derived an expression for the impedance of an oxide film in which an interfacial conductivity profile influences the conductivity of the film. On the basis of this derivation, the EIS results obtained in this work were fitted to the model. The results of the fitting shown in Fig. 8 with lines demonstrate a good agreement with experimental results. The agreement with the Young model makes it possible to estimate the potential dependence for the capacitance C of the film, the intrinsic resistivity ρ_0 and the interfacial resistivity of defect generation ρ_d in the film. The intrinsic resistivity is ascribed to the ionic conductivity of the bulk oxide film. This kind of estimation is shown for the Fe-25%Cr alloy in Fig. 11.

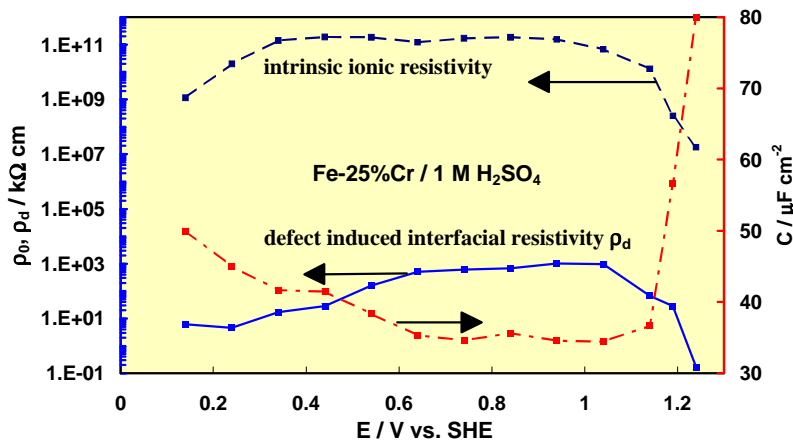


Figure 11. Potential dependences of the capacitance C , intrinsic resistivity ρ_0 and the interfacial resistivity of defect generation ρ_d for Fe-25%Cr.

The estimation shows that the defect induced interfacial resistivity is considerably lower than the intrinsic resistivity at all the studied potentials. Thus the interfacial resistivity is likely to determine the resistance of the whole film, if it extends over a considerable part of the film and/or the thickness of the film is within the tunneling range.

A qualitative explanation to the observed behaviour in the passive region is that polarisation at negative potentials results in a reduction process leading to the generation of lower valency defects at metal/film interface, while polarisation at positive potentials results in an oxidation process leading to the generation of higher valency defects at film/solution interface. Thus the conductivity profile at negative potentials is due to the reduction process and has its maximum at the inner interface, whereas the profile at positive potentials is due to the oxidation process and has its maximum at the outer interface.

A mechanistic description for the processes taking place and leading to conductivity profiles at the interfaces can be given on the basis of the surface charge approach [14, 15]. This approach is partly based on the point defect model [16, 17] for anodic films, but it takes into account the possibility of very high electric field within the oxide film. The film is represented as an n-type semiconductor - insulator - p-type semiconductor (n-i-p) junction, in which positive charge carriers (e.g. oxygen vacancies or metal interstitials as depicted in Fig. 12) injected at the metal / film interface play the role of electron donors and negative charge carriers (e.g. metal vacancies, Fig. 12) injected at the film / solution interface play the role of acceptors. It is noteworthy to mark that the situation will be electrically the same if the donor species are metal interstitials at the metal / film interface (e.g. Fe^{2+} in the structure of the passive film on iron) or high-valency species accumulated at the film / solution interface (e.g. Cr^{6+} in the structure of the passive film on Cr and Fe-Cr alloys at high potentials).

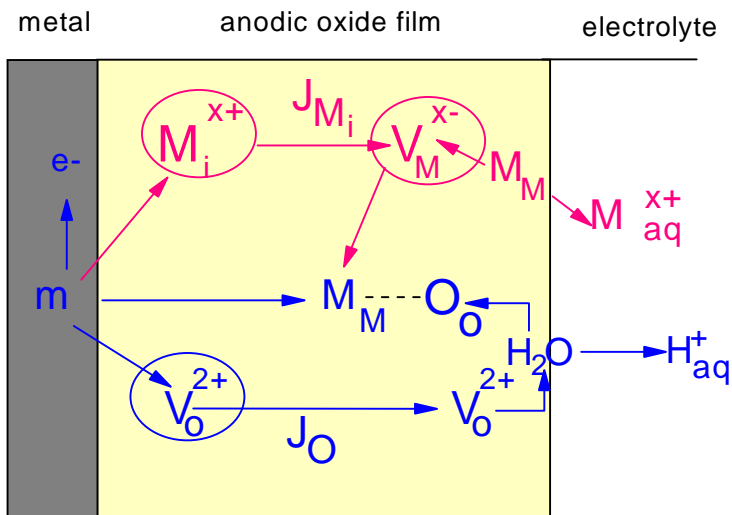


Figure 12. A scheme of the processes taking place within an oxide film according to the surface charge approach.

At sufficiently high positive potentials the oxide film on Fe-Cr alloys and Cr becomes conductive enough for the transpassive oxidation to start. This can be modelled on the basis of the processes depicted in a simplified reaction scheme shown in Fig. 13.

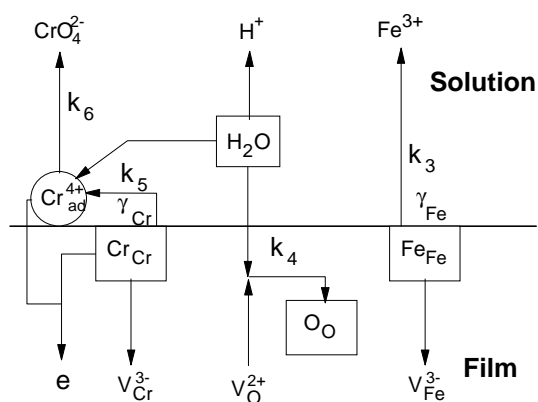
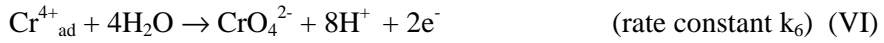
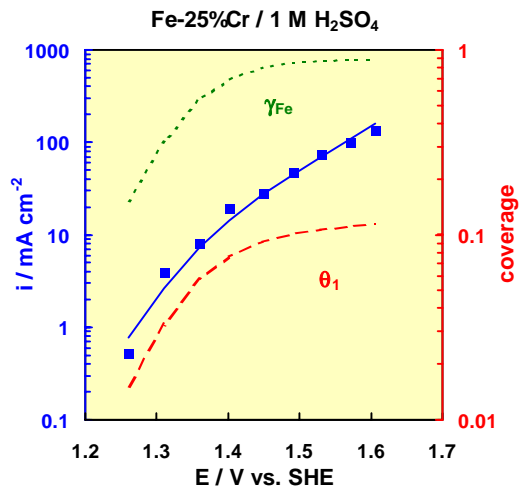


Figure 13. Scheme for the processes taking place at the anodic film/solution interface during the transpassive oxidation and dissolution of Fe-Cr alloys.

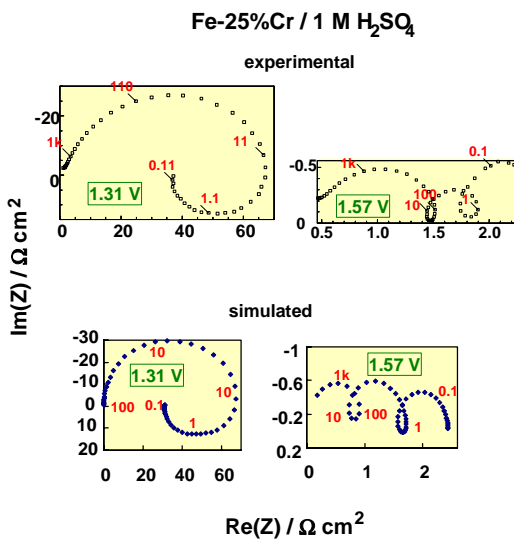
Transpassive dissolution of Cr can be regarded as a two-step reaction with an adsorbed intermediate taking place at the Cr positions in the outermost cation layer:



Based on the surface charge approach, expressions for the steady state current and impedance response of the growing film, of the metal/film interface and of the film/soluton interface can be derived. The total impedance can then be calculated as the sum of the impedances of the interfaces and of film bulk. The experimental polarisation curves and impedance spectra could be well simulated on the basis of the equations derived above. As an example, the simulated polarization curve and impedance spectra for the Fe-25%Cr alloy in the range 1.2...1.7 V are presented in Fig. 14. The simulation was found to be insensitive to changes in the parameters at the metal/film interface, i.e. they did not influence the impedance response significantly.



a)



b)

Figure 14. a) Experimental (points) and simulated (solid line) steady state polarization curve for the Fe-25%Cr alloy in an acidic sulphate solution together with the calculated potential dependence of the steady state fraction of Fe in the outermost layer of the anodic film and the coverage of the film surface with a Cr(IV) intermediate. b) Experimental and simulated impedance spectra for the transpassive dissolution of the Fe-25%Cr alloy in an acidic sulphate solution. Parameter is frequency in Hz.

4.3 Concluding remarks on modelling of oxide films

The anodic film formed on Fe-Cr alloys and Cr can be depicted as a very thin, essentially insulating layer. In the proposed model the film is treated as a doped n-i-p junction structure due to the continuous injection of oxygen vacancies or metal interstitials at the substrate/film interface and metal vacancies or high-valency interstitials at the film/electrolyte interface. Due to anodic or cathodic polarisation, oxidative or reductive changes of the stoichiometry in the first layers of the film near the interfaces lead to defect induced conductivity of the whole film. Because the thickness of the film is very close to the tunneling distance limit, sufficient accumulation of defects at the two interfaces leads to the transformation to a conducting film and subsequent release of soluble products both in the active and transpassive region.

The transpassive oxidation of Fe-Cr alloys can be modelled as a two-step transpassive dissolution of Cr including an adsorbed Cr(IV) intermediate and the enrichment of Fe in the outermost cation layer. The model describes quantitatively the steady state and transient response of Fe-12%Cr and Fe-25%Cr alloys in the transpassivity range.

The presence of Cr affects the active dissolution and transpassive behaviour of Fe in opposite ways: In the active-to-passive transition Cr acts as a passivating agent, diminishing considerably both the potential range of active dissolution and the amount of soluble products released. In the transpassive region, the presence of Cr leads to significant dissolution of the substrate material through the anodic film, whereas film growth is suppressed. In the transpassive range, Fe acts as a secondary passivating agent after its sufficient enrichment in the outermost layers of the passive film.

5. Development of electrochemical techniques for high-temperature measurements

5.1 Thin-layer electrode arrangement

Electrochemical measurements carried out in solutions simulating LWR coolant conditions or in actual plant conditions are complicated due to the low conductivity of the coolant, especially in typical BWR environments. To obtain useful information of reactions and transport processes occurring on and within oxide films, a thin-layer electrode arrangement for versatile electrochemical measurements was developed [18, 19].

5.1.1 Description of the technique

The principle of the thin layer electrode arrangement is shown in Figure 15. In this arrangement the working electrode and the inert counter electrode (usually made of Ir-metal) are constructed as two parallel surfaces (tips of small diameter rods). The distance between the electrodes can be adjusted with an accuracy of 10^{-9} m up to about 100 μm by means of a step motor and spring system developed originally for contact electric resistance (CER) measurements. The reference electrode is situated at the side of the working electrode. When the working electrode is polarised, the current flows between the working and counter electrodes across the μm -range gap, while the potential is measured from the side of the specimen thus greatly suppressing the effect of the ohmic drop in the electrolyte.

The bulk solution can be pumped through the counter electrode ensuring that representative solution chemistry prevails between the electrodes during the measurements. Therefore, this test arrangement can also be conveniently used to study the effects of solution flow rate and novel water chemistries on the electrochemical properties of oxide films. A detector electrode, analogous to the ring electrode in a conventional rotating ring-disk electrode set-up, can also be included in the arrangement to identify soluble species released during corrosion.

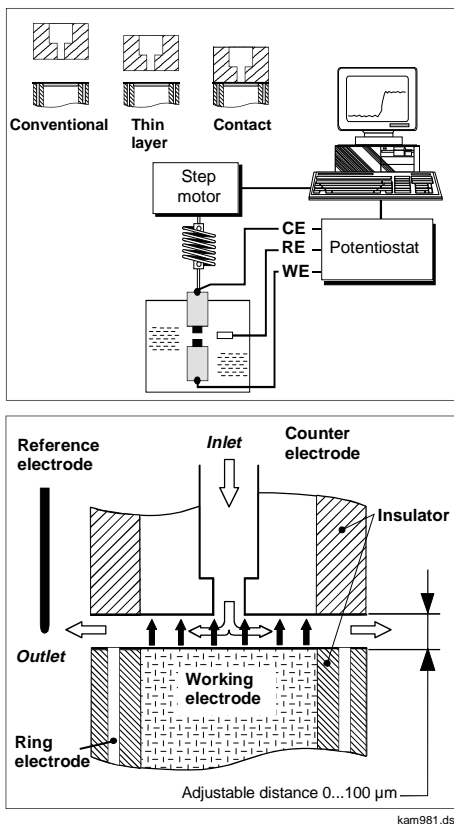


Figure 15. A scheme of the experimental set-up for thin-layer electrochemical measurements

The arrangement shown in Figure 15 can be employed to obtain electronic and electrochemical information of the oxide films on the studied construction materials by using the following measurements:

Thin layer electrochemical measurements

* Thin Layer Electrochemical Impedance (TLEI) measurements to characterise the oxidation and reduction kinetics and mechanisms of metals as well as properties of metal oxide films even in low conductivity aqueous environments.

* Thin Layer Walljet (TLW) measurements to detect soluble products released from the working electrode.

* Other controlled potential and controlled current measurements.

Solid contact measurements

* Contact Electric Resistance (CER) measurements to investigate and/or to monitor the electronic properties of surface films

* Contact Electric Impedance (CEI) measurements to measure the solid contact impedance spectra of oxide films.

5.1.2 Experimental verification

The versatility of information which can be obtained when using the thin layer electrode arrangement is demonstrated in Figures 16 and 17. The polarisation curve of AISI 316L in 0.1 M $\text{Na}_2\text{B}_4\text{O}_7$ at 200°C is shown as a function of potential in Figure 16, together with the potential dependence of the electronic resistance of the oxide film measured with the CER technique. The curves show the potentials region where the material is passive and where transpassive oxidation and secondary passivation take place, as well as the correlations between these phenomena and the electronic resistance of the film.

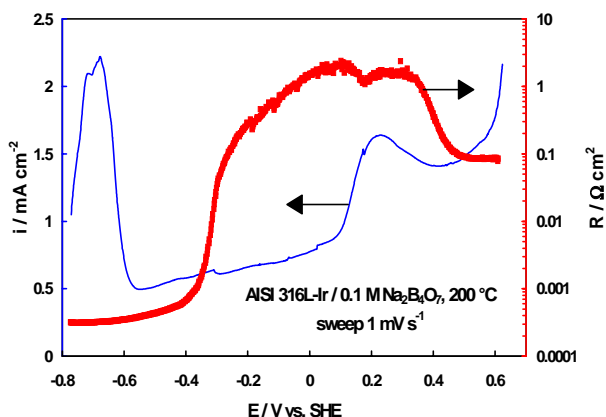
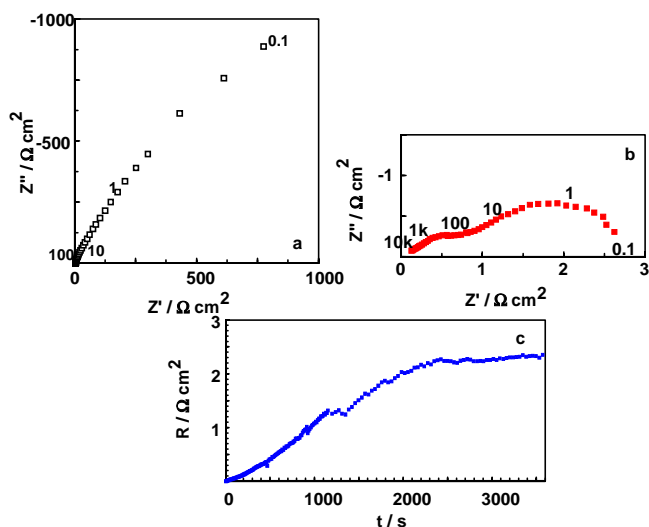


Figure 16. Polarisation curve of AISI 316L stainless steel, together with the resistance vs. potential curve.

The conventional impedance diagram measured at 0.22 V comprises a high-frequency time constant and a Warburg line at low frequencies (see Fig. 17a). The values of the impedance magnitude at low frequencies are of the order of $1 \text{ k}\Omega\text{cm}^2$. The value of the impedance magnitude at high frequencies can be attributed to the ohmic resistance of the whole system. This value is of the order of $2 \text{ }\Omega\text{cm}^2$ and thus approaches the value of the resistance of the electrolyte. The dc electronic resistance of the film determined with the CER technique (see Fig. 17c) is of the same order of magnitude (i.e. about $2.5 \text{ }\Omega\text{cm}^2$). Together these results demonstrate that the film is a good electronic conductor. This is further substantiated by the results from the measurement of the contact electric impedance, in which two relaxations are detected (see Fig. 17b). The depressed semicircle at high frequencies probably depicts the distributed geometric capacitance of the film, whereas a finite length Warburg-like response at intermediate frequencies suggests a diffusion-migration mechanism of electron transport. The low frequency limit of the contact electric impedance spectrum is practically identical to the value measured by the dc resistance CER technique.



316 L oxidised at 0.22 V vs. SHE in 0.1 m $\text{Na}_2\text{B}_4\text{O}_7$ at 200 °C

Figure 17. a) A conventional impedance spectrum of AISI 316 L. b) A contact impedance spectrum of the AISI 316 L - Ir couple. c) A dc resistance vs time curve of AISI 316 L by the CER technique.

5.1.3 Concluding remarks on thin-layer electrochemistry

A thin-layer electrode arrangement for impedance, dc resistance (CER) and other electrochemical measurements in low conductivity, high temperature aqueous electrolytes allows for a characterisation of the corrosion performance of construction materials in such environments. The combination of impedance and CER measurements facilitates a comprehensive characterisation of both the electric properties of the oxide films formed on construction materials, the ionic transport through the films and the kinetics of corrosion reactions at the film/electrolyte interface. The proposed arrangement includes also the possibility of contact electric impedance measurements as a tool for in-situ investigation of the mechanism of electronic conductivity of the oxide layers. Identification of the different soluble products is important for more reliable estimation of the corrosion rate and for accurate determination of the processes involved in phenomena such as activity build-up and stress corrosion cracking.

5.2 In-line monitoring of high temperature water chemistry

Improvements in the field of water chemistry control, more stringent guidelines and improvements in the in-line monitoring technologies have excellent chances to mitigate corrosion related problems of the existing nuclear power plants. As a consequence, the development of reliable and accurate high temperature sensors for the measurement of parameters such as pH_T (thermodynamic pH), ECP (electrochemical corrosion potential) and conductivity is essential to be able to characterise the "true" operational environments at high temperatures and pressures. This is manifested in the participation of VTT in the IAEA WACOL program (On-line monitoring of water chemistry and corrosion) resulting in continuous updating of the current status of the different high temperature water chemistry techniques. Approximately 20 participants from 13 countries provide contributions aimed at introducing proven monitoring techniques into plants on a regular basis and filling the gaps between plant operator needs and available monitoring techniques.

The aim of this part of the present research program was to develop Teflon-free reference and pH electrodes for applications in which the temperature exceeds 300°C to meet the needs of increased operating temperatures. In addition, the development of an in-core reference electrode for reactor applications in co-operation with the OECD Halden project was set as a goal for this project. The final objective in the in-core reference electrode development work was to construct a sensor which can be used for several years giving reliably the reference potential.

5.2.1 Development of in-core reference electrodes

The effects of different kinds of water chemistries on the response of an in-core reference electrode have been tested at VTT. Additional tests in Assembly Test Loop at Halden test reactor (OECD Halden Reactor Project) showed that the electrode can produce reliable and accurate reference potentials under various oxidizing and reducing aqueous environments even in high primary coolant flow rates. In addition, a new small size in-core Pd-electrode was developed by VTT and the OECD Halden Reactor Project. This miniaturised sensor has been shown to be helium leak tight during temperature cycling in an air oven and in high temperature water inside an autoclave. [20]

The Metal-Ceram Electrical Insulating Seals which are essential parts of the in-core electrodes have been tested in in-core location for 80 days of operation in a PWR loop in the Halden Boiling Water Reactor showing no sign of degradation. These tests have demonstrated that this type of sealing technology can be used as a basis for development of in-core reference electrodes.

5.2.2 Concluding remarks on in-line monitoring

The co-operation between VTT and OECD Halden Reactor Project has resulted in the development of a prototype of an in-core Pd reference electrode which can be used for several years in in-core locations for corrosion potential measurements. This is a significant step in performing in-line water chemistry monitoring in in-core locations of boiling water reactors since the life time and accuracy of the commercially available sensors is limited to less than one fuel

cycle. Long term in-core and calibration runs will be performed at Halden test reactor during the years 1999–2000. Improvements in the in-line monitoring technology due to these new high temperature sensors allow for an improved analysis and narrow range control of “true” operational environments.

6. Conclusions

The main conclusions from this subproject dealing with oxide films in high temperature aqueous environments are:

- Installation of a TrendChem high-temperature water chemistry monitoring system at Loviisa plant has enabled the establishment of correlations between the applied water chemistry, oxide film properties and the extent of activity incorporation on primary circuit material surfaces.
- The development of a thin-layer electrode arrangement has made it possible to conduct versatile electrochemical measurements in simulated power plant coolants, even in poorly conductive BWR coolants.
- The combination of results obtained using the developed electrochemical and new surface analytical techniques together with mechanistic modelling has facilitated the clarification of the mechanisms of phenomena related to activity build-up on primary coolant surfaces and to different types of corrosion.

The studies focused so far mainly on grown-on oxide films need to be extended to cover also the deposited layer of the oxide film. This is how the transport of species through the whole oxide film can be modelled and the impact of transport properties on activity incorporation and corrosion rate can be estimated. Investigations in carefully controlled simulated conditions need to be continuously supported by plant experiments in order to guarantee the relevance of the experiments. This can be best accomplished if the developed techniques are installed and can be tested in Finnish nuclear power plants.

7. Acknowledgements

The reported work was part of the Finnish Research Programme on the Structural Integrity of Nuclear Power Plants 1995 - 1998, subproject RAVA5 on Material Degradation in Reactor Environment. This subproject was not included in the original RATU2 plans, but increased interest in behaviour of oxide films and activity pickup gave reason to launch this RAVA5 subproject starting in 1997. The work for Chapter 2 was completed in 1997 - 1998, Chapter 3 in 1997, Chapter 4 in 1998 and Chapter 5 in 1997 - 1998.

Co-operation with Seija Suksi and Juhani Hinttala from the Radiation and Nuclear Safety Authority (STUK), Thomas Buddas, Magnus Halin, Kimmo Tompuri and Ossi Hietanen from IVO and Anneli Reinvall, Erkki Muttilainen and Olli-Pekka Luhta from TVO, together with many other colleagues is gratefully acknowledged. The work was coordinated to the co-operation with the OECD Halden Reactor Project, Norway.

References

1. Robertson, J. Corrosion Science, 1991. Vol. 32, pp. 443-465.
2. Buddas, T., Halin, M., Laitinen, T., Mäkelä, K. and Tompuri, K. Influence of primary circuit water chemistry on oxide films on stainless steel during a fuel cycle at Loviisa Unit 2, 1998 JAIF International Conference on Water Chemistry in Nuclear Power Plants, Kashiwazaki, Japan, 13-16 Oct. 1998.
3. Bojinov, M., Laitinen, T., Mäkelä, K., Saario, T. and Sirkiä, P. Activity incorporation into zinc doped PWR oxides. Enlarged Halden Programme Group Meeting, Lillehammer, Norway, 15-20 March 1998.

4. Aaltonen, P., Bojinov, M., Ehrnstén, U., Lagerström, J., Laitinen, T., Saario, T. and Sirkiä, P. The effect of environment on the electric and electrochemical properties of surface films on alloy 600 and alloy 690 in pressurised water reactor primary water. Fontevraud IV (International Symposium on the contribution of materials investigation to the resolution of problems encountered in pressurised water reactors), 14–18 Sept. 1998, Fontevraud, France.
5. Fish, J. S., Lewis, N., Yang, W. J. S., Perry, D. J. and Thompson, C. D. Proc. of Eighth International Symposium on Environmental Degradation of Materials in Nuclear Power Systems - Water Reactors, Vol. 1. American Nuclear Society Inc., La Grange Park, Illinois, USA, 1997. Pp. 266-273.
6. Lagerström, J., Ehrnstén, U., Saario, T., Laitinen, T. and Hänninen, H. Proc. of the Eighth International Symposium on Environmental Degradation of Materials in Nuclear Power Systems - Water Reactors. Vol. 1. American Nuclear Society Inc., La Grange Park, Illinois, USA, 1997. Pp. 349-356.
7. Bojinov, M., Betova, I., Fabricius, G., Laitinen, T., Raicheff, R. and Saario, T. The stability of the passive state of iron-chromium alloys in sulphuric acid solution, Corrosion Science, in print.
8. Bojinov, M., Fabricius, G., Laitinen, T. and Saario, T. Transpassivity mechanism of metals and alloys studied by AC impedance, DC resistance and RRDE measurements. Electrochim. Acta, in press.
9. Bojinov, M., Fabricius, G., Laitinen, T. and Saario, T. The mechanism of the transpassive dissolution of chromium in acidic sulphate solutions, J. Electrochem. Soc., 1998, Vol. 145, pp. 2043-2050.
10. Bojinov, M., Fabricius, G., Laitinen, T., Saario, T. and Sundholm G. Conduction mechanism of the anodic film on chromium in acidic sulphate solutions. Electrochim. Acta, 1998. Vol. 44, pp. 246-261.
11. Young, L. Trans. Faraday Soc., 1955, Vol. 51, 1250.
12. Cahan, B. and Chen, C.T. J. Electrochem. Soc., 1982. Vol. 129, 921.

13. Müller, N. PhD Thesis, Erlangen, Germany, 1980.
14. Bojinov, M., Kanazirski, I. and Girginov, A. *Electrochim. Acta*, 1996. Vol. 41, 2695.
15. Bojinov, M. *Electrochim. Acta*, 1997. Vol. 42, 3489.
16. Chao, C.Y., Lin L. F., Macdonald D. D. J. *Electrochem. Soc.*, 1981, Vol. 128, pp. 1187-1194.
17. Macdonald, D. D. J. *Electrochem. Soc.*, 1992, Vol. 139, pp. 3434-3449.
18. Bojinov, M., Laitinen, T., Mäkelä, K., Saario, T. and Sirkiä, P. Characterisation of material behaviour in high temperature water by electrochemical techniques, Enlarged Halden Programme Group Meeting, Lillehammer, Norway, 15–20 March 1998.
19. Bojinov, M., Hinttala, J., Laitinen, T., Muttilainen, E., Mäkelä, K., Reinvall, A., Saario, T. and Suksi, S. Development of electrochemical techniques to study oxide films on construction materials in high temperature water. 1998 JAIF International Conference on Water Chemistry in Nuclear Power Plants, Kashiwazaki, Japan, 13–16 Oct.1998.
20. Mäkelä, K. Current status of PD-reference electrode development work, Enlarged OECD Halden Project Meeting, Loen, Norway, 24–28 May 1996.

Development of tools and models for computational fracture assessment

Heli Talja, Kari Santaoja*
VTT Manufacturing Technology
Helsinki University of Technology*
Espoo, Finland

1. Introduction

The aim of the work presented in this paper has been to develop and test new computational tools and theoretically more sound methods for fracture mechanical analysis. The applicability of the engineering integrity assessment system MASI for evaluation of piping components has been extended. The most important motivation for the theoretical development have been the well-known fundamental limitations in the validity of J-integral, which limits its applicability in many important practical safety assessment cases. Examples are extensive plastic deformation, multimaterial structures and ascending loading paths (especially warm prestress, WPS). Further, the micromechanical Gurson model has been applied to several reactor pressure vessel materials. Special attention is paid to the transferability of Gurson model parameters from tensile test results to prediction of ductile failure behaviour of cracked structures.

2. Automated engineering integrity assessment

Capabilities for fast engineering integrity assessment are very important e.g. if cracks are found in primary circuit components during the annual outage of a nuclear power plant. In such cases very fast decisions have to be made about the acceptability of the cracked component. For such computations a program system called MASI has been developed at VTT (Talja 1995b, Talja et al. 1997). It consists of several computational programs which have been implemented into the system as executable files and are run by a graphical user interface.

The first version of the system was especially tailored for pressurised thermal shock analyses of the reactor pressure vessel (Kantola 1986, Mikkola 1992, Raiko 1993, Raiko et al. 1994). The system has been extended to support also fatigue assessment (Viitala & Talja 1995).

2.1 Assessment of sub-cladding cracks

One possibility to assess cracks located below the cladding of a reactor pressure vessel is to simplify the case by replacing the actual configuration with an “equivalent” through-cladding crack, for which analytical solutions exist. This approach, however, leads to overly conservative assessments. So the capabilities of MASI system have been extended to more realistic analysis of sub-cladding crack cases (Hanson 1997).

Several models for sub-cladding cracks, which were found in literature, were programmed and tested. A pressurised thermal shock loading case was used as the test case. Three analytical models were compared with finite element results obtained using the Abaqus program (ABAQUS 1995), in order to evaluate their validity for the solution for the stress intensity factor for a crack appearing under the cladding on the inside of a cylinder. The models covered both axial and circumferential cracks, and the stress intensity factor was usually calculated at crack tips in both base metal and at the interface between the base metal and the cladding. When applying the analytical models, also the thermal and stress analyses were performed using the engineering analysis tools included in the MASI system.

The stress intensity factor is not a very useful tool when evaluating the crack tip at the interface between the cladding and the base metal. The J-integral is not path-independent there, and the plastic deformations are significant. The integrity may be estimated, however, using other models.

For an axial elliptical sub-cladding crack, the model by Ovchinnikov (1986) gave plausible results for both crack tips, as shown in Fig. 1 for the crack tip at base material. The results with plasticity correction would be preferred in a safety analysis, since they would ensure conservative results. The analytical stress intensity factor results with no correction agreed well with the finite

element results as well as for the. The model by EPRI did not generate acceptable results for this crack type.

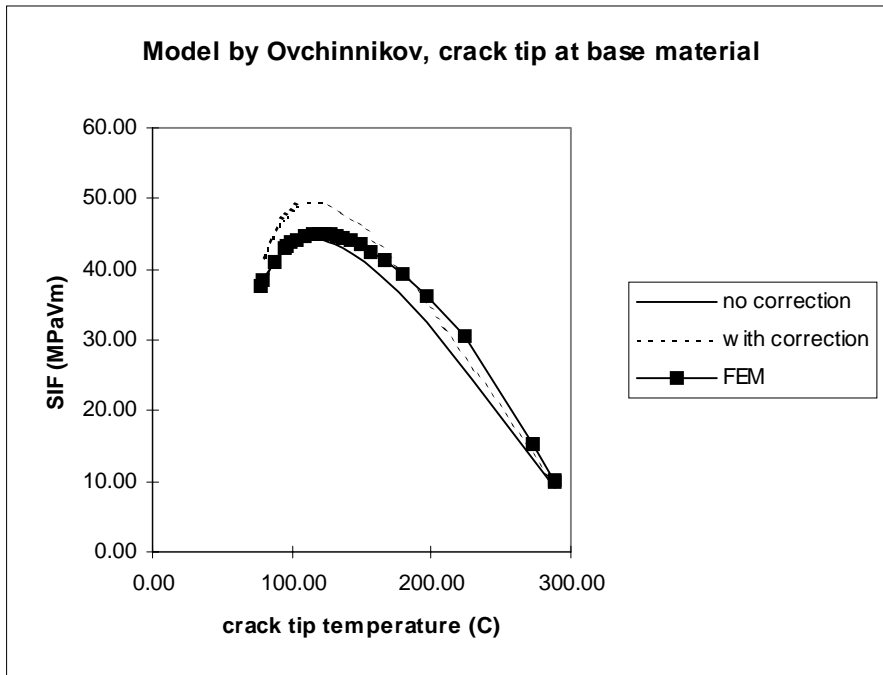


Figure 1. Comparison of analytical results with the model by Ovchinnikov to two-dimensional finite element results.

The models by Hodulak et al. (1995, Blauel et al. 1997)) and EPRI (Anonymous, 1990) covered circumferential cracks. Both models generated very similar results for the crack tip in the base metal. The results without corrections followed nicely those of the finite element analysis. Also in this case, the results with corrections would be preferred to ensure conservative results. The model by Hodulak et al. did not provide a solution for the stress intensity at the interface, and the model by EPRI generated very poor results for that crack tip.

As a conclusion the models by Ovchinnikov (1986) and Hodulak et al. (1995) have been selected for axial and circumferential sub-cladding crack cases, correspondingly.

2.2 Automated analyses for piping components

Special features needed in automated integrity evaluations of cracked piping components (Talja 1995a) have been added to the MASI system, which will be integrated as part of the piping assessment system of TVO. The program has been outlined so that it can either fully utilise the data stored in the databases by TVO or the user can define the necessary input parameters with help of the graphical user interface, Fig. 2.

At first only straight piping components and crack growth by fatigue or stress corrosion are considered. The system performs fatigue assessments for cracks which are either postulated or actually found in a (weld of a) piping component. As the main result of the computation, an estimate of crack growth due to the loading cycles implied during a certain time period is obtained.

The criticality of a crack grown by fatigue is checked using the rules given in ASME XI (1995). A special program module has been developed for this purpose (Talja & Lipponen 1998). From the computation it is further judged how long the cracked component can still be used - whether it can be used until the next planned plant outage, or a suggested necessary repair date is given. The assessment is repeated for several pipe components and cracks.

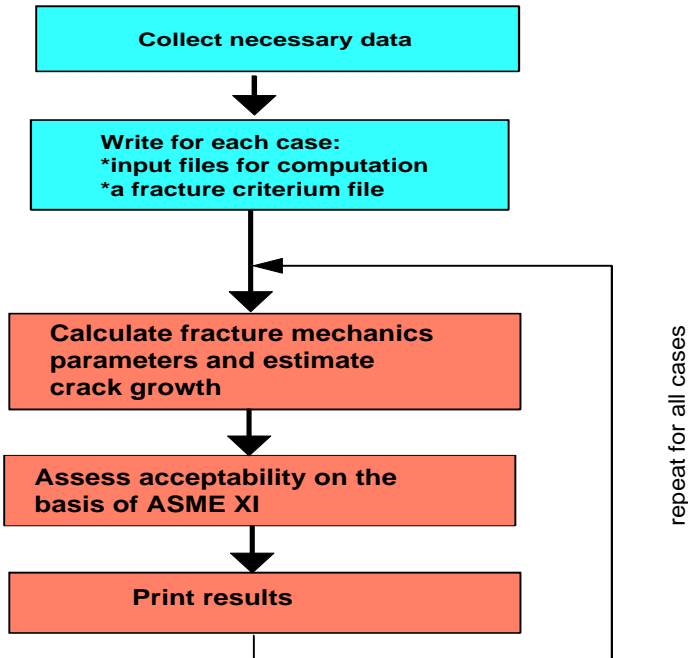


Figure 2. Automated piping analysis procedure of the MASI system.

3. Modelling of ductile cracking for structural analysis

A new theory called the ‘J-vector theory’ is derived for crack growth assessment of nuclear power plant components. The J-vector theory is an extension to the well-known J-integral concept. The J-integral is one of the today’s main tools in safety and availability analyses of pressure vessels in Western nuclear power plants. The main advantages of the J-vector theory beyond the J-integral are the following: (a) it predicts the crack growth direction, (b) it gives the amount of crack growth and (c) it is prepared for materials in general and (d) in contrast to the J-integral concept it does not assume the unrealistic singular stress-strain field (see e.g. Santaoja 1992) at the crack tip.

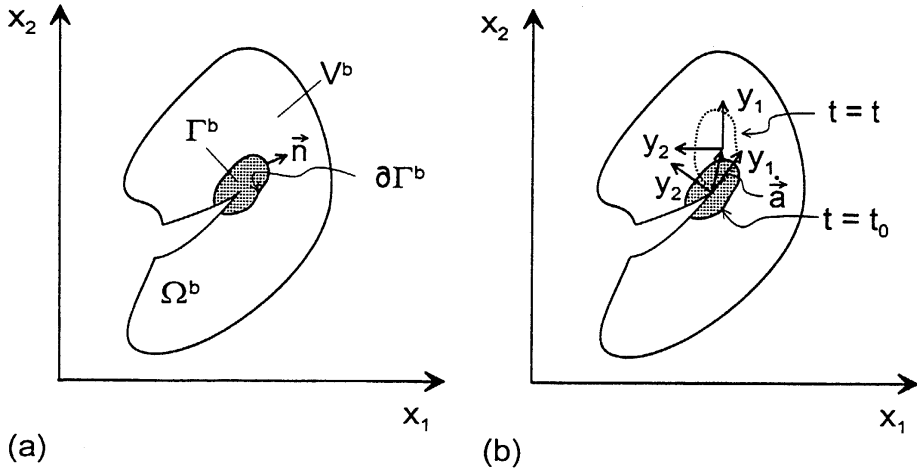


Figure 3. (a) Separation of the body V^b into two different subdomains Ω^b and Γ^b . (b) The subdomain Γ^b and the moving coordinate system (y_1, y_2) are attached to the crack tip.

The fundamental idea of the J-vector theory is the mathematical separation of the body V^b into two different domains denoted by Ω^b and Γ^b , as shown by Fig. 3. The domain Γ^b encloses the crack tip and is imagined to be attached to the crack tip and to move with the moving frame (y_1, y_2) through the body with a growing crack, see Fig. 3(b). For this separated body V^b the basic laws of thermomechanics apply. Thermomechanics is a science that combines thermodynamics and mechanics. The basic laws of thermomechanics are e.g. Newton's second law of motion, i.e. $F = ma$, and the first and second laws of thermodynamics. Those basic laws hold of course for crack growth in a non-separated body, but in that case the expressions of thermodynamics do not give any tool to predict the crack growth. The novelty of the separation is that it provides the following equation:

$$\dot{\vec{a}} = \eta \frac{\partial \phi^C(\vec{J} - 2\vec{\gamma}; \dots)}{\partial(\vec{J} - 2\vec{\gamma})}, \quad (1)$$

where $\dot{\vec{a}}$ is the crack growth velocity, $\phi^C()$ is the function giving the model for crack growth, \vec{J} the J-vector and $2\vec{\gamma}$ is the crack growth resistance. For

where $\dot{\vec{a}}$ is the crack growth velocity, $\phi^C()$ is the function giving the model for crack growth, \vec{J} the J-vector and $2\vec{\gamma}$ is the crack growth resistance. For rectilinear crack growth and for straight crack front the J-vector \vec{J} takes the following appearance:

$$\begin{aligned} \vec{J} := & \oint_{\partial\Gamma^b} [\rho\psi\vec{n} - \vec{n} \cdot \boldsymbol{\sigma} \cdot (\vec{u}\vec{\nabla})] ds \\ & + \int_{\Gamma^b} \left[\rho\dot{\vec{v}} \cdot (\vec{u}\vec{\nabla}) - \rho \frac{\partial\psi}{\partial T} (T\vec{\nabla}) - \rho\vec{b} \cdot (\vec{u}\vec{\nabla}) - \rho \frac{\partial\psi}{\partial h} (h\vec{\nabla}) \right] dA. \end{aligned} \quad (2)$$

In Eq. (2) the terms on the second line are as follows: The influence of inertia forces, the influence of inhomogeneous temperature field, the influence of body forces and the last two terms are for influence of inhomogeneous material. The variables on the upper line of Eq. (2) are as follows: ρ is the density of the material, ψ is the specific Helmholtz free energy, \vec{n} is the outward unit normal to the path $\partial\Gamma^b$, see Fig. 3(a), $\boldsymbol{\sigma}$ is the stress tensor, \vec{u} is the displacement vector and $\vec{\nabla}$ is the vector operator del acting on the preceding quantity. If the deformation is pure elastic and the temperature effects are neglected (hyperelastic material behaviour), the strain energy density $w = \rho\psi$. The stress tensor $\boldsymbol{\sigma}$ is defined by $\vec{t} := \vec{n} \cdot \boldsymbol{\sigma}$. If also the effect of the inertia forces and the body forces are neglected and the material is homogeneous, Definition (2) yields:

$$\vec{J}_1^e = \oint_{\partial\Gamma^b} \left[wn_1 - \vec{t} \cdot \left(\frac{\partial\vec{u}}{\partial x_1} \right) \right] ds, \quad (3)$$

which means that the first component of the hyperelastic J-vector equals to the J-integral. It can be shown (Santaoja 1996 and 1994) that for hyperelasticity the following holds:

$$\frac{\partial\Pi}{\partial\vec{a}} = -\vec{J}^e, \quad (4)$$

where Π is the potential energy. The corresponding expression to Result (4) is widely used for the J-integral (see Rice 1968, Eq. 68). By taking a simple model

for φ^C in Evolution Eq. (1) the following expression for the onset of crack growth is obtained:

$$\bar{J} = 2\bar{\gamma}, \quad \text{which with Equation (4) yields} \quad -\frac{\partial \Pi}{\partial \bar{a}} = 2\bar{\gamma}. \quad (5)$$

Eq. (5b) contains the same information as the expression by Griffith (1920, Eq. 11) which was the starting shot for fracture mechanics.

The above quite cumbersome mathematical presentation was carried out to demonstrate that the J-vector theory is an extension to Griffith's work and to the J-integral concept. Actually the J-integral concept is a simple model and the J-vector theory is the theory for crack growth. One can prepare a simple model within the J-vector theory to obtain the J-integral concept and the result obtained by Griffith.

The J-vector theory requires a constitutive equation for material behaviour and a model for crack growth. The latter is the function φ^C in Eq. (1). The J-vector theory uses thermomechanics with internal variables which is the most promising dialect of thermomechanics (thermodynamics) for preparation of material models. In the framework of this dialect there is an extensive gallery of models to cover a wide range of material behaviour (see e.g. Lemaitre & Chaboche 1990) including almost all the 'traditional constitutive equations'. The Gurson-Tvergaard model, which is very important in fracture mechanics, obtained its thermomechanical appearance very recently (Santaoja 1997). Thus, the thermomechanical representation of the material model is not a problem. The crack growth model is something new beyond traditional thermomechanics and fracture mechanics. The investigation, however, can be started from the simple model that, with hyperelastic material behaviour, gives the J-integral concept.

The application of the J-vector theory needs computation. There are few - if any - examples that can be solved analytically. The computer program has to be capable to adapt material models written in the form of thermomechanics with internal variables. Furthermore, crack growth has to be simulated. As far as the author knows such a commercial code is not available. Certainly the most widely used finite element method (FEM) code for structural analysis is

ABAQUS (1995). ABAQUS provides the user with an opportunity to implement new constitutive equations expressed by thermomechanics with internal variables. VTT has used ABAQUS for several years with great success.

In order to keep the amount of work limited the J-vector theory implementation is planned to be done as follows. A method having two FEM meshes will be introduced. The coarse mesh is the standard one for the whole structure provided by ABAQUS. On the top of the coarse mesh there is a finer mesh. This latter mesh covers only a small volume around the crack front and it moves with the growing crack. The advantage of this method is that the critical volume around the crack front is always covered by a fine mesh whereas the rest of the body has also an acceptable not too fine mesh. The reduction in computer costs is remarkable. Furthermore, the J-vector path is a fixed path within the fine which makes the computing of the value for the J-vector straightforward. This kind of an approach is known in the theory of plasticity and in fluid mechanics. We have a candidate to do this work as a doctoral thesis.

The main advantage of the J-vector theory is that it describes crack growth in materials in general which means that it has a very general basis and therefore it does not have such limitations in validity as the classical J-integral concept. The theory for simulation of crack growth is valid for all kinds of crack growth processes including brittle and ductile crack growth and also fatigue crack growth. This originates from the fact that the development of the J-vector theory is based only on the basic laws and axioms of thermomechanics. No extra restrictive assumptions are adopted. As long as the Newtonian mechanics hold good, also the J-vector theory is valid. The constitutive equation and the model for crack growth determine the capability of the application to model the crack growth. The development of the J-vector theory has been closely linked to the investigation of thermomechanics with internal variables carried out at VTT (Santaoja 1997, 1998).

4. Use of micromechanical material modelling in predicting ductile fracture resistance

In the case of realistic nuclear reactor pressure vessel materials, only a very limited amount of material is usually available for testing. With the help of

micromechanical material models, fracture mechanical parameters can be estimated by testing small tensile specimens only. An important advantage of micromechanical material models over classical fracture mechanics is that, at least in principle, the parameters do not depend on specimen size or geometry. This makes micromechanical material modelling at present a subject of world-wide intensive research.

Ductile fracture occurs in metals as nucleation, growth and coalescence of microvoids. Microvoids are caused by inclusions and carbides breaking or debonding from the matrix material. Among micromechanical material models for ductile fracture, the Gurson-Tvergaard-Needleman model is the most widely used. Gurson (1977) derived the original yield condition for porous materials by analysing a spherical void in a rigid-plastic spherical solid. It was later modified by Tvergaard (1981) to improve the agreement with numerical analyses. The modified yield condition is:

$$\Phi = \frac{3\sigma_{ij}\sigma_{ij}}{2\sigma^2} + 2qf \cosh\left(\frac{\sigma_{kk}}{2\sigma}\right) - \left[1 + (qf)^2\right] = 0, \quad (6)$$

where Φ_{ij} is the Cauchy stress tensor, Φ is the current flow stress of the matrix material, f the void volume fraction and q a parameter introduced by Tvergaard. In the case of zero porosity Eq. (6) reduces to the well-known von Mises yield condition. Further modifications were undertaken by Tvergaard and Needleman (1984) to consider the final material failure by void coalescence, which starts when a critical porosity f_c is reached. They replaced f by a “damage” function f^*

$$f^* = \begin{cases} f & \text{for } f \leq f_c \\ f_c + K(f - f_c) & \text{for } f > f_c \end{cases} \text{ with } K = \frac{f_u^* - f_c}{f_f - f_c}, \quad (7)$$

and introduced a model to consider void nucleation. The ultimate porosity value, at which the stress carrying capacity vanishes according to (6) is $f_u^* = 1/q$ and final porosity f_f is the value at which stress carrying capacity has been observed to occur in reality. Gurson model parameters can be classified into initial and

critical parameters f_c and f_r . The initial parameters are the initial porosity f_0 and the volume fraction of void nucleating parameters f_n .

The main problems in applying the modified Gurson model are the large number of parameters and the difficulties in determining their values experimentally. According to a methodology developed at Fraunhofer-Institut für Werkstoffmechanik (IWM) in Germany, the damage parameter values are obtained by numerical fitting of tensile test results and then used to predict J_R curves. If a parameter set succeeds in describing different tests correctly, it can be regarded as material parameter values.

Extensive numerical and experimental studies were performed jointly by IWM and VTT to assess the applicability of the methodology on several reactor pressure vessel materials: besides Western ferritic steels 20 MnMoNi 5 5 (German nomination) and A533B also austenitic VVER-440 reactor pressure vessel cladding was considered (Schmitt et al. 1997, Talja 1998, Talja et al. 1997).

As part of the study, possibilities for correlating the scatter of tensile and J-R curve results were studied. Experimental data in three different orientations were utilised, and a simple method to treat the material anisotropy by using different parameter sets in different orientations was shown to be a good practical approach (Talja 1998). The Gurson model parameters were determined using two strategies: The scatter of tensile test results was first fitted by trying the value of parameter f_c between 3 and 6 % the parameter f_n was predominantly varied. In the second case f_n was kept constant and f_c was varied. Comparable agreement between measured and estimated scatter was found in both cases. The results of fitting were then applied to estimate J-R curves. This was repeated in three orientations. The results for the first fitting strategy and orientation T are shown in Figures 4 and 5. Experimental J-R data correspond to orientation T-L.

The results reproduce the non-uniqueness problem mentioned e.g. by Zhang (1996), meaning that parameters describing well one test type are not necessarily able to describe another test. So in safety assessments it is important not to rely on simple fitting only in the parameter definition but at least to check the values by simulation to another test type. Table 1 shows that the values of J-

integral at crack growth initiation, J_i , and tearing modulus T are much more sensitive to variations in f_c than in f_n . By varying the initial parameter a rather good agreement was reached in estimating the scatter of experimental J-R results.

Table 1. Steel 20 MnMoNi 5 5: Comparison of calculated J_i and tearing modulus values in orientations L-T, T-L and T-S using the damage parameter values of two different fitting strategies.

Orientation & case		f_n	f_c	J_i [N/mm]	T [-]
L-T, varying f_c	min	0.002	0.03	247	237
	aver	0.002	0.045	273	285
	max	0.002	0.06	288	359
L-T varying f_n	min	0.00195	0.06	291	320
	aver	0.00165	0.06	298	320
	max	0.00135	0.06	302	325
T-L, T-S varying f_c	min	0.004	0.018	194	210
	aver	0.004	0.04	235	232
	max	0.004	0.10	301	457
T-L, T-S varying f_n	min	0.006	0.03	207	219
	aver	0.004	0.04	235	281
	max	0.002	0.03	247	237

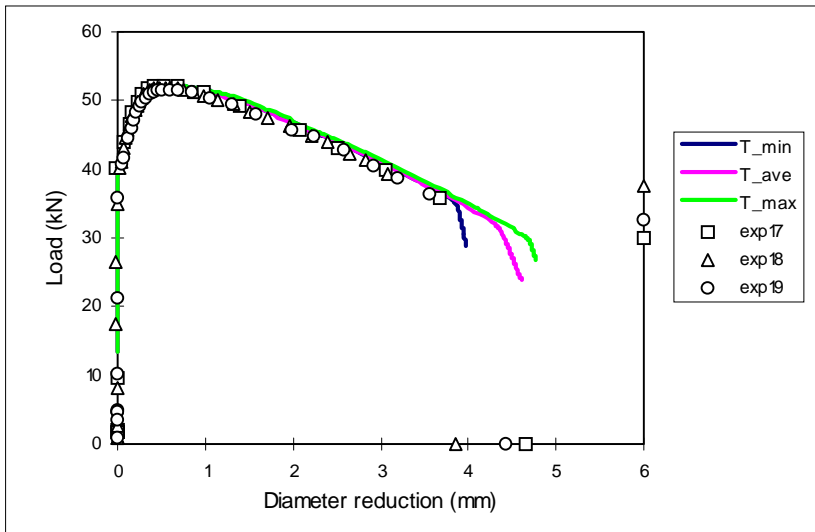


Figure 4. Steel 20 MnMoNi 5 5: comparison of calculated and measured load values as a function of diameter reduction in orientation T. Gurson model parameters have been fitted by trying to keep f_c between 3 and 6%.

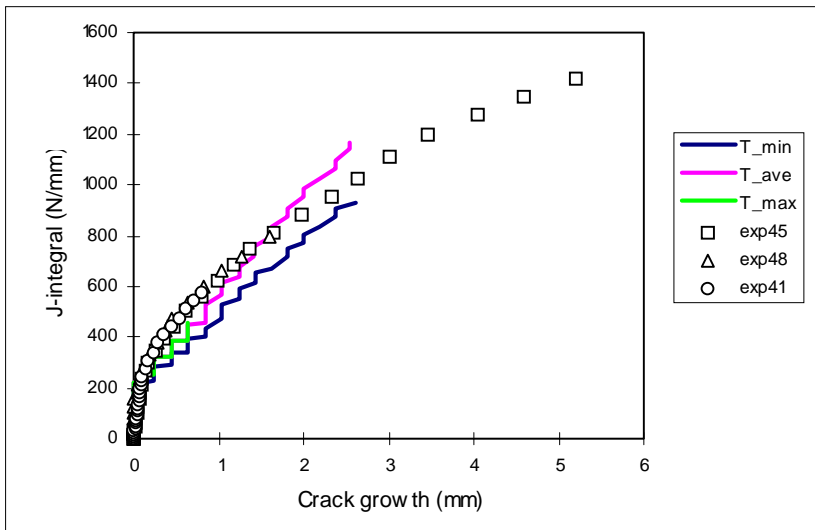


Figure 5. Steel 20 MnMoNi 5 5: Comparison of calculated and measured J-R curves in orientation T-L.

5. Conclusions

Capabilities of the engineering integrity assessment program system MASI have been extended to analysis of sub-cladding cracks and to facilitate automated integrity evaluations of cracked piping.

A new theory called the 'J-vector theory' has been derived for crack growth assessment of nuclear power plant components. The J-vector theory is an extension to the well-known J-integral concept. The main advantage of the J-vector theory is that it describes crack growth in materials in general which means that it has a very general basis and therefore it does not have such limitations in validity as the classical J-integral concept.

Capabilities for predicting stable crack growth were extended by taking the micromechanical Gurson-Tvergaard-Needleman model into use. Good results were obtained for ferritic reactor pressure vessel materials. The transferability of model parameters from tensile to fracture mechanical test results was studied, and in the analysed case it was possible even to find a correspondence between the scatter of the results of the different test types. A practical way to treat material anisotropy was presented.

6. Acknowledgements

The reported work was part of the Finnish Research Programme on the Structural Integrity of Nuclear Power Plants 1995 - 1998, subprojects RAKE1-2 on Structural Analyses for Nuclear Power Plant Components. The work for Chapter 2 was completed in 1995 and 1997 - 1998, for Chapter 3 in 1996 - 1997 and for Chapter 4 in 1996 - 1998.

Co-operation with Rauli Keskinen and Rainer Rantala from the Radiation and Nuclear Safety Authority, STUK, Paulus Smeekes from TVO, Alpo Neuvonen from IVO Ltd. together with Aarne Lipponen from VTT, Mimmi Hanson (at present at Hightech Engineering, Sweden) and many other colleagues is gratefully acknowledged. The numerical work on Gurson model was performed during a stay as visiting research scientist at Fraunhofer-Institut für Werkstoff-

mechanik (FhIWM) in 1996. Co-operation with Dr. Winfried Schmitt, Dr. Horst Kordisch and Dr. Dong-Zhi Sun from FhIWM is gratefully acknowledged.

References

ABAQUS Theory Manual 1995 (version 5.5). Rhode Island, USA: Hibbitt, Karlsson & Sorensen, Inc.

Anonymous 1990. French Verification of Pressurised Water Reactor Vessel Integrity. Paris, France: Electric Power Research Institute. EPRI NP-6713.

ASME XI 1995. ASME Boiler and Pressure Vessel Code. Section XI Rules for Inservice Inspection of Nuclear Power Plant Components. 1995 Edition. New York: The American Society of Mechanical Engineers.

Blauel, J. G., Hodulak, L., Nagel, G., Schmitt, W. & Siegele, D. 1997. Effect of Cladding on the Initiation Behaviour of Finite Length Cracks in an RPV under Thermal Shock, Nuclear Engineering and Design, Vol. 171, No. 1-3, pp. 179-188.

Griffith, A. A. 1920. The phenomena of rupture and flow of solids. Philosophical Transactions of the Royal Society of London, A221, pp. 163 - 197.

Gurson, A. L. 1977. Continuum theory of ductile rupture by void nucleation and growth: Part 1 - Yield criteria and flow rules for porous ductile media. Transactions of the ASME, January, pp. 2 - 15.

Hanson, M. 1997. Analysis of subclad cracks. Stockholm: Royal Institute of Technology, Diploma Thesis. 28 p. + app. 36 p.

Hodulak L. & Siegele, D. 1995. Calculation for stress intensity factors for cracks under thermal shock transients. American Society for Testing and Materials Special Technical Publications 1220: Fracture Mechanics. Pp. 637 - 645.

Kantola, K. 1986. Jännitysintensiiteettikertoimen laskeminen painofunktio menetelmällä (Calculation of the stress intensity factor by the weight function method). Espoo: Technical Research Centre of Finland, Nuclear Engineering Laboratory. 40 p. (Technical Report YRT-3/86). (In Finnish).

Lemaitre, J. & Chaboche J.-L. 1990. Mechanics of solid materials. New York, USA: Cambridge University Press. 556 p. [Originally published in French as: Mécanique des matériaux solides 1985. Paris, France: Dunod (and Bordas)].

Mikkola, T. P. J. 1992. Numerical analysis methods of surface cracks. Espoo: Technical Research Centre of Finland. 42 p. + app. 85 p. (VTT Publications 119).

Ovchinnikov, A. 1986. Approximate equation for determining the stress intensity factor, K_I , for bodies with subsurface cracks. Strength of Materials, Vol. 18, pp. 1479 - 1482.

Raiko, H. 1993. The plastic limit load of cracked structures. Espoo: Technical Research Centre of Finland. 34 p. (Work report LUJA-2/93). (in Finnish).

Raiko, H., Ikonen, K. & Mikkola, T. 1994. DIFF, an analysis program for PTS. Espoo: Technical Research Centre of Finland. 27 p. (Work report LUJA-1/94). (In Finnish).

Rice, J. R. 1968. Mathematical analysis in the mechanics of fracture. In: H. Liebowitz (Ed.), Fracture, An advanced treatise: Vol. II. Mathematical fundamentals. New York, USA: Academic Press.

Santaoja, K. 1992. Some remarks upon fracture mechanics. Espoo, Finland: Technical Research Centre of Finland. 66 p. + app. 8 p. (VTT Publications 100).

Santaoja, K. 1994. Transport theorem and material derivatives in the description of crack growth processes by thermomechanics. Espoo, Finland: Technical Research Centre of Finland. 45 p. (VTT Publications 212).

Santaoja, K. 1996. Rectilinear crack growth in hyperelastic materials. Espoo, Finland: Technical Research Centre of Finland. 77 p. + app. 13 p. (VTT Publications 275).

Santaoja, K. 1997. Thermomechanics of solid materials with applications to the Gurson - Tvergaard material model. Espoo, Finland: Technical Research Centre of Finland. 162 p. + app. 14 p. (VTT Publications 312).

Santaoja, K. 1998. J-vector theory for simulation of rectilinear crack growth. Espoo, Finland: Technical Research Centre of Finland. 81 p. + app. 18 p. (VTT Publications 360).

Schmitt, W., Talja, H., Böhme, W., Oeser, S. & Stöckl, H. 1998. Characterization of upper-shelf fracture toughness based on subsized Charpy and tensile test results. ASTM STP 1329. Pp. 63 - 81.

Talja, H. 1995a. Automated integrity assessment for piping components. Espoo: VTT Manufacturing Technology. 32 p. + app. 4 p. (Report VALB120).

Talja, H. 1995b. Program system MASI for fracture assessment. Version 1.0. Status report and user instructions. Espoo: VTT Manufacturing Technology. 36 p. + app. 23 p. (Report VALB43).

Talja, H. 1998. Ductile fracture assessment using parameters from small specimens. Doctoral Thesis. Espoo, Finland: Technical Research Centre of Finland. 140 p. (VTT Publications 353).

Talja, H. & Lipponen, A. 1998. Automated integrity assessment of straight piping components. Espoo: VTT Manufacturing Technology. To be published as VALB Report).

Talja, H., Novák, J. & Lauerová, D. 1997. Numerical analyses for tensile and fracture mechanics specimens of VVER-440 reactor vessel cladding material. Freiburg: Fraunhofer-Institut für Werkstoffmechanik. 30 p. (Report IWM-T 11/97).

Talja, H., Raiko, H., Mikkola, T.P.J. & Zhang, Z.L. 1997. Structural integrity assessment with engineering integrity assessment tools. Computers & Structures, Vol. 64, pp. 759 - 770.

Viitala, T. & Talja, H. 1995. Implementing fatigue analysis capabilities into the MASI system - Version 1.1 (Väsymisanalyysivalmiuden lisääminen MASI-järjestelmään - versio 1.1). Espoo: VTT Manufacturing Technology. 16 p + app. 6 p. (Report VALB113). (In Finnish).

Tvergaard, V. 1981. Influence of voids on shear band instabilities under plane strain conditions. *International Journal of Fracture*, Vol. 17, No. 4, pp. 389 - 407.

Tvergaard, V. & Needleman, A. 1984. Analysis of the cup-cone fracture in a round tensile bar. *Acta Metallurgica*, Vol. 32, pp. 157 -169.

Zhang, Z. L. 1996. A sensitivity analysis of material parameters for the Gurson constitutive model. *Fatigue & Fracture of Engineering Materials & Structures*. Vol. 19, No 5, pp. 561 - 570.

(See Appendix 1 for a comprehensive listing of publications)

Structural analysis of NPP components and structures

Arja Saarenheimo, Heikki Keinänen and Heli Talja
VTT Manufacturing Technology
Espoo, Finland

1. Introduction

Capabilities for effective structural integrity assessment have been created and extended in several important cases. In the following presented applications deal with pressurised thermal shock loading, PTS, and severe dynamic loading cases of containment, reinforced concrete structures and piping components.

Hydrogen combustion within the containment is considered in some severe accident scenarios. Can a steel containment withstand the postulated hydrogen detonation loads and still maintain its integrity? This is the topic of Chapter 2. The following Chapter 3 deals with a reinforced concrete floor subjected to jet impingement caused by a postulated rupture of a near-by high-energy pipe and Chapter 4 deals with dynamic loading resistance of the pipe lines under postulated pressure transients due to water hammer.

The reliability of the structural integrity analysing methods and capabilities, which have been developed for application in NPP component assessment, shall be evaluated and verified. The resources available within the RATU2 programme alone cannot allow performing of the large scale experiments needed for that purpose. Thus, the verification of the PTS analysis capabilities has been conducted by participation in international co-operative programmes (Keinänen et al. 1998a). Participation to the European Network for Evaluating Steel Components (NESC) is the topic of a parallel paper in this symposium. The results obtained in two other international programmes are summarised in Chapters 5 and 6 of this paper, where PTS tests with a model vessel and benchmark assessment of a RPV nozzle integrity are described.

2. Steel containment analyses

Containment performance is of general interest for nuclear reactor safety assessment. Hydrogen detonation loads are considered within the scope of so-called severe accident analyses. Hydrogen combustion within containment rooms can lead to high pressures and temperatures, which may lose containment integrity. Transport and mixing of hydrogen inside the containment are critical factors determining the hydrogen burning mode. If the reacting gases, hydrogen and oxygen, are initially premixed, deflagration and detonation are possible combustion modes.

Gaseous detonations are shock waves driven by a chemical reaction. Unlike a deflagration, the chemical reaction is caused by shock wave compression in unburnt gas, and takes place slightly behind the shock wave. Typical speeds for detonation waves are 1000 - 2200 m/s, and they result in rapidly varying, dynamic pressure loads on containment structures.

The steel containment considered under hydrogen detonation conditions has the dimensions of the containment of Loviisa nuclear power plant. The initial hypothetical detonation loading data used in three-dimensional analyses was defined by the Radiation and Nuclear Safety Authority (STUK).

Dynamic structural analyses (Saarenheimo 1994) were performed with the commercial general purpose finite element code, ABAQUS 5.2 and 5.4. Several axisymmetric materially and geometrically non-linear analyses were carried out using different kinds of detonation impulses acting in the middle of the dome. Success criteria for dynamic loading were presented for elastic and inelastic analyses.

Extensive three-dimensional analyses comprised elastic, elastic-plastic and elastic-visco-plastic calculations under one detonation impulse at the belt line, at the same axial position where the fifth stiffener is located. According to materially non-linear three-dimensional calculations the containment succeeded this hypothetical detonation. The effect of the detonation is rather local and the effect of the strain rate to the yield strength is remarkable. Especially, when the strain rate dependence is considered, the period needed to achieve the maximum

peak value of the impulse is essential and affects considerably the results. The effect of the geometrical non-linearity is essential.

The amount of the plastic deformation is roughly taken dependent of the area of the triangle shaped impulse. According to the elastic-plastic and elastic-viscoplastic three-dimensional analyses the containment succeeded the criteria for free field strains considered in this study. Lack of considering geometrical non-linearity makes these results conservative.

Deformed shapes, P1D40

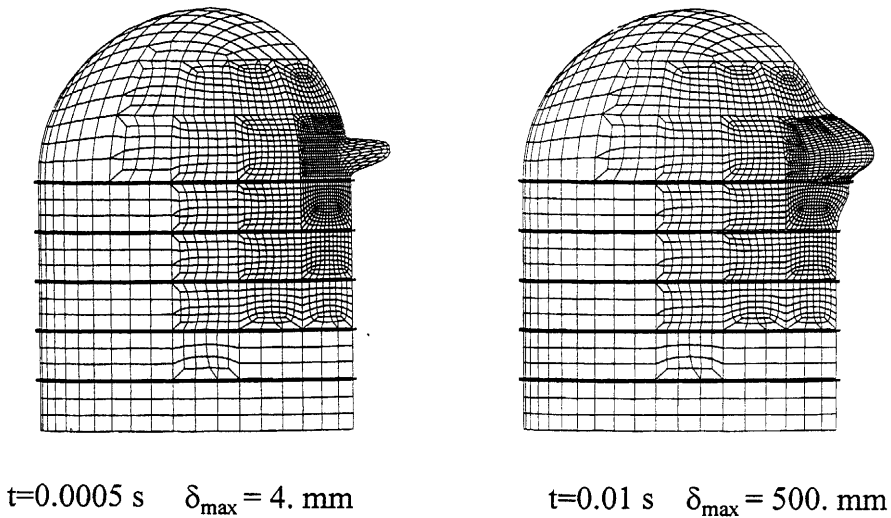


Figure 1. The displacements due to a hydrogen detonation impulse at the belt line of a steel containment.

Geometrically and materially non-linear analyses were carried out by using the ABAQUS/Explicit 5.4 code (Saarenheimo and Hyvärinen 1996). A simple procedure, based on the strong explosion theory, was developed by STUK for

detonation load evaluation. Two detonation pulses corresponding the amount of 5 kg and 10 kg hydrogen were analysed. The detonation centre located in the lower part of the dome 4 m from the wall, Fig. 1. Also the parameters simulating the strain rate dependence of the yield strength were varied in order to find out the effect of this phenomenon. With the assumptions used in this study the containment withstands the smaller load which corresponds to a maximum impulse of 12 kPa. The containment does not withstand the higher load corresponding to a maximum impulse of 26 kPa. Deformation rates were about $10 - 25 \text{ s}^{-1}$ and the effect of the strain rate on the yield strength is remarkable. The effect of the geometrical non-linearity is crucial. It is important to note that details like penetrations where stress peaks easily occur were not considered in this study. The main aim of this study was to determine detonation transients, predict the structural response and evaluate the capability of the tools available.

3. Reinforced concrete structures under impact loads

Safety-related reinforced concrete structures in nuclear power plants shall be designed to withstand specified operation and accident conditions. A particular concern is dynamic loading arising from ruptures of near-by high-energy piping. Such loading typically includes effects of pipe whip, missile and jet impingement.

In this study the capabilities of commercial general purpose finite element analysis programs ADINA and ABAQUS for analysing reinforced concrete structures under impact loads were evaluated and tested. The main differences between the programs lie in the constitutive modelling of concrete, in the available element types and in time integration procedures. Also the ways to model reinforcement varies a lot. Explicit time integration proved to be necessary for practical applications. Thus, the ABAQUS/Explicit program was chosen for further use.

ABAQUS/Explicit allows the combination of two- and three-dimensional solid elements with rebar layers. Brittle concrete Mode I cracking with crack closure and reopening can be modelled. Concrete is assumed to behave linearly elastic under compression. The tension softening model is user defined and based on

fracture energy, displacement or strain. The plastic deformations of the reinforcement are proportional to the plastic energy absorbed in the structure. Bond slip and dowel action at rebar/concrete interface can not be simulated.

Numerical examples were calculated to assess the capability of ABAQUS/Explicit to simulate numerically the behaviour of impact loaded reinforced concrete structures (Saarenheimo 1997a). Computational results were evaluated for impact loaded beams against test results found in the literature. The effects of modelling the load and choosing the parameters defining the concrete behaviour after cracking were studied. Fig. 2 compares calculated and measured strain values in the reinforcement of the lower surface of the beam. According to the results, ABAQUS/Explicit can be successfully applied in cases, where the compression crushing of concrete is not decisive.

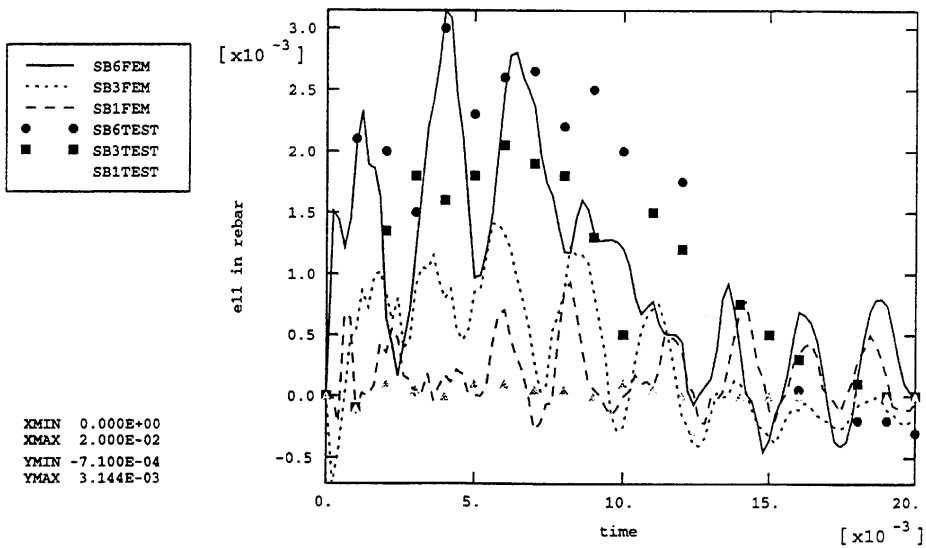


Figure 2. Calculated and measured strains as a function of time. Values in the reinforcement of the lower surface of the beam.

A further investigation was made into dynamic behaviour of a horizontal concrete floor subjected to jet impingement caused by a postulated near-by secondary circuit pipe rupture (Saarenheimo 1997b). The floor consists on double reinforced concrete slab lying on steel girders. Between the concrete slabs there is an isolation material layer. This problem was taken from a PWR plant.

A non-linear dynamic finite element analysis was carried out using ABAQUS/Explicit code. Special attention was given to material non-linearity which increases the energy absorption capacity at high strains and may lead to larger partially irreversible structural deformations. The jet impingement force was evaluated based on a thermal hydraulic analysis of the event. The loading of impingement was determined considering the deflection of the broken pipe.

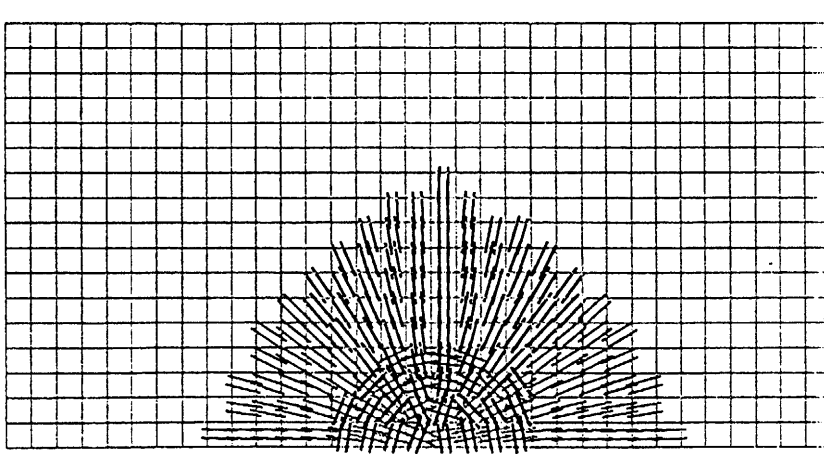


Figure 3. Cracking of the bottom of the upper slab of the floor due to jet impingement.

The results verified adequate structural strength, in spite of incipient cracking and plastic deformation at zones of maximum tensile stresses at the area where the water jet hits the slab. The lower slab remains uncracked. Fig. 3 shows the final crack distribution at the bottom of the upper slab. If the bottom surface of the

upper slab is assumed to lack the minimum reinforcement, the upper slab becomes cracked almost through the thickness.

4. Structural analysis of piping loaded by pressure transients

From the viewpoint of impact design it is important to determine the energy-absorbing capacity of structures. Because of the importance of inertia forces and material strain rate effects mainly simplified quasi-static methods are not acceptable.

When using nonlinear analysis the nonlinear response of the material must be known, including the effects of temperature changes and strain rate. Typical inelastic temperature dependent phenomena of metals are flow stress and yield stress, which decrease with increasing temperature. There are some exceptions, such as phase transformation and dynamic strain ageing which originate from the complex interaction between moving dislocations and the dissolution of impurities like nickel and carbon.

In rate dependent materials high strain rates increase the flow stress but decrease the ultimate rupture strain. In many metals, rate dependency at temperatures well below melting point is related to an additional stress required to generate and accelerate dislocations, i.e. to initiate changes in the rate of plastic flow. This effect is most prevalent in metals that have a distinct and easily defined yield stress. Low carbon steel is notoriously rate sensitive in this respect. At high strain rates (1000 /s) the yield stress can increase by more than a factor of two over a static value (Stronge & Yu 1993).

No proper acceptance criteria approved by regulatory bodies exist for these type of analysis. Some criteria for dynamic analyses and some success criteria can be found in the literature (Sammataro et al. 1993)

As an example, one of the main steam lines of the Loviisa Nuclear Power Plant, made of ferritic CT20 steel, has been considered under a pressure transient due to a condensation water hammer (Saarenheimo 1998). In these analyses two pressure transients were considered. In the first case the pressure transient was

caused by a condensation water hammer with velocity 5 m/s and in Case 2 the velocity was assumed to be 10 m/s. Thermal hydraulic analyses and pressure transient evaluations were carried out by IVO Power Engineering Ltd. Pressure transients due to the transient were determined in locations P1, B2-B4 and P5 shown in Fig. 4. The pressure transients in Case 1 are shown in Fig. 5. Transients at the straight pipelines were interpolated linearly from these point values. Near the rockwell the duration of the pulse was about 0.12 s and at the other end of the model the pressure increased about 25 ms later than at the rockwell. Also, the duration of the impulse at point P1 was roughly half that of the pulse at the rockwell. The velocity of the pressure transient was the same in both cases. Only the peak value is linearly dependent on the water hammer velocity.

The pipeline was modelled using ABAQUS (ABAQUS/Standard version 5.7 1997) PIPE and ELBOW elements. The weight of the water and possible isolation layers around the pipe were included in the effective material density. No damping was considered.

All the degrees of freedom at point P1 are fixed. Displacements perpendicular to the pipe axis are fixed at the point where the containment wall is located. Also displacements perpendicular to the pipe axis are prohibited at the point where the outlet pipe penetrates the roof. This simulates the steel construction located on the roof. There are two spring hangers denoted as S1 and S2 in Fig 4. The rotational stiffness at the end of the model is modelled using a rotational spring (S4). The other degrees of freedom at point P4 are fixed. At locations S5 and S6 the pipeline lies on rather stiff supports S5 and S6. At these supports the pipe can move upward but movement towards the support is prohibited by using a very stiff spring support. At support S5 displacement in the global X direction is prohibited.

Thermal stresses and stresses due to the self-weight of the pipeline were calculated before setting the transient loading. The duration of the transient was roughly 0.12 sec, as it clearly can be seen from the stress results. At the straight parts of the pipe circumferential stress due to the transient in Case 1 was 80 MPa and axial stress 40 MPa. The highest von Mises stress value near the T-section was 130 MPa. Stresses due to the transient in Case 1 are well below the material yield stress. In Case 2 the corresponding stress increases were 80 MPa

and 160 MPa, respectively. The highest von Mises stress value near the T-section was below 200 MPa.

According to the ASME NC-3600 Class 2, the allowable stresses for CT20 steel are 227 MPa and 252 MPa. The stress strain curve for CT20 material was evaluated by IVO at 50°C. The effect of operating temperature on the ferritic pipe material was estimated using the stress strain curves given in a Russian standard (PNAEG-7-002-86). The yield stress used in the analyses was 320 MPa.

According to these analyses the stresses at the T-connections are below the measured material yield stress. This yield stress value at 270 °C is based only on one measurement at 50°C and , however, can not be considered conservative. For more exact stress considerations in the near vicinity of the T-connection a more detailed finite element model is needed. Especially, the contact of the support S5 and the horizontal part of the pipe between these two T-connections needs more detailed analysis. Analyses with a detailed FE model will be completed by using shell elements in modelling the T-section.

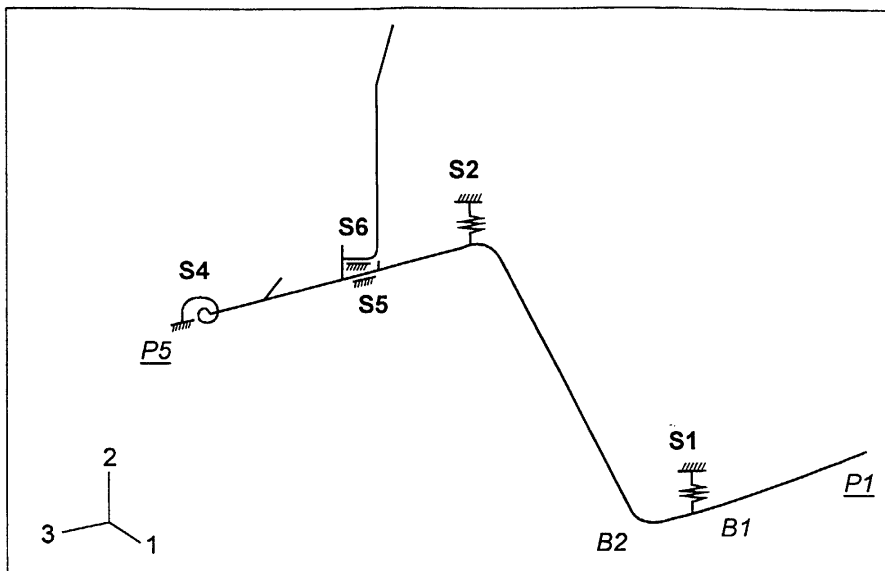


Figure 4. Steam pipeline.

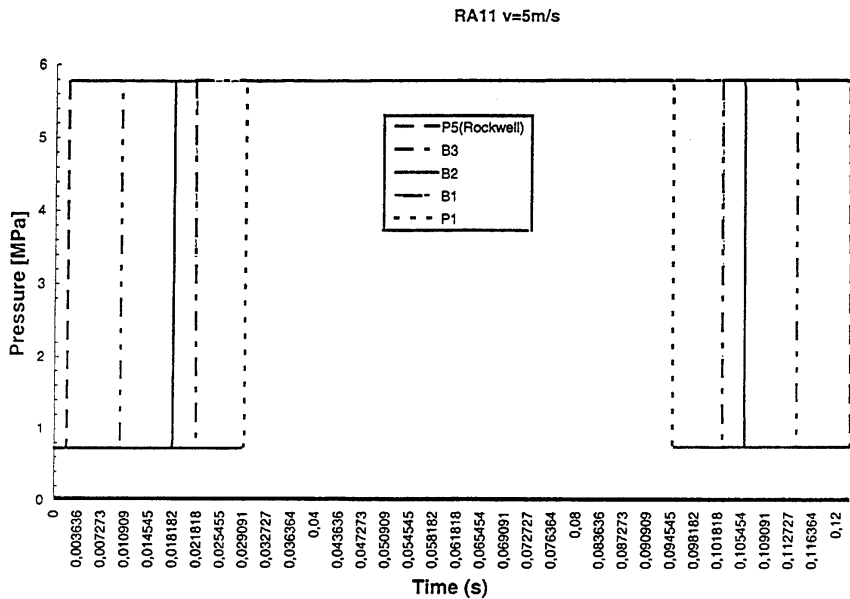


Figure 5. Pressure transients in Case 1.

5. Pressurised thermoshock tests on cladded model pressure vessel of VVER 440 RPV steel

This was a joint research program between IVO Power Engineering, VTT Manufacturing Technology and Central Research Institute of Structural Materials "Prometey" (1990 - 1996). The main objective of the research program was to create experimental knowledge of the crack behaviour under pressurised thermal shock (PTS) loading, as well as specific material property data for CrMoV type VVER-440 pressure vessel steel in simulated brittle condition. The program consisted of pressure vessel tests with two model pressure vessels (cladded and non-cladded), material characterisation, computational fracture analyses and evaluation of the results (Keinänen et al. 1998b).

Three PTS tests were carried out on the second, cladded model pressure vessel, Fig. 6 (Keinänen et al. 1997). The vessel material was in under-tempered (tempering temperature 610°C) condition to simulate the decrease of base

material fracture toughness due to irradiation embrittlement in a real reactor pressure vessel. Both under-clad and through-clad axial cracks in the outside surface were tested, Table 1.

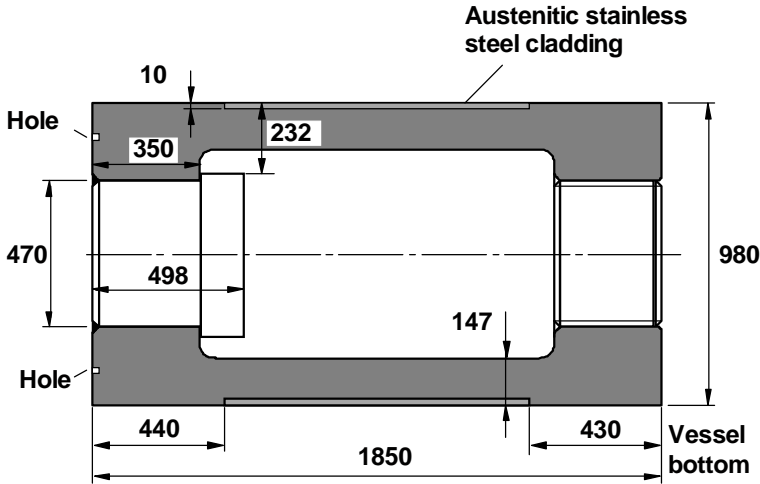


Figure 6. The geometry of the cladded model pressure vessel.

Table 1. Different tests and flaws in the case of the cladded model vessel. T_c is coolant (water) temperature and T_{ini} is initial temperature of the vessel.

Test	1	2	3
Pressure (bar)	0	>600	>300 ^a
T_{ini} (°C) ^b	295	300	300
T_c (°C)	10	10	10
Crack no.	2 ^c	2 ^c	3
Crack type	sub-clad	sub-clad	through-clad

^aDue to leak constant pressure was not maintained. ^bApproximated initial temperature at vessel midlength. ^cCrack 2 remained through the whole testing history.

Table 2 summarises crack behaviour during different testing phases. The vessel had in the first test two cracks located 180° from each other. Crack 1 was a trough-clad crack and crack 2 was an under-clad crack. The NDT measurements of cracks 1 and 2 before pre-pressurisation showed that cracks 1 and 2 have

grown under the cladding in the vessel length direction in the manufacturing phase of the model vessel. The through-clad crack 1 initiated in the first pre-test pressurisation, and consequently vessel rupture occurred in the second pressurisation at the pressure of 259 bar. As there was a leak through crack 1, the first test was performed without pressure. In the test, the crack 1 initiated again and extended.

Table 2. Summary of the crack behaviour in the different phases of testing.

Event	Pre-pressurisation	Test 1	Test 2	Test 3
surface crack 1	Initiation and rupture		Repaired before test by welding	Leak in the repair weld
sub-clad crack 2	Initiation and arrest	Initiation and arrest	Initiation and arrest	Initiation and arrest
surface crack 3	-	-	No initiation	No initiation
surface crack 4	-	-	-	In manufacture uncontrolled growth, repaired by welding
surface crack 5	-	-	-	No initiation
LOADING	Pressure	Thermal shock (TS)	Pressurised TS	Pressurised TS
REMARKS	Rupture of vessel, repaired before test 2	No pressure in thermal shock	New heat treatment before test	Many cracks in pressure vessel ⇒ interaction?

After the first test the vessel was repaired from ruptured crack 1 area by welding and a new through-clad crack (crack 3) was manufactured 90° from the previous through-clad crack 1. After the repair welding of vessel and the crack 3 manufacture, a tempering heat treatment was performed before the second test. After the second test two new through-clad cracks (crack 4 and 5) were manufactured. In the case of crack 4 a very deep crack (3/4 of wall thickness) was accidentally obtained. This was partly repaired by welding before test 3.

The initial and final depth of under-clad crack 2 was determined visually from the fracture surface after tests. Part of the fracture surface shown in Fig. 7 reveals brittle, cleavage type morphology. Several initiation and arrest zones can be visually found from the fracture surface. There is a clearly visible line showing crack location during tempering heat treatment, which was performed after the first test. The crack growth up to this line has occurred probably during the pre-test pressurisation. In the last two PTS tests crack initiation, propagation and arrest have occurred. The fracture surfaces reveal ductile intergranular fracture. The final crack extension has been ductile in the last test.

The computational analyses were made using finite element method, and ABAQUS 5.5 code. The through-clad and under-clad cracks (cracks 1 and 2) were analysed separately by using a three-dimensional slice model, which describes actually an infinitely long crack. In the case of the under-clad crack cleavage crack growth of 31 - 53 mm was simulated by releasing displacement constraint boundary conditions. A three dimensional model was created to analyse crack 3 opening (cutting of cladding) before the second test and crack 3 behaviour in the second test. The crack 3 shape was based on the NDT results. The cutting of cladding was simulated in the computation by gradually removing the displacement boundary conditions in the area of cladding.

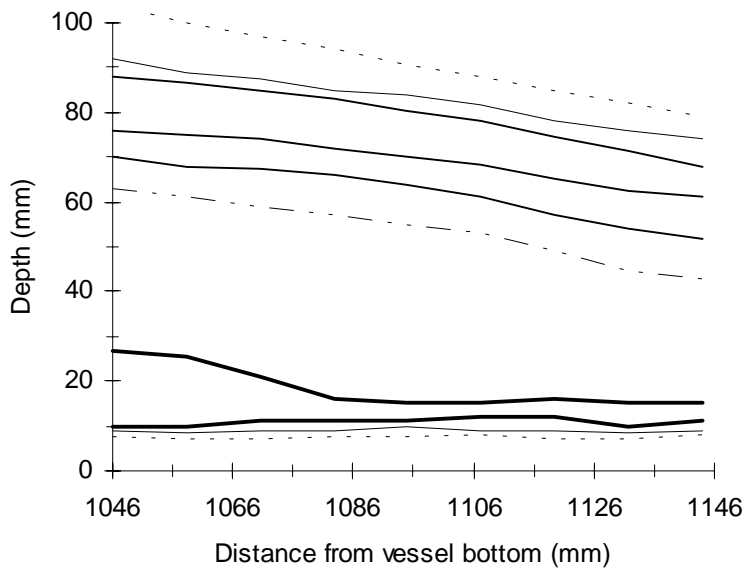
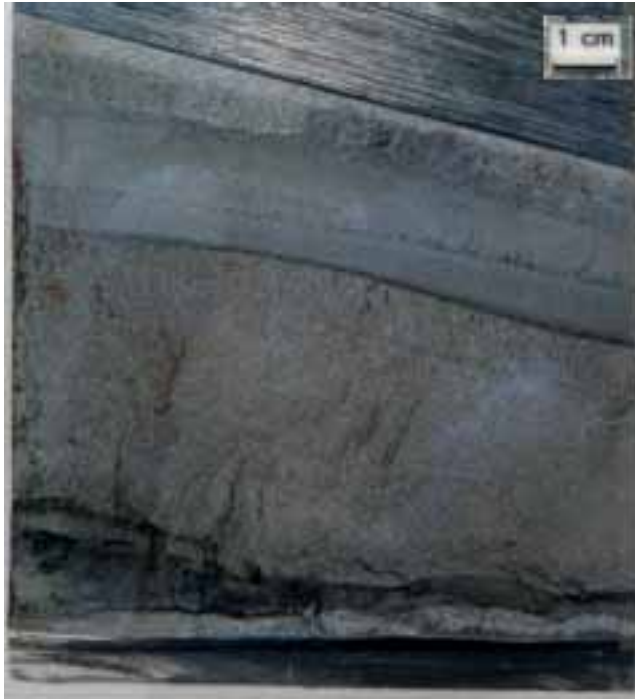


Figure 7. Presentation of a part of the sub-clad crack (crack 2) fracture surface. The location is a section of 1046 - 1146 mm from the vessel bottom.

Fig. 8 and 9 compare measured and computed strain on the cladding above the sub-clad crack 2 during pre-test pressurisation and first test. Crack propagation was also modelled in the computation. The computed strain shows almost linear behaviour on the contrary of the measured strain. At the final time step, 402 s, cleavage crack extension (31 - 53 mm) was simulated in the computation of the first test, Fig. 9. The cleavage crack growth causes an immediate jump in the computed strain value. There is a close correspondence between the computed and measured strain values at time values less than 50 seconds. The ductile intergranular crack growth during the test gives explanation for the measured quite rapidly growing strains without specific jumps.

The test behaviour of the clad vessel can be summarised as follows:

- Rupture of the vessel occurred through initiation and growth of the surface crack (crack 1) in pressurisation before test 2.
- The under-clad crack (crack 2) initiated and arrested several times in the pre-test pressurisations. Considerable amount of cleavage crack extension occurred.
- The extended under-clad crack initiated and arrested in the last two tests (tests 2 and 3). Crack extension type was ductile grain boundary fracture. The last (minor) part of the crack extension in test 3 was ductile.

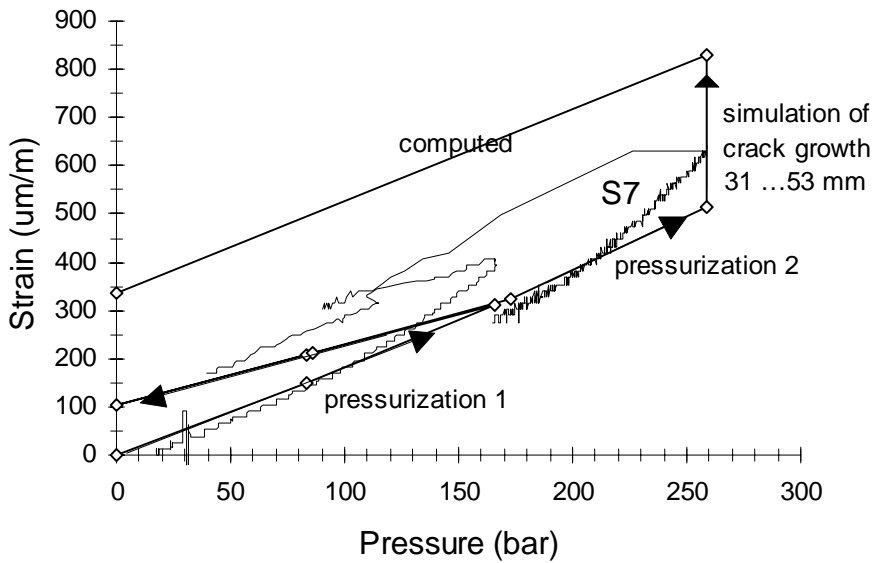


Figure 8. Comparison of measured and computed circumferential strain (10 mm from the crack plane) in the cladding above the sub-clad crack (crack 2) during pre-test pressurisation.

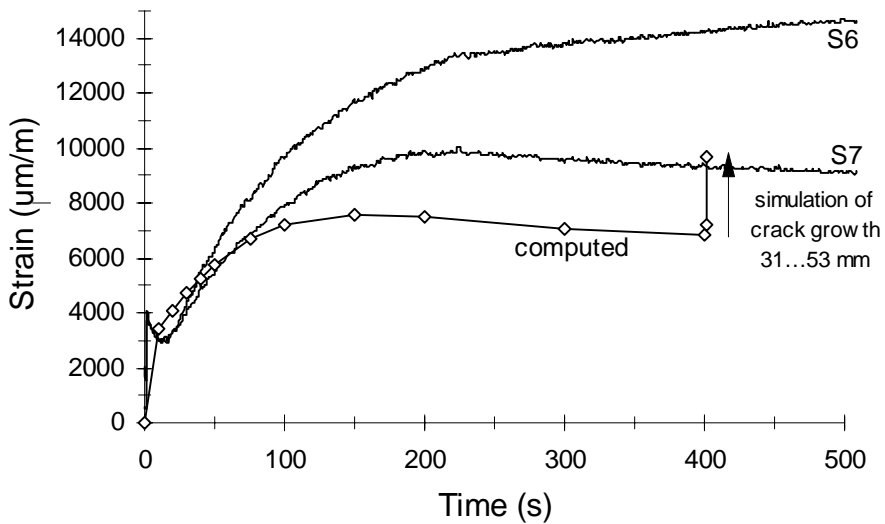


Figure 9. The computed maximum strain above the sub-clad crack together with measured strains S6 and S7 in the first thermoshock test.

6. Assessment of RPV primary nozzle integrity

The objectives of this IAEA Coordinated Research Programme (IAEA CRP) were to exchange information on the state-of-the art in assessing remaining life of the reactor pressure vessel (RPV) nozzles and mitigating effects of ageing, and to perform a collaborative case study. Organisations from Bulgaria, the Czech Republic, France, Germany, Hungary, Russia, the United Kingdom, Finland and USA as well as CEC/IAM Joint Research Centre were taking part in the programme (Erve 1995). The stage 2 of the programme was aimed at comparing methodologies for evaluating the current condition, assessing structural integrity and predicting remaining life of a selected VVER-440/213 RPV nozzle. The individual partners performed a detailed evaluation, considering brittle fracture, leak-before-break or fatigue failure phenomena and related assessment methods.

The brittle fracture analysis of the selected primary nozzle from one unit of the Hungarian VVER-440 nuclear power plant PAKS performed by VTT is presented here. It was assumed in the analysis, that there was a circumferential inside surface crack in the fusion line of a bi-metallic weld.

The nozzle was thought to be subjected to operational pressure and to emergency coolant flow transients. The first transient was stratified flow, which caused strip cooling loading conditions. The second one was perfect mixing, which caused axisymmetric cooling loading conditions. A detailed presentation of the brittle fracture analysis can be found in Keinänen & Talja (1996).

6.1 Finite element computation model

The numerical computations were made using Abaqus 5.4 finite element software. The analyses were thermo-elastic-plastic small strain and small displacement analyses. Materials were modelled using von Mises plasticity. J-integral was calculated using the contour integral method of Abaqus 5.4. From J-integrals stress intensities were calculated using the well-known plane strain formula.

A 30 degree section of the reactor pressure vessel (RPV) wall was modelled, Fig. 10. A circumferential crack with depth of 18.1 mm was modelled. The crack tip was modelled as a blunted notch with a radius of 0.05 mm.

The normal operating pressure 12.4 MPa and corresponding resultant forces were modelled on the free (vertical) surface of the pipe and on the horizontal lower surface of the pressure vessel wall. The initial temperature of the vessel was 265°C. The inner surface temperature varied from 133 to 265°C and the heat transfer coefficient from 1500 to 3000 W/m²K.

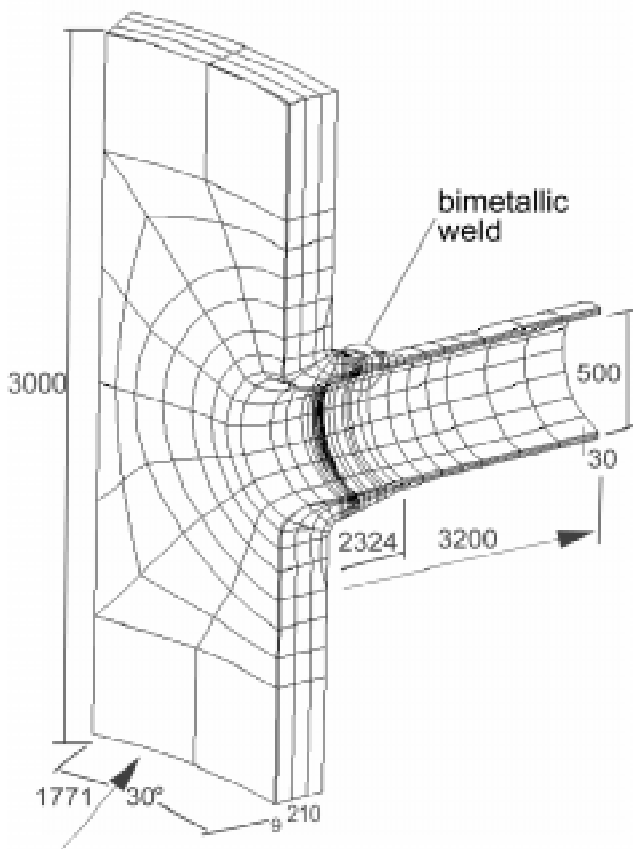


Figure 10. The finite element model of the RPV wall section (Keinänen & Talja 1996).

In the "free" face of the pipe the nodes were fixed to the initial plane which was free to translate but not to rotate ('free' boundary conditions). An alternative modelling was made in such a way that axial shrinkage of the pipe was hindered ('fixed' boundary conditions). A prescribed displacement was given to the "free end" of the pipe. The magnitude of the displacement corresponded to that caused by the pressure loading.

6.2 Simplified computation

For comparison, the analyses were performed also by simplified fracture assessment methods. The engineering fracture assessment program system "MASI" Talja (1995) was applied. Because there were not direct solutions for the nozzle geometry in the program system, some essential simplifications were made.

The geometry was described as an infinitely long cylinder with constant radius and wall thickness. The wall thickness corresponded to that at the location of the crack. In the case of strip cooling the program does not consider the circumferential heat flow. This gave slightly too small (conservative) temperature values in the strip area.

In stress intensity factor computation there was no solution available for R/t values smaller than 5. The temperature and stress distributions due to the thermal shock are mainly defined by the wall thickness, not by the radius. Thus, the inner radius was taken as 475 mm and the internal pressure value was correspondingly scaled down to 6.48 MPa. In the stress intensity factor calculation an axisymmetric crack case with axisymmetric loading was utilised.

6.3 Assessment of brittle fracture

To assess brittle fracture the 'emergency condition' -curve from the former Soviet code (Standards for Strength and Calculations of Components and Piping of Nuclear Power Plants, Energoatomizdat, Moscow, USSR (1989)) was used giving $K_{I3} = 26 + 36 e^{0.02(T-T_k)}$. In this case the given value for T_k was 50°C.

In the perfect mixing loading case the ‘fixed’ boundary condition gave higher stress intensity factor values than ‘free’ boundary conditions. In the stratified flow loading case the differences were small.

Fig. 11 shows the calculated stress intensity factors as a function of crack tip temperature for the stratified flow loading case with ‘free’ boundary conditions. The material toughness curve is not presented, because it would be located on the left (safe) side of the figures outside the scaling range. The results confirm, that safety margin against brittle fracture is relatively large under the assumed conditions.

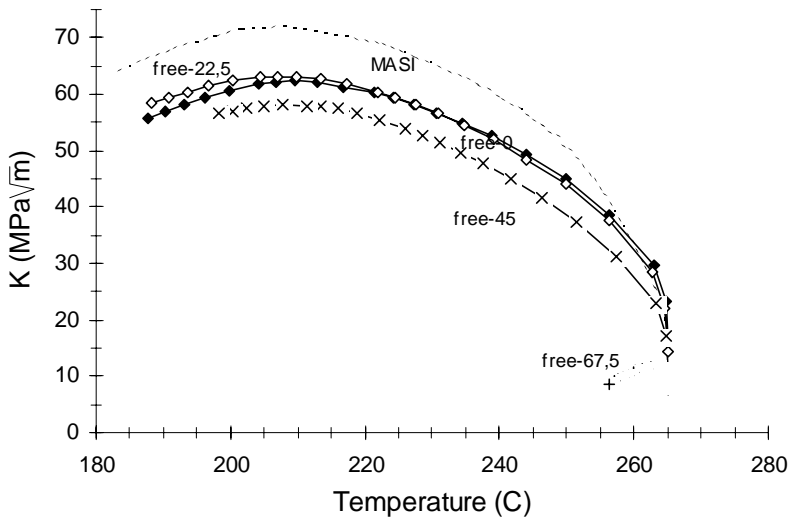


Figure 11. Calculated stress intensity factors as a function of crack tip temperature, stratified flow loading conditions causing strip cooling. Results are shown for ‘free’ boundary conditions at selected crack front locations (angular distance from crack plane ($^{\circ}$) is shown).

Welding residual stresses were not taken into account in the finite element computations. The modelling of the boundary condition at the free edge of the inlet pipe had a significant effect on the results. A simplified engineering assessment provided results with a reasonable agreement with the detailed finite element analysis.

The brittle fracture analysis was performed also by plant designer EDO Hidropress, Nuclear Power Plant Paks and VUJE (NPPRI) (Erve 1996). For the given transient all the results were similar.

EDO Hidropress performed additional analysis for a beyond design based accident transient, which produced more severe results. In this case brittle fracture provision for the vessel nozzle is met if emergency core cooling system (ECCS) water is pre-heated to a temperature of 55°C.

7. Conclusions

The reliability of the structural integrity analysing methods and capabilities, which have been developed for application in NPP component assessment especially for dynamic and PTS loading cases, was evaluated and verified. This was mainly done by comparison with experimental data from large scale tests.

The behaviour of a steel containment was assessed under two detonation pulses while the focus to determine detonation transients, predict the structural response and evaluate the capability of the tools available. The effect of geometrical non-linearity and strain rate dependence of material behaviour proved to be crucial.

Further investigations were made into dynamic behaviour of reinforced concrete structures. According to test analysis results, ABAQUS/Explicit can be successfully applied in cases, where the compression crushing of concrete is not decisive. A horizontal concrete floor of a PWR plant, subjected to jet impingement caused by a postulated near-by secondary circuit pipe rupture, was analysed. The jet impingement force was evaluated based on a thermal hydraulic analysis and the loading of impingement was determined considering the deflection of the broken pipe. The results verified adequate structural strength, in spite of incipient cracking and plastic deformation at zones of maximum tensile stresses at the area where the water jet hits the slab.

One of the main steam lines of the Loviisa Nuclear Power Plant, made of ferritic CT20 steel, was considered under a pressure transient due to a condensation water hammer. Thermal hydraulic analyses and pressure transient evaluations

were carried out by IVO Power Engineering Ltd. Based on a model using pipe and elbow elements, the stresses were below the measured material yield stress. However, for more exact stress considerations in the near vicinity of the T-connection a more detailed finite element model is needed.

In a joint research program between IVO Power Engineering, VTT Manufacturing Technology and Central Research Institute of Structural Materials "Prometey" crack behaviour was studied under pressurised thermal shock loading. The program consisted of pressure vessel tests with two model pressure vessels in simulated brittle condition. Three PTS tests were carried out on the second (cladded) model pressure vessel. Both under-clad and through-clad axial cracks in the outside surface were tested. Considerable amount of cleavage extension of the under-clad crack occurred in the pre-test pressurisations. The extended under-clad crack initiated and arrested in the last two tests. Crack extension type was ductile grain boundary fracture. Computational analyses were made using ABAQUS. With help of these analyses the behaviour of the under-clad crack could be clarified.

Within an IAEA Coordinated Research Programme a brittle fracture analysis of a primary nozzle from one unit of the NPP PAKS was performed by several organisations. A circumferential crack in the fusion line of the bimetallic weld was assumed. In addition to operational pressure, a stratified flow transient and a perfect mixing cooling case were considered. In computations detailed finite element models and simplified fracture assessment methods were applied. Simplified engineering assessment provided results with a reasonable agreement with the detailed finite element analysis. The results confirmed, that the safety margin against brittle fracture is relatively large under the assumed conditions.

Generally, all the analyses reported here showed that good predictions of complex loading cases can be obtained with modern computational tools. Again it proved out that very careful consideration of boundary conditions is necessary.

8. Acknowledgements

The reported work was part of the Finnish Research Programme on the Structural Integrity of Nuclear Power Plants 1995 - 1998, subprojects RAKE3-4 on Structural Analyses for Nuclear Power Plant Components. The work for Chapters 2 - 3 was completed in 1995 - 1997, Chapter 4 in 1997 and Chapters 5 - 6 in 1995 - 1997.

Co-operation with Rauli Keskinen and Rainer Rantala from Radiation and Nuclear Safety Authority (STUK), Paulus Smeeke from TVO, Ralf Ahlstrand, Alpo Neuvonen and Yrjö Hytönen from IVO Ltd. together with many other colleagues is gratefully acknowledged. The work reported in Chapter 6 was a cooperative task between IVO, Prometey Institute from Russia and VTT. The work reported in Chapter 6 was coordinated to the IAEA CRP Programme.

References

Erve, M. 1995. Brittle fracture evaluation in the dissimilar weld. In IAEA Coordinated Research Programme (CRP) "Management of Ageing of Reactor Pressure Vessel (RPV) Primary Nozzle". Results of stage I, Appendix 1, Part B. Vienna: IAEA (Working material IWG-LMNPP-95/2).

Erve, M. 1996. Pilot studies on management of ageing of nuclear power plant components. IAEA-Coordinated Research Programme "Management of Ageing of Reactor Pressure Vessel (RPV) Primary Nozzle". Final Report (1st draft). Erlangen, 20.12.1996.

Keinänen, H. & Talja, H. 1996. Brittle fracture analysis of primary nozzle of VVER-440 nuclear power plant PAKS. Espoo: VTT Manufacturing Technology (Report VALB115).

Keinänen, H., Talja, H., Rintamaa, R., Ahlstrand, R., Nurkkala, P., Karzov, G., Timofeev, B. & Blumin, A. 1997. Pressurized thermoshock tests with a clad model vessel (vessel 2). Test results evaluation. Espoo: Technical Research Centre of Finland. 44 p. + app. 20 p. (Report VALB149).

Keinänen, H., Talja, H., Rintamaa, R. 1998a. Computational methods assuring nuclear power plant structural integrity and safety: an overview of the recent activities at VTT. Nuclear Engineering Design, Vol. 183, pp. 41 -51.

Keinänen, H., Talja, H., Rintamaa, R., Planman, T., Ahlstrand, R., Nurkkala, P., Karzov, G., Timofeev, B. & Blumin, A. 1998b. Lessons learned from large scale PTS testing. 5th Int. Conference on Material Issues in Design, Manufacturing and Operation of Nuclear Power Plant Structures and Equipment, St. Petersburg, Russia, June 7-14, 1998. 11 p.

PNAEG-7-002-86. 1989. Strength Calculation Standards for Components and Pipelines of Nuclear Power Plants. Energoatomizdat, Moscow.

Saarenheimo, A. 1994. Preliminary analyses of a steel containment under detonation conditions. Espoo: Technical Research Centre of Finland. 33 p. + app. (Report VALB52).

Saarenheimo, A. & Hyvärinen J. 1996. Finite element analyses of a steel containment under detonation conditions. Accepted provisionally for presentation at the Fourth International Conference on Structures under Shock and Impact, 3 - 5 July, Udine, Italy.

Saarenheimo, A. 1997a. Iskukuormitettujen teräsbetonirakenteiden analysointi elementtimenetelmäohjelmalla. Espoo: VTT Manufacturing Technology. 24 p. (Report VALB181). (In Finnish).

Saarenheimo, A. 1997b. Non-linear analysis of a reinforced concrete slab subjected to jet impingement. Espoo: VTT Manufacturing Technology. (Report VALB209).

Saarenheimo, A. 1998. Structural analysis of piping loaded by pressure transients. Espoo: VTT Manufacturing Technology. 48 p. + app. 31 p. (Report VALB332).

Sammataro, R. F., Solonic, R. W. & Edwards, N. W. 1993. A generic approach for steel containment vessel success criteria for severe accidents loads. Nuclear Engineering and Design, Vol. 145, pp. 289 - 305.

Stronge, W. J. & Yu, T. X. 1993. Dynamic models for structural plasticity. London: Springer-Verlag. 279 p.

Talja, H. 1995. Program system MASI for fracture assessment. Version 1.0. Status report and user instructions. Espoo: VTT Manufacturing Technology. 36 p. + app. 23 p. (Report VALB43).

(See Appendix 1 for a comprehensive listing of publications)

Verification of analysis methods through participation in the NESC1 programme

Rauno Rintamaa, Tapio Planman, Heikki Keinänen,
Heli Talja and Pentti Kauppinen
VTT Manufacturing Technology
Espoo, Finland

1. Introduction

The evaluation and verification of the capabilities and reliability of the structural integrity assessment methods and tools, which have been developed in the RATU2 programme, has been conducted by participation in several international co-operative programmes. In such programmes the computational capabilities can be verified by comparison of results with those of other specialists and with experimental data.

The results obtained through participation into the European Network for Evaluating Steel Components, NESC1 programme are presented in this paper.

2. European Network for Evaluating Steel Components (NESC)

2.1 Collaborating principles

In general, the objective of the NESC network is to organise and manage an international network of organisations around experimental programmes which will:

- Enable information to be exchanged about the entire process of structural integrity assessment
- Stimulate the undertaking of specific collaborative studies

- Work towards the use of best practice and support the harmonisation of international standards.

The network structure for NESC is based on the use of an independent operating agent (JRC) and the division of the individual tasks into Task Groups such that these can be kept at a manageable size and in general be supported by “in-kind” contributions from the partners.

The role of the Joint Research Centre (JRC) of the European Commission was fixed by the “club type” Collaboration Agreement which was the basis of the NESC co-operation. This agreement, as for all the other European Networks, ENIQ, AMES and EPERC is based on the following principles:

- International consensus of achieving results
- Contribution in kind, no cash flow
- Steering Committee representative of all participants
- Projects within Structural Integrity of Ageing Components
- Neutral independent laboratory for Reference Laboratory, refereeing and daily management.

In order to carry out the work of the Network a number of Task Groups were set up:

Task Group 1	Inspection
Task Group 2	Material Properties
Task Group 3	Structural Analysis
Task Group 4	Instrumentation
Task Group 5	Evaluation.

All these Task Groups report to a Steering Committee at which each partner is represented and where any important decisions affecting the Programme are taken.

2.2 NESC 1 spinning cylinder project

The NESC1 spinning cylinder project (Hurst et al. 1996) was started in 1994 and it will be completed during 1999. It is the first project started in the European Network for Evaluating Steel Components (NESC). The purpose of NESC is to study and verify the entire process of structural integrity assessment of steel structures and the associated methods. In NESC1 the focus is on methods used in studying the behaviour of under-clad and through-clad cracks in PWR vessel steels.

The NESC 1 network has comprised members from 33 different organisations from 12 different countries. VTT has participated in the testing of materials, analysed the measured material data as well as co-ordinated the work of the material characterisation task group (TG 2). In addition, VTT performed pre- and post-test NDT-inspection of the cylinder and structural analysis.

The simulated pressurised thermal shock experiment (PTS), one of the most demanding tasks of the NESC1 project, was carried out successfully in spring 1997 using the spinning cylinder test facility of AEA Technology PLC (AEA). The structural analyses of the experiment as well as the destructive examination of the cylinder will be completed by the end of 1998. Draft final evaluation report has been scheduled for the end of March 1999.

3. Material properties for the spinning cylinder

Materials Task Group (TG2) chaired by R. Rintamaa has been responsible for gathering and collating the material property data used in the stress and fracture analyses (Rintamaa et al. 1997). It is worthy of note that these tests produced not only tensile and fracture properties but also thermal and other physical properties and that cladding, base material and heat affected zone were covered by the tests. These tests were carried out on an actual off-cut from the test cylinder clad using exactly the same procedure as the cylinder. It is considered that the NESC test cylinder is almost certainly the best characterised piece of steel in the world and a NESC report collating all the data has already been produced. Nine European institutes participated in the extensive material characterisation programme (Table 1).

Table 1. Participants of the material characterisation programme in NESC 1 project.

Institut für Werkstoffmechanik (IWM), Germany
ENEL, Italy
AEA Technology/Rolls Royce and Ass., United Kingdom
VTT Manufacturing Technology (VTT), Finland
Materialprüfungsanstalt Stuttgart (MPA), Germany
Framatome, France
Netherlands Energy Research Foundation (ECN)
Energy Centre Nederland (ECN), The Netherlands
Siemens-KWU, Germany

In the following, material property data produced or analysed by VTT will be given.

3.1 Material characterisation and analysis methods (VTT)

The test programme consisted of, e.g., tensile, instrumented Charpy and static and dynamic fracture toughness tests of the cylinder base metal (Planman et al. 1996, Rintamaa et al. 1997, Rensman et al. 1998, Rintamaa et al. 1998). The fracture mechanical tests were mainly carried out using Charpy size three-point bend specimens with initial crack length $a_0/W = 0.5$ (tests with $a_0/W = 0.1$ were performed by Framatome). Charpy-V specimens were used for measuring the transition temperatures of impact toughness and for estimating the mean temperature corresponding to the crack arrest force of 4 kN. The static and dynamic fracture toughness test data were analysed according to the Master Curve method (ASTM E 1921-97).

The crack arrest fracture toughness (K_{Ia}) of the cylinder material was determined in two ways. Test data were measured according to the standard method (by MPA Stuttgart) and analysed statistically to determine the reference temperature (T_0) of K_{Ia} (by VTT) (ASTM E 1921-97). The K_{Ia} -temperature curves were also estimated from the measured Charpy data using a correlation based on the crack arrest force (by VTT).

Supplementary fracture toughness and Charpy tests were performed on the heat-affected zone (HAZ) of the base metal locating under the welded inside cladding because the thickness of this layer was as large as 10 mm max. and could thus have affected the fracture behaviour of the vessel. The fracture surfaces of some tested specimens were examined by electron microscopy (SEM) to make sure that the dominating fracture mode has been cleavage. Susceptibility to intergranular mode was expectable since the material had been tempered in a temperature regime where temper embrittlement is likely. The exceptional heat-treatment had been applied to simulate irradiation embrittlement. The wall thickness of the cylinder was 170 mm and the base metal grade A 508 B type forged steel.

3.2 Basic results

Some of the basic results measured in the material characterisation programme are given here. For example, Charpy tests were carried out by VTT and AEA. The transition temperatures corresponding to impact energy 41 J, lateral expansion 0.89 mm and 50% shear fracture were 78°C, 97°C and 92°C, respectively. The measured data and the transition curve fitted to VTT's data are shown in Fig. 1.

The static fracture toughness tests measured with Charpy size and 25 mm thick three-point bend specimens were carried out by VTT and ENEL. The measured data and the calculated fracture probability curves adjusted to 25 mm specimen thickness are shown in Fig 2. The results, including all data, gave $T_0 = 68^\circ\text{C}$.

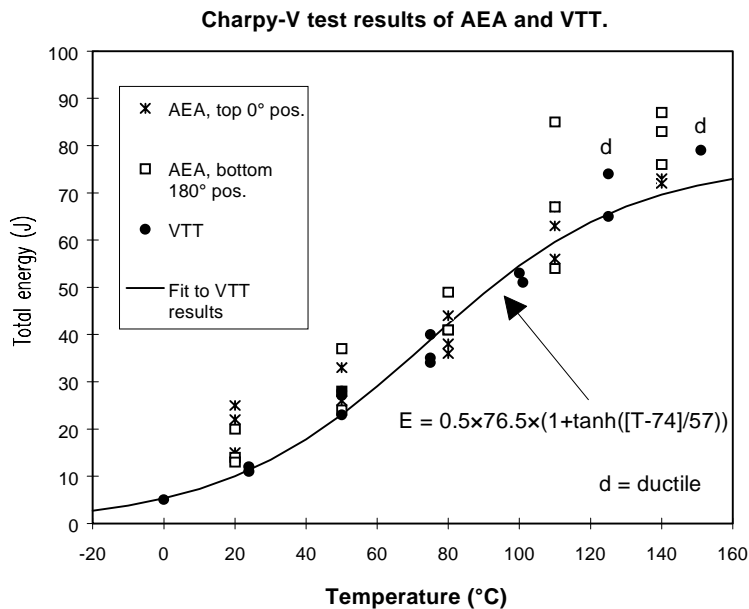


Figure 1. Charpy test results of the base metal (the AEA data from cylinder No. 4).

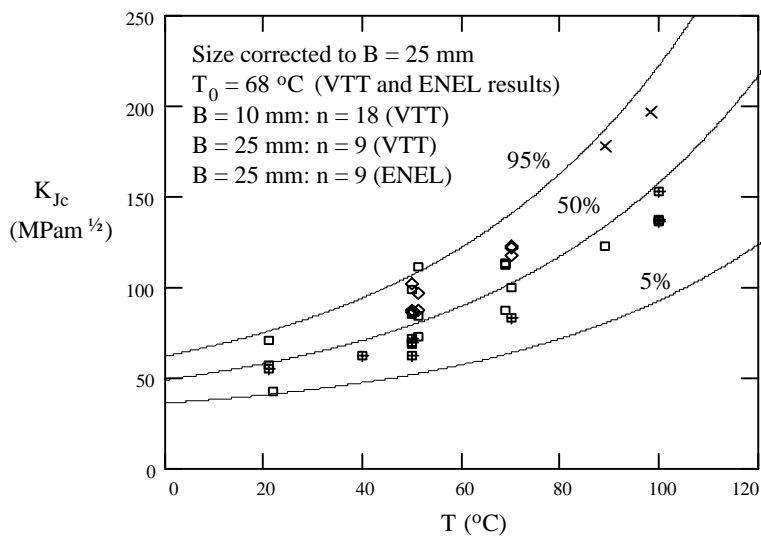


Figure 2. Fracture toughness of the base metal measured with specimen thickness 10 and 25 mm (adjusted to 25 mm specimen thickness). $\square = 10 \times 10$ mm (VTT), $\diamond = 25 \times 25$ mm (VTT), $\times = 10 \times 10$ mm, ductile (VTT) and $\oplus = 25$ mm CT specimen (ENEL).

The mean (50% fracture probability) crack initiation and crack arrest fracture toughness of the base metal are shown as a function of temperature in Fig. 3. The 4 kN crack arrest force temperature was on the average 73°C which corresponds to, according to the proposed correlation, the crack arrest fracture toughness reference temperature of 84°C (Planman et al. 1996). The reference temperature (T_0) estimated using the correlation of the 100 MPa√m crack arrest fracture toughness and the 4 kN crack arrest force transition temperatures was thus close to the T_0 of the measured K_{Ia} data (Fig. 3). The K_{Ia} data measured by MPA Stuttgart have been analysed statistically using the Master Curve method.

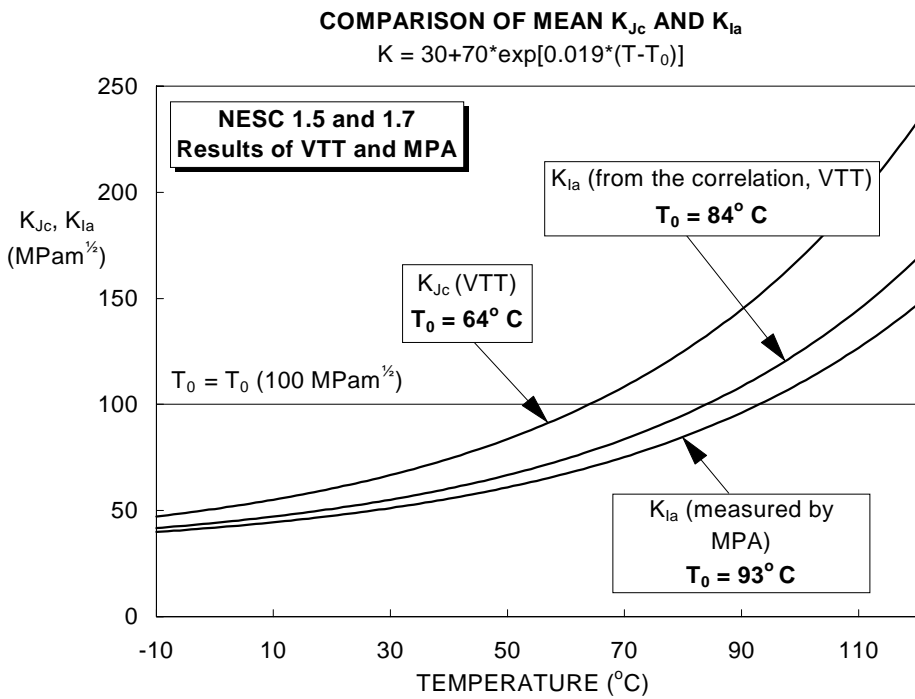


Figure 3. Comparison of K_{Jc} and K_{Ia} vs. temperature (50% fracture probability) calculated from the measured test results (K_{Jc} and K_{Ia}) and using the proposed correlation (K_{Ia}).

The reference temperatures T_0 (100 MPa√m) and the 41 J impact energy (E) transition temperature measured for the base metal are compared in Table 2. The results show nearly equal T_0 for both the static and dynamic fracture toughness (K_{Jc} and K_{Jd}) but over 20°C higher value for the crack arrest

toughness (K_{Ia}). The temperature (T_0) measured for the heat-affected zone of the base metal locating under the cladding was about 50°C lower than in the base metal outside the heat-affected zone. The nil-ductile transition temperature based on the Pellini tests was measured to be close to +35°C.

Table 2. Comparison of 100 MPa√m transition temperatures T_0 and $T_{41 J}$.

Material	K_{Jc} T_0 (°C)	K_{Jd} T_0 (°C)	K_{Ia} T_0 (°C)	E $T_{41 J}$ (°C)	E $T_{68 J}$ (°C)
Base metal $a_0/W = 0.5$	64 ¹⁾ 68 ²⁾	68	93	78	134
Base metal $a_0/W = 0.1$	32 ¹⁾				
HAZ under cladding	16				

1) Three-point bend specimens

2) All specimens

The instrumented Charpy test results of the programme were also used to validate the correlation developed for estimating the 100 MPa√m K_{Ia} crack arrest fracture toughness transition temperature ($T_{K_{Ia}}$) of various structural steels (Planman et al. 1997). The correlation is calculated from the transition temperature of the Charpy specimen crack-arrest force of 4 kN which according to the experience seems to be measurable for most structural steels.

The revised version of the correlation (including all the data currently available) and the linear regression fit are shown in Fig. 4. The NESCI result thus follows well the correlation.

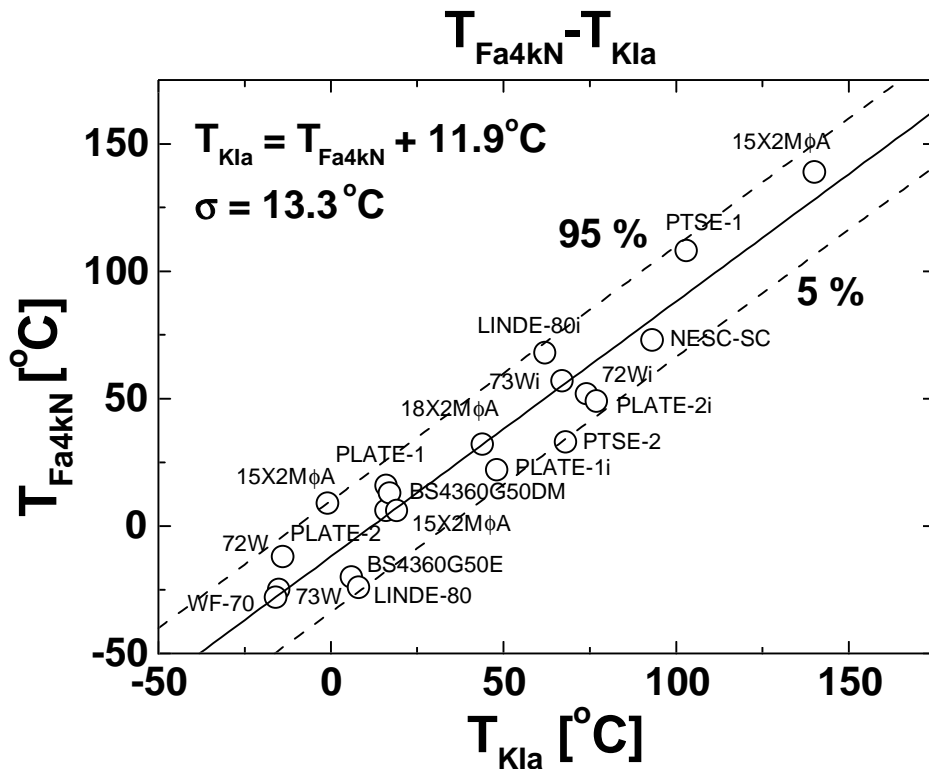


Figure 4. Correlation between the transition temperatures for the Charpy specimen 4 kN crack-arrest force and the 100 MPa√m K_{Ia} crack-arrest fracture toughness (Planman et al. 1997).

3.3 Findings on the material properties

Based on the results of the material tests carried out in NESC1 Task Group 2, the following key conclusions have been made:

- Hardness measurements and metallographical studies have indicated that the width of the HAZ under the cylinder cladding is 5 to 10 mm. This means that the HAZ should be considered in modelling the behaviour of the under-clad and through-clad cracks. The fracture toughness of the HAZ is higher than that of the base metal (the difference in T_0 is about 50°C).

- The fracture toughness with the shallow crack ($a_0/W = 0.1$) is higher than with the deep one (the value of T_0 was 32°C with the shallow crack and 64°C with the normal one, i.e. $a_0/W = 0.5$).
- The difference in the static and dynamic fracture toughness is almost negligible.
- The value of T_0 ($100 \text{ MPa}\sqrt{\text{m}}$) of the crack arrest toughness is about 30°C higher than that of the crack initiation fracture toughness.
- The crack arrest toughness of the base metal follows the proposed transition temperature correlation based on the 4 kN crack arrest force measured by Charpy tests.

All results are still in evaluation process, and final conclusions will be drawn in the first half of 1999.

4. Numerical analyses for the experiments

VTT has participated in the pre-test analysis phase of NESCI by providing pre-test analyses using the MASI system (some of the preliminary pre-test computations were conducted using detailed thermo-elastic three-dimensional models) and computations for fitting the heat transfer coefficient values to experimental thermal data (Talja et al. 1997).

Due to the use of simplified methods, only the behaviour of a surface breaking crack at the deepest point was predicted during the NESCI experiment. Due to linear elastic stress analysis these calculations were obviously quite conservative. No crack initiation or growth in the direction of the wall thickness was predicted and thus the computational results confirmed that there was no risk of catastrophic failure due to the most critical crack.

The heat transfer coefficient values during the test were estimated by fitting finite element results to measured temperature data and by thermohydraulic heat transfer analyses. As the temperature measurement at the inner surface might have been affected by the cooling water, it seemed most appropriate to use values below but near the surface in the fitting.

Four different choices of heat transfer coefficient values were tested. One of them was to apply values provided by a thermohydraulic analysis. Calculated temperature values were compared to the measured ones at different depths in the cylinder wall in the four cases. Temperature and stress distributions from the different analyses were compared to each other. Thermo-elastic-plastically calculated stress distributions in the four cases were almost identical and so also the effect on fracture assessment results would be very small. As also the calculated temperature values differed only slightly from each other, no big difference in the safety assessment is caused due to applied fracture toughness values.

The post test analyses were started in Autumn 1998 when the results of fractographic studies were available. They will be completed by the end of the year. These computations include:

- 1) an assessment using the ASME procedure,
- 2) a detailed 3D analysis for the initial crack geometry (Fig. 5) and applying the master curve method to assess initiation of brittle crack growth and
- 3) a 3D analysis with a “slice model”, corresponding to the deepest point of the crack, to estimate ductile crack growth both in base material and in cladding.

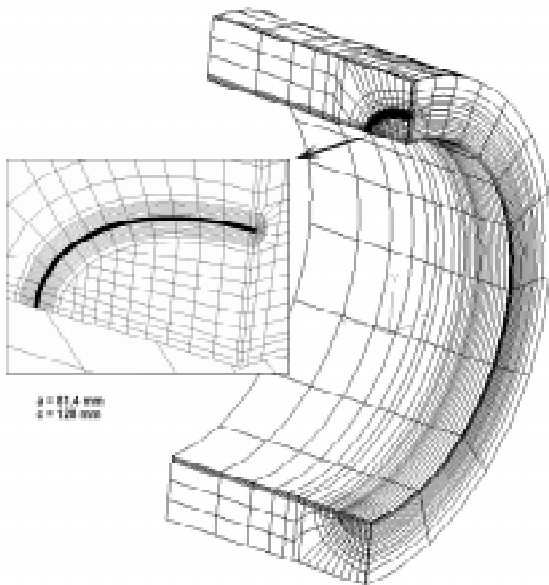


Figure 5. Finite element mesh for the post-test analyses of NESCI experiment.

5. Nondestructive testing

VTT performed the preservice and inservice inspections of the NESC cylinder in 1996 and 1997 by using a mechanized ultrasonic equipment shown in Fig. 6. The same equipment is used in the inservice inspections of several components and piping welds in the Finnish nuclear power plants. The equipment includes a mechanized scanner that is moving along the surface to be inspected guided by a rubber-belt. The scanning was performed on the outside surface of the cylinder. The ultrasonic part of the inspection system consists of a multichannel ultrasonic flaw detector (SUMIAD) and a data analysis system (MASERA).

The inspection procedure used for detection of defects was based on the use of both normal incidence and angle beam probes (31° , 41°). The angles of incidence were selected in order to optimize the corner reflection from possible cracks. For detection of axial cracks two probes in opposite directions were used. During scanning all signals exceeding the noise level were recorded.

For the sizing of flaws the crack tip reflection technique was used. In addition, the analysis of selected flaws was performed by applying the SAFT-technique. All indications which were assessed to be caused by flaws were reported in full details (position, length, width, height). For two main defects the crack profiles were given in the report.

The results of both preservice and inservice inspections have been reported to JRC Petten in confidential reports containing also the description of the inspection procedure applied. The evaluation of the results of different participating teams is still in progress and no results can be presented here. A summary report containing the results of destructive analysis performed and the results of different teams is expected to be available in the spring 1999.



Figure 6. Inspection of the NESC cylinder with the mechanized ultrasonic equipment of VTT.

6. Conclusions

As the results of NESC 1 project are still in the evaluation process, no well defined general technical conclusions can be done. However, preliminary evaluations indicate that some further research is needed concerning the accuracy and qualification of in service inspection (ISI), relevancy of material parameters to be used in structural analysis as well as selection of structural integrity assessment methods.

In general, the network is an efficient forum to perform large projects with general joint interest, and to exchange information, expertise, know-how and experience in a very useful way.

7. Acknowledgements

The reported work was part of the Finnish Research Programme on the Structural Integrity of Nuclear Power Plants 1995 - 1998, subproject RAKE4 on Structural Analyses for Nuclear Power Plant Components and subproject AIRI2 on Reliability of Non-destructive Inspections of Nuclear Power Plants.

Co-operation with Rauli Keskinen, Rainer Rantala and Matti Ojanen from the Radiation and Nuclear Safety Authority (STUK), Ralf Ahlstrand and Alpo Neuvonen from IVO Ltd., Paulus Smeekes from TVO Ltd. together with many other colleagues is gratefully acknowledged. The work reported was VTT's contribution to the co-operative NESC1 programme within the European Network for Evaluating Steel Components, which is co-ordinated by the EU JRC, Institute of Advanced Materials, Petten.

References

ASTM E 1921-1997. Test method for the determination of reference temperature, T_0 , for ferritic steels in the transition range. ASTM Books of Standards.

Hurst, R., Wintle, J. and Hemsworth, B. 1996. NESC: The Network for Evaluating Steel Components. Int. Conference on Pressure Vessel Technology, Vol 1.

Planman, T., Valo, M., Wallin, K. and Rintamaa, R. 1996. NESC1 Material Characterization.. Espoo: VTT Manufacturing Technology. 25 p. + app. 72 p. (Report VALC-270).

Planman, T., Wallin, K. and Rintamaa, R. 1997. Evaluating crack arrest fracture toughness from Charpy impact testing. SMIRT -97, Structural Mechanics in Reactor Technology. Lyon, France, 17 - 22 August 1997. 8 p.

Rensman, J., Horsten, M.G, Rintamaa, R., Blauel, J.-G., Keim, E. and Wardle, G. 1998. Comprehensive pre-test material characterisation: Results of the characterisation of the HAZ and the cladding in view of ductile fracture of the NESC 1 spinning cylinder. In: Bhandardi, S. (Ed.) Severe Accidents and Topics in the NESC Project. PVP-Vol. 362. New York: The American Society of Mechanical Engineers. Pp. 229–235.

Rintamaa, R., von Estorff, U. and Wintle, J. B. 1997. Pre-test material characterisation of the NESC spinning cylinder. Proceedings of ICONE 5, 5th International Conference on Nuclear Engineering. Nice, France, 26 - 30 May 1997. In: CD, 1997 ASME/SPEM/JSME ICONE-5, Proceedings of the 5th International Conferences on Nuclear Engineering, ASME. 6 p.

Rintamaa, R., von Estorff, U., Fedeli, G., Gillot, R. and Houssin, B. 1998. Comprehensive pretest material characterization - a view to cleavage fracture of the NESC1 spinning cylinder. In: Bhandardi, S. (Ed.) Severe Accidents and Topics in the NESC Project. PVP-Vol. 362. New York: The American Society of Mechanical Engineers. Pp. 221–227.

Talja, H., Saarenheimo, A., Miettinen, J. and Lindholm, I. 1997. NESC1 project - simplified pretest analyses and sensitivity analysis for heat transfer coefficient. Espoo: VTT Manufacturing Technology. 16 p. + app. 28 p. (Report VALB245).

(See Appendix 1 for a comprehensive listing of publications)

Non-destructive inservice inspections

Pentti Kauppinen, Matti Sarkimo and Kari Lahdenperä
VTT Manufacturing Technology
Espoo, Finland

1. Introduction

In order to assess the possible damages occurring in the components and structures of operating nuclear power plants during service the main components and structures are periodically inspected by non-destructive testing techniques. The reliability of non-destructive testing techniques applied in these inservice inspections is of major importance because the decisions concerning the needs for repair of components are mainly based on the results of inspections. One of the targets of this research program has been to improve the reliability of non-destructive testing. This has been addressed in the sub-projects which are briefly summarised here.

2. Validation of ultrasonic inspection

The Finnish utilities and the nuclear regulatory body, STUK have shown increasing interest in the methodology and practises for qualification of non-destructive testing techniques used in the inservice inspections of Finnish nuclear power plants. As a background to this work are the requirements for Performance Demonstration presented in the Appendix 8 of the ASME Code Section XI. It has been clear from the beginning that the approach presented in ASME can't be followed in a country where only a few nuclear plants are in operation. The costs caused by the manufacture of the test specimen needed in ASME-type performance demonstration would be very high and in some cases also technically impossible due to the lack of representative material, manufacturing technology etc.

At the European level an alternative methodology for inspection qualification has been under development in the European Network for Inspection Qualification (ENIQ). VTT has participated this network from the early beginning of the work as a technical adviser to the Finnish utilities. The European regulatory bodies have formed similar working group that has been participated by the representative of STUK. Both working groups have prepared documents describing the European methodology for inspection qualification from their points of interest.

In Finland the work has had two focus areas:

- The establishment of the national practise for inspection qualification
- The development of technology for fabrication of test blocks containing defects that simulate service induced defects.

The development of the Finnish practise for inspection qualification has been carried out in a national working group formed by the representatives of the utilities, major inspection companies and VTT. The work has been based on the documents drafted in the two European working groups and therefore the practise drafted is following the main lines of the European methodology for inspection qualification.

The overall description of the national NDT-qualification methodology is still under preparation and the target is to have the proposed practise accepted in 1997. The draft document has been discussed in the national working group and in a meeting between the Finnish nuclear regulatory body and the utilities. The general outlines of the proposed practise have been presented in the meeting of the Finnish Welding Society (Kauppinen 1997). In some specific inspection items the qualification of inspection has been performed as a pilot study in order to get practical experience in the qualification procedure. For the qualification of the ultrasonic inspection of the welds in the primary piping of Loviisa PWR a test specimen and qualification procedure was developed in cooperation with Imatran Voima Oy. The vendor was selected by IVO based on this qualification performed with a blind test specimen containing several welds and a lot of defects. The results of this work have been reported by Paussu and Särkiniemi (1997).

The test block assembly used for the qualification of the automatic ultrasonic inspection of the primary circuit welds of Loviisa PWR contained a base metal ring, a ring with circumferential weld and a sector of elbow with longitudinal welds. The different parts of the assembly are schematically shown in Fig. 1.

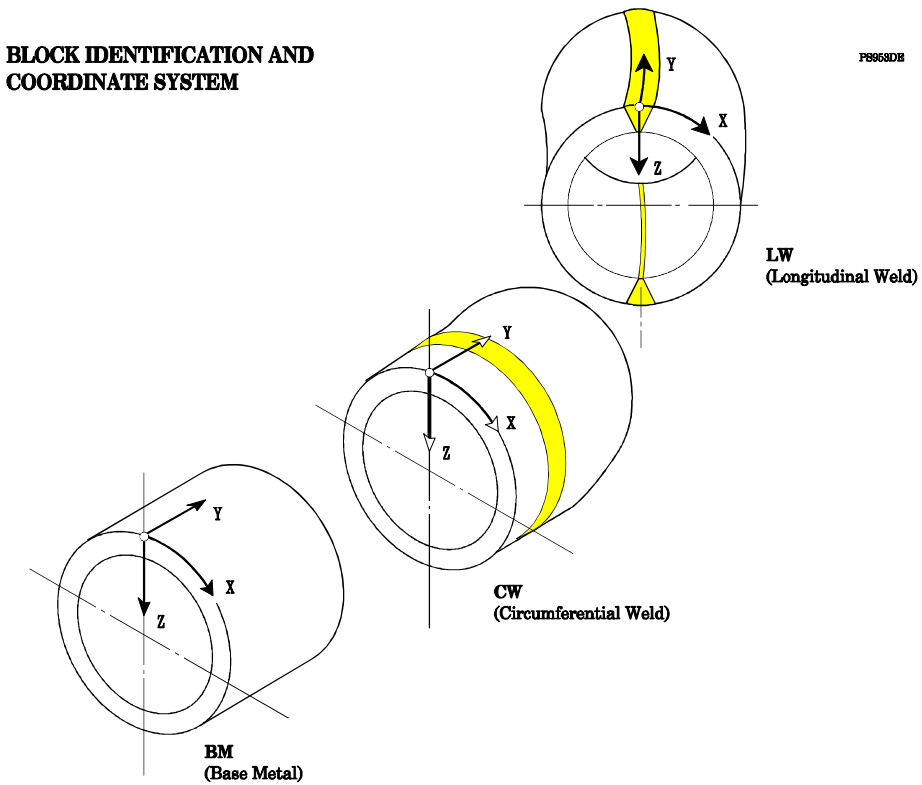


Figure 1. The parts of the test block assembly used for the qualification of the automatic ultrasonic inspection of the primary circuit welds of Loviisa PWR.

The main reflectors used in the qualification test are real implanted cracks (TGSCC) opening to the inside surface of the specimen. In order to evaluate the capability to detect deep defects having varying orientations EDM notches were used. Furthermore, some welding defects were fabricated to assess the capability to detect subsurface defects. To be sure that the noise caused by additional welds of implants do not reveal the defects several misleading defects (repair areas and blank implants) were included in the specimen.

The ultrasonic measurements performed showed that the attenuation caused by EB-welds was insignificant. The manual welds of implants could be detected in the base metal due to the increased ultrasonic noise. When these implants were in the weld metal of wide weld root area the implants could not be detected.

In order to evaluate the results of the qualification test the evaluation criteria were drafted in the spirit of Appendix 8 of ASME Code Section XI. Tolerance boxes were determined based on the practice used in the PISC III exercise. The evaluation was based on detection probability of all defects. Both deep and shallow defects were evaluated. The errors in defect sizing were calculated but not considered as determinant because no real sizing techniques were used in the qualification test.

Defect detection probability was calculated using formula $DDP = n / N$, where n is the number of defects detected and N is the total number of defects in the specimen. False-call rate was calculated using formula $FCR = f / (f + n)$, where f is the number of false-calls. Reliability of detection (ROD) is formed by two factors. The first is ability to detect defects and second to avoid false-calls. ROD is calculated using formula

$$ROD = DDP (1 - w \bullet FCR), \quad (1)$$

where w is a weighting factor describing the severity level of false calls. These criteria were used to select the vendor for inservice inspections in 1996 and to continue the optimisation of the inspection technique.

The results of the first measurements showed the necessity to further develop the inspection procedure and to perform additional measurement with improved procedure. This measurement was performed already on site just before starting the actual inspection in the plant. In this measurement satisfying results, just on the acceptable limit, were achieved.

The experience from this inspection qualification exercise can be summarised as follows:

- The techniques developed for manufacture and implanting of defects were successful.

- Implanting with EB welding gave optimal result. Noise level doesn't reveal implant.
- Implanting with manual welding can be used for longitudinal implants of welds.
- The short circumferential defects of weld root area were poorly detected.
- Axial defects of weld root area were not detected.
- Defect sizing and characterisation was inaccurate.
- The test block contained too many defects and interest areas.

Based on the good experience from this first large scale qualification similar approach is scheduled also for other inspection items.

The first pilot study of qualification of inspectors in Finland was performed in February 1997 in cooperation with the utilities and major inspection companies. The test specimen described above was one of the test specimens used in the qualification. This type of qualification process will be continued in 1998 - 1999 as a pilot phase for the Finnish inspection qualification practise.

Furthermore, the mechanised ultrasonic inspection of welds in the austenitic piping of Olkiluoto BWR was qualified with open test and technical justification. In cooperation with the utilities a blind test has been arranged for inspectors performing ultrasonic testing of austenitic piping. The experience achieved in these practical qualifications will be taken into account when preparing the national qualification practise.

The second activity has been the fabrication of test specimen for inspection qualification purposes. The work started with development of technology for creation of intergranular stress corrosion cracks in austenitic piping specimen. The target has been to create cracks under laboratory conditions directly in the specimen without implanting. The cracks should be located close to the weld and the same test specimen should contain both blank grading units (areas without flaws) and flawed grading units. The depths of the cracks should vary between 5 - 80% of the wall thickness and the crack morphology should be representative to the cracks detected in operating plants. In 1995 - 1996 the technique for producing stress corrosion cracks in austenitic pipes has been developed. With the technique developed the depths of the cracks can be controlled and the required areas from the specimen can be kept sound. From

ultrasonic point of view the cracks are representing the IGSCC detected in austenitic piping. The metallographical study showed that the cracks are propagating through the grains (not intergranular). The clear advantage of introducing the defects directly in the specimen is that the defect areas can not be detected based on the ultrasonic signals received from the welds used in implanting the coupons containing defects. This issue has raised strong criticism against the implanting technology in the ENIQ-group.

An other defect type being of interest is the thermal fatigue crack. For creation of this type of crack in laboratory the experiments were started in 1996. The first successful cracks were produced in 1997 and after that the technique has been further developed. As latest innovation cracks have been introduced in the roots of threads in threaded holes. Technique has been developed to produce cracks in different orientations and with variable depths.

3. Automatic ultrasonic inspection

In order to improve the reliability of inservice inspections of primary circuit components of nuclear power plants mechanised and automatic inspection equipment have been developed. The results of the PISC-programme demonstrated the generally superior performance of automatic inspection procedures, although some teams received extremely good results in manual inspection. In inconvenient and hazardous working conditions (radiation exposure, noise, elevated temperature etc.) a careful inspection and full coverage in scanning can only be guaranteed by using mechanised scanning devices. Since 1995 VTT is using in mechanised ultrasonic inspections the SUMIAD-system developed by Tecnatom/Spain. This system allows recording of full A-scan data from 8 channels simultaneously. The results are presented in C-, B- and D-scan images which enable evaluation of flaw position, orientation and main dimensions. One example of the test result presentations is given in Fig. 2 where indications originating from a inspection of steel component with austenitic cladding on one surface can be seen. For detailed analysis of results the MASERA-programme included in the system can be used. The system has been used in the inservice inspections of Loviisa NPP and Olkiluoto NPP. Additionally the system was used in the preservice and inservice inspection of the NESC-cylinder.

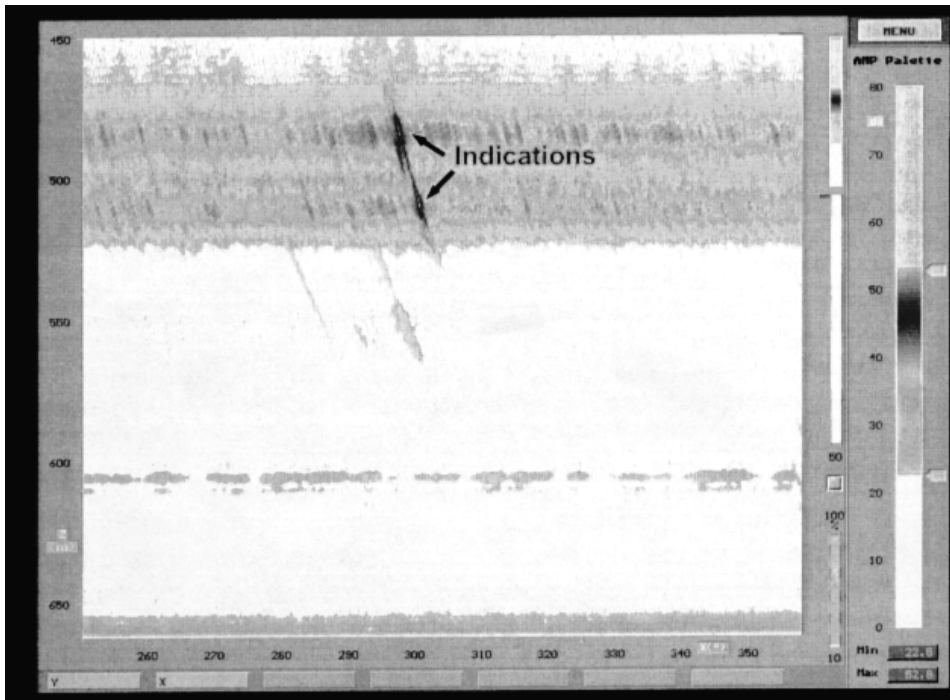


Figure 2. A printout produced by the new automatic ultrasonic inspection system showing indications from a small defect in the interface zone between the base material and cladding. The base material is shown in black and the cladding in blue back ground colour.

4. Reliability of inspection of heat-exchanger tubing

One of the sub-projects of the international PISC-programme completed in 1994 was the inspection of steam-generator tubing. Due to the large amount of data gathered in the round robin exercises the analysis of results was delayed and the final results of this sub-project were presented in late 1995. The reliability of inspection techniques proved to be lower than expected and clearly indicated urgent needs to develop inspection techniques. In the round robin exercises the teams using a combination of eddy current and ultrasonic techniques were in general the most successful ones. The teams using only eddy current technique

did not perform as well, which can be seen in Fig. 3 showing the flaw detection frequencies of different teams. The team of VTT used only eddy current technique.

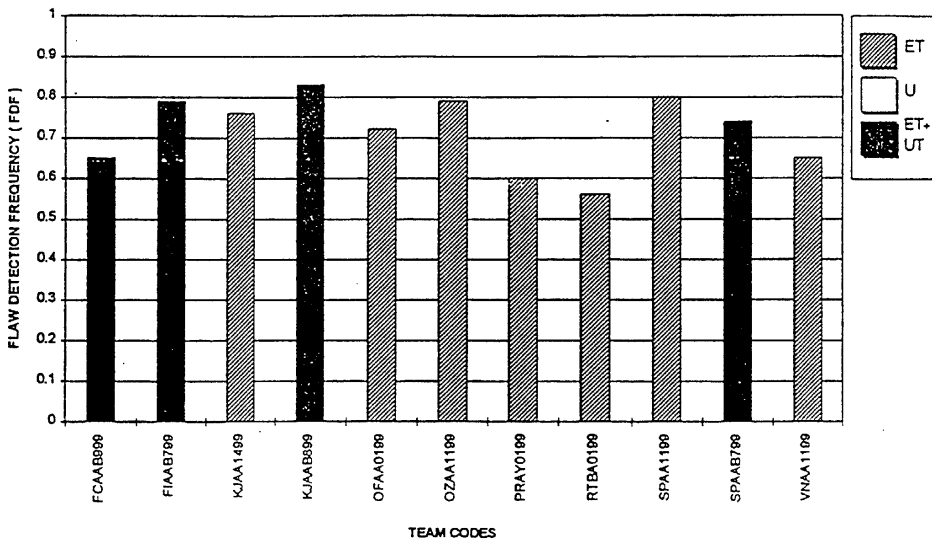


Figure 3. The flaw detection frequencies of different teams participating in the PISC steam generator tubing inspection programme.

5. On-line monitoring

On-line monitoring can be considered in the future more and more important issue ensuring the safe operation of ageing nuclear power plants. Transducer techniques, data acquisition and analysing capabilities of today make many advanced applications possible. On-line monitoring is able to give rapid response to malfunctions and failures and thus quick corrective operation can be taken to limit the damage and prevent secondary losses. In many cases it is also possible to get pre-warning of incipient failure and prevent the catastrophic

break down of the machinery or component. These aspects can be seen most important in process areas that are not accessible during operation. Online monitoring and data acquisition can also produce information to be used as guidance when the in-service inspection areas are selected. If non-destructive examinations can be focused to the most critical locations safety enhancement and also economic benefits are obvious. Also the planning of the repair operations will benefit from successful on-line monitoring and one can ensure that the necessary tools and spare parts are available when an outage starts. Finally, if the on-line monitoring data can be linked with the operating parameters, very important knowledge about the most critical operation conditions will be obtained.

The literature review performed covered the most usual on-line monitoring techniques applied at nuclear power plants. Various methods and techniques to detect malfunctions of the machinery and defects in the components could be identified. Many of the methods are used or could be applied also to the conventional power plants or process industry.

Vibration measurement techniques of rotating machinery are well established. These systems are capable to indicate for example misalignment, unbalance, shaft cracking and bearing failure of machinery. At some nuclear power plants also vibration monitoring of the primary circuit components is applied. Special vibration monitoring application based on the neutron flux noise measurement is used to detect changes in the vibration and movement characteristics of the reactor internal parts.

There are several on-line monitoring applications based on the utilisation of acoustic emission technology. Leak detection is often based on various indirect measurements but today also acoustic signals generated by high pressure flow through crack opening or leaking valve can be detected using piezoelectric sensors mounted on the piping system. An other well established acoustic measurement system is loose part monitoring. Such systems are installed at many nuclear power plants and those are capable to indicate the presence of impacting metal parts inside the primary coolant system and can thus indicate breaking or loosening of components. Several research projects have been directed to develop methods that are able to reveal generation and growth of cracks using on-line acoustic emission monitoring. In spite of the operating

systems in some industrial sectors and existence of the applicable ASME Code (Continuous acoustic emission monitoring, ASME Boiler and Pressure Vessel Code, Section V, Article 13) the crack monitoring installations applying acoustic emission seem only to be performed in research projects when the nuclear industry is concerned.

There is wide interest to apply transient and fatigue monitoring systems that use the existing plant instrumentation measuring capabilities to collect the data for calculations. The behaviour of critical component and piping system areas are simulated with mathematical models to which the measured pressure, flow and temperature values are fed periodically. The new developing measuring techniques, that are based on the capabilities of the optical fibre, could be used in the near future for on-line instrumentation. Applying these systems a large number of temperature or strain measurement points could be covered with a single fibre.

Today there exists considerable interest to measure material degradation using non-destructive methods. This is very important application area in the nuclear industry considering for example the measurement of radiation embrittlement of the reactor pressure vessel material. Many techniques have been developed and much research work is going on but still most of these techniques can be applied only under laboratory conditions. Much work can be foreseen in this field to develop and to verify these methods. Probably none of these measuring techniques can today be regarded as continuous monitoring method and on the other hand the periodical application of the methods would be in the most cases quite sufficient.

During the later phase of the project it was discussed with the Finnish utilities and regulatory body about the possible needs to develop applications of the on-line monitoring techniques. Intention was to find applications that would utilise non-destructive methods to monitor the structural integrity of components during operation. It seems that there are not visible at the moment probable situations where such an application could be necessary. Anyway possible situation could be for example monitoring of a crack that cannot be repaired during outage or detection of a defect initiation in a suspected component section. According to the literature there has been developed successful laboratory application where ultrasonic testing could be used to monitor the

crack growth during fatigue loading in high temperature (300 °C). Also eddy current technique could be used to monitor the crack behaviour when it is open to the inspection surface. To be able to apply these methods to real components and situations considerable research and development work should be performed in laboratory scale. The basic facilities and know-how of the technology are necessary if an application in an outage situation should be installed.

6. Conclusions

The general target of the research work carried out in the AIRI-project in 1995 - 1998 has been the improvement of the reliability of non-destructive techniques used in the inservice inspections of nuclear power plants. Compared to the previous research program completed in 1997 the work has been more focussed on the factors affecting the practical performance of the inspection and the development of the inspection techniques has been addressed only in some specific cases.

The automation of inspections is a world-wide tendency to improve the reliability of inspections and also in Finland this work is in progress. In 1995 - 1998 mechanised inspection techniques have been developed and the techniques have been applied in the inservice inspections of piping welds in Finnish nuclear power plants. The work will be continued in order to develop techniques applicable to more challenging inspection items having difficult geometry, limited access etc.

Another important way to improve the reliability of inspections is the qualification. The qualification of inspections was included in the AIRI-project from the beginning of the project and since that remarkable progress has been made. A document describing the Finnish practise for inspection qualification has been drafted and several pilot qualifications have been performed. Furthermore, the techniques needed in the manufacture of test specimen for qualification tests have been developed. The research work carried out in AIRI-project forms a good basis for the future development of inspection qualification in Finland.

7. Acknowledgements

The reported work was part of the Finnish Research Programme on the Structural Integrity of Nuclear Power Plants 1995 - 1998, project AIRI on Reliability of Non-destructive Inspections of Nuclear Power Plants.

Co-operation with Olavi Valkeajärvi from the Radiation and Nuclear Safety Authority, STUK, Mauri Heltimoinen and Raimo Paussu from IVO Ltd., Matti Nyman from TVO and Liisa Muurinen from Helsinki Energy are gratefully acknowledged.

The work concerning the qualification of inspection was coordinated to the ENIQ-programme. In the ENIQ-group formed by the European nuclear power plant utilities the Finnish representative has been Matti Nyman from TVO and the work in Finland has been coordinated by a national working group. The European Methodology for Inspection Qualification was drafted by ENIQ in 1996 the proposal for Finnish qualification practise in 1997. The cooperation with JRC Petten as well as with Finnish and other European utilities and inspection vendors is acknowledged.

The participation of VTT to the inspection tasks of the NESC-programme was included in the AIRI-project. The preservice inspection of the spinning cylinder was performed in 1996 and the inservice inspection in 1997. The evaluation of results is still in progress.

References

Kauppinen, P. 1997. Tarkastuksen päteväittäminen. SHY:n NDT-päivät, Lappeenranta 12. - 13.3.1997. Suomen Hitsausteknillinen Yhdistys (SHY). 6 p. (in Finnish).

Kauppinen, P. & Sillanpää, J. 1995. NDT - luotettavaa tietoa vioista? BALTICA III Energiatuotannon kunnossapitokokemukset, Helsinki - Stockholm, 6 - 8 June, 1995. Espoo: Espoo: VTT Manufacturing Technology. 11 p. (In Finnish).

Kauppinen, P., Särkiniemi, P. & Jeskanen, H. 1995. Manual ultrasonic inspection of austenitic and dissimilar welds. In: Hietanen, S. & Auerkari P.

(eds.) BALTICA III, International Conference on Plant Condition & Life Management, Vol. II. Espoo: Technical Research Centre of Finland. Pp. 677 - 684. (VTT Symposium 151).

Kauppinen, P., Särkiniemi, P. & Jeskanen, H. 1995. Reliability of ultrasonic detection and sizing of flaws in austenitic welds. XV St. Petersburg Conference on Ultrasonic Non-destructive testing of Metal Construction. Repino, St. Petersburg, Russia, 30 May -1 June, 1995. Pp. 25 - 28.

Kauppinen, P., Pitkänen, J., Särkiniemi, P. & Jeskanen, H. 1995. Ultrasonic detection and sizing of flaws in austenitic cladding and dissimilar metal welds. Seminar "Dissimilar welded joints in NPP equipment and pipings: Problems and means to solve them". Vyborg, Russia, 18 - 22 September, 1995. 7 p.

Lahdenperä, K. 1995. Austeniittisten valujen ja kaksimetalliliitosten testaus. Hitsausteknillisen yhdistyksen NDT-päivät. Turku, 15. - 16.3.1995. 16 p. (in Finnish).

Paussu, R. & Särkiniemi, P. 1997. Capability demonstration of inspection techniques for Loviisa NPP using a blind test block assembly. EC OECD IAEA Specialists Meeting on NDE Techniques Capability Demonstration and Inspection Qualification. Petten, The Netherlands, 11 - 13 March 1997. 5 p.

Pitkänen, J. & Kauppinen, P. 1995. Ultraääni- ja sähkömagneettisten menetelmien kehitysnäkymiä. Hitsaustekniikka, Vol. 45, No. 3, pp. 36 - 40. (In Finnish).

Pitkänen, J., Kauppinen, P., Jeskanen, H. & Schmitz, V. 1995. Evaluation of ultrasonic indications by using PC-based synthetic aperture focusing technique (PCSAFT). Proceedings of the International Conference on Computer Methods and Inverse Problems in Non-destructive Testing and Diagnostics. Minsk, Belarus, 21 - 24 November, 1995. Pp. 291 - 302.

Sarkimo, M. 1998. Jatkuvan monitoroinnin menetelmät rakenteiden eheyden varmistamiseen ydinvoimaloissa. Espoo: Technical Research Centre of Finland. 41 p. (VTT Tiedotteita 1882). (In Finnish).

(See Appendix 1 for a comprehensive listing of publications)

Analysis of maintenance strategies

Kari Laakso and Kaisa Simola
VTT Automation
Espoo, Finland

1. Introduction to the maintenance strategy

The most nuclear power utilities have established goals and objectives for their nuclear power plants, including e.g. 1) operating the plant effectively from primarily the safety and secondly the economic point of view, 2) ensuring safety of the public and the plant workers, and 3) providing uninterrupted electric power to the shareholders with long-term minimum cost. The maintenance goals should reflect these goals at a more functional level.

In a larger perspective, the goal of the plant maintenance and operability activities may be assurance of long-term asset management by keeping the plant continuously in a good condition like new (Mokka 1996). Avoiding faults causing plant disturbances during the operating period may be the most important performance goal which should not be put in danger by minimising the number of maintenance work during the annual maintenance and refuelling outage. More detailed goals and objectives may be to carry out the necessary work at the optimal time during the outages or operation, and to minimise the unavailability time of safety related equipment. One internal objective may be to carry out the maintenance work at budgeted cost. It is expected that every maintenance organisation will, together with its parent organisation, identify its own goals and objectives (EURO-MAINE 1997).

Figure 1 illustrates a rough idea how a target steered model for maintenance management, including control of ageing, could be constructed (Laakso, Dorrepaal & Skogberg 1998). The maintenance *goals* and objectives should have the following characteristics: 1) they are realistic and challenging, 2) they are understandable and clearly communicated to the staff, and 3) action plans are documented describing how the goals or objectives will be achieved. From

the maintenance objectives, such as safety, availability and cost related, one can establish quantitative targets or *acceptance criteria*, against which the level and trend of performance can then be measured (Schjøllberg 1996). *Indicators*, such as unavailability of technical equipment, are compared to some reference value in order to determine if they are significantly deviating (NKS/SIK-1 1994).

The maintenance *strategy* gives guidelines on how the resources should be prioritised and allocated on different systems and components in order to achieve the objectives. An optimal allocation of preventive maintenance, testing, condition monitoring, repairs and modification work on the components and structures should be achieved and the efforts should be carried out at the correct time in a correct way. This requires also decisions for revising the maintenance programs and ranking the safety related modifications. In a nuclear power plant, the maintenance strategy can be currently defined to base on preventive maintenance and condition diagnosis of components and systems (Vuorenmaa 1997). The maintenance strategy is reflected in the *maintenance program* which includes the maintenance action planning and related maintenance support elements (Martin-Onraet et al. 1996).

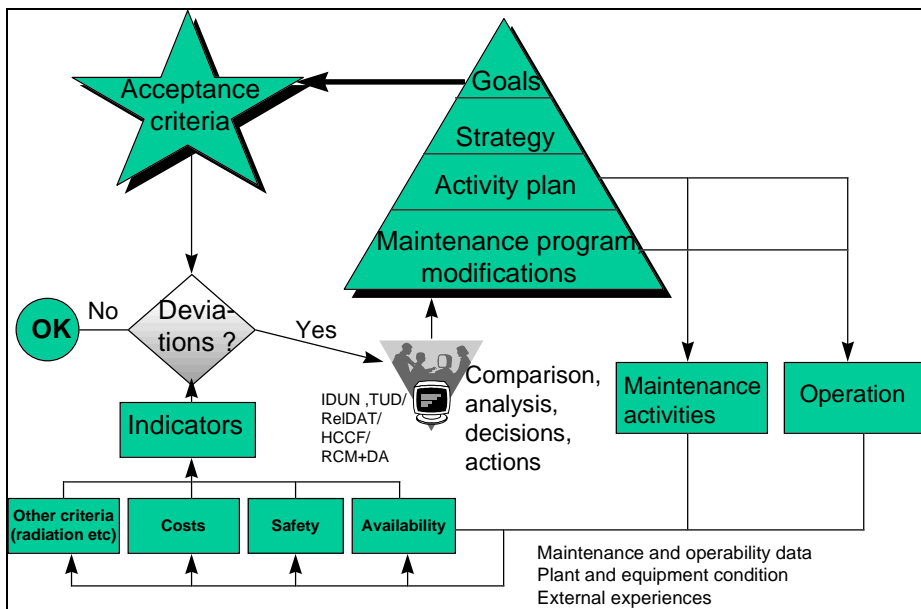


Figure 1. A target steered model of maintenance management.

The concrete performance of the maintenance actions requires *support* (resource) *functions* such as people, information, material and tools (SKI Reference Book: Maintenance 1993, Sanden & Chockie 1995). Based on the maintenance strategy, it will be possible to single out the most important net investments on the maintenance *support elements* to achieve better the maintenance objectives. For instance, a developmental element to be planned can be RCM analysis of technical systems which are most important from the safety, availability and cost point of view. Another project in the *activity plan* may be introduction of a computerised processing system of maintenance indicators to facilitate a user friendly utilisation of the maintenance history data base for experience feedback of maintenance effectiveness.

2. Maintenance analysis

A model was developed for aiding evaluation of the effectiveness of existing maintenance action programs of a power plant. The maintenance actions concerned are given as follows.

Table 1. Maintenance actions.

- Functional testing which can be periodic motioning of a closing valve,
- Calibration control such as check of a limit switch,
- Non-destructive testing which can be ultrasonic testing of a weld,
- Servicing such as cleaning and lubrication of a valve stem,
- Periodic replacements e.g. replacement of rubber items in a solenoid valve,
- Condition monitoring e.g. measurement of motor power during valve actuation,
- Repairs such as stem packings tightened, and
- Modification works based on redesign of equipment.

The analysis model combines a review of historical data on faults and repairs with an analysis of the history of functional testing and preventive maintenance (Laakso 1997). The results of maintenance analysis pinpoint proposals on

changes in maintenance and testing justified for fault reduction and earlier detection (Laakso et al. 1995b).

The model was firstly developed via pilot analyses on the maintenance of motor-operated closing valves and automatic protection systems in Finnish and Swedish nuclear power units (Hänninen & Laakso 1993, Laakso et al. 1995a). Parallely, the developments benefitted from ageing analyses of certain safety related components and NPP protection automation (OECD 1995, Simola 1998).

The applications of the maintenance analyses resulted in verification of the maintenance action programs and justification of changes in them from the point of view of system reliability, availability and maintenance work cost. The proposed changes were adjustment of the intervals of testing and preventive maintenance and introduction of more effective preventive actions. The analysis model is summarised in the upper part of the Fig. 2.

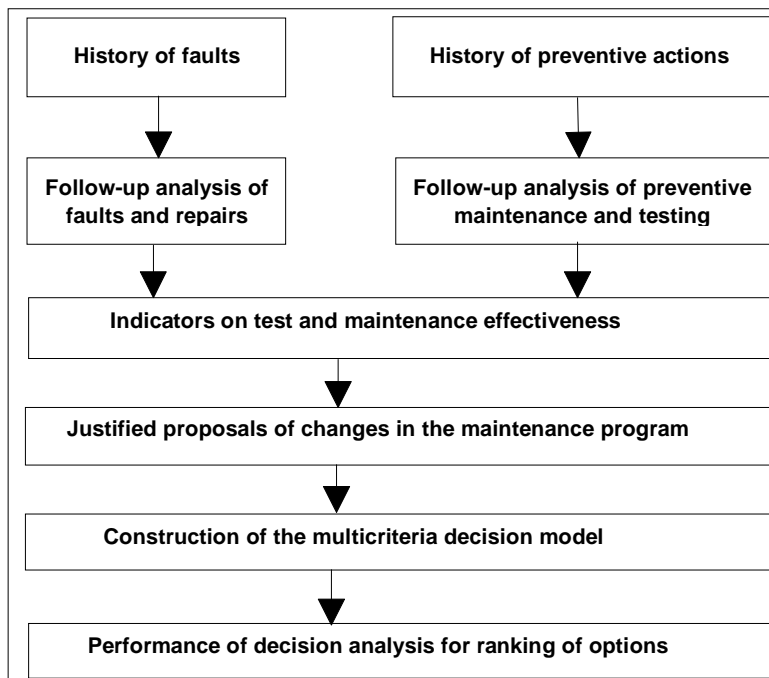


Figure 2. Brief steps in the model of maintenance and decision analysis.

We experienced that several recommendations were implemented at the plants but understood that a proper decision requires consideration of more, often conflicting, decision criteria. Such can be plant safety, availability, maintenance cost, work culture and radiation protection.

Decision analytic approaches were concurrently developed for enhanced use of probabilistic safety assessment in decision making on operational safety issues (NKS-SIK-1 1994, Holmberg & Pulkkinen 1993). Experiences from these studies indicated that decision and maintenance analyses should be used together to support complex maintenance related decisions.

3. Decision modelling

A systematic decision support structure is needed for identifying and ranking the significant criteria, information needs and options for a decision (Laakso, Sirola & Holmberg 1997). The results from maintenance analysis can be used in the decision analysis, together with other analyses and expert judgement, to evaluate how well the decision criteria are met. Experiences from the earlier decision analyses, to correspond the needs identified, were operationalized by definition of a decision support tool (Sirola, Holmberg & Laakso 1997). The quantitative decision model of the tool is based on an additive multi-attribute value function defined by the equation:

$$v_{tot}(a_i) = \sum_{j=1}^n w_j v_j(a_i), \quad (1)$$

where a_i means the decision option i , w_j is the weight coefficient of the criterion j and $v_j(a_i)$ is the scaled score of the decision option a_i compared to the decision criterion j (French 1986). The decision model presupposes a mutual preferential independence of the attributes measuring the achievement of the decision objectives j .

By analysing a more extensive collection of decisions, one could apparently identify the most significant decision criteria for different typical decision cases. This approach also identifies the needs for developing decision mechanisms and enhances the understanding and quality of the decisions. Gradually, qualitative

decision models related to maintenance and safety have been structured based on experiences from the decision and reliability analyses, e.g. (NKA/RAS-450 1990, Holmberg & Pulkkinen 1993, Laakso 1997). The drafted models have been completed and updated by using interviews and comments from personnel at Nordic nuclear and conventional power plants and safety authorities (Laakso & Paulsen 1995, Laakso, Dorrepaal & Skogberg 1998). The models include decision criteria and attributes for selected cases. Such cases are decisions on maintenance program changes, modifications and installation of condition monitoring (Hänninen & Laakso 1993, Laakso et al. 1995a, Laakso et al. 1995b, Laakso 1997). Also a model of plant shutdown decision in a questionable fault situation was included (Holmberg & Pulkkinen 1993, Holmberg et al. 1994). The decision models have been stored in the data base of the decision analysis tool to make the accumulating knowledge operational for the tailored applications.

4. Decision support procedure for maintenance, safety and economy

The tool, its database and the method have been tested and demonstrated with two end users in decision analysis exercises. The first case concerned acceptance of repair of a blocked check valve during power operation with an exception permit (Sirola, Holmberg & Laakso 1997). In the second case, items from about 1400 components in a standby safety system were ranked for analysis based on several strategic selection criteria, which are presented in Table 2. The most significant components were selected as Analysis Significant Items (ASIs) for further consideration.

Table 2. Criteria and indicators for strategic selection of items for analysis. The weights of criteria are given by comparing them in pairs.

- Reactor safety
 - FSAR safety class
 - PSA risk importance
- Functional reliability
 - Failure rates
- Repair costs
 - Man-hours
- Preventive maintenance costs
 - Man-hours
- Radiation protection
 - Radiation zone

The reactor safety criteria were taken into account through the safety classes in the Final Safety Analysis Report and the risk increase factors from the Probabilistic Safety Assessment. Worker safety was considered through radiation exposures in the work spaces. Items covered by repeated faults or extensive preventive resources were also considered as the selection criteria of Analysis Significant Items (ASIs).

A detailed and resource-demanding re-assessment of the maintenance action program was directed to the selected ASIs. Indicators on maintenance and test effectiveness are automatically calculated for single and redundant components from the maintenance history data in the maintenance information system. A qualitative follow-up analysis of the underlying failure and maintenance data was firstly done on items exhibiting deviating levels or trends of indicators. The analyses resulted in justification of changes compared to the existing preventive maintenance and periodic testing (Simola, Laakso & Skogberg 1998). The maintenance effectiveness of the remaining significant items was parallelly verified.

The formal decision analyses demonstrated the potential of a systematic decision analysis procedure to support the decision maker and experts in identification of the most important decision criteria and best decision options

or to rank components in complex decision situations. The structured maintenance and decision analysis also helped to document the bases, and review, of a maintenance action program with a view to target steered maintenance management (Laakso, Dorrepaal & Skogberg 1998).

A further development of the tool, methods and models with an aim to accomplish a proven decision support procedure for maintenance, based on safety and economic targets, continues in future applications.

5. Conclusions

The main areas addressed and studied were:

- analysis model and methods to evaluate maintenance action programs and support decisions to make changes in them, and
- understanding of maintenance strategies in a systems perspective as a basis for future developments.

The subproject showed how systematic models for maintenance analysis and decision support, utilising computerised and statistical tool packages, can be taken into use for evaluation and optimisation of maintenance of active systems from the safety and economic point of view.

Acknowledgements

The reported work was part of the Finnish Research Programme on the Structural Integrity of Nuclear Power Plants 1995–1998, subproject KUNTO 1 on Maintenance Strategies and Reliability and the Nordic research project Strategies for Reactor Safety 1994–1997, subproject NKS/RAK-1.4 on Maintenance Strategies and Ageing. The work for Chapter 1 was performed during 1994–1998, Chapter 2 during 1994–1996, Chapter 3 during 1996–1997 and the present work for the Chapter 4 was completed in 1998.

Co-operation with Barsebäck Kraft AB, Finnish Radiation and Nuclear Safety Authority, Forsmarks Kraftgrupp AB, Helsinki Energy, Imatran Voima Oy,

Swedish Nuclear Power Inspectorate and Teollisuuden Voima Oy is gratefully acknowledged. A special thank is directed to the participants of the Nordic NKS/RAK-1.4 group who provided information and contributed with their expertise in the discussions of the working group meetings. Another special thank is directed to the maintenance, safety and development personnel of Finnish and Swedish nuclear power plants. The involved personnel discussed openly with the researchers their experiences and expert opinions in the interviews on Maintenance Strategies and Equipment Ageing as well as in other informal and innovative meetings.

References

EURO-MAINE. 1997. Euromaintenance Guidelines. Phase 2. Objectives and strategies. The Swedish part. Eureka-Maine Project 1073, July 1997. 104 p.

French, S. 1986. Decision theory. An introduction to the mathematics of rationality. Chichester: Ellis Horwood.

Holmberg, J. & Pulkkinen, U. 1993. Regulatory decision making by decision analysis. Helsinki: Finnish Centre for Radiation and Nuclear Safety. 34 p. (Report STUK-YTO-TR 61).

Holmberg, J., Pulkkinen, U., Pörn, K. & Shen, K. 1994. Risk decision making in operational safety management. Experience from the Nordic benchmark study. Risk Analysis, Vol. 14, No. 6, pp. 983 - 991.

Hänninen, S. & Laakso, K. 1993. Experience based reliability centred maintenance - An application on motor operated valve drives. Helsinki: Finnish Centre for Radiation and Nuclear Safety. 61 p. (Report STUK-YTO-TR 45).

Laakso, K., Hänninen, S. & Hallin, L. 1995a. How to evaluate the effectiveness of a maintenance programme. Baltica III, International Conference on Plant Condition & Life Management. Helsinki - Stockholm, 6 - 9 June 1995. 10 p.

Laakso, K., Hänninen, S. & Simola, K. 1995b. Experience based reliability centred maintenance - A case study of the improvement of the maintenance programme for valve drives. International Journal Maintenance, Vol. 10, No. 1, pp. 3 - 7.

Laakso, K. & Paulsen, J. 1995. Maintenance strategies and ageing of equipment. Nordic NKS/RAK-1.4 questionnaire survey. Questionnaire. 29.4.1995. 9 p.

Laakso, K., Sirola, M. & Holmberg, J. 1997. Decision modelling for maintenance and safety. ESReDA Seminar on Decision Analysis and its Applications in Safety and Reliability. Espoo, Finland, May 15 - 16. 10 p. + 2 app.

Laakso, K. 1997. Assessing the effectiveness of a maintenance programme. Euromaintenance 96 Conference, Copenhagen, Denmark, 21 - 23 May. Maintenance & Asset Management, Vol. 12, No. 1, pp. 19 - 24.

Laakso, K., Dorrepaal, J. & Skogberg, P. 1998. Maintenance analysis and decision support for safety and availability of active systems. Final report of the Nordic research subproject NKS/RAK-1.4 Maintenance strategies and ageing. Laakso, K. (Ed.). Draft NKS/RAK-1(97)12 Report. Roskilde: NKS sekretariatet. 101 p.

NKA/RAS-450 1990. Optimization of technical specifications by use of probabilistic methods. A Nordic Perspective. Final Report of the NKA project RAS-450. Laakso, K (Ed.). Prepared by Laakso, K., Knochenhauer, M., Mankamo, T. Pörn, K. Copenhagen. NORD Series 1990:33. 156 p.

NKS/SIK-1. 1994. Safety evaluation by living probabilistic safety assessment and safety indicators. Final report of the Nordic Nuclear Safety Research Project SIK-1. Laakso, K. (Ed.). Report prepared by Holmberg, J., Laakso, K., Lehtinen, E. and Johanson, G. Copenhagen. TemaNord 1994:614. Pp. 29 - 33.

Martin-Onraet, M., Degraeve, C. & Meuwisse, C. 1996. Integrated logistic support concepts in the design of nuclear power plants. EDF paper. 6 p.

Mokka, R. 1996. O&M Cost Management in TVO NPP. Nuclear Europe Worldscan. Vol. XVI, No. 11-123, November-December. P. 46.

OECD(NEA/CSNI/R(95)9. 1995. Evidence of ageing effects on certain safety related components. A generic study performed by Principal Working Group 1 of The Committee for Safety of Nuclear Installations. Volume 2: Contributions

of participating countries. Volume 2B: Finland. 290 p. (Compiled by Laakso, K., Simola, K., Pulkkinen, U. & Hänninen, S.).

Sanden, P.-O. & Chockie, A. 1995. A regulatory tool for the assessment of maintenance program improvements. International Conference Human Factors and Organisation in NPP Maintenance Outages: Impact on Safety. Stockholm, Sweden, 18 - 22 June. 10 p.

Schjøllberg, P. & Hunstad, S. 1996. Application of maintenance indicators in maintenance management. Proceedings of the 13th European Maintenance Conference and Fair. Euromaintenance 96 Conference. Copenhagen, May 21 - 23. Pp 249 - 264.

Simola, K. 1998. Experience based ageing analysis of NPP protection automation. In: Mosleh, A. & Bari, R.A. (Eds.) Proceedings of the 4th International Conference on Probability Safety Assessment and Management. Vol. 1. London: Springer-Verlag. Pp. 483 - 488.

Simola, K., Laakso, K. & Skogberg, P. 1998. Evaluation of existing maintenance programs using RCM methodology. Proceedings of the European Conference on safety and reliability - ESREL'98, Trondheim, Norway, 16 - 19 June. Safety and Reliability, Vol. 1. A. A. Balkema, Rotterdam, Brookfield. Pp. 207 - 213.

Sirola, M., Holmberg, J. & Laakso, K. 1997. Computerized decision analysis tool - Decision tool. Program document. Report VTT/AUT/TAU-7013/97 and KUNTO(96)17. 6 p. + app. (Limited distribution of appendices).

SKI Reference Book, Maintenance 1993. Prepared for the Swedish Nuclear Power Inspectorate by Battelle Seattle Research Centre. Seattle, Washington. USA. 97 p.

Vuorenmaa, A. 1997. How to cope with maintenance in a unit requiring a high availability performance. Case: IVO Oy. Seminar in Finnish on improvement of the productivity of machine and equipment investments, Helsinki, 4 - 5 June. 8 p. + app. (In Finnish).

Models on reliability of non-destructive testing

Kaisa Simola and Urho Pulkkinen
VTT Automation
Espoo, Finland

1. Introduction

The reliability of ultrasonic inspections has been studied in e.g. international PISC (Programme for the Inspection of Steel Components) exercises. These exercises have produced a large amount of information on the effect of various factors on the reliability of inspections. The information obtained from reliability experiments are used to model the dependency of flaw detection probability on various factors and to evaluate the performance of inspection equipment, including the sizing accuracy. The information from experiments is utilised in a most effective way when mathematical models are applied. Here, some statistical models for reliability of non-destructive tests are introduced. In order to demonstrate the use of inspection reliability models, they have been applied to the inspection results of intergranular stress corrosion cracking (IGSCC) type flaws in PISC III exercise (PISC 1995). The models are applied to both flaw detection frequency data of all inspection teams and to flaw sizing data of one participating team.

2. Models for non-destructive inspection data

Statistical models were studied and applied for the evaluation of the results of non-destructive testing (NDT) (Simola & Pulkkinen 1998). The reliability of non-destructive inspections was approached from three directions. First, flaw sizing models were studied based on the assumption that the measured flaw size is a simple function of true depth and random noise due to measurement errors. Second, probability models for the uncertainty in the flaw detection were

considered. Finally, we introduced a procedure for combining the information from sizing accuracy with possible prior knowledge on the flaw size in order to express the confidence on the sizing result.

2.1 Flaw sizing models

The studies of flaw sizing models were based on an assumption that the measured flaw size is a simple function of true depth and random noise due to measurement errors. A model based on lognormal distribution has been used e.g. by Berens (1989). We introduced an alternative approach, based on the logit transformation of the relative flaw depth (flaw depth/wall thickness). In the logit model, the measured flaw size \hat{a} is related to the true flaw size a in the following way:

$$\ln\left(\frac{\hat{a}}{d-\hat{a}}\right) = \beta_0 + \beta_1 \ln\left(\frac{a}{d-a}\right) + \xi \quad (1)$$

where d is the wall thickness, ξ is a normally distributed random error term with zero mean value and variance σ_ξ^2 , and β_0 and β_1 are the regression parameters.

The advantage of the logit model is that it is physically more feasible than the lognormal model. Further, the model is very flexible in describing various kinds of relationships between the measured and true flaw sizes.

The behaviour of the logit model is presented for some parameter values in Figure 1. For values $\beta_0 = 0$ and $\beta_1 = 1$, the median of the measured depth equals to the true depth. With values $\beta_1 > 1$, the measurement tends to overestimate flaw sizes with $a/d > 1/2$, and to underestimate other flaws. If $0 < \beta_1 < 1$, the measured relative flaw size is pulled from the true relative flaw size toward $\exp(\beta_0)/[1+\exp(\beta_0)]$. As β_1 approaches zero, the measurement result becomes independent of the true flaw size, and the measured flaw size is completely determined by random noise. With large values of β_1 the function becomes steep (see the thick solid line) which corresponds to a measurement intended for only detecting flaws without any sizing efforts.

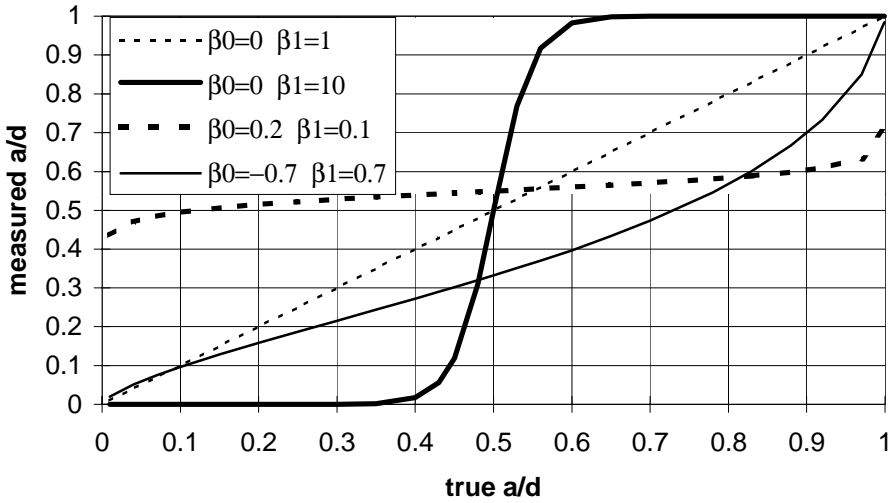


Figure 1. Logit model behaviour for some parameter values.

2.2 Flaw detection models

Probability models for the uncertainty in the flaw detection were considered. Again the models were based on logarithmic and logit transformations of the relative flaw sizes. The logarithmic model is following:

$$\text{POD}(a/d) = \Phi(c_1 + c_2 \ln(a/d)) \quad (2)$$

where Φ is the cumulative distribution of (0,1)-normal distribution, a/d is the relative flaw depth, and $c_1 \in \mathbf{R}$ and $c_2 > 0$ are model parameters.

A very similar POD function can be obtained for the logit model:

$$\text{POD}(a/d) = \Phi\left(c_1 + c_2 \ln\left(\frac{a}{d-a}\right)\right) \quad (3)$$

Besides the flaw depth, the flaw size is characterised by the length of the flaw. In order to take into account the impact of the flaw length on the detection

probability, the models can be modified to include also the relative length as a variable.

2.3 Models for updating flaw size distributions

When a flaw is observed in a periodic in-service inspection, an evaluation is carried out whether the flaw size is acceptable. The uncertainty of the measurement result should be taken into account in designing inspection policies and making decisions on corrective actions. The measurement reliability can be managed by using Bayesian models for the updating of the flaw size distributions. These models combine the results from several inspections, providing the decision makers with better knowledge on the flaw size. Further, it is theoretically possible to optimise the inspection policies by applying the Bayesian measurement models and stochastic optimisation techniques, as demonstrated by (Pulkkinen 1994).

A procedure for combining the information from sizing accuracy with possible prior knowledge on the flaw size was introduced in the project. In this connection, also models for updating the number of flaws in an inspected area were developed.

2.4 Application to IGSCC data

To illustrate and compare the models, they have been applied to flaw sizing data and flaw detection frequency data from a PISC III exercise (PISC 1995). The data consisted of ultrasonic inspection results of intergranular stress corrosion cracking type flaws.

The parameters of the sizing reliability models were estimated from the sizing data of the Finnish inspection team for both the lognormal and the logit sizing reliability models. The goodness of the models was compared statistically. This comparison indicated, that the logit model fitted slightly better to the data than the lognormal model this case.

In our application, the probability of flaw detection (POD) as a function of flaw size was determined by estimating the model parameters from detection frequency data generated in the PISC III exercise. In the first analysis, the POD was expressed as the function of flaw depth. Figure 2 (Simola & Pulkkinen 1997) presents the POD functions based on the maximum likelihood estimates. The logit model (eq. 3) and the lognormal model (eq. 2) result to rather similar POD functions.

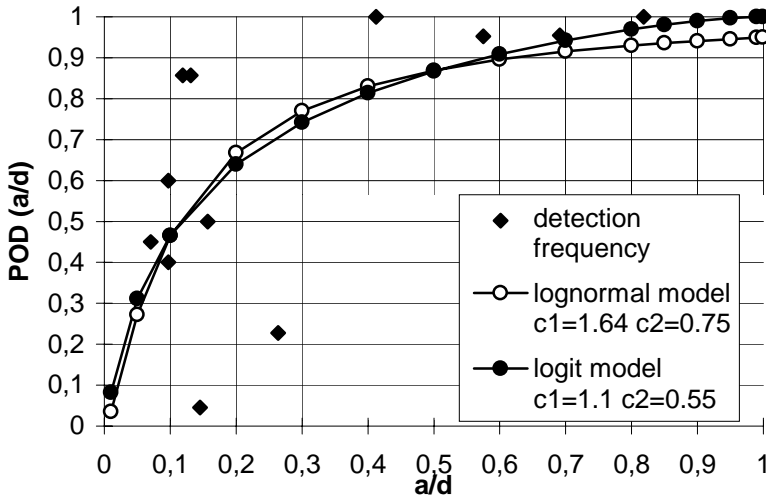


Figure 2. POD functions estimated from detection frequency data. Lognormal and logit models.

The model in which the detection probability depends both on the flaw depth and length did not result to significantly better fit compared to cases where flaw depth was the only variable. This was partly due to the fact that the ratio of relative depth and length did not vary much in the data. To get more information on the impact of flaw length on the detection probability, more variety in the flaw aspect ratios would be needed.

3. Conclusions

We have modelled the flaw sizing performance, the probability of flaw detection, and developed models to update the knowledge of true flaw size based on sequential measurement results and flaw sizing reliability model. In

discussed models the measured flaw characteristics (depth, length) were assumed to be simple functions of the true characteristics and random noise corresponding to measurement errors, and the models were based on logarithmic transforms.

Compared to the lognormal model the sizing model based on logit transformation has a greater physical realism and flexibility. In our example, the logit model fitted better to the actual sizing data than the lognormal model. Similarly, in our example on detection probability based on PISC III data, the model utilising the logit was slightly better than the model based on logarithmic transformation.

A Bayesian procedure for combining information and updating knowledge on number and size of flaws was introduced. Practical applications of this approach could be found in support of inspection and maintenance decisions (Pulkkinen 1994) and in qualification of NDT systems. These models could contribute e.g. to the definition of an appropriate combination of practical assessments and technical justifications in NDT system qualifications, as expressed by the European regulatory bodies (NRWG 1996).

The management of inspection programs is developing towards a risk informed approach - risk based inspection of structures. The approach requires an integration of the inspection reliability models, structural analyses, PSA studies and human factors by means of decision analysis. Closely related to this subject, a survey of probabilistic methods for evaluation of structural component integrity (Simola & Koski 1997) was done. The survey identified needs of data collection and modelling for structural reliability analyses as an input for probabilistic safety analyses and optimisation of maintenance programs of structures.

4. Acknowledgements

The reported work was part of the Finnish Research Programme on the Structural Integrity of Nuclear Power Plants 1995 - 1998, subprojects KUNTO2 on Maintenance Strategies and Reliability. The work was completed in 1997.

Co-operation with Rauli Keskinen from the Radiation and Nuclear Safety Authority, STUK, and Pentti Kauppinen from VTT Manufacturing Technology is gratefully acknowledged. The work was also coordinated to the Nordic Nuclear Safety (NKS) programme.

References

Berens, A. P. 1989. NDE reliability data analysis. In *Metals Handbook*, 9th edition, 17, ASM Int., pp. 689 - 701.

NRWG 1996. Common position of the European regulators on qualification of NDT systems for pre- and inservice inspections of light water reactor components. Final report prepared by the Nuclear Regulators Working Group. European Commission. EU 16802.

PISC III. 1995. Report on the evaluation of the inspection results of the wrought-to-wrought PISC III. Assemblies No. 31, 32, 33, 34, 35 and 36. Luxembourg: Office for official publications of the European Commission. (Report No. 33).

Pulkkinen, U. 1994. Statistical models for expert judgement and wear prediction. Espoo: Technical Research Centre of Finland. 65 p. + app. 80 p. (VTT Publications 181).

Simola, K. & Pulkkinen, U. 1998. Models for non-destructive inspection data. *Reliability Engineering and System Safety* 60 (1998), p. 1 - 12.

Simola, K. & Koski, K. 1997. A survey of probabilistic methods for evaluation of structural component integrity. VTT KUNTO Report (p5)7. 56 p.

Simola, K. & Pulkkinen, U. 1997. Models for reliability and management of NDE data. In Soares (ed.) *Advances in Safety and Reliability*. Proceedings of the ESREL '97 International Conference on Safety and Reliability, June 17 - 20, 1997. Lisboa, Portugal. Pp. 1491 - 1498.

Human and organisational factors in the reliability of non-destructive testing (NDT)

Leena Norros
VTT Automation
Espoo, Finland

1. Introduction

Non-destructive testing used in in-service inspections can be seen as a complicated activity system including three mutually related sub-activities:

- definition of inspection programs and necessary resources,
- carrying out diagnostic inspections, and
- interpretation of the results from the view of plant safety and corrective measures.

Various studies to investigate and measure the NDT performance have produced disappointing result. No clear correlations between single human factors and performance have been identified even though general agreement exists concerning the significance of human factors to the reliability of testing ([NUREG/CR-4600 1986, Koutaniemi et al. 1988, Dahlgren & Skånberg 1993, PISC III 1994, 1995). Another incentive for our studies has been to test and evaluate the applicability of the international results in the Finnish circumstances. Three successive studies have thus been carried out on the human and organisational factors in non-destructive testing.

2. Review of the international literature on human factors of non-destructive testing

The aim of this study (Kettunen & Norros 1996) was to chart human and organisational factors influencing the reliability of NDT. Being a literary survey the study was mainly based on the international and Finnish research available on the topic. In consequence, the results achieved reflected the ideas of the international research community. In addition to this, Finnish partners and actors participating in this activity provided the research team with valuable information of NDT theory and practice.

The literary survey indicated that a good and coherent picture of human and organisational factors influencing the reliability of in-service inspections is still missing. However, it has been undoubtedly proved that the inspectors possess different flaw detection capacities, and that an inspector's capability may considerably vary within a working day. There does not seem to be any statistically significant correlation between formal certification level and ultrasonic testing capability, either. In general, a reliable inspection procedure is based on a profound understanding of the inspection methods and principles, and adequate scope and scheduling of in-service inspection programs. On the other hand, in nuclear power plants the reliability of inspection may deteriorate e.g. due to tight time schedules, fear of radiation and deficient motivation. We concluded that, on the basis of the international literature, no single human or organisational factor is responsible for the NDT performance fluctuations obtained in various reliability studies, and that there seems to be a close connection between inspection management and the general reliability of NDT operations.

3. Beliefs concerning the reliability of NPP in-service inspections

In the course of the above described literary survey we also carried out interviews among Finnish NDT experts and supervisors in order to get acquainted with the NDT branch. As the interviews were planned, carried out and registered in a systematic manner the data could later be utilised for more

profound analysis. We were interested to study how well the international opinions concerning the factors influencing NDT reliability would correspond with the views of the Finnish experts.

Thus, the aim of the second study was to find out the belief systems held by the officials responsible for planning and supervision of NDT operations within the Finnish nuclear industry. The interviewees were asked to express their opinions on:

1. the reliability of NDT methods in general,
2. the factors influencing the reliability of in-service inspections, and
3. the degree of reliability of the current inspection operations conducted by means of NDT methods in the Finnish nuclear power plants.

Another goal of the study was to assess the adequacy of the officials' belief systems using the results of the international studies and the subjects' own justifications as reference.

This study (Kettunen 1997) indicated that the overall reliability of NDT methods was considered very high among the representatives of Finnish utilities and inspection organisations. On the other hand, the opinion assumed by the representatives of the nuclear regulatory body was more qualified. There was a strong belief in all interest groups that the reliability of in-service inspections do depend on various human and organisational factors of which inspectors' attitudes towards their work was perhaps regarded as the most important one. Other common factors were an understanding of inspection items, inspection costs, time schedules, personnel qualification, and radiation. The current inspection activities in the Finnish NPPs were generally considered to be of high quality. Officials' belief systems on the reliability of NDT methods in general and the factors influencing the reliability of in-service inspections were considered adequate.

4. Analysis of the decision-making demands of the inspectors' work

We were struck of the inconsistency of the results regarding human reliability in in-service inspections. We assumed that this might be due to the positivistic methodology used in the studies. We suggested that instead of interpreting inspection as an abstracted signal detection problem, it should be considered as intentional activity in meaningful physical and social contexts. The case studies performed within the NDT domain have taken the context of the activity into account. The problem in these studies, again, is that they usually report what went wrong in the inspection. This information has significance for the management of inspections, but it is still insufficient while not making explicit the generic functional constraints of the regulation of the normal inspection activity aiming at high-quality results under demanding conditions. We therefore decided to use a research approach that would in a concrete way reflect the intentional and contextual nature of the activity. The method used was under development at the VTT Automation Man-machine psychology group. It focuses on the decision making in natural working environments, which is conceptualised as an adaptive interaction between the subject and the environment (Hukki & Norros 1996, Norros & Hukki 1996, Klemola & Norros 1997, Hukki & Norros 1998).

The ultrasonic inspections during the 1996 annual maintenance outages of both Finnish nuclear power plants were investigated (Norros & Kettunen 1998). All 15 NDT inspectors who participated in the work were interviewed. When transcribed into word-to-word protocols the interview data consisted of 200 pages. We also observed and video-recorded the complete course of four actual inspection task performances. This material was meant to provide the basis for developing a method for a later analysis of decision-making in real working situations.

The interview material was analysed in two ways. Firstly, we wanted to find out what factors the inspectors would consider to effect the reliability of inspections, and how well their opinions seemed to correspond with the international results and with the opinions of the NDT experts of the Finnish nuclear power plants and inspection organisations. Secondly, we were interested

in the inspectors' conceptions of the decision-making demands of their work. We assumed that differences in these conceptions would indicate different habits of action. In our methodology habits of action are defined as the way the actor takes into account the possibilities and constraints of the task situation as the boundary conditions of action and how he uses the available resources. A systematic discourse analysis was carried out on the interview material (see e.g. Silverman 1993, Charmaz 1995).

The results indicated that the situation of NDT inspections in Finnish NPPs was fairly good. Factors that according to the international experience were evaluated as threats to the reliability of inspections, i.e. tight time schedules, lacking interests from the utility, fear of radiation or deficient motivation, were not found problems by the inspectors. The inspectors strongly and unanimously emphasised the role of the foremen for reliable inspection. The foremen were considered to be a significant resource for the inspectors during the outages through preparing the work, co-ordinating the individual activities, and monitoring the radiation exposure. The inspectors' point of view was in coherence with the beliefs of the experts and officials interviewed in the previous study. This observation indicated good communication and co-operation among the different personnel groups involved in the inspections. This was also explicitly evaluated as one of the key factors for successful work during maintenance outages.

We also evaluated the inspectors' conceptions concerning the decision-making demands of their work. Our assumption was that inspectors' construction of the object of work, and particularly their insight of the uncertainties of the inspection, would be decisive for understanding the ultimate demands of work. We approached this question through analysing first the inspectors' conceptions about the result of work. Differences were found in the conceptions concerning how quality of inspections can be achieved in daily work, and these correlated with conceptions concerning the nature of professional expertise. Thus, two main approaches to quality emerged: In the first the inspectors emphasised personal expertise and interpretative skills, because they saw these as the essential means to cope with the inherent uncertainty in the inspection task. Other inspectors, representing the second approach, found the standardised, procedure-oriented performance as central, because it was seen the essence of inspection. The inherent uncertainties of the task were not considered. Some of

the inspectors acknowledged the uncertainty, but saw that it can be coped with standard performance. These inspectors were classified in the latter approach. When we further analysed the conceptions concerning co-operation we found that those inspectors who emphasised personal expertise and interpretative skills considered co-operation as a resource for problem solving, whereas those emphasising the standardised, procedure-oriented performance saw co-operation as a mean to increase the effectiveness of performance.

We also analysed the inspectors' conceptions concerning the ways of carrying out inspection tasks. In our material all inspectors were allowed to carry out detection inspection in the NPP, but only six out of fifteen inspectors had the normative qualifications for characterisation of defects in the NPP. We therefore asked the inspectors opinions about the demands of the detection task and the role of the inspection protocol in the work. Again two major conceptions emerged: In the first one the inspectors described the perception-action cycle that has to be created in order to reach the diagnostic-interpretative aims. These persons saw the production of the inspection protocol as a phase of the inspection and as a tool for the comprehension of the result of the inspection. In the other approach the inspectors emphasised the prescribed task to detect the fault but did not consider it from the human performane point of view. The protocol was considered as a formal document of the work. Furthermore, it was found out that all but one of those inspectors who also carried out the more qualified task of the characterisation of defects emphasised the diagnostic-interpretative skills in both the detection and the characterisation tasks. Respectively, only two inspectors out of nine who only carry out detection tasks, emphasised the diagnostic-interpretative nature of the detection task.

Through comparing the results concerning the quality conceptions and the conceptions of the demands on inspection, i.e. the skill conception, we could infer the existence of two habits of action. The result is indicated in Table 1.

Table 1. The emerging of the two habits of action through comparing the inspectors' conceptions on quality and inspection skills. The figures in each cell indicate the number of inspectors.

QUALITY CONCEPTION	SKILL CONCEPTION	
	Activity centred	Task centred
Focused on personal expertise	6	2
Focused on standardised performance	1	6

The two different habits of action among the inspectors were:

- interpretative habit of action (focus on personal expertise, and emphasis on the perception-action cycle with diagnostic-interpretative aims) , or
- procedural habit of action (focus on standardised performance and emphasis on the carrying out the prescribed task).

5. Conclusions

The results provide evidence to the belief of the NDT experts and foremen of the earlier study (Kettunen 1997) that the attitudes of the inspectors influence the performance. The defined two working practices (habits of action) can be interpreted as practical expressions of different attitudes. The results indicate also that a strong division of tasks among the inspectors carrying out detection tasks and characterisation of defects may promote procedural habit of action and hinder the identification of the interpretative possibilities and demands present in all inspections. The diagnostic-interpretative task demands were, however, acknowledged in the interpretative habit of action. Because these demands may be considered as general core demands of inspection, insight of their significance and orientation towards their fulfilment may be assumed to affect the adequacy of the inspection that is difficult to measure directly. For the development of interpretative habits of action it would be necessary to increase the theoretical, problem-oriented analysing of the core demands of inspection during training. Also many-sided utilisation of professional skills should be encouraged in the daily work e.g. through increasing co-operation between the

two groups of inspectors, those carrying out the detection tasks and those taking care of the more qualified characterisation of defects.

6. Acknowledgements

The reported work was part of the Finnish Research Programme on the Structural Integrity of Nuclear Power Plants 1995 - 1998, subproject KUNTO 3 on Maintenance Strategies and Reliability. The study was carried out during 1995-1997.

Co-operation with the Radiation and Nuclear Safety Authority (STUK), Teollisuuden Voima Oy Olkiluoto Power Plant, Imatran Voima Oy Loviisa Nuclear Power Plant, Oy Huber Testing Ab and Polartest Oy is gratefully acknowledged. A special thank is directed to all the NDT-inspectors who participated in the study and openly discussed their expert opinions with the research team.

References

Charmaz, K. 1995. Grounded theory. In: Smith, J.A, Harré, R. & Van Langenhove, L. (Eds.) *Rethinking Methods in Psychology*. London: Sage Publications. Pp. 27 - 49.

Dahlgren, K. & Skånberg, L. 1993. Felaktigt utförd provning av rörböjar i system 321. (A wrongly performed inspection of pipe bends in system 321. In Swedish). *Drifterfarenheter från svenska och utländska kärnkraftverk*. Stockholm: Statens Kärnkraftsinspektion. Pp. 12 - 13. (Rapport nr 8.13-930477).

Hukki, K. & Norros, L. 1996. Lajinvaihto paperikoneen ohjaajien päätöksenteon kohteena. (Quality change-over as a decision case for paper machine operators, in Finnish). *Työ ja Ihminen*, 4/96, Pp. 307 - 320.

Hukki, K. & Norros, L. 1998. Subject-centered and systemic conceptualisation as a tool for simulator training. *Le Travail Humain*, 4, pp. 313 - 331.

Kettunen, J. 1997. Uskomuksia ydinvoimalaitoksissa suoritettavien tarkastusten luotettavuudesta. (Beliefs concerning the reliability of nuclear power plant in-service inspections, in Finnish.). KUNTO(96)11. 49 p. + app. 9 p. (STUK-YTO-TR 121). ISBN 951-712-173-3

Kettunen, J. & Norros, L. 1996. Inhimillisten ja organisatoristen tekijöiden yhteys NDT-tarkastusten luotettavuuteen. Katsaus kansainväliseen kirjallisuuteen. (Human and organizational factors influencing the reliability of non-destructive testing. In Finnish). 59 p. (STUK-YTO-TR 103). ISBN 951-712-118-0

Klemola, U.-M. & Norros, L. 1997. Analysis of the anesthetist's activity: Recognition of uncertainty as basis for new practice. *Medical Education*, 31, pp. 449 - 456.

Koutaniemi, P., Siidorow, A. & Sillanpää, J. 1988. Ultraäänitestaajien pätevyystutkintojen analysointi. Espoo: Technical Research Centre of Finland. 22 p. + app. 47 p. (VTT Research Notes 918).

Norros, L. & Hukki, K. 1996. Development of a simulator training method for nuclear power plants. 2nd International Conference on Human Factors Research in Nuclear Power Operations (ICNPO 2). Berlin, 28 - 30 November, 1996.

Norros, L. & Kettunen, J. 1998. NDT-tarkastajien toimintatavat ammattitaitoa ja tarkastustehtävää koskevien käsitysten perusteella (Analysis of NDT-inspectors' working practices. In Finnish). STUK-YTO-TR 147, 45 p. ISBN 951-712-279-9. Helsinki.

NUREG/CR-4600. 1986. Wheeler, W., Rankin, W., Spanner, J., Badalamente, R., & Taylor, T. Human factors study conducted in conjunction with a mini-Round Robin assessment of ultrasonic technician performance. Springfield: National Technical Information Service.

PISC III. 1994. Human reliability in inspection. Final report on action 7 in the PISC III programme. Luxembourg: Office for official publications of the European Commission. (Report No. 31).

PISC III. 1995. Report on the evaluation of the inspection results of the wrought-to-wrought PISC III. Assemblies No. 31, 32, 33, 34, 35 and 36. Luxembourg: Office for official publications of the European Commission. (Report No. 33).

Silverman, D. 1993. *Interpreting Qualitative Data*. London: Sage Publications.

Fire safety

Olavi Keski-Rahkonen, Jouni Björkman, Simo Hostikka, and Johan Mangs
VTT Building Technology
Espoo, Finland

Risto Huhtanen
VTT Energy

Helge Palmén, Arto Salminen and Antti Turtola
VTT Automation

1. Introduction

According to experience and probabilistic risk assessments, fires present a significant hazard in a nuclear power plant. Fires may be initial events for accidents or affect safety systems planned to prevent accidents and to mitigate their consequences. The project consists of theoretical work, experiments and simulations aiming to increase the fire safety at nuclear power plants.

The project has four target areas:

- to produce validated models for numerical simulation programmes,
- to produce new information on the behavior of equipment in case of fire,
- to study applicability of new active fire protecting systems in nuclear power plants, and
- to obtain quantitative knowledge of ignitions induced by important electric devices in nuclear power plants.

The topics explained below in detail have been solved mainly experimentally, but modelling at different level is used to interpret experimental data, and to allow easy generalisation and engineering use of the obtained data.

Numerical fire simulation has concentrated in comparison of CFD modelling of room fires, and fire spreading on cables on experimental data. So far the success has been good to fair. A simple analytical and numerical model has been developed for fire effluents spreading beyond the room of origin in mechanically strongly ventilated compartments.

For behaviour of equipment in fire several full scale and scaled down calorimetric experiments were carried out on electronic cabinets, as well as on horizontal and vertical cable trays. These were carried out to supply material for CFD numerical simulation code validation. Several analytical models were developed and validated against obtained experimental results to allow quick calculations for PSA estimates as well as inter- and extrapolations to slightly different objects.

Response times of different commercial fire detectors were determined for different types of smoke, especially emanating from smoldering and flaming cables to facilitate selection of proper detector types for replacement of old systems in our NPPs.

Electrical derating of cables in temperatures exceeding long term ambient were determined experimentally, and modelled simply to understand the main physicochemical process of derating. Decrease in insulation resistance of circuitry exposed to smoke for half an hour was an order of magnitude, but still small enough to influence the performance of used microcircuits considerably. Also several other measured effects were small. Failure time distribution of instrument cable in flames was measured experimentally, and consequences of created open or short circuits determined for a pressure transmitter. Ignition experiments were made for a representative set of potential electronic components under heavy overload. A statistical study of power and instrument cables ignition probability was carried out.

2. Numerical fire simulation

2.1 Fire simulation

For the validation of the new field model code SOFIE, a fire in a single room ($2.8 \times 2.8 \times 2.2$ m) was calculated (Björkman & Keski-Rahkonen 1996). The results correlated well with experimental data.

A simple fire spread model for cables developed earlier has been improved by utilizing more accurately the existing cone calorimeter tests. A fit for the heat release rate and duration of local burning as a function of incident heat flux has been proposed. The fit is specific for PVC cables used generally in Finnish NPPs. The more accurate estimate for rate of heat release makes it possible to perform more reliable simulations for cable fires.

The experimental setup of horizontal cable trays described in section 3.2 has been used as a tool in testing and developing the fire spread model. The model gives a rather fair agreement of heat release rate if the combustion properties of cables are known. However, there seems to be large uncertainties in the material properties of cables. There is also some uncertainty in the ignition criteria of new targets (Huhtanen 1998b).

The first task of the international numerical fire simulation code validation round robin was initiated (Keski-Rahkonen 1993) and organised by VTT. Totally 21 participants from 12 countries using 12 different codes participated. The preliminary report (Keski-Rahkonen 1996) showed rather large scatter of predictions between users and codes. However, most of the participants were able to solve the problems to a reasonable accuracy as far as the use of results is concerned. For Scenario B participation was somewhat smaller, but both blind and open simulations were made using experimental data carried out at VTT for Technische Universität Braunschweig. Preliminary results showed, that the user is the most critical link in the chain of simulations. The codes themselves were fairly similar. Even the difference of zone- and cfd-codes was not striking. The codes could at best predict gas temperatures in rooms at 20...30% accuracy, (Keski-Rahkonen 1998). Final report of the Scenario B (Hostikka & Keski-Rahkonen 1999), and the Scenario C are under preparation.

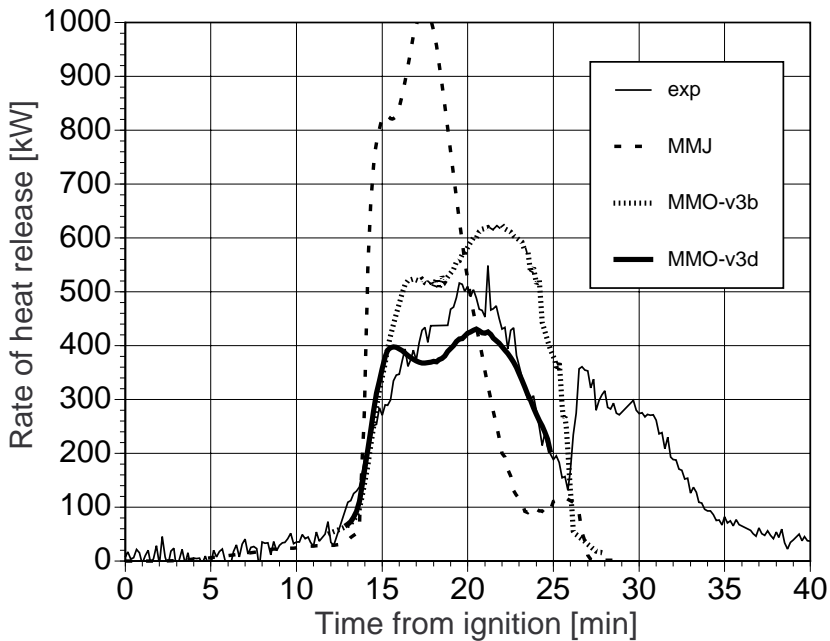


Figure 1. Rate of heat release in a horizontal cable fire experiment. Experimental measurement vs. simulated results. MMJ denotes heat release calculated with material properties of MMJ cable. MMO denotes the heat release calculated with material properties of MMO cable which was the material used in the experiment. In case MMO-v3b all five cable trays ignite during the first stage (which is not the case in the experiment). In case MMO-v3d ignition of two trays is restricted for comparison.

The purpose of the numerical computer code validations is to demonstrate, to what degree different mathematical models are able to predict behaviour in fires of real size in NPPs. Validation is hampered by the lack of good enough experimental data. Use of our data obtained under 3.2, and 4.1 for international blind fire simulation code testing is being considered.

2.2 Spread of smoke inside nuclear power plant control building

The spread of smoke generated by fire was studied inside a nuclear power plant control building (Hostikka & Keski-Rahkonen 1998). The ventilation manifold was modeled as a simple adiabatic network connecting fully mixed compartments. Model allows both analytical and numerical solutions of the smoke spread. This is the main advantage of the current model, when compared to the traditional network modeling concept. Smoke fraction, gas temperature and species concentrations in the system were calculated for an experimentally determined example fire in an electronic cabinet. The effects of some ventilation parameters and the sensibility to the RHR input were studied based on the numerical solutions.

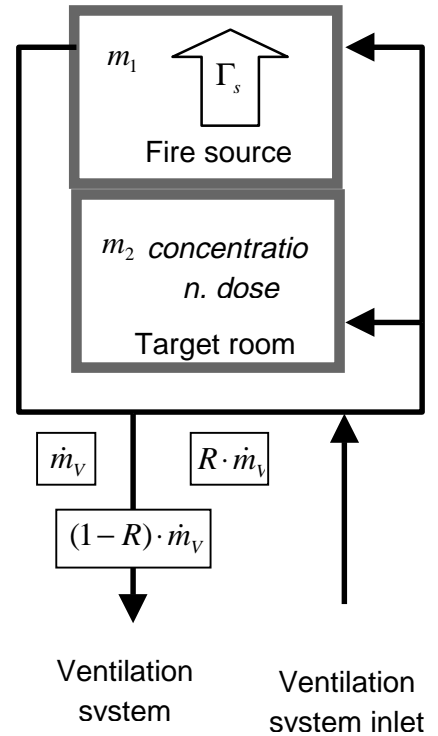


Figure 2. Two room model.

For analytical solutions of the smoke fraction and species concentrations the model was simplified by introducing an equivalent two-room model presented Figure 2. A fire is located in the first room and the rest of the system is described by the target room. For practical purposes the model can be further simplified by balancing the ventilation conditions. Based on the developed model the concentrations of toxic products are governed by two processes with characteristic time scales: (1) Dilution of smoke by a ventilation ($T_1 = m / (1-R)\dot{m}_v$), and (2) mixing in the burn room ($T_2 = m / \dot{m}_v$). Here m is the total mass of air inside the compartments ($m = m_1 + m_2$), \dot{m}_v is the mass flow of the ventilation and R is the feedback ratio of the ventilation system. The analytical solutions of the simplified model were compared with the numerical

solutions of the more detailed model to assess the error caused by the simplifying assumption.

Finally, an equation for dose D was derived for the long time accumulation of toxic combustion products to a person staying in a room apart from the fire source room:

$$D = \frac{R}{1 - R} \frac{\Gamma_s}{\dot{m}_v} \quad (1)$$

where Γ_s is the total released mass of the combustion product. Equation (1) gives a practical method to assess the safe ventilation rate and feedback ratio when the yield of a toxic product is known.

3. Behavior of equipment in fire

3.1 Full scale experiments on electronic cabinets

Continuing earlier work a second series of three full scale fire experiments on electronic cabinets have been carried out. In the experiments (Figure 3 left hand side) one cabinet, the fire cabinet, was fitted with relays, connectors, wiring, cables and circuit boards (Mangs & Keski-Rahkonen 1996). A mock-up cabinet made of thin steel sheets was attached to the fire cabinet in order to study the spread of fire into an adjoining cabinet. Still another cabinet was placed at a distance of 1 m opposite the fire cabinet to represent a neighbouring row of cabinets. The contents of the fire cabinet was ignited with a small propane burner either at the bottom of the cabinet beneath a vertical cable bundle or beneath a wiring bundle.

Rate of heat release (RHR, Figure 3 right hand side) by means of oxygen consumption calorimetry, mass change, CO₂, CO, and smoke production rate, as well as gas and wall temperatures in all three cabinets were measured as a function of time. The key role of the ventilation conditions in the cabinet when determining the rate of heat release was clearly shown.

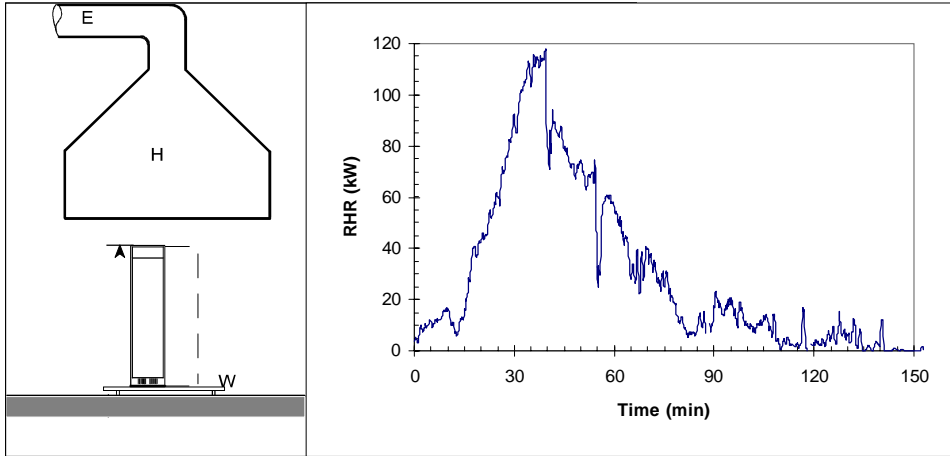


Figure 3. Electronic cabinet A on scales W under a hood H (left) for determination of total rate of heat release (RHR) as a function of time (right).

Ignition power and energy sufficient for sustained burning leading to flashover in the cabinet was determined. The ignition power and energy levels seem to be fairly near the limit ignition/no ignition of the cabinet (Figure 4). The fire growth rate after ignition was estimated to be slow according to NFPA 72E classification.

A simple analytical formula was derived (Mangs and Keski-Rahkonen 1994) for maximum Q_{\max} rate of heat release in a gas tight metal cabinet, where air flows in from the lower part through an opening of area A_i and exhausts from the upper part from an opening of area A_e . The vertical distance between openings is H . The maximum possible rate of heat release after flashover in the oxygen limited burning is given by

$$Q_{\max} \approx 4.8 \text{ MW} \sqrt{\frac{H}{3.3 / A_e^2 + 1 / A_i^2}} \quad (2)$$

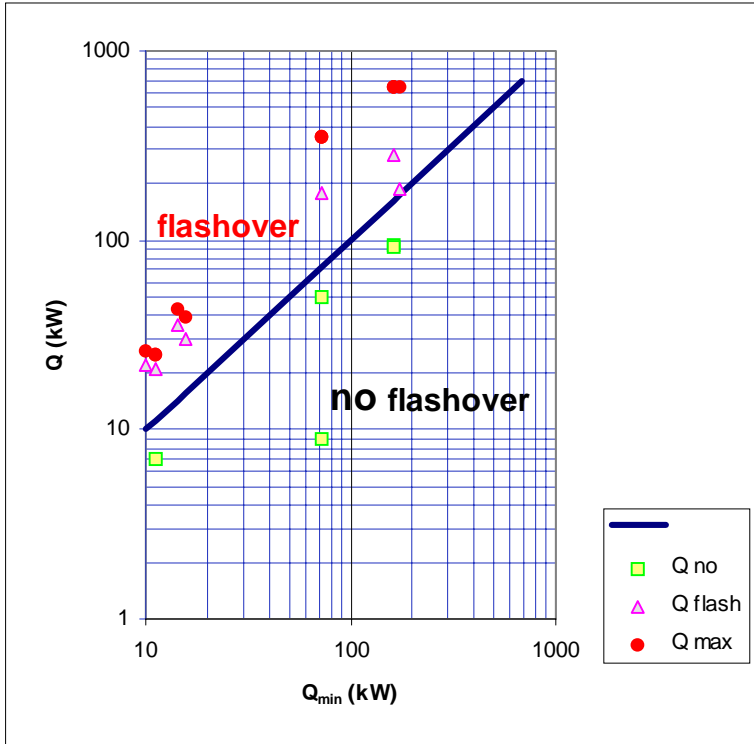


Figure 4. Predicted minimum RHR Q_{min} for flashover (heavy line) in an electronic cabinet according to Equation (3). On vertical scale observed RHR (triangle and square symbols) as a function (horizontal scale) of calculated minimum RHR. Filled circles indicate the predicted maximum RHR according to Equation (2).

Similarly an analytic formula was derived for the minimum RHR Q_{min} needed to drive a cabinet to flashover (Keski-Rahkonen and Mangs 1996)

$$Q_{min} \approx 19.3 \text{ kW} \sqrt{h_k A_w A \sqrt{H}} \quad (3)$$

where h_k is the effective heat transfer coefficient through the wall of the cabinet, A_w the total area of the cabinet envelope, and A the weighted average of the entrance and exit openings.

Proposed analytical formulas were checked (Figure 4) against our small and full scale data and two other full scale experiments (Keski-Rahkonen & Mangs 1996), and good agreement was obtained although the number of tests is still too small for total validation. Paananen(1996) in his master's thesis made a careful comparison of Equation (2) with his small scale data, and found the proposed formula agrees well with the observations.

The use of Equation (2) is in PSA analyses to extend the directly measured data to obtain only through geometrical data a reliable value for the maximum RHR to be used to estimate maximum risk or as an input to numerical fire simulation code to calculate fire development in a room containing these cabinets.

The use of Equation (3) is in PSA analyses to estimate the minimum RHR needed to transfer an established local burning around the ignition point to a burning destroying quickly everything inside the cabinet.

A very practical results of the fire experiments of the cabinets was to demonstrate, how sensitive a function of air flow is the RHR inside the cabinet. To limit fire and smoke spread, and other harmful consequences of the fire, the cabinets must be kept carefully closed at all times.

3.2 Full scale experiments on cable trays

Two full scale fire experiments on PVC cables used in nuclear power plants were carried out, one with cables in vertical position and one with cables in horizontal position. Before full scale experiments a series of scaled down experiments were carried out to determine, what size of ignition source is needed to drive the cables to full flame involvement.

Cables in vertical position

The vertical cable bundle, 3 m high, 300 mm wide and 30 mm thick, was attached to a steel cable ladder. The vertical bundle experiment was carried out in nearly free space with three walls near the cable ladder guiding air flow in order to stabilize flames (Figure 5). The vertical cable bundle was ignited with a small propane gas burner beneath the lower edge of the bundle.

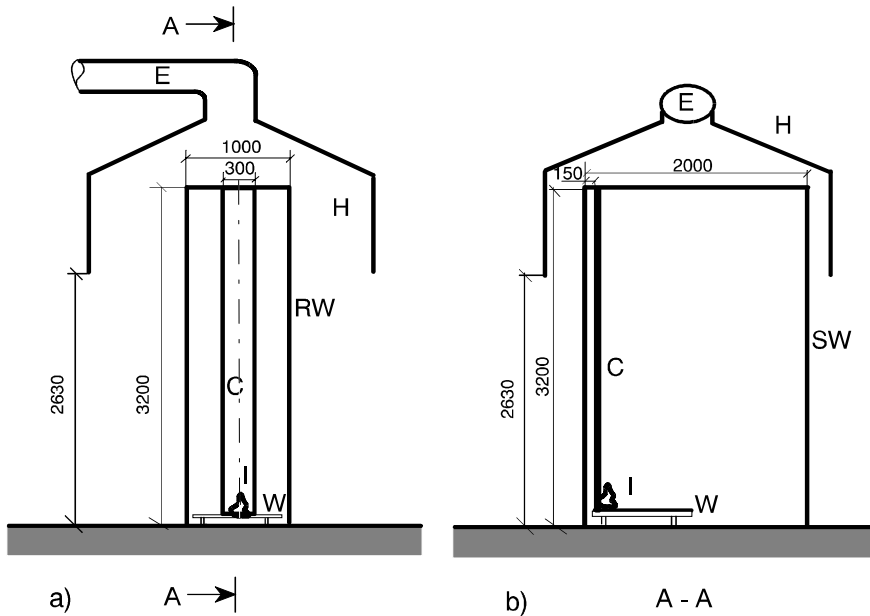


Figure 5. The configuration of the vertical cable tray experiment, a) front view, b) side view. C cable bundle, I location of ignition with propane burner, RW rear wall, SW side wall, W weighing device, H hood and E exhaust duct. Dimensions in mm.

Rate of heat release by means of oxygen consumption calorimetry, mass change, CO₂, CO and smoke production rate and cable surface, gas and wall temperatures were measured as a function of time.

Cables in horizontal position

The horizontal cable tray experiment was carried out in a small room with five cable bundles attached to steel cable ladders. Three of the 2 m long cable bundles were located in an array equally spaced above each other near one long side of the room and two correspondingly near the opposite long side (Figure 6). The horizontal cable bundles were ignited with a small propane burner beneath the centre of the lowest bundle in the array of three bundles.

Rate of heat release by means of oxygen consumption calorimetry, mass change, CO₂, CO and smoke production rate, cable surface and gas temperatures, gas

flow velocities, times to sprinkler operation and times to electric failure of cables were measured as a function of time.

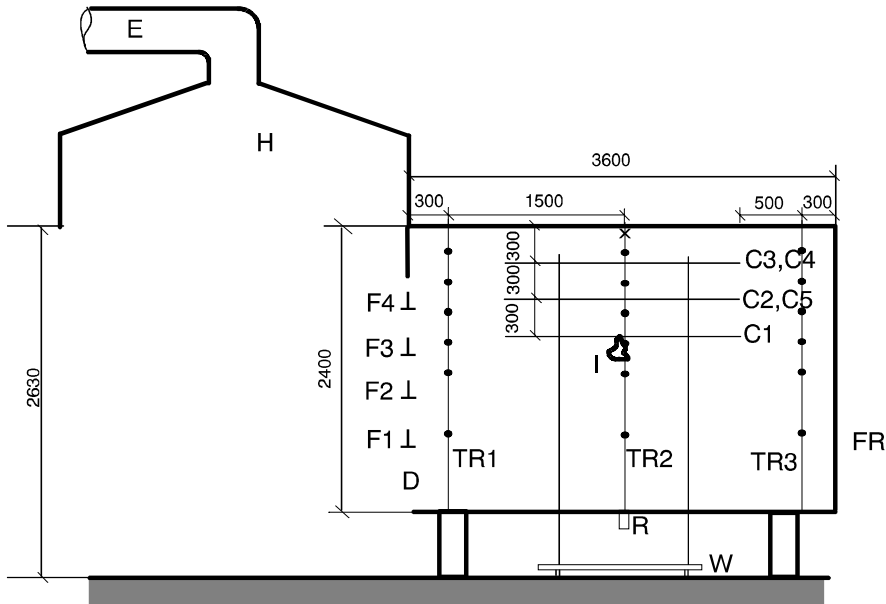


Figure 6. The configuration for the horizontal cable tray experiment, side view. FR fire room, C1-C5 cable trays, I location of ignition with propane burner, W weighing device, H hood, E exhaust duct, TR1, TR2, TR3 thermocouple rakes, R radiometer, F1 - F4 bidirectional probes and X sprinklers. Dimensions in mm.

The results from the vertical and horizontal cable tray experiments will be published in a delayed way (Mangs & Keski-Rahkonen 1997). The information from experiments is used in developing the simple model of fire spread on cable trays. Comparisons of simulations with experimental data will allow assessing the capability of new fire spread models implemented into CFD-codes to predict large scale cable fires.

3.3 Performance of instruments in case of fire

Heat transfer into the measuring unit and electronic unit of a working pressure transmitter and valve actuator with electric motor was considered using theoretical calculations and experimental methods. An important part of the study was also to investigate performance, damages and failures of the equipment at elevated temperatures beyond the normal operation limits. The pressure transmitter was suddenly exposed in a test furnace at temperatures of +40°C, +70°C, +140°C and +250°C corresponding to high operation temperature, upper limit of normal operation temperature and beyond the temperatures, where the device is likely to damage, respectively. In normal operation temperature range the pressure output signal stayed in required limits up to the upper limit of use temperature +70°C. At higher temperatures pressure signal went out of the prescribed limits (at 140°C) and short circuit occurred (at 250°C) damaging the equipment. Temperature development in the apparatus corresponded reasonably with the theoretical calculations. The valve actuator with electric motor was suddenly exposed in a test furnace at temperatures +40°C, 140°C and 250°C corresponding to common upper limit of normal operation temperature in plants, maximum operation temperature of electric motor and temperature, where coils are likely damage. In the valve actuator the microswitch failed at 230°C and electric motor damaged at 250°C. Time constants for heating for the studied equipment were determined. As final results extreme value diagrams were given for determining the critical exposure time at different temperatures for various components (Figure 7 and Figure 8 as an example).

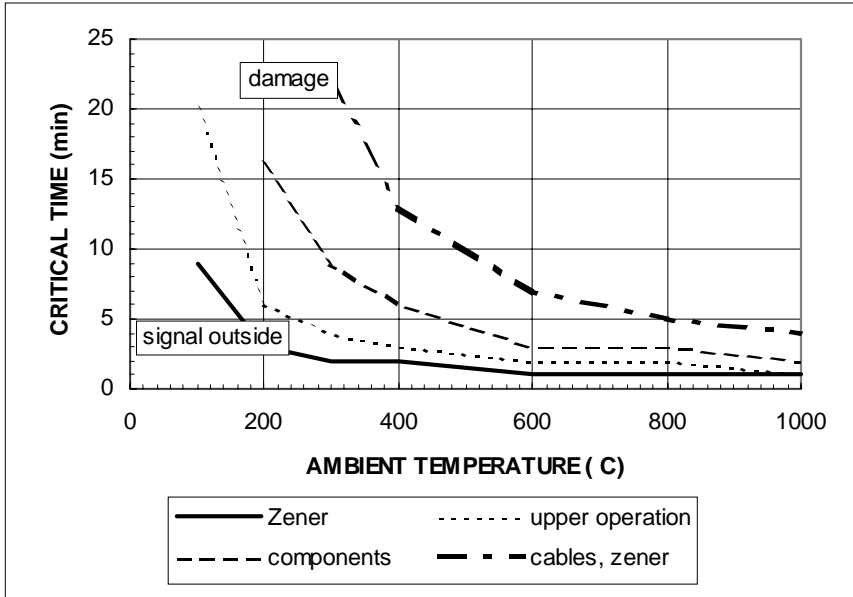


Figure 7. Extreme values of exposure times at different ambient temperatures for the interior of electronic box of the pressure transmitter. Temperatures +50°C, +70°C, +120°C and 200°C correspond to upper operation limit of Zener diode, heat balance with upper limit of operation temperature of the pressure transmitter, short circuit, damage of cables and Zener diode, respectively. (upper limit of operation temperature of resistors, transistors, PVC-cables). Malfunctions and failures discovered in the experiments are shown in the figure: pressure signal out of the confidence limits at 140°C (signal outside) and short circuit and damage at 250°C in 40 minutes (damage). Curves have been extrapolated far from the range of relating experiments. Accordingly, extreme values beyond, say 500°C, should be applied with care.

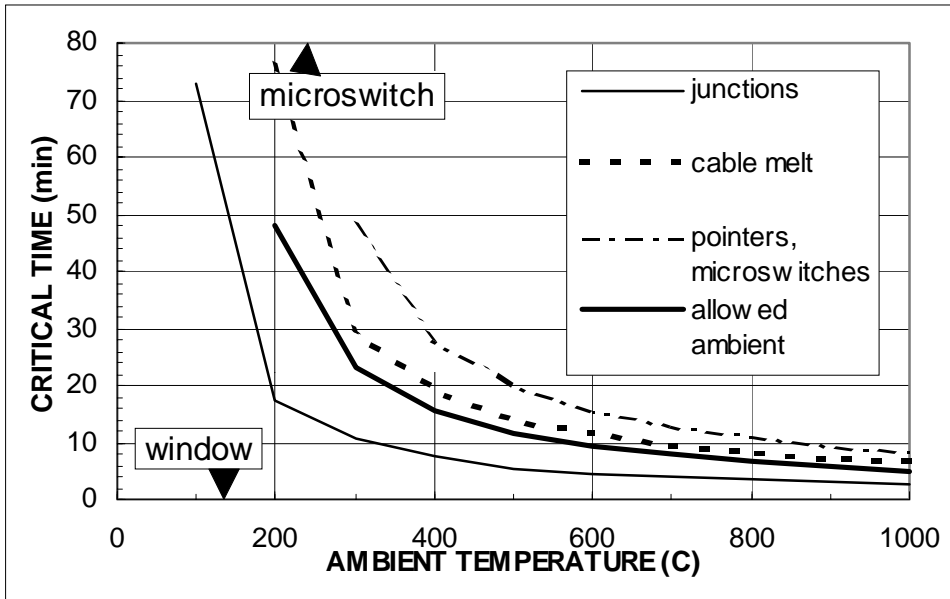


Figure 8. Conservative extreme values of exposure times at different ambient temperatures for the interior of electronic box of the valve actuator. Temperatures + 90°C, 155°C, +180°C and +230°C correspond to damaging of light junctions, heat balance with upper limit of ambient operation temperature (F-class), cables melting and failing microswitches and pointers, respectively. Malfunctions and failures discovered in the experiments are shown in the figure: positioners window was broken at 140°C (window) and microswitch failed at 250°C in about 3 hours (microswitch). *Curves have been extrapolated far from the range of relating experiments. Accordingly, extreme values beyond, say 500°C, should be applied with care.*

4. Fire protection systems

4.1 Response of fire detectors

The response of different smoke detectors to standard test fires as well as smoldering and flaming cable material fires was studied (Björkman & Keski-Rahkonen 1997a) to backup selection of new fire detection systems to existing Finnish NPPs. The response time and smoke density of each detector were

measured. The experiments were carried out in the smoke density laboratory designed according to EN 54-9 standard.

The laboratory was instrumented with additional equipment (Björkman & Keski-Rahkonen 1997b) to allow detailed comparison with numerical prediction by CFD simulation. Blind validation of the simulation has been performed inside VTT (Huhtanen 1998a), and an international validation round is considered. Experimental data report (Björkman & Keski-Rahkonen 1997b) is printed but not distributed before these blind simulations are carried out.

5. Electrical components and devices in fire

5.1 Fire behaviour of cables

A method to measure conductivity of cables used in NPPs at temperatures exceeding the long term rating was developed (Keski-Rahkonen et al. 1997). The problem is to predict how long and at what temperatures cables function under emergency situations. The structure and materials of the relevant cables were reviewed, and high temperature properties were sought from literature sources.

Literature review revealed the major physical mechanism of conduction of electricity through a good insulator is ionic conductivity. Fragments of polymerization chemicals form simple ions, which in electric field move leading to conductivity σ

$$\sigma = \sqrt{K_0 n_0} e(\mu_+ + \mu_-) \exp\left(-\frac{\Delta W}{2\epsilon_s kT}\right) \quad (4)$$

which has an Arrhenius type temperature behaviour. In Equation (4) all other symbols than temperature T and permittivity ϵ_s are material dependent constants independent of temperature. Therefore, presenting measured conductivities on Arrhenius plot like in Figure 9 as a function of inverse absolute temperature $1/T$, data fall on a linear curve, from which the material

dependent constants can be determined. The permittivity ϵ_s is a strong function of moisture. Therefore, even minute concentrations of water inside the insulation deteriorate the resistivity of the material.

Two series of tests were carried out for a number of cables to check the validity of theory and the test method. As shown by Figure 9 the proposed simple model seems to work for PVC based materials. The bars with a letter label indicate: U maximum normal operation temperature, E emergency operation temperature, S short circuit temperature, and M melting temperature limits for PVC cable materials according to manufacturing quality control standards. Measured data points above melting temperature (M) seem to fall roughly on a linear curve.

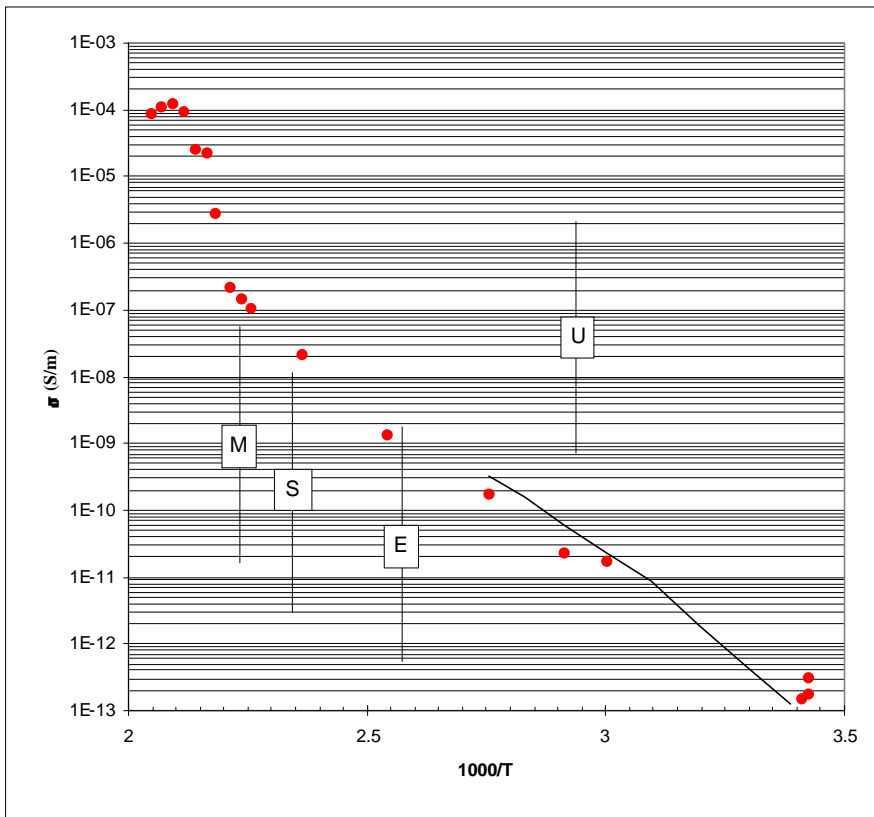


Figure 9. Electric conductivity σ (S/m) of a **PVC-cable** as a function of inverse absolute temperature T (in units of $1000/K$). For comparison literature data are drawn in a full line. After melting, the wires of the cable could become air insulated, which explains the high rise in conductivity observed below 2.2.

Thus derating of a cables at high temperatures can be reduced to derating of cable insulation material. The proposed method allows a handy method to obtain quantitative data on conductivity of real cable materials, which is difficult to obtain for high temperatures but is needed for fire risk analyses of NPPs.

5.2 Effects of smoke on electrical components

Smoke is generated by many sources and is released to the environment, causing pollution, reduction in visibility, and nonthermal short-term and long-term damage as discoloration, odor, electrical shorting and conduction, corrosion etc. In case of fires there have been found large variations in smoke particle size. As the smoke moves away from the fire origin large particles settle down to the floor and surface of equipment, leaving small particles in the gas phase, similar to the long -range transport in the atmosphere. Smoke can significantly affect electronic equipment especially digital electronics. Short-term damage may include circuit bridging and in the long term smoke can lead to corrosion of metal parts. Summary of the work to date and component-level tests carried out by Sandia National Laboratories for the U.S. Nuclear Regulatory Commission to determine the impact of smoke on digital instrumentation and control equipment as well as work carried out in Oak Ridge National Laboratory has been reviewed.

Small-scale experiments at VTT were carried out in order to evaluate the impact of smoke on instrumentation. The work is focused on short-term damage. Longer-term effect of gases and corrosion is beyond the scope of the study. Results of these studies may improve the safety of nuclear power plants as they modernize and replace their analog with digital equipment under renovation. In the experiments circuit boards were placed in the smoke chamber. Smoke was produced by heating the fuel (25 g of PVC cable material commonly used in Finnish nuclear power plants) with a radiative panel locating in the chamber. Combustion mode was smouldering. The exposure conditions were mainly characterized by means of smoke density, temperatures in the smoke chamber and ambient, fuel type and fuel loss. Performance of three identical circuit boards with microcircuits, DIP-switches and cob-structures of leads were measured.

Each board contained the following housing on top side: one 74HC00 and one 74LS00 (quad dual NAND) in quad DIL-package, one 74LS00 (quad dual NAND) in DIL-package, DIP-switch with eight separate switches, four comb figures having 0.2/0.2 mm, 0.3/0.3 mm, 0.5/0.5 mm, 0.7/0.7 mm line widths as clearances. Additionally, 100 nF by-pass capacitors used between 5 V and ground for the IC-circuits.

The following measurements were made:

- 1) The delay between input and output rising edge, the rise time of output edge and the output high logic level were measured with oscilloscope from 74HC00 and 74LS00. The four NAND-gates were connected in series and 10 kHz square wave was fed to the both inputs of the first gate.
- 2) The input impedance of each gate from 74LS00 was measured with the insulation from 74LS00 resistance meter with 10 V.
- 3) The contact resistance of each switch was measured with milliohm meter from the DIP switch. The switches were set to on-position and they were not manipulated during the exposures.
- 4) The insulation resistances were measured with 10 V from the four comb figures

Most prominent effect of smoke can be seen in the comb figures: the resistance falls more than two orders of magnitude (Figure 10). However, the resistance is still very large after the change. The resistance recovers partially when the conditioning terminates. All boards behaved in a similar way.

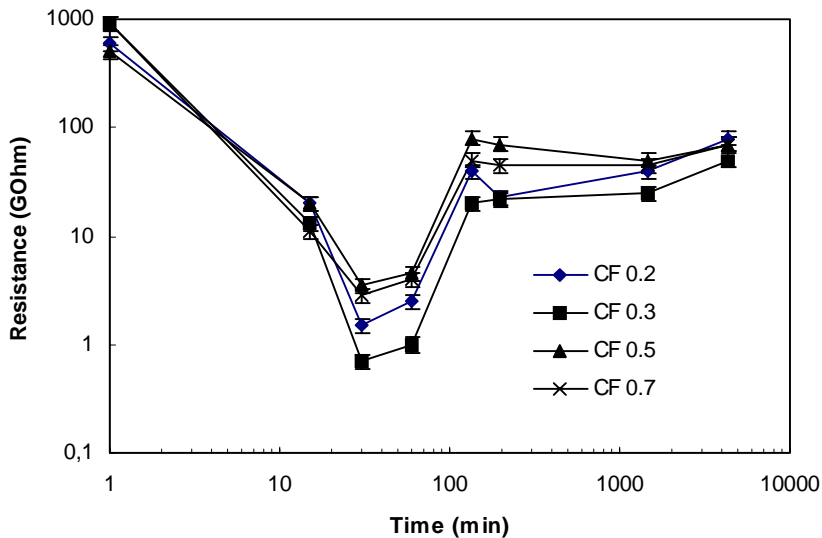


Figure 10. Insulation resistances of comb figures on the printed circuit board A.

The measurements of the printed circuit boards show that exposure of smoke effects only circuitry with high resistance values by forming parasitic low impedance paths. The effect is considerable: in the input impedance and in the insulation resistance measurements the change is one order and two orders of magnitude, respectively. The effect on the electrical parameters of ICs, and on the contact resistances is not significant. After smoke ventilation circuitry partially recovers leaving the worst case deviation from the original values a factor of 10 in insulation resistance. According to the results the detected variations could be assumed to alter only little the functional performance of a circuitry consisting of similar types of boards as studied. If the performance of boards would deteriorate due to these observed changes the related circuitry would be inappropriate for intended environmental conditions.

5.3 Failure distribution in instrumental cables in fire

The performance of a four-conductor instrumental cable exposed to fire has been investigated. Failure modes and consequences of short circuits in a four-conductor cable connected to a pressure transmitter were first studied with different short circuit resistors without fire exposure. Results from this pre-study

and earlier cable fire experiments presented in literature were used when designing the fire experiments. Two types of automation cable were studied in two series of fire experiments carried out under similar circumstances.

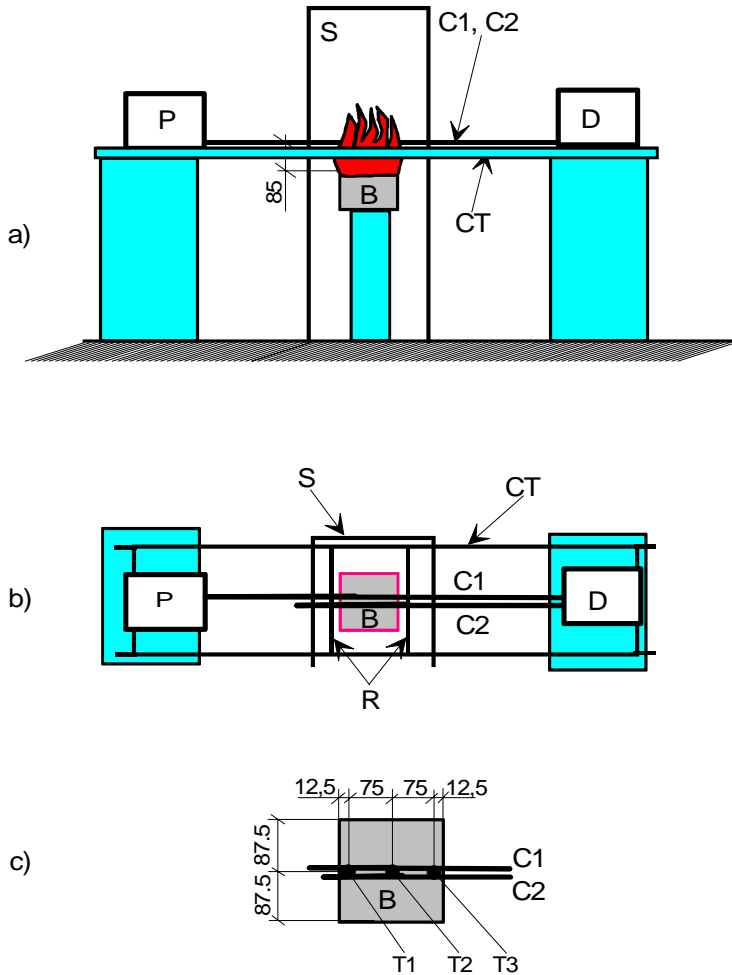


Figure 11. The experimental configuration in instrumental cable fire experiments. a) side view, b) top view and c) thermocouple T1, T2 and T3 location, top view. P pressure transmitter, B propane gas burner, CT steel cable tray, C1 pressure transducer cable, C2 resistance measurement cable, D data acquisition unit and S mineral wool shield in order to stabilise flames. Dimensions in mm.

Each experiment considered two cables, one energised cable C1 connected to the pressure transducer P and one non energised open circuit cable C2 for monitoring short circuiting through insulation resistance measurements. The cables were exposed to flames from a 170 mm x 170 mm propane gas burner B beneath the cables (Figure 11).

Times to first disturbance in supply voltage to and current output signal from the pressure transducer (cable C1) was monitored as well as times to short circuits between significant pairs of conductors in cable C2 through direct insulation resistance measurements.

The distribution of times to first disturbance was characterised by fitting probability distributions to the observed cumulative frequencies. Fitting of a Weibull cumulative distribution

$$F(t) = 1 - \exp\left\{-\left[\frac{(t - \tau)}{\beta}\right]^\alpha\right\} \quad (5)$$

to time t to first disturbance in voltage supply to the pressure transducer is presented in Figure 12 as an example.

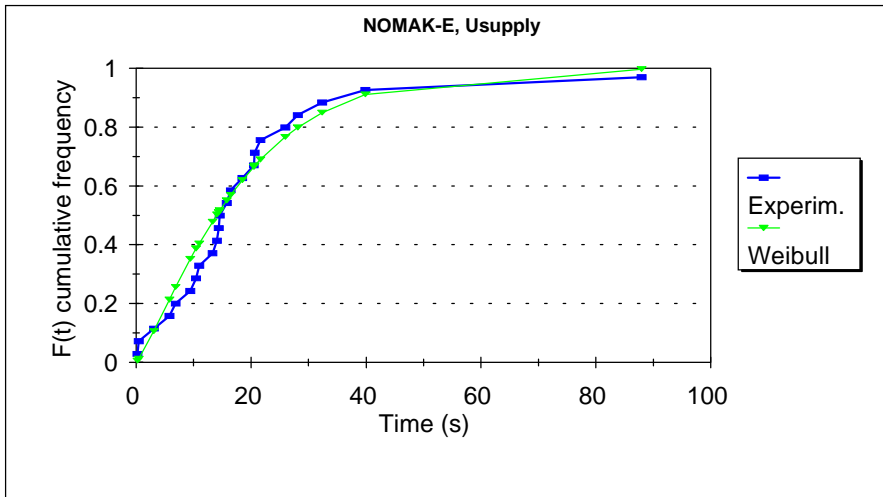


Figure 12. Weibull cumulative distribution with parameters $\alpha = 1.2$, $\beta = 19$ s and $\tau = 38$ s fitted to observed cumulative frequencies of times to first voltage supply disturbance in fire experiment with four-conductor automation cable connected to pressure transmitter.

6. Electrically induced ignition of electrical components

6.1 Literature review

A literature review on ignition mechanisms, critical components and first ignited materials in electrically induced fires has been carried out. Nuclear power plant event data bases as well as general public information on electrical fire causes was utilised.

Short circuit, ground fault or arcing was the most frequent ignition mechanism in the NPP event data bases. Three specific groups of critical components in nuclear power plants could be identified:

1. switches, breakers and relays
2. cables and contacts, splices and terminals
3. transformers.

Oil from transformers, breakers, etc. was the leading first material ignited followed by cable insulation.

It was also noted that the considerable amount of electrical fire causes recorded as unspecified electrical fault or appliance introduce uncertainty into the statistics. Further many of the specified ignition mechanisms and failed components are presented as “possible” or “supposed” in the databases. Ignition and development into sustained burning is also in many cases the result of a chain of faults which lead to difficulties in defining the true root cause.

6.2 Fire experiments on electrical components

Fire experiments on electrical components such as microcircuits, tantalum capacitors and power transistors mounted into printed circuit boards have been carried out. The components were chosen from a sample of typical printed circuit board assemblies used in Finnish nuclear power plants. The main criteria

in choosing components was that they could tolerate enough power for ignition to be possible.

Proposed electrical faults leading to ignition were overvoltage and faulty polarity of power supply in experiments with printed circuit boards with microcircuits and tantalum capacitors. Power transistors were overloaded with gradually increasing current.

The experiments were carried out under the hood of a cone calorimeter for rate of heat release measurements. Neither the external heat flux cone nor the spark ignitor of the cone calorimeter apparatus were used in the experiments.

Three experiments were carried out with power transistors. The surface of the printed circuit board ignited in two experiments, leading to distinct flaming fire of duration 25 and 70 s, respectively. The flames went out when the wiring to the transistor broke due to overloading. Maximum rate of heat release was 450 W in these power transistor experiments.

Seven experiments were carried out with microcircuits and tantalum capacitors. Capsules of microcircuits and tantalum capacitors ignited and burned with a small flame for 5 ... 30 s in some of the experiments without igniting adjacent components or circuit board. The rate of heat released from these components were below the detection level of the cone calorimeter. Other observed effects on micro circuits and capacitors were sparking, slight smoke production and breaking of component capsules.

The experiments indicated that of the present components power transistor was the only component with potential to ignite adjacent combustible material.

6.3 Ignition mechanisms and frequencies in control and power circuits in nuclear power plants

Ignition mechanisms and ignition frequencies for control and power cables and circuits in nuclear power plants have been estimated from event databases. Ignition frequencies per reactor year and unit length of cable indicate that cable

fires are approximately by a factor 40 more frequent in power circuits than in control circuits.

7. Summary

Numerical fire simulation has concentrated in comparison of CFD modelling of room fires, and fire spreading on cables on experimental data. So far the success has been good to fair. A simple analytical and numerical model had been developed for fire effluents spreading beyond the room of origin in mechanically strongly ventilated compartments.

For behaviour of equipment in fire several full scale and scaled down calorimetric experiments were carried out on electronic cabinets, as well as on horizontal and vertical cable trays. Analytical models were developed for the rate of heat release of the cabinets, which were validated against obtained experimental results. Cable tray fires were carried out to supply material for validation of CFD code performance in simulating fire spread on cables. Failure times of pressure transmitters, and valve actuators were measured by placing them in a furnace at different temperatures, highest of which exceeded much the specified long term ambient conditions. Heat transfer models were written and compared with measured temperatures at different parts of the equipment to be able to understand the heating process, and to locate the most sensitive parts. Simple heat transfer modelling seems to work well and allow generalising the obtained results to other similar equipment. Graphs for failure times at different ambient temperatures were prepared for easy use in PSA-work.

Response times of different commercial fire detectors were determined for different types of smoke, especially emanating from smoldering and flaming cables to facilitate selection of proper detector types for replacement of old systems in our NPPs. Additionally, the fire room was richly instrumented to allow prediction for temperature and flow fields to be used for validation of CFD modelling in predicting smoke detector response.

Electrical derating of cables in temperatures exceeding long term ambient were determined experimentally, and modelled simply to understand the main physicochemical process of derating. Experimental values of conductivity

obtained for the most important types of PVC cables behaved reasonably according to this simple theory. Long term decrease in insulation resistance of circuitry exposed to smoke for half an hour was an order of magnitude, but still small enough to influence the performance of used microcircuits considerably. Also several other measured effects were small. Failure time distribution of instrument cable in flames was measured experimentally, and consequences of created open or short circuits determined for a pressure transmitter. Ignition experiments were made for a representative set of potential electronic components under heavy overload. Most of the components were destroyed by overload, but did not ignite surroundings. Only power transistors were able to ignite adjacent circuit board. According to a statistical study power cables seemed to be 40 times more frequent (per length of a cable) to ignite a fire than instrument cables.

References

Björkman, J. and Keski-Rahkonen, O., 1996. Simulation of the Steckler room fire experiment by using SOFIE CFD-model. Espoo: Technical Research Centre of Finland, VTT Publications 265. 28 p.+ app. 3p.

Björkman, J. and Keski-Rahkonen, O., 1997a. Response of fire detectors to different smokes. Espoo: Technical Research Centre of Finland, VTT Publications 295. 33 p.

Björkman, J. and Keski-Rahkonen, O., 1997b. Full scale experiments with different smokes. Espoo 1997, Technical Research Centre of Finland, VTT Publications 332. 18 p. + app. 62 p.

Hostikka, S. and Keski-Rahkonen, O. 1999. Results of CIB W14 Round Robin for Comparison of Fire Simulations. (to be published).

Hostikka, S. and Keski-Rahkonen, O. 1998. Modelling of Smoke Spreading inside a nuclear power plant control building. Espoo: VTT Building Technology, Research Report RTE10202/98. 34 p.

Huhtanen, R., 1998a. Simulation of a smoke detector test. Espoo: VTT Energy, Research report ENE21/8/98. 44 p + app. 3 p.

Huhtanen, R., 1998b. Fire spread model for horizontal cable trays. Espoo: VTT Energy. Research report ENE21/xx/98. To be published.

Keski-Rahkonen, O., 1993. Proposal for the validation of simulation computer programmes, Prepared for The FORUM for International Cooperation on Fire Research, meeting at Espoo, September 1 - 3, 1993, Technical Research Center of Finland, Fire Technology Laboratory, 18 p. (unpublished).

Keski-Rahkonen, O., 1996. CIB W14 Round Robin for Code Assessment. A Comparison of Fire Simulation Tools. Open International Symposium on Fire Safety Design of Buildings and Fire Safety Engineering. 19 - 20 August 1996, Oslo, Norway. 11 p. + app. 3p.

Keski-Rahkonen, O., Björkman, J. and Farin, F., 1997. Derating of cables at high temperatures. Espoo 1997, Technical Research Centre of Finland, VTT Publications 302. 57 p + app. 2 p.

Keski-Rahkonen, O. 1998. Quantifying tools : possibilities, limits, and hazards, 2nd International Conference on Fire and Explosion Protection, 21-23 October, 1998, Zurich, Switzerland. Institute of Safety & Security. Zurich. (1998), 1-22.

Keski-Rahkonen, O. & Mangs, J., 1996. Maximum and minimum rate of heat release during flashover in electronic cabinets of NPPs, in Faillace, R., Müller, K., Röwekamp, M. & Schneider, U (ed.), Proceedings of SMiRT 13 Post Conference Seminar No. 6, August 21-24, 1995, Fourth International Seminar on Fire Safety in Power Plants and Industrial Installations, Gramado, Brasil. SR 2092 / INT 9047, GRS-V-Bericht 9, 1996. P. 19-31.

Mangs, J. & Keski-Rahkonen, O., 1994. Full scale fire experiments on electronic cabinets. Espoo 1994, Technical Research Centre of Finland, VTT Publications 186. 50 p. + app. 37 p.

Mangs, J. & Keski-Rahkonen, O., 1996. Full scale fire experiments on electronic cabinets II. Espoo, Technical Research Centre of Finland, VTT Publications 269. 48 p. + app. 6 p.

Mangs J. & Keski-Rahkonen O., 1997. Full scale fire experiments on vertical and horizontal cable trays. Espoo, Technical Research Centre of Finland, VTT Publications 324. 58 p. + app. 44 p.

Paananen, J., 1996. Instrumenttikaapin palon suurimman tehon kokeellinen määrittäminen [Experimental determination of the maximum rate of heat release of an electronic cabinet]. Master's thesis. Helsinki University of Technology. Structural Engineering and Building Physics, Fire and Safety Engineering 1996. 111 p. + app. 22 p. (in Finnish)

(see appendix 1 for a comprehensive listing of publications)

RATU2 research objectives and achievements

Jussi Solin and Matti Sarkimo
VTT Manufacturing Technology
Espoo, Finland

1. Introduction

The Finnish research programme on the structural integrity of nuclear power plants, RATU2 was launched in 1995 for four years to coordinate the independent national research and development work aiming for structural safety in NPP's. The general planning and goal setting of the programme was based on the research need assessment and evaluation of the previous RATU programme. The research plans have been updated and refined annually on the basis of available funding.

This paper provides a summary of the achievements related to the original objectives for the RATU2 programme from an administrative point of view. An overview on the new facilities and human resources is also given. The main conclusions of the interim evaluation are also reported. The major scientific and technical results are described in more detail in the technical papers of this symposium.

2. Achievements compared to plans

When launching the programme, general aims and work plans for the first two years were specified (VTT, 1994). Thereafter, the detailed work plans have been annually updated.

The main tasks set for the whole programme (1995 - 1998) and the related achievements in each research project are summarised in the following.

2.1 Material degradation in the reactor environment (RAVA)

The main tasks and their progress can be summarised as follows:

- The usability of fracture mechanics-based material values in structural analyses with respect to constraint is investigated analytically and experimentally with special emphasis on surface cracks and small test specimens.
 - *The VTT approach for statistical treatment of brittle fracture toughness data, known as the Master Curve approach, has gained wide international acceptance. An ASTM testing standard, based on the development work done in this and the previous RATU programme has been published (ASTM E 1921-97). Simultaneously, the Master Curve approach has initiated work for codification changes within ASME and the PVRC in USA. The method has also been implemented in an European code for steel structures (Eurocode 3). Furthermore, several international round robins on the Master Curve have begun or are beginning (IAEA, MPC etc.)*
 - *A doctoral thesis dealing with constraint effects in surface cracks has been published.*
- Testing methods are developed for the routine testing of small test specimens including active materials, surface flaws, and new, simplified techniques, for the determination of the dynamic fracture resistance and crack arrest toughness.
 - *Testing of fracture resistance curves by Charpy-size specimens is on routine level and the procedure has been validated for various structural steels.*
 - *Testing capabilities have now been developed further to ultra small specimens (e.g. $3 \times 4 \times 27 \text{ mm}^3$ 3pb) and the measuring capacity of such specimens has been estimated.*
 - *A restraining K_{Ia} -test has been developed and validated.*
 - *Testing and analysis techniques for elastic-plastic mixed-mode (I/II) fracture toughness testing have been developed.*

- The test specimen reconstitution technology used by VTT, both for impact and fracture resistance specimens is validated in international test programmes and networks like European Action Group for Ageing Materials Evaluation and Studies (AMES).
 - *The international round robin activity has not yet ended, but participation to AMES network has been active.*
 - *Validation tests have been performed within VTT for irradiated VVER RPV base metal.*
- A theoretical model describing the statistical effect of pre-stressing (WPS) on the fracture resistance is developed and validated.
 - *This task has been withdrawn due to reduced funding.*
- More accurate correlations between different test methods, presently used for irradiation embrittlement monitoring, and various fracture resistance parameters are developed and validated, especially focusing on the Charpy-V test. Based on the results, a new generation of irradiation embrittlement monitoring programmes is developed.
 - *Further experimental support has been obtained for the determination of crack arrest toughness transition temperature from instrumented Charpy-V tests based on the previously developed correlation.*
 - *A new correlation between static initiation toughness and crack arrest toughness has been developed.*
 - *A description of the effect of loading rate on fracture toughness has been developed.*
 - *An improved correlation, based on fracture mechanical analogy, has been developed between standard and miniature size Charpy-V parameters.*
- The effect of irradiation and thermal annealing on the material micro-structure and fracture behaviour is studied. The work includes both theoretical modelling and material testing and is performed in co-operation with the International Group on Radiation Damage Mechanisms (IGRDM).

- *Micromechanical models are being sought by participating to the IGRDM activity. By participation to the group, in addition to the modelling experiences, confidential data is received from all partners.*
- Stress corrosion cracking mechanisms of materials in nuclear power plant environments are modelled and irradiation-induced material changes, which lead to stress corrosion in the reactor core environment, are established.
 - *A new selective dissolution vacancy-creep (SDVC) model has been proposed and successfully applied on a qualitative level to modelling of stress corrosion cracking in nuclear power plant environments. A prerequisite of the SDVC model, generation of excessive amounts of vacancies during metal oxidation has been verified using the internal friction technique. Vacancy generation under conditions known to enhance the environmental impact on materials degradation has been verified for brass, pure copper, nickel base alloys and stainless steels. Characterisation of surface films in situ at high temperature environments has provided further insight to the role of surface films in controlling vacancy generation rates.*
 - *At low doses the synergistic effect of thermal ageing, sensitisation and irradiation, not irradiation per se, was shown to make the stainless steel heat affected zones susceptible to environmentally assisted cracking (EAC). This effect was observed both with the slow strain rate technique (SSRT) using tensile specimens as well as with the rising displacement test method using reconstituted three point bend specimens.*
- Various effects on the environment-assisted crack growth in stainless steels are defined quantitatively and possibilities to prevent material failures in the reactor core conditions are established. Furthermore, the effect of thermal ageing on stainless steel weld joints and stainless castings is investigated.
 - *The experimental work is underway and this activity has been linked to the international EPRI CIR programme in order to characterise the irradiation assisted stress corrosion cracking (IASCC). Both the thermal ageing, i.e. heat input during welding process as well irradiation effects have been shown to increase materials susceptibility to environmentally assisted cracking.*

- *The effects of thermal ageing on mechanical properties and microstructural changes in cast Ti-stabilised stainless steels have been determined.*
- New test methods and facilities for environmentally and irradiation assisted cracking studies are developed.
 - *A pneumatic servo-controlled fracture resistance measuring (PSFM-device) device for EAC and IASCC studies was developed. Advantages of the new test system are enhanced load control and measurement precision due to avoided friction effects, possibility to test small 3PB specimens as well as flexible and easy control over test type and procedure.*
 - *A test device based on PSFM technique was developed for simultaneous testing of six 3PB specimens. This enables EAC data production for statistical treatment.*
- The progress of materials technology from the point of view of nuclear power plant manufacturing and repair technologies is continuously monitored.
 - *The published literature and data banks are continuously followed and collected.*
- The correlations between the high temperature water chemistry, stress corrosion susceptibility and rise of radiation levels through contamination are identified. Monitoring of the water chemistry is applied to prevent failures and activity rise.
 - *Correlations between applied water chemistry, oxide film properties and the extent of activity incorporation on primary circuit material surfaces at Loviisa power plant were established using a TrendChem high-temperature water chemistry monitoring system, including material samples, installed at the plant.*
 - *A thin-layer electrode arrangement was developed, facilitating versatile electrochemical measurements in simulated power plant coolants - even in poorly conductive BWR water.*

- *Results obtained using the developed electrochemical and new surface analytical techniques were combined and used as input data for mechanistic modelling to clarify the mechanisms of phenomena related to activity build-up on primary coolant surfaces and to different types of corrosion.*

2.2 Reliability of non-destructive inspections of nuclear power plants (AIRI)

The main tasks and their progress can be summarised as follows:

- The main principles of Finnish validation practice will be created by validating chosen pilot objects. Active participation in the European Network for Inspection Qualification (ENIQ) will ensure strong international and European perspective.
 - *The first pilot qualification tests concerning inspection procedures and personnel have been performed in 1996-1997 in close cooperation with the Finnish utilities.*
 - *For fabrication of qualification test specimens, the techniques for producing stress corrosion cracks and thermal fatigue cracks in stainless steel specimens have been developed as well as techniques for implanting different defects by EB-welding in piping assemblies. Test specimens containing cracks have been manufactured to the utilities for qualification purposes.*
 - *VTT researchers - together with the utility staff - have actively participated to the work of ENIQ. The ENIQ-methodology has been introduced to Finnish inspectors in national symposiums.*
 - *The proposal for Finnish practise to be followed in the qualification of inservice inspections of Finnish nuclear power plants has been prepared in a national working group participated by the utilities, major inspection vendors and VTT.*

- In the international project coordinated by the Network for Evaluating Steel Components (NESC), the NDE results will be used as input for structural analysis. An integrated view of the reliability of the methods used to assess structural safety is sought.
 - *The preserve and inservice inspections of the spinning cylinder of the NESC-project have been carried out in VTT in 1996 and 1997. In both these inspections the automatic ultrasonic inspection system has been used for flaw detection and analysis of indications. The final results of the project that would allow the evaluation of the accuracy and reliability of the inspection methodology are not yet available.*

- Modern ultrasonic equipment and analysis software will be combined with existing scanners. The system will be used in automatic inspections of the most important components.
 - *The automatic ultrasonic inspection system has been utilized in the inservice inspections of piping welds in Olkiluoto 1-2 BWR and in inspections of main gate valves in Loviisa 1-2 PWR. Based on the experience gained in these practical inspections the system has been further developed.*
 - *The automatic ultrasonic inspection system was also used for flaw detection and analysis of indications in the inspections of the NESC spinning cylinder.*

- New NDE techniques and capabilities will be sought. The applications will involve combinations of various techniques, novel data analysis methods and on-line monitoring systems.
 - *A literature review covering the most usual on-line monitoring techniques applied in nuclear power plants has been performed. The decisions on the concrete research tasks will be made together with the utilities. No practical measurements were performed within this project.*

2.3 Structural analyses for nuclear power plant components (RAKE)

The main tasks and their progress can be summarised as follows:

- Development of the engineering fracture assessment programme system MASI and tailoring it for life time assessments of chosen components.
 - *The engineering integrity assessment system MASI developed during the previous RATU programme, especially for pressurised thermal shock analyses of the reactor pressure vessel, has been extended to support fatigue and stress corrosion crack growth assessment. Capabilities for assessment of sub-cladding cracks have been added to the system.*
 - *The system has been tailored for automatic integrity assessment of piping components with the aim to be integrated as part of the piping assessment system of TVO. Capabilities for evaluation of straight piping components with basic flaw geometries have been created. A program module was created for evaluating the criticality of a crack using the ASME XI rules.*
- Development of effective methods and computation tools for fracture mechanics parameter evaluation.
 - *The micromechanical Gurson-Tvergaard material model was successfully applied on the numerical prediction of ductile fracture resistance of several reactor pressure vessel materials, when the model parameters had been fitted to tensile test results. Also a correlation between the scatter of tensile and fracture mechanical test data was successfully reproduced.*
 - *A new theory called the ‘J-vector theory’ was derived. The present formulation of the J-vector theory predicts rectilinear crack growth. The material and the temperature field can be inhomogeneous and also dynamic crack growth can be evaluated. The main advantage of the theory is that it describes crack growth in materials in general which means that it has a very general basis and therefore it does not have such limitations in validity as the classical J-integral concept.*

- Incorporation of the flow mechanics with structural analysis.
 - *The goal has been modified first to concentrate on the development of suitable facilities for analysing thermal hydraulic problems to obtain realistic estimates of loads subjected to the piping components and to create an in-house program which transforms the temperature results of fluid dynamic analysis in a suitable form for structural analysis. An agreement of the focused funding basis for this activity has been reached.*

- Structural integrity under impact type loads caused by accidents.
 - *The scope of this sub-project was to consider dynamic loading cases of important NPP structures. The expertise gained can also be utilised when assessing containment behaviour.*
 - *Steel containment behaviour was studied under severe postulated hydrogen detonation impulse loads with extensive nonlinear dynamic analyses. A simple procedure, based on the strong explosion theory, was developed by STUK for detonation load evaluation. Two detonation pulses corresponding the amount of 5kg and 10 kg hydrogen were analysed. Deformation rates were 10-25 s⁻¹ and the effect of strain rate to yield strength was remarkable. The effect of geometrical non-linearity was crucial.*
 - *The capabilities of ABAQUS/Explicit code for analysing reinforced concrete structures under impact loads were verified against some test results of impact loaded beams found in the literature. Dynamic behaviour of a concrete floor subjected to jet impingement was assessed after a postulated near by secondary circuit pipe rupture. Special attention was given to material non-linearity which increases the energy absorption capacity at high strain and may lead to partially irreversible structural deformations.*
 - *A literature study was carried out concerning nonlinear dynamic analysis of piping, especially success criteria and strain rate and temperature dependence of material strength properties. As an example one of the main steam line of the Loviisa NPP was considered under a pressure transient due to a condensation water hammer.*

- Verification of the analysis methods using full scale test results obtained in international research programmes, such as the NESC (Network for Evaluating Steel Components) coordinated by CEU/JRC/Petten, the FALSIRE (Fracture Analysis of Large Scale International Reference Experiments) project by OECD, IAEA coordinated research programmes, and pressurized thermal shock tests at the Prometey Institute in Russia.
 - *Extensive material testing and the pre-test preliminary analyses have been performed for the NESC spinning cylinder test which took place at the AEA Technology plc. in spring 1997. Comprehensive structural analyses together with analysis according to ASME XI are being performed in late 1998.*
 - *For priority reasons, the participation of the VTT team to the FALSIRE project was withdrawn during the annual project planning for 1997.*
 - *Within an IAEA coordinated research programme, comparative analyses were conducted for a circumferential surface crack in a bimetallic nozzle weld. A summary report is the duty of IAEA.*
 - *The investigations of the model pressure vessel tests at Prometey Institute in Russia were completed. The crack behaviour in the case of the clad vessel was clarified.*

2.4 Maintenance strategies and reliability (KUNTO)

The main tasks and their progress can be summarised as follows:

- A systematic maintenance analysis approach is to be developed and used as input for maintenance decision. The work has started with a Nordic survey on the maintenance strategies, ageing of equipment and the use of related information technology at the plants.
 - *A model was developed for aiding evaluation of the effectiveness of existing maintenance programs. The results of this maintenance analysis pinpoint proposals on changes in maintenance and testing tasks justified for fault reduction and detection.*

- *The analysis model was completed by a computerized decision analysis and decision models to support complex safety related decisions.*
- *It was shown how systematic models for maintenance analysis and decision support, utilising computerised and statistical tool packages, can be taken into use for evaluation and optimisation of maintenance of active systems from the safety and economic point of view.*
- *Maintenance strategies in a systems perspective were outlined and a rough model of target steered maintenance management was defined to be used as a basis for future developments.*
- For management of the nuclear piping integrity, probabilistic models on flaw growth and on the detection effectiveness of non-destructive testing (NDT) will be developed.
 - *Models based on the logit transformations of the relative flaw depth have been introduced both for the flaw detection probability and flaw sizing accuracy. The logarithmic models have been applied to the flaw sizing data and flaw detection frequency data from a PISC III exercise concerning ultrasonic inspection of intergranular stress corrosion cracking. In addition a Bayesian procedure for combining information and updating knowledge on number and size of flaws was introduced.*
 - *A survey of probabilistic methods for evaluation of structural component integrity and prediction of flaw growth was done. It identified needs of data collection and modelling as an input for probabilistic safety analyses and optimisation of maintenance programs of structures.*
- The research on human and organizational factors in non-destructive testing starts by a national and international survey of the NDT work and the human factors contributing to its effectiveness. A detailed plan will be prepared for identification of the human and organizational developmental factors.
 - *The results of a literature review on human factors influencing the reliability of NDT were compared to the views of the Finnish experts and officials.*

- *The continuing man-machine psychological analysis of the inspectors' work provided evidence to the views from the earlier study that the attitudes of the inspectors influence the inspection performance.*
- *Through analysing and comparing the results concerning quality conceptions and the conceptions of the demands on inspection, i.e. skill conception, two habits of action could be inferred. They were interpretative habit of action and procedural habit of action among the inspectors.*

2.5 Fire safety (PALOTU)

The main tasks and their progress can be summarised as follows:

- In order to predict heat release rate and flame spread velocity for solid burning materials, especially for cables, a theoretical model for pyrolysis rate will be developed and compared with experimental data.
 - *A fit for the heat release rate and duration of local burning as a function of incident heat flux has been proposed. The fit is specific for PVC cables used generally in the Finnish NPPs.*
 - *The more accurate estimate for rate of heat release makes it possible to perform more reliable simulations for cable fires. The presented models serve engineering purposes. More ambitious models are under development at different places around the world.*
- Development of CFD codes for fire applications (SOFIE) will be supervised and new versions of the code validated. User interfaces including databases and flexible couplings to other codes will be created for zone models used in routine calculations.
 - *Development of the SOFIE code has been supervised actively and an international validation procedure has been started outside the project but initiated by us. Two scenarios with good international participation have been calculated. A preliminary report quantifies the state of art accuracy of of temperature prediction to 20 ...30%. To the quality of results the user is more important than the selected*

code. Although cfd-models should be superior because of mathematical formulation, no great difference between zone and cfd-codes were observed for the scenarios studied.

- In case of fire, electric devices may still work, although their nominal, long term ambient limits have been exceeded. Short term limits and time delays can be determined by theoretical work and measurements on energised systems.
 - *It was shown that determination of cable performance at temperatures exceeding the long term rating reduces to demonstration of cable insulation material performance.*
 - *Pressure transmitters and valve actuators were measured in an oven at different temperatures, and times for failure measured. Theoretical models were developed and validated against measurements allowing easy application for similar equipment without direct measurements.*
 - *Failure times and mechanisms were determined for a pressure transmitter cables exposed to a flame temperature, and a Weibull distribution was fitted on data to allow calculating reliability.*
 - *In a preliminary study different electronic components and circuit boards were exposed on smoke for half an hour, and acute effects on the function of the circuits were measured. Leakage resistance decreased permanently by an order of magnitude, but the effect on the performance of the circuits were found rather small.*
- Applicability, reliability and technical parameters of active fire protection systems in nuclear power plants will be studied.
 - *The response of different smoke detectors to standard test fires as well as smouldering and flaming cable material fires was studied to backup selection of new fire detection systems to existing Finnish NPPs. The response time and smoke density at the response of each detector were measured. Also temperature and flow fields were measured, and compared with cfd-calculations to validate models for predicting reaction times of detectors.*

- Electrically induced ignition will be studied by determining ignition mechanisms and delays, carrying out ignition experiments by measuring ignition energy and the following rate of heat release using real components and electric cabinets.
 - *Continuing earlier work a second series of three full scale fire experiments on electronic cabinets have been carried out. These experiments demonstrated, how sensitive function of air flow the RHR inside the cabinet is.*
 - *Two full scale fire experiments on PVC cable trays were carried out, one with cables in vertical position and one with cables in horizontal position.*
 - *According to best statistical data bases available from NPPs probability of ignitions of power cables (per length unit) is approximately 40 times as high as for instrument cables.*

3. Other achievements

3.1 Development of human resources

Many experts have gained education and experience through participation into the research work. The academic degrees gained within this RATU2 programme are listed under References and summarised in Table 1.

A comprehensive listing of the 280 publications which have been prepared within this programme is given in Appendix 1 of this proceedings, and a survey of the publication types is shown in Table 2.

Several RATU2 researchers have stayed abroad for longer periods in leading research institutes or universities in aim to import relevant technologies to Finland and to strengthen the mutual co-operation. Normally this has been realised as one year exchange programmes. Such longer visits were addressed to Germany (3), United States (2) and Norway (1). One Swedish student made her Master of Science thesis to the Swedish Royal Institute of Technology (KTH) during her stay at VTT.

Table 1. Academic degrees gained within the RATU2 programme.

Project	Academic degrees		
	Doctor of Technology	Licentiate of Technology	Master of Science
RAVA	2	1	6
AIRI		1	
RAKE	1	1	1
KUNTO			1
PALOTU		1	3
RATU2	3	4	11

Table 2. Publications prepared within the RATU2 programme.

Project	Publications			
	Original papers in periodicals	Thesis publications	Conference papers ⁽¹⁾	Reports and others ⁽²⁾
RAVA	17	9	61	31
AIRI	2	1	11	16
RAKE	7	3	11	25
KUNTO	4	1	8	16
PALOTU	2	4	8	16
TUHTI			2	25
RATU2	30	18	103	129

(1) International conferences, including reviewed proceedings

(2) VTT, STUK and other reports, domestic seminars, international workshops

3.2 Development of networks

Both domestic and international research networks have been established and strengthened as a result of this RATU2 programme. Although each of the research projects has specific objectives and budget, the research work joins the project teams in flexible ways into the task groups. As the practical problems are multidisciplinary, some are dealt with in several projects within the RATU2 programme and/or linked to other international programmes.

The networks, such as AMES, NESC and PISC, co-ordinated by the Joint Research Centre (JRC) of the European Union, as well as the Nordic NKS co-operation are considered very important for technology transfer and international exchange of results. The participation to the international CIR program co-ordinated by EPRI, to the OECD Halden reactor project, to the EURATOM Nuclear Fission Safety (NFS) projects and some other international projects was also organised through the RATU2 programme. This arrangement provided a forum for co-ordinated domestic funding and steering of these related activities. It also made it possible to use the existing technology transfer channels and reference groups together with the Finnish authorities and utilities.

3.3 Development of new research facilities

The following new research facilities and capabilities have been adopted within the RATU2 Research Programme:

3.3.1 Fracture mechanics

- A four-point bending, mixed-mode testing system for elastic-plastic mode I/II fracture toughness testing. The facility makes it possible to measure materials tearing resistance with varying degrees of mode mixity with small to medium size specimens.
- A restraining crack arrest testing facility. The facility makes it possible to modify the crack driving force-crack length-dependence in a K_{Ia} -test and increases the possibility of obtaining valid test results.

- Capability for elastic-plastic testing and numerical analysis of surface cracked bend specimens.
- A hot cell fracture resistance testing facility for miniature bend specimens $3 \times 4 \times 27 \text{ mm}^3$. The facility makes it possible to measure material toughness from very small samples, e.g. from samples taken from Charpy specimens tested in previous surveillance programs.

3.3.2 Environment assisted cracking

- A hot cell three point bending testing facility for Charpy-size specimens ($10 \times 10 \times 55 \text{ mm}^3$) suitable for fracture resistance testing in reactor water environment and elevated temperature, i.e. in an autoclave.
- A pneumatic servo-controlled fracture resistance measuring device (PSFM-device) for environmentally assisted cracking (EAC) studies. The testing system enables constant load, constant displacement and constant displacement rate test performance in simulated light water environments using small three point bend specimens with minimum and maximum dimensions of $3 \times 4 \times 27 \text{ mm}^3$ and $10 \times 10 \times 55 \text{ mm}^3$. Also based on the same technology, a test facility was developed for testing six specimen simultaneously.

3.3.3 Oxide films

- Development of a thin-layer electrode arrangement which makes versatile electrochemical measurements possible even in poorly conductive power plant coolants at high temperatures and pressures.
- Capability of performing electrochemical impedance spectroscopic measurements in high-temperature aqueous electrolytes.

3.3.4 Non-destructive testing

- An automated multichannel ultrasonic inspection system containing a multipurpose scanner for different piping welds and software for data

analysis. The facility enhances reliability of non-destructive testing. It also reduces the radiation doses of the inspection personnel during inspection of NPP components.

3.3.5 Structural analysis

- Capability for assessment of ductile fracture using micromechanical material modelling. The micromechanical Gurson-Tvergaard material model has been successfully applied on the numerical prediction of ductile fracture resistance of several reactor pressure vessel materials.
- A new theory called the ‘J-vector theory’ for rectilinear crack growth. The main advantage of the theory is that it describes crack growth in materials in general which means that it has a very general basis and therefore it does not have such limitations in validity as the classical J-integral concept.
- An engineering integrity assessment program system MASI for time- and cost-effective assessment of cracked pressure vessels and piping. New capabilities for fatigue and stress corrosion crack growth assessment and for assessment of sub-cladding cracks. A new program module for evaluating the criticality of a crack using the ASME XI rules.
- Verified procedures for performing PTS assessments. Verification of the analysis methods using full scale test results obtained in international research programmes, concerning especially clad pressure vessels, stratified thermal loads and bimetallic nozzle welds.
- Capability for structural integrity evaluation demonstrated for several cases under impact type loads caused by accidents: steel containment behaviour under severe postulated hydrogen detonation impulse loads, reinforced concrete structures under impact loads and nonlinear dynamic analysis of piping (a main steam line under a pressure transient due to a condensation water hammer).
- Incorporation of the flow mechanics with structural analysis. Development of suitable facilities for analysing thermal hydraulic problems to obtain realistic estimates of loads. An in-house program to transform the temperature results of fluid dynamic analysis to structural analysis.

3.3.6 Maintenance and reliability

- A systematic analysis model for evaluation of maintenance programs and to support decisions to change them with a view to improve safety and economy. The system has been applied for improvement of maintenance effectiveness and reliability.
- Logit model for presentation of sizing accuracy and detection probability of flaws from non-destructive inspection data.
- Man-machine psychological analysis of skill conceptions among NDT inspectors facilitating development of interpretative habits of action.

3.3.7 Fire safety

- New versions of the fire simulation code "SOFIE" allowing advanced simulation of fires, and a versatile presentation of calculation results. Simulation results matching with the experimental results have been obtained for several practically relevant cases.
- A new generation of fire technology has been achieved through utilising field model concepts for design of the large scale experiments together with extensive instrumentation to allow detailed comparisons with the field model predictions.
- A significant step towards the global acceptance of fire simulation codes has been achieved by VTT's strong contribution to an international impartial validation of the numerical fire simulation code packages.
- As a results of these efforts VTT has been able to cope with and lead developing on technology on fast growing market demand of fire technology for designing special buildings outside nuclear industry using performance based principles in a sense of fire risk analysis of NPPs.

4. Interim evaluations

The achievements in the RATU2 research programme were twice systematically evaluated. In 1996 an internal evaluation was carried out by the steering group

and project reference groups. The results were used for successive annual planning. For an independent assessment, the Ministry of Trade and Industry commissioned external evaluators, who visited the programme in 1998. The results were used for planning of a follow-on programme.

4.1 External evaluation

The RATU2 programme, together with the parallel RETU program on reactor safety, was evaluated in January 1998 by Dr. Claude Faidy of EdF, France and Prof. Mike Hayns of Aston University, U.K. Their evaluation summary included the following assessment on the performed work:

“The evaluation showed the continuing very high quality of staff deployed on the program, with a very high specific output rate. For a small overall resource, the team was very supporting of the policy of using these programs for the education and training of the next generation of specialists. This will clearly have long term benefits, as well as already having some of its most innovative work emerging through PhD theses and dissertations. The parallel policy of technology transfer is also supported, with the integration of the work into the VTT structure adding value through synergies between technical disciplines and exposure to many different potential end users.” (Faidy and Hayns, 1998)

A clear recommendation of future research priorities was also included in their report:

“The evaluation team recognized a number of future trends which could have a strong influence on the direction of the programs. These include the continuing possibility of a fifth nuclear power plant, membership of the EU and hence access to its nuclear fission safety programs, the aspirations of the Utilities to increase the performance of the plant and the requirements of the regulatory authority for long term safety reviews. Above all, however, the team recognized that the Finnish plant are now at least twenty years old and, whilst they still have a long way to go before the end of their useful lives, they will require increasing attention to issues related to plant aging. Along with many other countries, therefore, we anticipate a move towards research topics more directly related to underpinning the continued safe operation of the plant. ” (Faidy and Hayns, 1998)

5. Conclusions

The RATU2 programme has brought many significant scientific findings and useful applications of new knowledge. As the international evaluators pointed out, in many cases the achievements were of outstanding good quality and gave remarkable input to the common knowledge on materials behaviour and structural integrity of NPP's.

Of course, the herein reported achievements would not have been possible if the work had been started from zero. Fortunately, the new research aims were specified in an early phase and the start-up after the previous RATU programme was smooth enough to ensure continuous progress. The long term planning has also enabled recruiting of many young researchers and allowed the investments on developing human resources and experimental facilities.

In domestic scales, the RATU2 programme has been a remarkable investment, but still forming a minor part of the international research on the relevant topics. Active participation into the international networks and research programmes has increased the output value of this research programme. On the other hand, this active technology transfer could not happen without extensive research of our own. Participation to international co-operation has been broad, but yet focused to certain technology areas where VTT's position is strong and new technology can be transferred to domestic use for ensuring the reliability of NPP components. International acceptance of the results has also provided valuable feedback and benchmarking as well as additional motivation for the researchers to continue their work.

Another, and not the least, key success factor is considered to be the balanced mixing of basic research and problem solving activities together with the open communication between the researchers and end users, i.e., the authority and and utility staffs. This provides a good environment for target oriented long term research.

6. Acknowledgements

The reported work covers the Finnish Research Programme on the Structural Integrity of Nuclear Power Plants 1995 - 1998 financed by the Ministry of Trade and Industry (KTM), Technical Research Centre of Finland (VTT), the Radiation and Nuclear Safety Authority (STUK), Imatran Voima Oy (IVO) and Teollisuuden Voima Oy (TVO).

The reported achievements have been gained by a great number of researchers and other staff who participated in this programme. The project leaders Kim Wallin, Pentti Kauppinen, Heli Talja, Kari Laakso and Olavi Keski-Rahkonen have supervised the work and summarised the achievements.

The members of the steering group of the programme Mr. Matti Ojanen, (Chairman), the Radiation and Nuclear Safety Authority, Mr. Ralf Ahlstrand, IVO Power Engineering Ltd., Mr. Juho Hakala, Teollisuuden Voima Oy, Prof. Hannu Hänninen, Helsinki University of Technology, Dr. Timo Haapalehto, Ministry of Trade and Industry, Dr. Lasse Mattila, VTT Energy, Dr. Rauno Rintamaa, VTT Manufacturing Technology, as well as the reference groups of each project have given a significant contribution to steering of this research programme and are gratefully acknowledged of this co-operation.

References

Faidy, C. & Hayns, M. R. 1998. Evaluation of the RATU2 and RETU Research Programs. Helsinki: Ministry of Trade and Industry, Finland. 65 p. (Studies and Reports 8/1998).

VTT 1994. Ydinvoimalaitosten rakenteellinen turvallisuus (RATU2) 1995 - 1998, Tutkimusohjelman suunnitelma. Espoo: VTT Manufacturing Technology. 50 p. (Report VALB41). (In Finnish).

Theses for academic degrees prepared within the RATU2 programme

Aulamo, H. 1997. Ydinvoimalaitoksen kaapelipaloriski (Cable fire risk of a nuclear power plant). Master's Thesis. Helsinki University of Technology, Department of Engineering Physics and Mathematics. 117 p. (In Finnish).

Björkman, J. 1998 Palonilmaisun mallintaminen [Modeling of fire detection]. Lisensiaatintutkinto, Helsingin yliopisto, Fysiikan laitos. Helsinki, 55 p.

Hanson, M. 1997. Analysis of subclad cracks. Stockholm: Royal Institute of Technology, master thesis. 28 p. + app. 36 p.

Hostikka, S. 1997. Palopatsasmallit tulipalon simuloinnissa [Plume models in numerical simulation of fire]. Master's Thesis. Helsinki University of Technology, Department of Engineering Physics and Mathematics. 79 p. + app. 8 p. (In Finnish).

Ihonen, J., 1997. Anodic behaviour of chromium in aqueous solutions. Master's Thesis. Helsinki University of Technology, Laboratory of Physical Chemistry and Electrochemistry. 76 p + Appendices.

Itäaho, M. 1995. Ympäristön vaikutus materiaalien virumiseen ja murtumiseen (The effect of environment on the creep and fracture behavior of materials). Master's Thesis. Helsinki University of Technology, Faculty of Mechanical Engineering. 103 p. (In Finnish).

Kettunen, J. 1997. Uskomuksia ydinvoimalaitoksissa suoritettavien tarkastusten luotettavuudesta. (Beliefs concerning the reliability of nuclear power plant in-service inspections). Helsingin yliopisto. Psykologian laitos. Pro gradu - tutkielma. 49 p. + app. 9 p. (Report STUK-YTO-TR 121) .(In Finnish).

Kinnunen, P., 1998. Nikkelillä ja nikkeli-kromilejeeringeillä esiintyvien oksidifilmien karakterisointi (Characterisation of oxide films on nickel and nickel-chromium alloys). Master's Thesis. Helsinki University of Technology, Laboratory of Physical Chemistry and Electrochemistry. 89 p. + Appendices. (In Finnish).

Laukkanen, A. 1997. The effect of asymmetric loading on fracture toughness of metallic materials. Master's Thesis. Helsinki University of Technology. Laboratory of Engineering Materials. 198 p.

Moilanen, P. 1995. Pneumaattinen servo-ohjattu murtumisvastuslaitteisto (Pneumatic servo controlled fracture resistance measuring device). Master's Thesis. Helsinki University of Technology, Faculty of Mechanical Engineering. 87 p. (In Finnish).

Mäkelä, K. 1995. The effect of high temperature water chemistry on corrosion reactions in primary coolant systems of nuclear power plants. Licentiate thesis. University of Helsinki, Department of Chemistry. 28 p. + Appendices.

Nevalainen, M. 1997. The effect of specimen and flaw dimensions on fracture toughness. Doctoral thesis, Helsinki University of Technology. Espoo: Technical Research Centre of Finland. 60 p. + Appendices. (VTT Publications 314)

Paananen, J. 1996. Instrumenttikaapin palon suurimman tehon kokeellinen määrittäminen (Experimental determination of the maximum rate of heat release of an electronic cabinet). Master's Thesis. Helsinki University of Technology, Structural Engineering and Building Physics, Fire and Safety Engineering. 111 p. + app. 22 p. (In Finnish).

Pyykkönen, M. 1997. Pienten koesauvojen särönpituuden mittaus murtumismekaanisissa kokeissa käyttäen sähköistä menetelmää. Diploma thesis. Helsinki University of Technology. 75 p. (in Finnish)

Saarenheimo, A. 1996. Elementtimenetelmän käyttö stabiilin särönkasvun arvioinnissa. (Evaluation of stable crack growth by using the finite element method). Licentiate Thesis. Helsinki University of Technology. Espoo: VTT. 114 p. + app. 122 p. (VTT Julkaisuja - Publikationer 819). (In Finnish).

Saario, T. 1995. Development and Applications of the Contact Electric Resistance Technique. Doctor's Thesis. Helsinki University of Technology, Department of Materials Science and Rock Engineering. 34 p.

Sarkimo, Matti. 1995. Suurten paineastioiden eheyden analysointi akustisella emissiolla. (The analysis of the structural integrity of large pressure vessels by acoustic emission testing). Licentiate Thesis. Helsinki University of Technology, Faculty of Mechanical Engineering. 105 p. (In Finnish).

Talja, Heli. 1998. Ductile fracture assessment using parameters from small specimens. Doctoral thesis, Helsinki University of Technology. Espoo: VTT Manufacturing Technology. 140 p. (VTT Publications 353).

(See Appendix 1 for a comprehensive listing of publications)

Appendix 1: List of Publications

The Finnish Research Programme on The Structural Integrity Of Nuclear Power Plants (RATU2)

Material Degradation in the Reactor Environment

Aaltonen, P. 1995. Sirkonioksidikalvojen käyttö pH:n mittaukseen korkeissa lämpötiloissa. Funktionaaliset materiaalit ja älykkäät rakenteet koneenrakennuksessa [Functional materials and intelligent structures in mechanical design]. In: Hänninen, H., Brederholm, A. & Ullakko, K. (Eds.). Espoo: TKK Materiaalitekniikan laboratorio. ISBN 951-22-2523-9 (In Finnish).

Aaltonen, P., Mäkelä, K. & Buddas, T. 1995. Characterization of oxide scales from Loviisa units 1 and 2. 7th International Symposium on environmental degradation of materials in nuclear power systems - water reactors. Breckenridge, Colorado, USA, 6 - 10 August, 1995. 11 p.

Aaltonen, P., Saario, T., Karjalainen-Roikonen, P., Piippo, J. & Tähtinen, S. 1996. Vacancy-creep model for EAC of metallic materials in high temperature water. Corrosion '96. The NACE International Annual Conference and Exposition. Denver, Colorado, USA, 24 - 29 March 1996. Paper No. 81. 12 p.

Aaltonen, P., Saario, T., Ehrnstén, U., Itäaho, M. & Hänninen, H. 1996. Vacancy-creep model for EAC of brass. Eurocorr '96. Nizza, France 24 - 26 November 1996. 4 p.

Aaltonen, P., Jagodzinski, Y., Tarasenko, A., Smouk, S. & Hänninen, H. 1997. Influence of hydrogen charging on mechanical behaviour of Inconel-600 Alloy measured by internal friction. 8th Env. Deg. of Materials in Nuclear Power Systems - Water reactors. NACE, Amelia Island, USA, 10 - 14 August 1997. Pp. 325 - 332.

Aaltonen, P., Saario, T., Ehrnstén, U., Itäaho, M., Hänninen, H. 1997b. Selective dissolution-vacancy-creep model for EAC of brass. In: Magnin, Thierry (Ed.) Corrosion-Deformation Interactions CDI '96. Second International Conference on Corrosion-Deformation Interactions in conjunction with EUROCORR'96. Nice, France, 1996. The Institute of Materials. Pp. 35 - 44.

Aaltonen, P., Bojinov, M., Ehrnstén, U., Lagerström, J., Laitinen, T., Saario, T. & Sirkiä, P. 1998. The effect of environment on the electric and electrochemical properties of surface films on alloy 600 and alloy 690 in pressurised water reactor primary water (Poster). Proceedings of the International Symposium Fontevraud IV contribution of materials investigation to the resolution of problems encountered in pressurised water reactors, Vol. II. Fontevraud, France, 14 -18 September, 1998. Pp. 861 - 872.

Aaltonen, P., Jagodzinski, Yu., Tarasenko, A., Smouk, S. & Hänninen, H. 1998. Internal friction in brasses after oxidation in tap water by anodic polarisation. *Acta Mater.*, Vol. 46, No. 6, pp. 2039 - 2046.

Aaltonen, P., Jagodzinski, Yu., Tarasenko, A., Smouk, S. & Hänninen, H. 1998. Low-frequency internal friction of pure copper after anodic polarisation in sodium nitrite solution. *Corrosion Science*, Vol. 40, No. 6, pp. 903 - 908.

Aaltonen, P., Mäkelä, K., Venz, H. & Meier H.-P. 1998. X-ray diffraction characterisation of oxide films on primary circuit surfaces at Beznau Unit 1. *Eurocorr '98*, Utrecht. 6 p.

Aaltonen, P., Jagodzinski, Yu., Tarasenko, A., Smouk, S. & Hänninen, H. 1998. Study of Snoek-type relaxation in hydrogenated Inconel 600. *Philosophical Magazine A*, Vol. 78, No. 4, pp. 979 - 994.

Amaev, A., Platonov, P., Krugov, A., Strombakh, Y., Ahlstrand, R., Nikolaev, V.A. & Valo, M. 1998. Characterisation of the decommissioned Novovoronezh-1 pressure vessel wall material properties by through wall trepans. 19th ASTM Symposium on Effects of Radiation on Materials. Seattle, USA, 16 - 18 June 1998. 20 p.

Arilahti, E., Beverskog, B., Bojinov, M., Hansson-Lyyra, L., Laitinen, T., Markgraf, J. F. W., Moilanen, P., Mäkelä, K., Mäkelä, M., Saario, T. & Sirkiä P. 1998. Advanced in-situ characterisation of corrosion properties of LWR fuel cladding materials. IAEA Technical Committee Meeting on Water Chemistry and Corrosion Control of Cladding and Primary Circuit Components. Hluboka nad Vltavou, Czech Republic, 28 September - 2 October, 1998.

ASTM E 1921-1997. Standard Test Method for Determination of Reference Temperature, T_0 , for Ferritic Steels in the Transition Range. ASTM Books of Standards. American Society for Testing and Materials.

Bojinov, M., Laitinen, T. & Saario, T. 1997. Mechanism of transpassive corrosion of chromium in neutral aqueous solutions. EUROCORR '97, Vol. II. The European Corrosion Congress. Trondheim, Norway, 22 - 25 September 1997. Pp. 617 - 622.

Bojinov, M., Fabricius, G., Itonen, J., Sundholm, G., Piippo, J., Saario, T. & Laitinen, T. 1997. Combination of different electrochemical techniques to characterize the anodic behaviour of chromium. Int. Symposium on Electrochemical Methods in Corrosion Research - EMCR 97. Trento, Italy, 25 - 29 August 1997. 9 p.

Bojinov, M., Betova, I., Raicheff, R., Fabricius, G., Laitinen, T. & Saario, T. 1997. Mechanism of the transpassive dissolution and secondary passivation of chromium in H_2SO_4 solutions. 6th Int. Symposium on Electrochemical Methods in Corrosion Research - EMCR'97. Trento, Italy, 25 - 29 August 1997.

Bojinov, M., Fabricius, G., Laitinen, T. & Saario, T. 1997. The mechanism of the transpassive dissolution of chromium in weakly acidic sulphate solutions. Abstract No. 318 in 1997 Joint International Meeting: 192nd Meeting of The Electrochemical Society, Inc. and 48th Annual Meeting of the International Society of Electrochemistry. Paris, France, 31 August - 5 September, 1997.

Bojinov, M., Fabricius, G., Laitinen, T. & Saario, T. 1998. The mechanism of the transpassive dissolution of chromium in weakly acidic sulphate solutions. In: Natishan, P. M., Isaacs H. S., Janik-Czachor, M., Macagno, V. A., Marcus, P. and Seo, M. (Eds.) Proc. Symposium on Passivity and its Breakdown. 1997 Joint International Meeting of The Electrochemical Society, Inc. Paris, France, 31 August - 5 September, 1997. Vol. 97-26. Pp. 108 - 119.

Bojinov, M., Fabricius, G., Ihonon, J., Sundholm, G., Piippo, J., Saario, T. & Laitinen, T. 1998. Combination of different electrochemical techniques to characterize the anodic behaviour of chromium. Materials Science Forum, 289-292 (1998) 117.

Bojinov, M., Laitinen, T., Mäkelä, K., Saario, T. & Sirkiä, P. 1998. Characterisation of material behaviour in high temperature water by electrochemical techniques. Enlarged Halden Programme Group Meeting, Norway, Lillehammer, 15 - 20 March, 1998. 20 p.

Bojinov, M., Laitinen, T., Mäkelä, K., Saario, T. & Sirkiä, P. 1998. Activity incorporation into Zinc Doped PWR oxides. Enlarged Halden Programme Group Meeting, Lillehammer, Norway, 15 - 20 March 1998.

Bojinov, M., Fabricius, G., Laitinen, T., Saario, T. & Sundholm, G. 1998. Conduction mechanism of the anodic film on chromium in acid sulphate solutions. *Electrochimica Acta*, 44, 246-261.

Bojinov, M., Fabricius, G., Laitinen, T. & Saario, T. 1998. The mechanism of the transpassive dissolution of chromium in acid sulphate solutions. *Journal of the Electrochemical Society*, 145, pp. 2043 - 2050.

Bojinov, M., Fabricius, G., Laitinen, T. & Saario, T. 1998. Transpassivity mechanism of metals and alloys studied by AC impedance, DC resistance and RRDE measurements. *Electrochim. Acta*. In press.

Bojinov, M., Laitinen, T., Mäkelä, K., Saario, T. & Sirkiä, P. 1998. A combination of AC impedance and DC resistance techniques to study corrosion in high temperature aqueous environments. Proceedings of the 4th International Symposium on Electrochemical Impedance Spectroscopy. Rio de Janeiro, Brazil, 2 - 7 August, 1998. Pp. 393 - 395.

Bojinov, M., Fabricius, G., Ihonen, J., Laitinen, T., Piippo, J. & Saario, T. 1998. The passive and transpassive behaviour of chromium in neutral aqueous solutions at ambient and high temperatures. ELECTROCHEM '98, 2 - 4 September, 1998. The University of Liverpool, UK.

Bojinov, M., Laitinen, T., Saario, T., Fabricius, G. & Sundholm, G. 1998. Conduction mechanism of the anodic film on chromium and iron-chromium alloys in acidic sulphate solutions. 49th Annual Meeting of the International Society of Electrochemistry. Kitakyushu, Japan, 13 - 18 September, 1998.

Bojinov, M., Mäkelä, K., Laitinen, T., Saario, T., Hinttala, J., Suksi, S., Muttillainen, E. & Reinval, A. 1998. Development of electrochemical techniques to study oxide films on construction materials in high temperature water. 1998 JAIF International Conference On Water Chemistry in Nuclear Power Plants. Kashiwazaki, Japan, 13 -16 October, 1998. 5 p.

Bojinov, M., Betova, I., Fabricius, G., Laitinen, T., Raicheff, R. & Saario, T. 1998. The stability of the passive state of iron-chromium alloys in sulphuric acid solution. Corrosion Science. In print.

Bojinov, M., Fabricius, G., , Laitinen, T., Mäkelä, K., Saario, T. & Sundholm, G. 1998. Conduction mechanism of the anodic film on Cr and Fe-Cr alloys in H₂SO₄ solution, EUROCORR'98, 28.9.-1.10.1998, Utrecht, The Netherlands.

Bojinov, M., Fabricius, G., Ihonen, J., Laitinen, T. & Saario, T. 1998. The effect of temperature on the passive and transpassive behaviour of chromium in neutral aqueous solutions, EUROCORR'98, 28.9.-1.10.1998, Utrecht, The Netherlands.

Bojinov, M., Betova, I., Raicheff, R., Fabricius, G., Laitinen, T., Mäkelä, K. & Saario, T. 1998. The mechanism of transpassive dissolution of iron-chromium alloys, EUROCORR'98, 28.9.-1.10.1998, Utrecht, The Netherlands.

Bojinov, M., Laitinen, T., Mäkelä, K., Saario, T. & Sirkiä, P. 1998. A novel technique for electrochemical measurements in low conductivity environments, EUROCORR'98, 28.9.-1.10.1998, Utrecht, The Netherlands.

Bojinov, M., Betova, I., Raicheff, R., Fabricius, G., Laitinen, T. & Saario, T. 1998. Mechanism of the transpassive dissolution and secondary passivation of chromium in H₂SO₄ solutions. Materials Science Forum, 289-292, 1019.

Buddas, T., Halin, M., Laitinen, T., Mäkelä, K. & Tompuri, K. 1998. Influence of primary circuit water chemistry on oxide films on stainless steel during a fuel cycle at Loviisa Unit 2, 1998 JAIF International Conference on Water Chemistry in Nuclear Power Plants, 13 - 16 October, 1998. Kashiwazaki, Japan.

Ehrnstén, U., Lagerström, J., Laitinen, T., Piippo, J. & Saario, T. 1996. Characterisation of material behaviour by means of simultaneous monitoring of water chemistry and of surface film electric resistance. Water chemistry of nuclear reactor systems 7. Proceedings of the conference organized by the British Nuclear Energy Society. Bournemouth, UK, 13 - 17 October, 1996. Pp. 277 - 279.

Ehrnstén, U., Lagerström, J., Saario, T., Piippo, J., Aaltonen, P., Tähtinen, S., Laitinen, T. & Hänninen, H. 1996. Environmentally assisted cracking of alloy 600 in PWR primary water. Eurocorr '96. Nizza, France, 24 - 26 September 1996. Paris: Societe de Chimie Industrielle. 10 p

Ehrnstén, U., Saario, T., Laitinen, T. & Lagerström, J. 1997. The effect of hydrogen concentration on surface films and EAC of Alloy 600 in PWR water. The 4th EPRI Workshop on PWSCC of Alloy 600 in PWR's.

Fabricius, G., Laitinen, T., Piippo, J., Saario, T., Salmi, K. & Sundholm, G. 1996. Electrochemical behaviour of chromium in sulphuric acid solutions. Eurocorr '96. Nizza, France, 24 - 26 November 1996. 4 p.

Fabricius, G., Laitinen, T., Piippo, J., Saario, T., Salmi, K. & Sundholm, G. 1996. Passivation and dissolution of chromium in sulphuric acid solutions. Baltic Conference on Interfacial Electrochemistry. Tartu, Estonia, 14 - 18 June 1996. 3 p.

Ihonen, J. 1997. Anodic behaviour of chromium in aqueous solutions. Master's Thesis. Helsinki University of Technology, Laboratory of Physical Chemistry and Electrochemistry. 76 p + app.

Itäaho, M. 1995. Ympäristön vaikutus materiaalien virumiseen ja murtumiseen [The effect of environment on the creep and fracture behavior of materials]. Master's Thesis. Helsinki University of Technology. Faculty of Mechanical Engineering. 103 p. (In Finnish).

Karjalainen-Roikonen, P., Aaltonen, P., Ehrnstén, U. & Hietanen, O. 1995. Long-term ageing of cast Ti-stabilised stainless steel. CSNI/CEC Workshop on aged and decommissioned materials for structural integrity purpose. Mol, Belgium, 27 - 28 June 1995. 12 p.

Karjalainen-Roikonen, P., Toivonen, A. & Moilanen, P. 1996. The use of small fracture mechanical specimens in research of environmentally assisted cracking in simulated light water reactor environments. Enlarged Halden Programme Group Meeting on High Burn-up Fuel Performance, Safety and Reliability and Degradation of In-Core Materials and Water Chemistry Effects. Loen, Norway, 19 - 24 May 1996. 5 p.

Kinnunen, P. 1998. Nikkelillä ja nikkeli-kromilejeeringeillä esiintyvien oksidifilmien karakterisointi (Characterisation of oxide films on nickel and nickel-chromium alloys). Master's Thesis. Helsinki University of Technology, Laboratory of Physical Chemistry and Electrochemistry. 89 p. + app. (In Finnish).

Koukkari, P., Laitinen, T., Olin, M. & Sippola, H. 1998. Vertailu kaupallisten laskentaohjelmien soveltuvuudesta metallioksidien termodynaamiseen stabiili-suustarkasteluun. [Comparison of the applicability of commercially available programs for calculation of thermodynamical stability of metal oxides]. To be published as a STUK-YTO-TR Report. (in Finnish).

Lagerström, J., Ehrnstén, U., Saario, T., Laitinen, T. & Hänninen, H. 1997. Model for environmentally assisted cracking of Alloy 600 in PWR primary water. In: Proceedings of the 8th International Symposium on Environmental Degradation of Materials in Nuclear Power Systems-Water Reactors. Florida, 10 - 14 August 1997. Vol. 1. Illinois: American Nuclear Society, Inc. Pp. 349 - 356.

Laitinen, T. & Saario, T. 1997. Characterisation of surfaces using the contact electric resistance technique. Finnish Chemical Congress, Helsinki, Finland, 11 - 13 November 1997.

Laitinen, T., Mäkelä, K. & Piippo, J. 1998. Electrochemical and water chemistry measurements in high-temperature aqueous environments, UKNCPS/IAPWS Symposium on Power Cycle Chemistry and Related High Temperature Corrosion, London, UK, 8 September 1998.

Laukkanen, A. 1998. Comparison between the engineering treatment model and R6 revision 3. *Engineering Fracture Mechanics*. 27 p.

Laukkanen, A. 1998. Analysis of experimental factors in elastic-plastic small specimen mixed mode I-II fracture mechanical testing. *Engineering Fracture Mechanics*.

Laukkanen, A. 1998. The effect of asymmetric loading on fracture toughness of metallic materials. Master's Thesis. Espoo: Technical Research Centre of Finland. 318 p. (VTT Publications 362).

Laukkanen, A. 1998. Fracture micromechanisms and resistance of ductile elastic-plastic metallic materials under asymmetric loading. *Engineering Fracture Mechanics*.

Laukkanen, A. 1998. Ductile elastic-plastic mixed-mode I-II crack propagation mechanisms and fracture resistance in metallic materials. 12th European conference on fracture. Sheffield, UK, 14 - 18 September, 1998. 6 p.

Laukkanen, A., Wallin, K. & Rintamaa, R. 1998. Evaluation of the effects of mixed-mode I-II loading on elastic-plastic ductile fracture of metallic materials. Symposium on Mixed-Mode Crack Behaviour. Atlanta, Georgia, USA, 6 - 7 May, 1998. 33 p.

Mimura, H. 1998. Note on "Fracture toughness Master Curve" approach. Bulletin of the Faculty of Engineering, Yokohama National University, Vol. 47, March 1998.

Moilanen, P. 1995 Pneumaattinen servo-ohjattu murtumisvastuslaitteisto [Pneumatic servo controlled fracture resistance measuring device]. Master's Thesis. Helsinki University of Technology. Faculty of Mechanical Engineering. 87 p. (in Finnish) .

Moilanen, P., Pyykkönen, M., Rintamaa, R., Tähtinen, S., Toivonen, A. & Saario, T. 1998. The feasibility of small size specimens for testing of environmentally assisted cracking of reactor core materials. Fontevraud IV. Fontevraud, France 14 - 18 September, 1998. 11 p.

Mäkelä, K. 1995. The effect of high temperature water chemistry on corrosion reactions in primary coolant systems of nuclear power plants. Licenciate Thesis. University of Helsinki, Department of Chemistry. 28 p. + app.

Mäkelä, K., Buddas, T. & Aaltonen, P. 1995. The effect of hydrazine dosing on high temperature pH_T and redox potentials under PWR environments. Corrosion 1995. Orlando, USA 26 - 31 March 1995. NACE International. 9 p.

Mäkelä, K. 1996. Current status of PD-reference electrode development work. Enlarged OECD Halden Project Meeting, 24 - 28 May 1996, Loen, Norway.

Mäkelä, K., Laitinen, T. & Buddas, T. 1996. The effect of the new feedwater distributor design on the impurity concentrations in one of the Loviisa 2 unit steam generators. Water chemistry of nuclear reactor systems 7. Proceedings of the conference organized by the British Nuclear Energy Society. Bournemouth, UK, October 13 - 17, 1996. Pp. 364 - 370.

Mäkelä, K., Laitinen, T. & Buddas, T. 1997. Concentrations of chemical species in one of the Loviisa unit steam generators during steady-state-operation. 3rd Int. Seminar on primary and secondary side water chemistry of nuclear power plants. Balatonfüred, Hungary, 16 - 20 September, 1997. 7 p.

Mäkelä K., Laitinen, T. & Bojinov, M. 1998. The influence of modified water chemistries on metal oxide films, activity build-up and stress corrosion cracking of structural materials in nuclear power plants. To be published as a STUK-YTO-TR Report.

Nevalainen, M. & Dodds, R. H. 1995. Numerical investigation of 3-D constraint effects on brittle fracture in SE(B) and CT(T) specimens. Urbana, IL: University of Illinois, USA. 41 p. (Civil Engineering Studies. Structural Research Series No. 598, UILU-ENG-95-2001).

Nevalainen, M., Planman, T. & Müller, K. 1995. Fracture mechanical evaluation of a reactor pressure vessel steel 18Kh2MFA. Espoo: VTT Manufacturing Technology. 22 p. (Report VALB119).

Nevalainen, M., Wallin, K. & Rintamaa, R. 1995. Crack depth effects measured by dynamic fracture toughness tests. Fracture Mechanics: Vol. 24, ASTM STP 1207. Philadelphia, USA: American Society for Testing and Materials. Pp. 108 - 1139.

Nevalainen, M. & Dodds, R. H. 1996. Numerical investigation of 3-D constraint effects on brittle fracture in SE(B) and C(T) specimens. International Journal of Fracture 74, 2, pp. 131 - 161.

Nevalainen, M. 1997. Fracture toughness comparison between a semielliptical surface crack in a 4PB plate and a through-thickness test specimen. Espoo: VTT Manufacturing Technology. 34 p. (VTT Publications 303).

Nevalainen, M. 1997. The effect of specimen and flaw dimensions on fracture toughness. Doctoral Thesis. Helsinki University of Technology. Espoo: Technical Research Centre of Finland. 60 p. + app. (VTT Publications 314)

Nevalainen, M., Wallin, K. & Planman, T. 1997. Staattisen ja dynaamisen särönpysähtymis - transitiolämpötilan välinen korrelaatio teräksillä BS 4360 Grade 50E ja BS 4360 Grade 50D Mod. Espoo: VTT Manufacturing Technology (Report VALB204). (In Finnish).

Nevalainen, M., Rahka, K., Ahlstrand, R. & Blomin, A. A. 1998. Modified crack-arrest fracture toughness determination for a nuclear reactor pressure vessel steel. Fontevraud IV. Fontevraud, France, 14 - 18 September, 1998.

Pelli, R. & Törrönen, K. 1995. State of the art review on thermal annealing. Luxembourg: European Commission, EUR 16278 EN. 43 p. (AMES Report No. 2).

Piippo, J., Saario, T., Laitinen, T. & Hinttala, J. 1996. Electrical properties of surface films formed on copper. Eurocorr '96. Nizza, France 24 - 26 September 1996. 4 p.

Piippo, J., Saario, T., Tegeder, V. & Stellwag B. 1996. Influence on zinc on properties and growth of oxide layers in simulated primary coolant. Water chemistry of nuclear reactor systems 7. Proceedings of the conference organized by the British Nuclear Energy Society. Bournemouth, UK, 13 - 17 October, 1996. Pp. 131 - 134.

Planman, T., Pelli, R. & Törrönen, K. 1995. Irradiation embrittlement mitigation. Luxembourg: European Commission, EUR 16072 EN. 90 p. (AMES Report No. 1).

Planman, T., Valo, M. & Wallin, K. 1995. Comparison of impact tests results on small and ISO-V type Charpy specimens. IAEA Specialists' Meeting on Irradiation Embrittlement and Mitigation, Espoo, Finland, 23 - 26 October 1995. 11 p.

Planman, T., Wallin, K., Valo, M., Ahlstrand, R. & Kohopää, J. 1995. Comparison of some impact test results on ISO-V and KLST type Charpy specimen. Espoo: VTT Manufacturing Technology. 13 p. (Report VALB93).

Planman, T., Wallin, K. & Rintamaa, R. 1995. Comparison of some indirect measures of crack arrest. Seminar on Crack Arrest Concepts for Failure Prevention and Life Extension, 27 September, 1995. Abington, UK: The Welding Institute. 9 p.

Planman, T. & Rintamaa, R. 1996. Ageing materials evaluation and studies (AMES). Espoo: VTT Manufacturing Technology. 7 p. + app. 14 p. (Report VALB161).

Planman, T., Valo, M., Wallin, K. & Rintamaa, R. 1996. NESC1 Material Characterization. Espoo: VTT Manufacturing Technology. 25 p. + app. 72 p. (Report VALC-270).

Planman, T. & Rintamaa, R. 1997. Ageing materials evaluation and studies (AMES). VTT:n osallistuminen yhteistyöhön v. 1996. VTT Manufacturing Technology VALB208. (In Finnish)

Planman, T., Wallin, K. & Rintamaa, R. 1997. Evaluating crack arrest fracture toughness from Charpy impact testing. SMIRT -97, Structural mechanics in reactor technology. Lyon, France 17 - 22 August, 1997. 8 p.

Planman, T., Keinänen, H., Rintamaa, R., Ahlstrand, R., Kryukov, A., Nikolaev, V. & Dragunov, Yu. 1998. Integrity assessment of the VVER 1000 RPV's including embrittlement aspects. 5th Int. Conference on Material Issues in Design, Manufacturing and Operation of Nuclear Power Plant Structures and Equipment. St. Petersburg, Russia, June 7 - 14, 1998. 12 p.

Pyykkönen, M. 1997. Pienten koesauvojen särönpituuden mittaus murtumis-mekaanisissa kokeissa käyttäen sähköistä menetelmää. Diploma Thesis. Helsinki University of Technology. 75 p. (in Finnish)

Saario, T. 1995. Development and applications of the Contact Electric Resistance technique. Helsinki University of Technology. Department of Materials Science and Rock Engineering. Doctor's Thesis. 34 p. (Report TKK - V - A13).

Saario, T. & Paine, J. P. N. 1995. Effect of the surface film electric resistance on eddy current detectability of surface cracks in alloy 600 tubes. 7th Int. Symposium on environmental degradation of materials in nuclear power systems - water reactors. Breckenridge, Colorado, USA, 6 - 10 August, 1995. 10 p.

Saario, T. & Piippo, J. 1995. A new electrochemical technique for in situ measurement of electric resistance and semiconductor characteristics of surface films on metals. Materials Science Forum, Vols. 185 - 188, pp. 621 - 628.

Saario, T. & Tähtinen, S. 1995. In-situ measurement of the effect of LiOH on the stability of fuel cladding oxide film in simulated PWR primary water environment. The NACE International Annual Conference and Corrosion Show. Orlando, USA, 25 - 31 March 1995. 15 p.

Saario, T., Aaltonen, P., Karjalainen-Roikonen, P., Piippo, J., Mäkelä, K., Tähtinen, S. & Hänninen, H. 1995. Selective dissolution - vacancy - creep model for IGSCC of alloy 600. 7th Int. Symposium on environmental degradation of materials in nuclear power systems - water reactors. Breckenridge, Colorado, USA, 6 - 10 August, 1995. 11 p.

Saario, T., Tähtinen, S., Piippo, J. & Kukkonen, J. J. V. 1995. In-situ measurement of the effect of LiOH on the stability of fuel cladding oxide film in simulated PWR primary water environment. 7th Int. Symposium on environmental degradation of materials in nuclear power systems - water reactors. Breckenridge, Colorado, USA, 6 - 10 August, 1995. 14 p.

Saario, T., Piippo, J. & Laitinen, T. 1996. The contact electric resistance (CER) technique. Eurocorr '96. Nizza, France, 24 - 26 September, 1996. 4 p.

Saario, T., Laitinen, T. & Piippo, J. 1997. Contact electric resistance (CER) technique for in-situ characterisation on surface films. Int. Symposium on electrochemical methods in corrosion research - EMCR 97. Trento, Italy, 25 - 29 August, 1997. 9 p.

Saario, T., Laitinen, T. and Piippo, J. 1998. Contact Electric resistance (CER) technique for *in situ* characterisation of surface films, Materials Science Forum, 289-292 (1998) 193.

Saario, T., Mäkelä K., Laitinen T, Bojinov, M. & Betova, I. 1998. The properties of and transport phenomena in oxide films on iron, nickel, chromium and their alloys in aqueous environments. To be published as a STUK-YTO-TR report.

Sokolov, M. A., Wallin, K. & McCabe, D. E. 1997. Application of small specimens to fracture mechanics characterization of irradiated pressure vessel steels. 28th National Symposium of Fracture Mechanics. Saratoga Springs, New York, June 1996. Fatigue and Fracture Mechanics: 28th Volume. ASTM STP 1321. J.H. Underwood, B.D. MacDonald, M.R. Mitchell (Eds.). Philadelphia: American Society for Testing and Materials.

Toivonen, A. & Karjalainen-Roikonen, P. 1996. Evaluation of environmentally assisted cracking using fracture resistance data. Eurocorr '96. Nizza, France 24 - 26 September 1996. 4 p.

Toivonen, A., Tähtinen, S., Moilanen, P. & Aaltonen, P. 1998. The feasibility of pre-fatigued sub size specimens to fracture mechanical studies in inert and in reactor core environments. Enlarged Halden Programme Group Meeting. Norway, Lillehammer 15 - 20 March, 1998. 18 p.

Wallin, K. 1995. Re-evaluation of the TSE results based on the statistical size effect. Espoo: VTT Manufacturing Technology. 30 p. (Report VALB97).

Wallin, K. 1995. Comparison of the scientific basis of Russian and European approaches for evaluating irradiation effects in reactor pressure vessels. Luxembourg: European Commission, EUR 16279 EN. 30 p. (AMES Report No. 3).

Wallin, K. 1995. Statistically defined safety factors and lower bounds signified by brittle fracture modelling. Proceedings of the 2nd Griffith Conference: Micromechanisms of Fracture and their Structural Significance. Sheffield, UK, 13 - 15 September 1995. London: The Institute of Materials. Pp. 131 - 140.

Wallin, K. & Rintamaa, R. 1995. Re-evaluation of the thermal shock experiment results based on the VTT approach for statistical treatment of fracture toughness data. In: 21. MPA Seminar. Approaches to lifetime extension of nuclear power plants. Stuttgart, Germany, 5 - 6 October 1995. Ed. K. Kussmaul. Vol. 1. Stuttgart: Staatliche Materialprüfungsanstalt (MPA) Universität Stuttgart. Pp. 2.1 - 2.18.

Wallin, K., Valo, M., Rintamaa, R., Törrönen, K. & Ahlstrand, R. 1995. Descriptive characteristics of different types of test for irradiation embrittlement. Nuclear Engineering and Design, Vol. 195, No. 1, pp. 69 - 80.

Wallin, K., Rintamaa, R., Valo, M., Planman, T. & Nevalainen, M. 1996. The VTT method for assessment of fracture resistance for structural steels from small material samples. Proc. of 11th Biennial European Conference on Fracture - ECF11. Poitiers-Futuroscope, France, 3 - 6 September 1996. In: ECF 11 Mechanisms and Mechanics of Damage and Failure. Vol. III. Ed. J. Petit. Warley, UK, EMAS. Pp. 2211 - 2216.

Wallin, K., Blauel, J. G. & Nagel, G. 1996. Vergleich der Bruchzähigkeitskurve nach ASME-Code bzw. KTA 3201.2 und der Masterkurve (ASTM Entwurf). MPA-Seminar. Staatliche Materialprüfungsanstalt (MPA) Universität. Stuttgart, Germany, 10 - 11 October 1996.

Wallin, K. 1997. Small specimen fracture toughness characterization - State of the art and beyond. 9th Int. Conference on Fracture. Sydney, Australia, 1 - 5 April, 1997. 12 p.

Wallin, K. 1997. Effect of strain rate on the fracture toughness. Reference temperature T_0 for ferritic steels. Symposium on Ductile Fracture - Recent Advances in Fracture. Orlando, Florida, 9 - 13 February 1997. The Materials Society TMS. 12 p.

Wallin, K., Brumovsky, M. & Steele, L. E. 1997. Results from the IAEA co-ordinated research programmes on irradiation embrittlement of reactor pressure vessel steels. ASME PVP '97 Report. 14 p.

Wallin, K., Valo, M., Planman, T. & Rintamaa, R. 1997. Applicability of smaller than Charpy specimens for fracture toughness characterization with the VTT. IAEA Specialists' meeting on irradiation effects and mitigation. Vladimir, Russia, 15 -19 September, 1997. 10 p.

Wallin, K. 1998. Master curve analysis of ductile to brittle transition region fracture toughness round robin data. The "EURO" fracture toughness curve. Espoo: Technical Research Centre of Finland. 58 p.(VTT Publications 367).

Wallin, K. 1998. The probability of success using deterministic reliability. Marquis & Solin (Eds), Fatigue Design 1998, vol.1. Espoo: VTT, Technical Research Centre of Finland. Pp. 49 - 60. (VTT Symposium 181).

Wallin, K. & Planman, T. 1998. RATU2-tutkimusohjelman RAVA-osaprojekti 1. Toteutumia ja tuloksia v. 1997. Espoo: VTT Manufacturing Technology. 14 p. (Report VALB296).

Wallin, K. & Rintamaa, R. 1998. Master Curve based correlation between static initiation toughness K_{IC} and crack arrest toughness K_{Ia} . 24th MPA-Seminar. Stuttgart, Germany. 8-9.10.1998. 19 p.

Wallin, K., Valo, M. & Rintamaa, R. 1998. Opportunities for structural integrity assessment from small specimen techniques. 5th Int. Conference on Material Issues in Design, Manufacturing and Operation of Nuclear Power Plant Structures and Equipment. St. Petersburg, Russia, June 7 - 14, 1998. 12 p.

Valo, M., Böhmert, J., von Estorff, U. & Törrönen, K. 1995. Proposed post service investigations on decommissioned Greifswald units. CSNI/CEC Workshop on aged and decommissioned materials for structural integrity purpose. Belgia, Mol, 27 - 28 June 1995. 14 p. + app.

Valo, M., Kohopää, J., Wallin, K., Planman, T. 1996. Annealing behaviour of Loviisa-1 surveillance materials measured with V-notched specimens and the current status of vessel anneal. 24th USNRC Water reactor safety information meeting. Washington, USA. 21 - 23.10.1996.

Valo, M., Wallin, K. & Planman, T. 1998. Fracture toughness and impact toughness as measures of irradiation embrittlement based on small specimen data of some pressure vessel steels. Espoo: VTT Manufacturing Technology. 13 p. (Report VALB339)

Valo, M., Wallin, K., Planman, T. & Rintamaa, R. 1998. Fracture toughness and impact toughness as measures of irradiation embrittlement based on small specimen data of some pressure vessel steels. 19th ASTM Symposium on effects of radiation on materials. Seattle, USA, 16 - 18 June 1998. 12 p.

Reliability of Nondestructive Inspections of Nuclear Power Plants

Jeskanen, H. 1997. Aaltomuodon muutostekniikat. SHY:n NDT-päivät. Suomen Hitsausteknillinen Yhdistys ry. 12 - 13.3.1997, Lappeenranta. 8 p. (In Finnish).

Kauppinen, P., Särkiniemi, P. & Jeskanen, H. 1995. Manual ultrasonic inspection of austenitic and dissimilar welds. BALTICA III, International conference on plant condition & life management. Helsinki - Stockholm, 6 - 8 June 1995. VTT Symposium 151. Vol. II. Eds. S. Hietanen & P. Auerkari. Pp. 677 - 684.

Kauppinen, P. & Sillanpää J. 1995. NDT - luotettavaa tietoa vioista? BALTICA III Energia-tuotannon kunnossapitokokemukset. Helsinki - Stockholm, 6 - 8 June, 1995. Espoo: VTT Manufacturing Technology. 11 p. (In Finnish).

Kauppinen, P., Särkiniemi, P. & Jeskanen, H. 1995. Reliability of ultrasonic detection and sizing of flaws in austenitic welds. XV St.Petersburg conference on Ultrasonic Nondestructive testing of Metal Construction. Repino, St.Petersburg, Russia, 30 May - 1 June 1995. Pp. 25 - 28.

Kauppinen, P., Pitkänen, J., Särkiniemi, P. & Jeskanen H. 1995. Ultrasonic detection and sizing of flaws in austenitic cladding and dissimilar metal welds. Seminar "Dissimilar welded joints in NPP equipment and pipings: Problems and means to solve them". Vyborg, Russia, 18 - 22 September 1995. 7 p.

Kauppinen, P. 1997. Tarkastuksen pätevyitys. SHY:n NDT-päivät. Suomen Hitsausteknillinen Yhdistys ry. 12. - 13.3.1997, Lappeenranta. 7 p. (In Finnish).

Kauppinen, P. 1998. Materiaaliominaisuuksien mittaaminen ultraäänitekniikalla. SHY NDT-päivät. 11.-13.3.1998. Suomen Hitsausteknillinen Yhdistys ry. 10 p. (In Finnish).

Lahdenperä, K. 1995. Austeniittisten valujen ja kaksimetalliliitosten testaus. Hitsausteknillisen yhdistyksen NDT-päivät. Turku, 15. - 16.3.1995. 16 p. (In Finnish).

Lahdenperä, K. 1996. ET PISC-Tulokset. SHY-NDT-päivät, Vaasa. 20. - 21.3.1996. (In Finnish).

Lahdenperä, K. & Kankare, M. 1996. Höyrystimien testaustekniikoiden vertailu PISC-projektissa. (Comparison of steam generator methods in PISC). Espoo: Technical Research Centre of Finland. 40 p. (VTT Julkaisuja - Publications 818). (In Finnish).

Lahdenperä, K. 1997. Pyörrevirtatarkastusten luotettavuuden parantaminen. Helsinki: Finnish Centre for Radiation and Nuclear Safety. (in Finnish).

Lipponen, A. 1996. Muokattujen austeniittisten putkien hitsausliitosten ultraäänitarkastuksen luotettavuus. Helsinki: Finnish Centre for Radiation and Nuclear Safety. 51 p. + app. (STUK-YTO-TR 117). (In Finnish).

Lipponen, A. 1996. Yhteiden ja kaksimetalliliitosten ultraäänitarkastuksen luotettavuus. Helsinki: Finnish Centre for Radiation and Nuclear Safety. 42 p. + app. (STUK-YTO-TR 118). (In Finnish).

Paussu, R. & Särkiniemi, P. 1997. Capability demonstration of inspection techniques for Loviisa NPP using a blind test block assembly. EC OECD IAEA Specialists' Meeting on NDE Techniques Capability Demonstration and Inspection Qualification. Petten, The Netherlands, 11 - 13 March 1997. 5 p.

Pitkänen, J. & Kauppinen, P. 1995. Ultraäänen ja sähkömagneettisten menetelmien kehitysnäkymiä. Hitsausteknillisen yhdistyksen NDT-päivät. Turku 15. - 16.3.1995. 21 p. (in Finnish).

Pitkänen, J. & Kauppinen, P. 1995. Ultraääni- ja sähkömagneettisten menetelmien kehitysnäkymiä. Hitsaustekniikka, Vol. 45, No. 3, pp. 36 - 40. (In Finnish).

Pitkänen, J., Kauppinen, P., Jeskanen, H. & Schmitz, V. 1995. Evaluation of ultrasonic indications by using PC-based synthetic aperture focusing technique (PCSAFT). Proceedings of the International Conference on Computer Methods and Inverse Problems in Non-destructive Testing and Diagnostics. Minsk, Belarus, 21 - 24 November, 1995. Pp. 291 - 302.

Pitkänen, J. 1996. Mekanisointi ja tulosten yhdistäminen. SHY-NDT-päivät, Vaasa, 20. - 21.3.1996. 13 p. (in Finnish).

Pitkänen, J. 1996. Mekanisoidun ultraäänitestauksen mittaustulosten esitystavat. Hitsaustekniikka. 8 p. (in Finnish).

Pitkänen, J. Kauppinen, P., Jeskanen, H., Särkiniemi, P. & Schmitz, V. 1996. Evaluation of ultrasonic indications by using PC-based synthetic aperture focusing technique (PC-saft). Proceedings of the 14th International Conference on NDE in the Nuclear and Pressure Vessel Industries. Pp. 459 - 463.

Pitkänen, J. 1998. Termisten säröjen määrittäminen ultraäänellä. SHY-NDT-päivät. 11. - 13.3.98. Suomen Hitsausteknillinen Yhdistys ry. 5 p. (In Finnish).

Pitkänen, J. 1998. Evaluation of ultrasonic indications by using synthetic aperture focusing technique. IAEA regional workshop on flaw discrimination and sizing methods and techniques. Madrid, Spain, 20 - 24 April, 1998. 7 p.

Pitkänen, J., Särkiniemi, P., Kauppinen, P. & Jeskanen, H. 1998. Ultrasonic measurement of a thermal fatigue crack field manually and with a simple handscanner. 7th European Conference on Non-destructive testing. Copenhagen, Denmark, 26 - 29 May, 1998. Pp. 746 - 750.

Pitkänen, J., Särkiniemi, P., Kauppinen, P. & Jeskanen, H. 1998. The ultrasonic detection and evaluation of defects in a thickwalled cylindrical component having cladding on inside surface. 7th European Conference on Non-destructive testing. Copenhagen, Denmark, 26 - 29 May, 1998. Pp. 1420 - 1425.

Pitkänen, J., Kuusinen, P., Särkiniemi, P. & Kauppinen, P. 1998. The effect of a shrinkage fit joint to ultrasonic inspectability of a component. 7th European Conference on Non-destructive testing. Copenhagen, Denmark, 26 - 29 May, 1998. Pp. 1980 - 1984.

Särkiniemi, P. & Paussu, R. 1998. Capability demonstration for vendor selection and inspection qualifications. 7th European Conference on Non-destructive testing. Copenhagen, Denmark, 26 - 29 May, 1998. Pp. 2008 - 2012.

Pitkänen, J. Särkiniemi, P. & Kauppinen, P. 1998. The application of RBI-concept to ultrasonic measurement of fatigue cracks. BALTICA IV, International conference on plant condition & life management. Helsinki - Stockholm, 7 - 9 September, 1998. Espoo: Technical Research Centre of Finland. Pp. 535 - 541. (VTT Symposium 185).

Sandlin, S. 1998. Mallinnus ultraäänitestauksen tukena. SHY NDT-päivät. 11. - 13.3.98. Suomen Hitsausteknillinen Yhdistys ry. 14 p. (in Finnish).

Sarkimo, M. 1995. Suurten paineastioiden eheyden analysointi akustisella emissiolla. (The analysis of the structural integrity of large pressure vessels by acoustic emission testing.) Licentiate Thesis. Helsinki University of Technology, Faculty of Mechanical Engineering. 105 p. (in Finnish).

Sarkimo, M. 1997. Jatkuvan monitoroinnin menetelmät rakenteiden eheyden varmistamiseen ydinvoimaloissa. Technical Research Centre of Finland. 41 p. (VTT Publications 1882).

Structural Analyses for Nuclear Power Plant Components

Hanson, M. 1997. Analysis of subclad cracks. Stockholm, Sweden: Royal Institute of Technology. Diploma Thesis. 28 p. + app. 36 p.

Keinänen, H., Rintamaa, R. & Talja, H. 1995. Computational methods assuring nuclear power plant structural integrity and safety - an overview of the recent activities at VTT. SMiRT 13, Post Conference Seminar 2. 9 p.

Keinänen, H., Talja, H., Rintamaa, R., Ahlstrand, R., Nurkkala, P., Karzov, G., Timofeev, B. & Blumin, A. 1995. Pressurized thermal shock tests with an uncladded and with a cladded model pressure vessel. SMiRT 13, Paper 349, Session G03. 6 p.

Keinänen, H., Talja, H., Rintamaa, R., Törrönen, K., Ahlstrand, R., Nurkkala, P., Karzov, G., Timofeev, B. & Blumin, A. 1995. Crack initiation and arrest in a pressurized thermal shock test for a model pressure vessel made of VVER-440 reactor pressure vessel steel. Nuclear Engineering and Design, Vol. 158, pp. 217 - 226.

Keinänen, H. & Talja, H. 1996. Brittle fracture analysis of primary nozzle of VVER-440 nuclear power plant PAKS. A stage 2 study of the IAEA coordinated research programme on management of ageing of reactor pressure vessel (RPV) primary nozzle. Espoo: VTT Manufacturing Technology. 25 p. + app. (Report VALB115).

Keinänen, H., Talja, H., Rintamaa, R., Ahlstrand, R., Rajamäki, P., Nurkkala, P., Karzov, G., Timofeev, B. & Blumin, A. 1995. Pressurized thermoshock tests with an uncladded model vessel, extensive summary report. Axial outside surface flaw in the model pressure vessel material (CrMoV, VVER-440 type) in under-tempered brittle state circumferential weld in the model vessel. Espoo: VTT Manufacturing Technology. 37 p. + app. (Report VALB114).

Keinänen, H., Talja, H., Rintamaa, R., Ahlstrand, R., Nurkkala, P., Karzov, G., Blumin, A. & Timofeev, B. 1996. PTS testing programme on model pressure vessels. 4th Int. Conf. on Material Science Problems in NPP Equipment Production and Operations. St. Petersburg, Russia, 16 - 23 June, 1996. 12 p.

Keinänen, H., Talja, H., Rintamaa, R., Ahlstrand, R., Nurkkala, P., Karzov, G., Blumin, A. & Timofeev, B. 1996. Thermal shock round robin. Prometey test PTS-2. Test number 9, 2nd PTS test with the cladded model pressure vessel, crack 3. Espoo: VTT Manufacturing Technology. 23 p. (Report VALB148).

Keinänen, H., Talja, H., Rintamaa, R., Ahlstrand, R., Nurkkala, P., Karzov, G., Timofeev, B. & Blumin, A. 1996. Pressurized thermoshock tests with a cladded model vessel (Vessel 2). Final report. Espoo: VTT Manufacturing Technology. 40 p. (Report VALB149).

Keinänen, H. & Talja, H. 1997. Brittle fracture analysis of primary nozzle of VVER 440 reactor pressure vessel. SMIRT -97, Structural Mechanics In Reactor Technology. Lyon, France 17 - 22 August 1997. 8 p.

Keinänen, H. & Talja, H. 1997. Brittle fracture analysis of VVER-440 primary nozzle. Espoo: VTT Manufacturing Technology. 16 p. + app. (Report VALB 260).

Keinänen, H., Talja, H., Rintamaa, R., Ahlstrand, R., Nurkkala, P., Karzov, G., Timofeev, B. & Blumin, A. 1997. Pressurised thermoshock tests on model pressure vessels of VVER 440 RPV steel. SMIRT -97, Structural Mechanics in Reactor Technology. Lyon, France, 17 - 22 August 1997. 8 p.

Keinänen, H., Talja, H., Rintamaa, R., Ahlstrand, R., Nurkkala, P., Karzov, G., Timofeev, B. & Blumin, A. 1997. Pressurized thermoshock tests with a cladded model vessel (Vessel 2) - Test results evaluation. Espoo: VTT Manufacturing Technology. 44 p. + app. (Report VALB149).

Keinänen, H., Talja, H. & Rintamaa, R. 1998. Computational methods assuring nuclear power plant structural integrity and safety: an overview of the recent activities at VTT. Nuclear Engineering and Design, Vol. 183, pp. 41 - 51.

Keinänen, H., Talja, H., Rintamaa, R., Planman, T., Ahlstrand, R., Nurkkala, P., Karzov, G., Timofeev, B. & Blumin, A. 1998. Lessons learned from large scale PTS testing. 5th Int. Conference on Material Issues in Design, Manufacturing and Operation of Nuclear Power Plant Structures and Equipment, St. Petersburg, Russia, June 7 - 14, 1998. 11 p.

Nevalainen, M. 1997. Determination of NDT-temperature for NESC1 material. Espoo: VTT Manufacturing Technology. 6 p. + app. (Report VALB278)

Pokela, H. 1998. Lämpötilatietojen siirto virtauslaskentaohjelmasta Fluent-elementtimenetelmäohjelmaan ABAQUS. Espoo: VTT Manufacturing Technology. 20 p. + app. (Report VALB323)

Rintamaa, R., Keinänen, H., Schulz, H., Hurst, R., Karzov, G., Timofeev, B. & Blumin, A. 1996. NESC2 Work Programme Proposal: Extended verification of the structural integrity assessment procedures for reactor pressure vessels of CrMoV-type steel. 4th Int. Conf. on Material Science Problems in NPP Equipment Production and Operations, St. Petersburg, Russia, June 16 - 23, 1996. 8 p.

Saarenheimo, A. 1995. Preliminary analyses of a steel containment under detonation conditions. Espoo: VTT Manufacturing Technology. 33 p. + app. (Report VALB52).

Saarenheimo, A., Eerikäinen, L. & Keskinen, R. P. 1995. Post-calculation of a feed water pipe break at the Loviisa nuclear power plant. SMiRT 13. 6 p.

Saarenheimo, A., Talja, H., Kordisch, H., Voss, B. & Neubrech, G.E. 1995. Crack Growth Evaluation of a Multimaterial CS-type Specimen. International Journal of Pressure Vessels and Piping 62, pp. 135 - 146.

Saarenheimo, A. & Hyvärinen, J. 1996. Finite element analysis of a steel containment under detonation conditions. Fourth Int. Conference on Structures under Shock and Impact, SUSI 96. In: Structures Under Shock and Impact IV. Eds. N. Jones, C. A. Brebbia, A. J. Watson. Southampton, UK, Computational Mechanics Publications. Pp. 15 - 24.

Saarenheimo, A. 1996. Elementtimenetelmän käyttö stabiilin särönkasvun arvioinnissa. (Evaluation of stable crack growth by using the finite element method.). Licentiate Thesis. Espoo: VTT. 114 p. + app. 122 p. (VTT Julkaisuja - Publikationer 819). (In Finnish).

Saarenheimo, A. 1997. Iskukuormitettujen teräsbetonirakenteiden analysointi elementtimenetelmä-ohjelmalla. Espoo: VTT Manufacturing Technology. 24 p. (Report VALB181). (In Finnish).

Saarenheimo, A. 1997. Non-linear analysis of a reinforced concrete slab subjected to jet impingement. Espoo: VTT Manufacturing Technology. (VALB209).

Saarenheimo, A. 1998. Structural analysis of piping loaded by pressure transients. Espoo: VTT Manufacturing Technology. 48 p. + app. (Report VALB332)

Santaoja, K. 1996. Rectilinear crack growth in hyperelastic materials. Espoo: Technical Research Centre of Finland. 77 p. + app. 13 p. (VTT Publications 275).

Santaoja, K. 1996. Validity of singular stress-strain field at the crack tip? Collection of transparents for the presentation held at the European Structural Integrity Society (ESIS) technical committee TC1 meeting in Espoo, Finland. 16 p.

Santaoja, K. 1997. Extension for the Gurson-Tvergaard material model based on thermomechanics and damage mechanics. Abstract. 3rd Euromech Solid Mechanics Conference. Stockholm, Sweden, 18 - 22 August, 1997. 1 p.

Santaoja, K. 1997. Thermomechanics of solid materials with application to the Gurson-Tvergaard material model. Espoo: Technical Research Centre of Finland. 162 p. + app. 14 p. (VTT Publications 312).

Santaoja, K. 1998. J-vector theory for simulation of rectilinear crack growth. Espoo: Technical Research Centre of Finland. 81 p. + app. (VTT Publications 360).

Sievers, J., Liu, X., Rajamäki, P., Talja, H. & Raiko, H. 1995. Comparative analyses concerning integrity of a VVER-440 reactor pressure vessel. Nuclear Engineering and Design, Vol. 159, pp. 63 - 68.

Talja, H. 1995. Automated integrity assessment for piping components. Espoo: VTT Manufacturing Technology. 31 p. + app. (Report VALB120).

Talja, H. 1995. Program system MASI for Fracture Assessment. Version 1.0. Status report and user instructions. Espoo: VTT Manufacturing Technology. 36 p. + app. 23 p. (Report VALB43).

Talja, H. & Viitala, T. 1995. Väsymisanalyysivalmiuden lisääminen MASI-järjestelmään - versio 1.1. Espoo: VTT Manufacturing Technology. 16 p. + app. (Report VALB113).

Talja, H., Koski, K., Rintamaa, R. & Keskinen, R., 1995. HDR-tutkimusohjelman tulosten arviointi. Helsinki: Finnish Centre for Radiation and Nuclear Safety. 96 p. (STUK YTO-TR 90). (In Finnish).

Talja, H., Raiko, H., Mikkola, T. P. J. & Zhang, Z. L. 1995. Structural safety analysis with engineering integrity assessment tools. Accepted for publication in Structural Engineering Review. 43 p.

Talja, H. & Keinänen, H. 1996. Application of engineering methods on reactor pressure vessel integrity assessment. Proc. of 11th Biennial European Conference on Fracture - ECF11. Poitiers-Futuroscope, France, 3 - 6 September 1996. In: ECF 11 Mechanisms and Mechanics of Damage and Failure. Vol. III. Ed. J. Petit. Warley, UK: EMAS. Pp. 2133 - 2138.

Talja, H. 1997. Numerical sensitivity study on path-independency of the J-integral. Espoo: VTT Manufacturing Technology. 14 p. + app. (Report VALB189).

Talja, H., Novák, J. & Lauerová, D. 1997. Numerical analysis for tensile and fracture mechanics specimens of VVER-440 reactor pressure vessel cladding material. Fraunhofer Institut für Werkstoffmechanik. Report T11/97. 30 p.

Talja, H., Raiko, H., Mikkola, T. P. J. & Zhang, Z. L. 1997. Structural integrity assessment with engineering integrity assessment tools. Computers & Structures 64(759-770).

Talja, H., Saarenheimo, A., Miettinen, J. & Lindholm, I. 1997. NESC1 project - simplified pretest analyses and sensitivity analysis for heat transfer coefficient. Espoo: VTT Manufacturing Technology. 16 p. + 28 p app. (Report VALB245).

Talja, H., Schmitt, W., Böhme, W., Oeser, S. & Stöckl, H. 1997. Charakterisierung der Hochlagenzähigkeit auf der Basis von miniaturisierten Charpy- und Zugversuchen. Fraunhofer IWM, Januar 1997. T 6/97. 9 p. + app.

Talja, H. 1998. Ductile fracture assessment using parameters from small specimens. Doctoral Thesis. Espoo: Technical Research Centre of Finland. 140 p. (VTT Publications 353)

Talja, H., Schmitt, W., Böhme, W., Oeser, S. & Stöckl, H. 1998. Characterization of ductile fracture toughness based on subsized charpy and tensile test results. ASTM Publication STP 1329: Small specimen test techniques, Eds. William R. Corwin, Stand T. Rosinski & Eric van Walle.

Turkki, T. 1997. ORMGEND3D-ohjelman testausraportti. Espoo: VTT Manufacturing Technology. 8 p. + app. (Report VALB254). (In Finnish).

Maintenance Strategies and Reliability

Kettunen, J. & Norros, L. 1996. Inhimillisten ja organisatoristen tekijöiden yhteys NDT-tarkastusten luotettavuuteen. Katsaus kansainväliseen kirjallisuuteen. [Human and organizational factors influencing the reliability of non-destructive testing]. Helsinki: Finnish Centre for Radiation and Nuclear Safety. 59 p. (STUK-YTO-TR 103). ISBN 951-712-118-0. (KUNTO(96)1). (In Finnish).

Kettunen, J. 1997. Uskomuksia ydinvoimalaitoksissa suoritettavien tarkastusten luotettavuudesta. [Beliefs concerning the reliability of nuclear power plant in-service inspections.] Helsingin yliopisto. Psykologian laitos. Pro gradu -tutkielma. 49 p. + app. 9 p. (STUK-YTO-TR 121). ISBN 951-712-173-3. (KUNTO(96)11) (In Finnish).

Kettunen, J. 1997. Uskomuksia ydinvoimalaitoksissa suoritettavien tarkastusten luotettavuudesta. Helsinki: Finnish Centre for Radiation and Nuclear Safety. 46 p. (STUK-YTO-TR 121). (In Finnish)

Laakso, K., Hänninen, S. & Simola, K. 1995. Experience based reliability centered maintenance - a case study of the improvement of the maintenance programme for valve drives. The International Journal Maintenance, Vol. 10, No. 1, pp. 3 - 7. (KUNTO(95)1)

Laakso, K. & Paulsen, J. L. 1995. NKS/RAK-1 Subproject 4/KUNTO. Maintenance strategies and ageing of equipment. Nordic questionnaire survey. Questionnaire 29.4.1995. NKS/RAK-1(95)6. (KUNTO(95)2). 9 p.

Laakso, K., Hänninen, S. & Hallin, L. 1995. How to evaluate the effectiveness of a maintenance program. BALTICA III, International Conference on Plant Condition and Life Management. VTT Symposium 151. Vol. II. Eds. S. Hietanen & P. Auerkari. (KUNTO(95)3). Pp. 597-606.

Laakso, K. 1996. Käyttövarmuuden parantaminen kunnossapitomallin avulla. Automaatioväylä 3/1996, pp. 31 - 32. (KUNTO(96)4)

Laakso, K. 1996. Assessing the effectiveness of a maintenance program. Presented at the 13th Euromaintenance 96 Conference. Copenhagen, Denmark, 21 - 23 May, 1996. (KUNTO(96)7). Pp. 279 - 289.

Laakso, K. 1996. Reliability centered maintenance (RCM). Suomalainen sovellus. Kunnossa-käynnissäpito '96. Ajankohtaisfoorumi 12. - 13.6.1996. Helsinki. IIR Finland Oy ja Kunnossapitoyhdistys ry. (KUNTO(96)12). 5 p. + app. (In Finnish).

Laakso, K. & Pyy, P. 1996. Use of reliability centered maintenance analysis for decision making. ESReDA 10th Seminar on Rotating Machinery Reliability and Maintenance. Chamonix, 4 - 5 April, 1996. (KUNTO(96)6). 17 p.

Laakso, K. 1997. Käyttövarmuuskeskeinen kunnossapitomalli. Voima ja Käyttö -lehti. 5 p. (In Finnish).

Laakso, K. 1997. Assessing the effectiveness of a maintenance programme. Selected from the Euromaintenance 96 Conference. Copenhagen, Denmark, 21 - 23 May, 1997. Maintenance & Asset Management, Vol. 12, No. 1, pp. 19 - 24.

Laakso, K., Sirola, M. & Holmberg, J. 1997. Decision modelling for maintenance and safety. Paper presented at the ESReDA seminar on decision analysis and its applications in safety and reliability. 15 - 16 May, 1997. Espoo, Finland. 10 p. + 2 app.

Laakso, K., Dorrepaal, J. & Skogberg, P. 1998. Maintenance analysis and decision support for safety and availability of active systems. Final report of the Nordic research subproject NKS/RAK-1.4 "Maintenance strategies and ageing". Report edited by Laakso, K. Draft NKS/RAK-1(97)12 Report. Roskilde, Denmark: NKS sekretariatet. 101 p.

Kunnossapidon luotettavuuskeskeinen arviointi. Kunnossapito-lehti 6/95, pp. 54 - 55. (KUNTO(95)10). (In Finnish).

Norros, L. & Kettunen, J. 1998. NDT-tarkastajien toimintatavat ammattitaitoa ja tarkastustehtävää koskevien käsitysten perusteella [Analysis of NDT-inspectors' working practices]. Helsinki: Finnish Centre for Radiation and Nuclear Safety. 45 p. ISBN 951-712-279-9. (STUK-YTO-TR 147). (In Finnish).

Simola, K. 1995. IAEA Research co-ordination meeting on management of ageing of motor operated isolation valve. Vienna, Austria, 3 - 7 April 1995. (KUNTO(95)4).

Simola, K. & Pulkkinen, U. 1995. Uses of reliability engineering methods and probabilistic models in MOV ageing analyses. IAEA meeting in the co-ordinated research program on management of ageing of motor operated isolating valve. Vienna, Austria, 3 - 7 April, 1995. (KUNTO(95)5). 18 p.

Simola, K. & Pulkkinen, U. 1995. Putkistojen kunnonvalvontamenetelmien luotettavuus. Väkiraportti 7.9.1995. (KUNTO(95)6). 12 p. (In Finnish)

Simola, K. & Pulkkinen, U. 1996. Statistical models for reliability and management of ultrasonic inspection data. 19.12.1996. (To be published in STUK-YTO-TR series 1997) (KUNTO(96)10). 33 p.

Simola, K. & Koski, K. 1997. A survey of probabilistic methods for evaluation of structural component integrity. Espoo: VTT Automation report. (KUNTO(95)7). 56 p.

Simola, K. & Pulkkinen, U. 1997. Models for reliability and management of NDE data. In: Soares (Ed.) Advances in Safety and Reliability. Proceedings of the ESREL '97 Int. Conference On Safety and Reliability. Lisboa, Portugal, 17 - 20 June, 1997. Pp. 1491 - 1498.

Simola, K. 1998. Experience based ageing analysis of NPP protection automation. In: Mosleh, A. & Bari, R.A. (Eds.) Proceedings of the 4th Int. Conference on Probability Safety Assessment and Management. Vol. 1. London: Springer-Verlag. Pp. 483 - 488.

Simola, K., Laakso, K. & Skogberg, P. 1998. Evaluation of existing maintenance programmes using RCM methodology. Proceedings of the European Conference on Safety and Reliability - ESREL'98. Vol. 1. Safety and Reliability. Trondheim, Norway, 16 - 19 June 1998. A. A. Balkema/Rotterdam/Brookfield. Pp. 207 - 213

Simola, K. & Pulkkinen U. 1998. Models for non-destructive inspection data. Reliability Engineering and System Safety, Vol. 60, No. 1-12. 12 p.

Sirola, M. 1996. Computerized decision analysis tool. EHPG-Meeting of the OECD Halden Reactor Project. Loen, Norway, 19 - 24 May 1996. (KUNTO(96)8). 10 p.

Sirola, M., Holmberg, J. & Laakso, K. 1997. Computerized decision analysis tool - Decision Tool. VTT Automation Report. (KUNTO(96)17). 6 p. + app.

IAEA. 1997. Co-ordinated research programme on management of ageing of motor operated isolating valve. Report of stage I of phase II. Reproduced by the IAEA, Vienna, Austria. Pp. 33 - 43. (KUNTO 95(8), prepared by Simola, K. 1996).

OECD(NEA/CSNI/R(95)9. 1995. Evidence of aging effects on certain safety related components. A generic study performed by Principal Working Group 1 of The Committee for Safety of Nuclear Installations. Volume 2: Contributions of participating countries. Volume 2B: Finland. 290 p. (Compiled in KUNTO by Laakso, K., Simola, K., Pulkkinen, U. & Hänninen, S., September 1995).

Fire safety

Aulamo, H. 1997. Ydinvoimalaitoksen kaapelipaloriski [Cable fire risk of a nuclear power plant]. Master's Thesis. Helsinki University of Technology. Department of Engineering Physics and Mathematics. 117 p. (In Finnish).

Björkman, J., Keski-Rahkonen, O. & Lewis, M. J. 1995. First simulations of the Steckler room fire experiment by using SOFIE. First European Symposium on Fire Safety Science. Zürich, Switzerland, 21 - 23 August 1995.

Björkman, J. & Keski-Rahkonen, O. 1996. Simulation of the Steckler room fire experiment by using SOFIE CFD-model. Espoo: Technical Research Centre of Finland. 28 p. + app. 3 p. (VTT Publications 265).

Björkman, J. & Keski-Rahkonen, O. 1997. Response of fire detectors to different smokes. Espoo: Technical Research Centre of Finland. 33 p. (VTT Publications 295).

Björkman, J. & Keski-Rahkonen, O. 1997. Response of fire detectors to cable fires. SMiRT 14, Fifth Post Conference Seminar No 6: Fire Safety in Nuclear Power Plants and Installations. Lyon, France 25 - 29 August 1997. 12 p.

Björkman, J. & Keski-Rahkonen, O. 1997. Full scale experiments with different smokes. Espoo: Technical Research Centre of Finland. 18 p. + app. 62 p. (VTT Publications 332).

Björkman, J. 1998. Palonilmaisun mallintaminen [Modeling of fire detection]. Licentiate Thesis. Helsinki University. 55 p.

Björkman, J. & Keski-Rahkonen, O. 1998. Pressure transmitter and valve actuator failure at high temperature. Espoo: VTT Building Technology. 59 p. (Research Report RTE10211/98). (To be published).

Björkman, J., Keski-Rahkonen, O., Salminen, A. & Palmen, H. 1998. Effects of smoke on electrical components. VTT Building Technology, Research Report RTE10216/98. (In preparation)

Heikkilä, L. & Keski-Rahkonen, O. (Eds.). 1996. Advanced numerical modelling of a fire. Final report. Espoo: Technical Research Centre of Finland. 24 p. (VTT Research Notes 1740).

Hostikka, S. 1997. Palopatsasmallit tulipalon simuloinnissa [Plume models in numerical simulation of fire]. Master's Thesis. Helsinki University of Technology, Department of Engineering Physics and Mathematics. 79 p. + app. 8 p. (In Finnish).

Hostikka, S. & Keski-Rahkonen, O. 1998. Modelling of smoke spreading inside a nuclear power plant control building. Espoo: VTT Building Technology. 34 p. (Research Report RTE10202/98).

Hostikka, S. & Keski-Rahkonen, O. 1998. Modelling of cable tunnel fire. Espoo, VTT Building Technology, Research Report RTE10220/98. (In preparation)

Huhtanen, R. & Keski-Rahkonen, O. 1995. CFD simulation of a fire in the containment of HDR Test Reactor. In: V. Molkov (Ed.) Proceedings of the First International Seminar on Fire and Explosion Hazard of Substances and Venting of Deflagrations. Moscow: All-Russian Research Institute for Fire Protection. Pp. 281 - 289.

Huhtanen, R. 1998. Simulation of a smoke detector test. Espoo: VTT Energy. 44 p. + app. 3 p. (Research report ENE21/8/98).

Huhtanen, R. 1998. Fire spread model for horizontal cable trays. Espoo: VTT Energy. (Research report ENE21/xx/98). (To be published).

Keski-Rahkonen, O. 1996. CIB W14 Round Robin for Code Assessment. A Comparison of Fire Simulation Tools. Open International Symposium on Fire Safety Design of Buildings and Fire Safety Engineering. Oslo, Norway, 19 - 20 August 1996. 11 p. + app. 3 p.

Keski-Rahkonen, O. & Mangs, J. 1996. Maximum and minimum rate of heat release during flashover in electronic cabinets of NPPs. In: Faillace, R., Müller, K., Röwekamp, M. & Schneider, U (Eds.) Proceedings of SMiRT 13 Post Conference Seminar No. 6, 21 - 24 August, 1995. Fourth International Seminar on Fire Safety in Power Plants and Industrial Installations, Gramado, Brasil. SR 2092 / INT 9047, GRS-V-Bericht 9, 1996. Pp. 19 - 31.

Keski-Rahkonen, O. 1997. Underlying research for fire protection upgrading. Fire and Safety Conference, 24 - 26 February 1997, London, UK. 19 p.

Keski-Rahkonen, O., Björkman, J. & Farin, F. 1997. Derating of cables at high temperatures. Espoo: Technical Research Centre of Finland. 57 p. + app. 2 p. (VTT Publications 302).

Keski-Rahkonen, O., Björkman, J. & Farin, J. 1997. Derating of cables at high temperatures. Fire and Safety Conference, London, UK, 24 - 26 February 1997. 17 p.

Keski-Rahkonen, O. 1998. CIB W14 Round Robin of fire simulation code comparisons. Fire-and-explosion hazard of substances and venting of deflagrations: Proceedings of the Second International Seminar, Moscow, Russia, 11 - 15 August 1997. Moscow: All-Russian Research Institute for Fire Protection. Pp. 87 - 101.

Keski-Rahkonen, O. 1998. Quantifying tools: possibilities, limits, and hazards. 2nd International Conference on Fire and Explosion Protection, Zürich, Switzerland, 21 - 23 October, 1998. Zürich: Institute of Safety & Security. Pp. 1 - 22.

Hostikka, S. & Keski-Rahkonen, O. 1998. Modelling of cable tunnel fire. Espoo, VTT Building Technology, Research Report RTE10220/98. (In preparation)

Mangs, J. & Keski-Rahkonen, O. 1996. Full scale fire experiments on electronic cabinets II. Espoo: Technical Research Centre of Finland. 48 p. + app. 6 p. (VTT Publications 269).

Mangs, J. & Keski-Rahkonen, O. 1997. Full scale fire experiments on vertical and horizontal cable trays. Espoo: Technical Research Centre of Finland. 58 p. + app. 44 p. (VTT Publications 324).

Mangs J. & Keski-Rahkonen, O. 1997. Calorimetric fire experiments of cable bundles. SMiRT 14, Fifth Post Conference Seminar No 6: Fire Safety in Nuclear Power Plants and Installations. Lyon, France, 25 - 29 August 1997. 10 p.

Mangs, J. & Keski-Rahkonen, O. 1998. Ignition mechanisms and frequencies in control and power circuits in nuclear power plants. Espoo: VTT Building Technology. 15 p. (Research Report RTE10208/98).

Mangs, J. & Keski-Rahkonen, O. 1998B. Failure distribution in instrumental cables in fire. VTT Building Technology, Research Report RTE10218/98. (In preparation)

Paananen, J. 1996. Instrumenttikaapin palon suurimman tehon kokeellinen määrittäminen [Experimental determination of the maximum rate of heat release of an electronic cabinet]. Master's Thesis. Helsinki University of Technology, Structural Engineering and Building Physics, Fire and Safety Engineering. 111 p. + app. 22 p. (in Finnish).

Coordination, Reporting and Dissemination

Faidy, C. & Hayns, M. R. 1998. Evaluation of the RATU2 and RETU Research Programs. Helsinki: Ministry of Trade and Industry, Finland. 65 p. (Studies and Reports 8/1998).

Forstén, J. & Rintamaa, R. 1995. Assuring structural integrity of ageing reactor steel components. OECD Halden Reactor Project Symposium, Tokyo, Japan, 22 - 23 May 1995. Pp. 1 - 21.

Rintamaa, R., Karjalainen-Roikonen, P., Aaltonen, P., Kauppinen, P., Pelli, R., Keinänen, H., Talja, H., Planman, T., Valo, M., Nevalainen, M. & Wallin, K. 1995. Overview on some recent results of the VTT's research programme on assuring nuclear power plant structural safety. International working group on life management of nuclear power plants, International Atomic Energy Agency. Vienna, Austria, 30 August - 1 September, 1995. Espoo: VTT Manufacturing Technology. 23 p. (Report VALB102).

Solin, J. 1997. RATU2 Suunnittelu, ohjaus ja raportointi; Tutkimusohjelman hallintomenettelyjen kuvaus. Espoo: VTT Manufacturing Technology. 15 p. + app. (Report VALB256). (In Finnish).

Solin, J. & Marquis, G. 1996. Long-life spectrum fatigue of welded components, experiments and analysis. Int. Conference on Fatigue of Welded Components and Structures. Société Française de Métallurgie et de Matériaux (SF2M). Senlis, France, June 12 - 14, 1996. 9 p.

Solin, J., Sarkimo, M. & Asikainen, M. (Eds.) 1996. RATU2 The Finnish Research Programme on the Structural Integrity of Nuclear Power Plants. Annual Report 1995. Espoo: VTT Manufacturing Technology. (Report VALB146).

Solin, J., Sarkimo, M. & Asikainen, M. (Eds.) 1997. Ydinvoimalaitosten rakenteellinen turvallisuus (RATU2), Vuosiraportti 1996. Espoo: VTT Manufacturing Technology. 19 p. + app. (Report VALB219). (In Finnish).

Solin, J., Sarkimo, M. & Asikainen, M. (Eds.) 1997. RATU2 The Finnish Research Programme on the Structural Integrity of Nuclear Power Plants, Interim Report 1995 - April 1997. Espoo: VTT, Technical Research Centre of Finland. 140 p. + app. (VTT Research notes 1843).

Solin, J., Sarkimo, M., Asikainen, M. & Niemi, J. (Eds.) 1998. Ydinvoimalaitosten rakenteellinen turvallisuus (RATU2), Vuosiraportti 1997. Espoo: VTT Manufacturing Technology. 15 p. + liitt. (Report VALB293). (In Finnish).

Solin, J., Sarkimo, M., Asikainen, M. & Åvall, Å. (Eds.) 1998. RATU2, The Finnish Research Programme on the Structural Integrity of Nuclear Power Plants, Synthesis of achievements 1995 - 1998. Espoo: VTT, Technical Research Centre of Finland. 334 p. + app. 42 p. (VTT Symposium).

VTT 1994. Ydinvoimalaitosten rakenteellinen turvallisuus (RATU2) 1995 - 1998, Tutkimusohjelman suunnitelma. Espoo: VTT Manufacturing Technology. 50 p. (Report VALB41). (In Finnish).

VTT 1994. Ydinvoimalaitosten rakenteellinen turvallisuus (RATU2), Toimintasuunnitelma vuodelle 1995. Espoo: VTT Manufacturing Technology. 48 p. (Report VALB45). (In Finnish).

VTT 1995. Ydinvoimalaitosten rakenteellinen turvallisuus (RATU2), Tilanneraportti I/1995. Espoo: VTT Manufacturing Technology. 12 p. + app. 56 p. (Report VALB91). (In Finnish).

VTT 1995. Ydinvoimalaitosten rakenteellinen turvallisuus (RATU2), Tilanneraportti II/1995. Espoo: VTT Manufacturing Technology. 12 p. + app. 58 p. (Report VALB103). (In Finnish).

VTT 1995. Ydinvoimalaitosten rakenteellinen turvallisuus (RATU2), Tilanneraportti III/1995. Espoo: VTT Manufacturing Technology. 16 p. + app. 63 p. (Report VALB118). (In Finnish).

VTT 1995. Ydinvoimalaitosten rakenteellinen turvallisuus (RATU2), Toimintasuunnitelma vuodelle 1996. Espoo: VTT Manufacturing Technology. 48 p. (Report VALB117). (In Finnish).

VTT 1996. Ydinvoimalaitosten rakenteellinen turvallisuus (RATU2) - Tilanneraportti I/96. Espoo: VTT Manufacturing Technology. (Report VALB147). (In Finnish).

VTT 1996. Ydinvoimalaitosten rakenteellinen turvallisuus (RATU2) - Tilanneraportti II/96. Espoo: VTT Manufacturing Technology. (Report VALB166). (In Finnish).

VTT 1996. Ydinvoimalaitosten rakenteellinen turvallisuus (RATU2) - Tilanneraportti III/96. Espoo: VTT Manufacturing Technology. (Report VALB196). (In Finnish)

VTT 1996. Ydinvoimalaitosten rakenteellinen turvallisuus (RATU2) - Toimintasuunnitelma vuodelle 1997. Espoo: VTT Manufacturing Technology. (Report VALB197). (In Finnish).

VTT 1997. Ydinvoimalaitosten rakenteellinen turvallisuus (RATU2), Tilanneraportti I/97. Espoo: VTT Manufacturing Technology. 15 p. (Report VALB227). (In Finnish)

VTT 1997. Ydinvoimalaitosten rakenteellinen turvallisuus (RATU2), Tilanneraportti II/97. Espoo. VTT Manufacturing Technology. 9 p. + app. (Report VALB244). (In Finnish).

VTT 1997. Ydinvoimalaitosten rakenteellinen turvallisuus (RATU2), Tilanneraportti III/97. Espoo. VTT Manufacturing Technology. 15 p. + app. (Report VALB270). (In Finnish).

VTT 1997. Ydinvoimalaitosten rakenteellinen turvallisuus (RATU2). Toimintasuunnitelma vuodelle 1998. Espoo: VTT Manufacturing Technology. 18 p. + app. (Report VALB283). (In Finnish).

VTT 1998. Ydinvoimalaitosten rakenteellinen turvallisuus (RATU2), Tilanneraportti I 1998. Espoo: VTT Manufacturing Technology. 14 p. + liitt. (Report VALB313). (In Finnish).

VTT 1998. Ydinvoimalaitosten rakenteellinen turvallisuus (RATU2), Tilanneraportti II 1998. Espoo: VTT Manufacturing Technology. 12 p + app. (Report VALB319). (In Finnish).

VTT 1998. Ydinvoimalaitosten rakenteellinen turvallisuus (RATU2), Tilanneraportti III 1998. Espoo: VTT Manufacturing Technology. 21 p. (Report VALB334). (In Finnish).

Appendix 2: Contact information

Steering Group of the RATU2 Programme

Mr. Matti Ojanen, (Chairman),
Radiation and Nuclear Safety Authority (STUK)
Mr. Ralf Ahlstrand, IVO Power Engineering Ltd.
Mr. Juho Hakala, Teollisuuden Voima Oy (TVO)
Prof. Hannu Hänninen, Helsinki University of Technology
Dr. Timo Haapalehto, Ministry of Trade and Industry
Dr. Lasse Mattila, VTT Energy
Dr. Rauno Rintamaa, VTT Manufacturing Technology

Coordination of the RATU2 Programme

VTT Manufacturing Technology
Mr. Jussi Solin
Tel. +358-9-456 6875
Fax +358-9-456 7002
Internet: Jussi.Solin@vtt.fi
P. O. Box 1704
FIN-02044 VTT, Finland
Street address: Kemistintie 3, Espoo

Coordination and reference groups of the RATU2 Projects

1. Material Degradation in Reactor Environment

Coordination:

VTT Manufacturing Technology
Dr. Kim Wallin
Tel. +358-9-456 6870
Fax +358-9-456 7002
Internet: Kim.Wallin@vtt.fi
P O Box 1704
FIN-02044 VTT, Finland
Street address: Kemistintie 3, Espoo

Reference group:

Juhani Hinttala	Radiation and Nuclear Safety Authority, STUK
Rainer Rantala	Radiation and Nuclear Safety Authority, STUK
Erkki Muttilainen	Teollisuuden Voima Oy
Heikki Raiko	VTT Energy
Ralf Ahlstrand	IVO Power Engineering Ltd
Ossi Hietanen	IVO Power Engineering Ltd
Hannu Hänninen	Technical University of Helsinki

2. Reliability of Nondestructive Inspections of Nuclear Power Plants

Coordination:

VTT Manufacturing Technology
Mr. Pentti Kauppinen
Tel. +358-9-456 6481
Fax +358-9-456 7002
Internet: Pentti.Kauppinen@vtt.fi
P O Box 1704
FIN-02044 VTT, Finland
Street address: Kemistintie 3, Espoo

Reference group:

Mauri Heltimoinen	IVO Loviisa
Liisa Muurinen	Helsinki Energy
Matti Nyman	Teollisuuden Voima Oy
Raimo Paussu	IVO Power Engineering Ltd
Olavi Valkeajärvi	Radiation and Nuclear Safety Authority, STUK
Kari Laakso	VTT Automation

3. Structural Analyses for Nuclear Power Plant Components

Coordination:

VTT Manufacturing Technology
Dr. Heli Talja
Tel. +358-9-456 4524
Fax +358-9-456 7002
Internet: Heli.Talja@vtt.fi
P O Box 1704
FIN-02044 VTT, Finland
Street address: Kemistintie 3, Espoo

Reference group:

Mauri Määttänen	Technical University of Helsinki
Rauli Keskinen	Radiation and Nuclear Safety Authority, STUK
Rainer Rantala	Radiation and Nuclear Safety Authority, STUK
Paulus Smeekes	Teollisuuden Voima Oy
Eero Torkkeli	Insinööritoimisto FEMdata Ky
Heikki Raiko	VTT Energy
Alpo Neuvonen	IVO Power Engineering Ltd.

4. Maintenance Strategies and Reliability

Coordination:

VTT Automation
Dr. Kari Laakso
Tel. +358-9-456 6465
Fax +358-9-456 6475
Internet: Kari.Laakso@vtt.fi
P O Box 1301
FIN-02044 VTT, Finland
Street address: Tekniikantie 12, Innopoli, Espoo

Reference group:

Rauli Keskinen	Radiation and Nuclear Safety Authority, STUK
Kari Nieminen	Teollisuuden Voima Oy
Alpo Savikoski	IVO Loviisa Power Plant
Osmo Viitasaari	IVO Tuotantopalvelut
Mihaly Makkai	Helsinki Energy
Risto Sairanen	VTT Energy
Veikko Rouhiainen	VTT Manufacturing Technology

5. Fire Safety

Coordination:

VTT Building Technology
Dr. Olavi Keski-Rahkonen
Tel. +358-9-456 4810
Fax +358-9-456 4815
Internet: Olavi.Keski-Rahkonen@vtt.fi
P O Box 1803
FIN-02044 VTT, Finland
Street address: Kivimiehentie 4, Espoo

Reference group:

DI Jouko Marttila	Radiation and Nuclear Safety Authority, STUK
DI Antti Nortta	IVO Power Engineering Ltd
DI Kari Taivainen	Teollisuuden Voima Oy
DI Heikki Tenhunen	Palotutkimusraati ry
TkL Risto Huhtanen	VTT Energy